UNIVERSITAT DE BARCELONA

Novel cell models for the identification of biomarkers and therapeutic targets in Inclusion Body Miositis

Judith Cantó Santos

Doctoral Thesis

Novel cell models for the identification of biomarkers and therapeutic targets in Inclusion Body Myositis

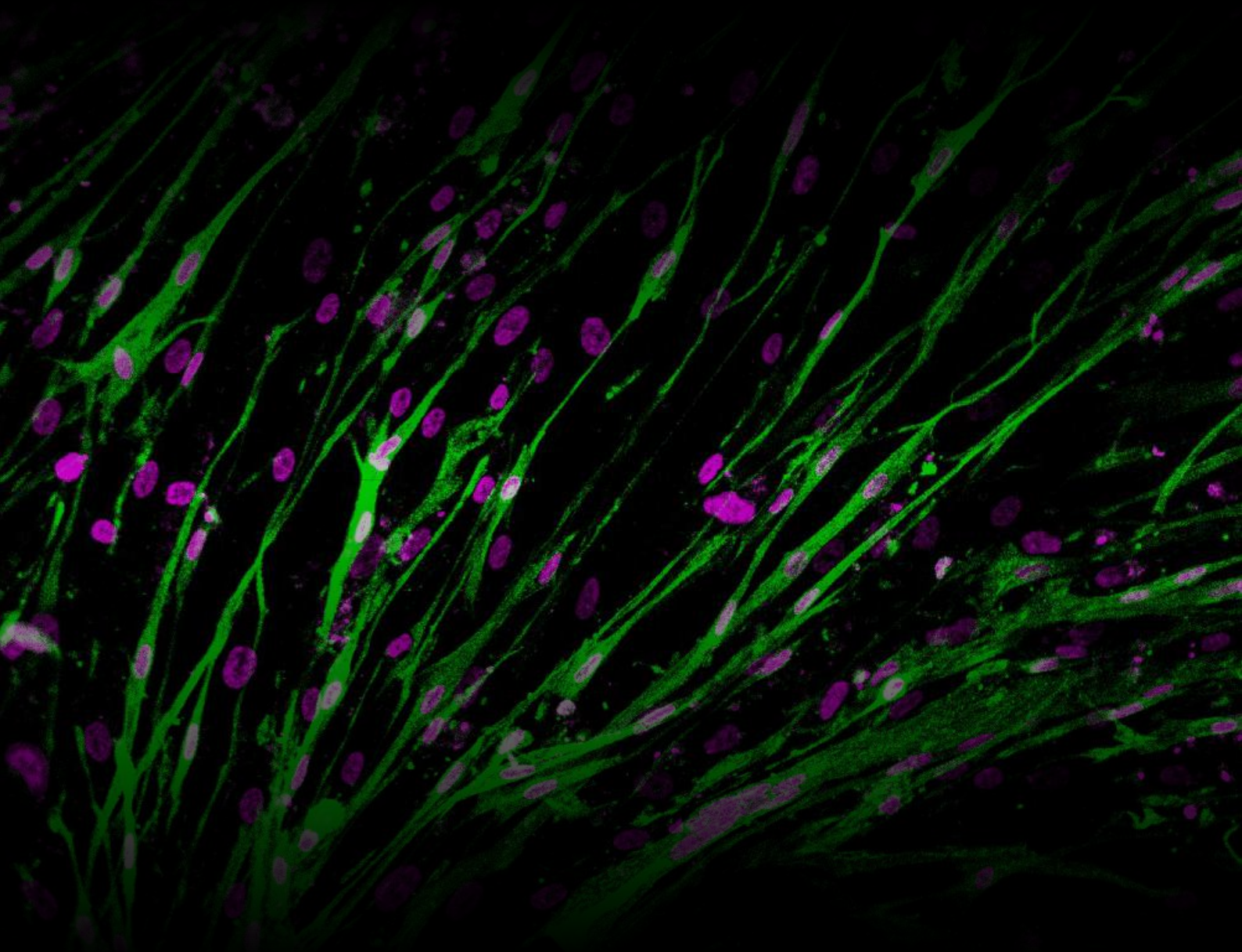

Judith Cantó Santos

Barcelona, July 2023

NOVEL CELL MODELS FOR THE IDENTIFICATION OF BIOMARKERS AND THERAPEUTIC TARGETS IN INCLUSION BODY MYOSITIS

Doctoral thesis dissertation presented by
JUDITH CANTÓ SANTOS
to apply for the doctoral degree at the University of Barcelona

Supervised by:
Dra. Gloria Garrabou
Department of Medicine, Faculty of Medicine and Life Sciences, University of Barcelona. Institut d'Investigacions Biomèdiques August Pi i Sunyer (IDIBAPS)

Dr. Josep Maria Grau Junyent
Department of Medicine, Faculty of Medicine and Life Sciences, University of Barcelona. Internal Medicine Department, Hospital Clinic de Barcelona. Institut d'Investigacions Biomèdiques August Pi i Sunyer (IDIBAPS)

Doctoral program in Medicine and Translational Research
Faculty of Medicine and Health Sciences
University of Barcelona
July 2023

FUNDING

This project has been funded by a fellowship from “Ajuts de personal investigador predoctoral en formació (APIF) 2019” by the University of Barcelona; by Fondo de Investigación para la Salud (FIS) PI18/00498, PI21/00935 supported by Instituto de Salud Carlos III (ISCIII) (Madrid, Spain) and by a project from CIBERER from the “Acciones Cooperativas y Complementarias Intramurales (ACCI)” 2022 call.

CONTENTS

LIST OF FIGURES

LIST OF TABLES

ABBREVIATIONS

A

AAV: adeno-associated virus

AD: Alzheimer disease

ADD: antidepressant drug

ADM: amyopathic dermatomyositis

AI: artificial intelligence

ALS: Amyotrophic lateral sclerosis

AMPK: AMP-activated protein kinase

APOE: apolipoprotein E

ASyS: antisynthetase syndrome

ATMPs: advanced therapy medicinal products

AβPP: amyloid beta precursor protein

B

BD2K: Big Data to Knowledge

C

CCL5: C-C motif chemokine 5

CCR5: C–C chemokine receptor type 5

cN1A: cytosolic 5'-nucleotidase 1A

CNV: copy number variants

COX-: cytochrome c oxidase deficient fibers

CS: citrate synthase

CXCL9: chemokine (C-X-C motif) ligand 9

D

DEG: differentially expressed gene

DM: dermatomyositis

DMD: Duchenne Muscular Dystrophy

E EMA: European Medicines Agency

ENMC: European Neuromuscular Centre

ER: endoplasmic reticulum

ERN Euro-NMD: European Reference Network for NMDs

EULAR/ACR: European League Against Rheumatism/ American College of Rheumatology

EURL/ECVAM: European Union Reference Laboratory for alternatives to animal testing

F FDA: Food and Drug Administration

FSHD: Facioscapulohumeral muscular dystrophy

FTD: frontotemporal dementia

FYCO1: FYVE and coiled-coil domain autophagy adaptor 1

G GA4GH: Global Alliance for Genomics and Health

GNE: glucosamine (UDP-N-Acetyl)-2-Epimerase/N-Acetylmannosamine kinase

GWAS: Genome-wide association studies

H HLA: human leukocyte antigen

I IBM: inclusion body myositis

IBMFRS: IBM functional rating scale

ICGC: International Cancer Genome Consortium

IFNγ: interferon gamma

IHEC: International Human Epigenome Consortium

IIBMCGS: International IBM Consortium Genetic Study

IIM: idiopathic inflammatory myopathies

IL1β: interleukin 1 beta

IMNM: immune-mediated necrotizing myopathy

iPSCs: induced pluripotent stem cells

IRDiRC: International Rare Disease Consortium

K KLRG1: Killer cell lectin-like receptor subfamily G member 1

L LAMA2: laminin subunit alpha-2

LC3: microtubule-associated protein light chain

LOH: loss of heterozygosity

M mAb: monoclonal antiobody

MCK: muscle creatine kinase

MDD: major depressive disorder

MELAS: mitochondrial myopathy, encephalopathy, lactic acidosis, and stroke-like episodes

MHC-I: major histocompatibility complex I

MMP: mitochondrial membrane pore

MPTP: 1-methyl-4-phenyl-1,2,3,6-tetrahydropyridine

MRC: mitochondrial respiratory chain

MRI: magnetic resonance imaging

mtDNA: mitochondrial DNA

MYH2: myosin heavy chain 2

MYOGEN: Myositis Genetic Consortium

N NMDs: Neuromuscular diseases

NRTI: Nucleoside reverse transcriptase inhibitors

O OKT3: monoclonal CD3 antibody

P PD: Parkinson disease

PM: polymyositis

PN: peripheral neuropathy

Q QMT: quantitative muscle testing

QoL: quality of life

R RNS: reactive nitrogen species

ROS: reactive oxygen species

S SDH+: succinate dehydrogenase positive fibers

SNP: single-nucleotide polymorphisms

SQSTM1: sequestosome 1

T T2DM: Type 2 Diabetes Mellitus diseases

TCA: tricarboxylic acid cycle

TDP-43: transactive response DNA-binding protein 43

TNFα: tumor necrosis factor alpha

TOMM40: translocase of the outer mitochondrial membrane 40

U UPR: unfolded protein response

V VCP: valosin-containing protein

VUS: variants of unknown significance

W WES: whole exome sequencing

WGS: whole genome sequencing

LIST OF ARTICLES IN THE THESIS

Thesis in the format of a compendium of publications.

The thesis consists of four objectives and four articles and one supplementary manuscript:

ARTICLE 1:

Judith Cantó-Santos, Laura Valls-Roca, Ester Tobías, Francesc Josep García-García, Mariona Guitart-Mampel, Anna Esteve-Codina, Beatriz Martín-Mur, Mercedes Casado, Rafael Artuch, Estel Solsona-Vilarrasa, José Carlos Fernandez-Checa, Carmen García-Ruiz, Carles Rentero, Carlos Enrich, Pedro J. Moreno-Lozano, José César Milisenda, Francesc Cardellach, Josep M. Grau-Junyent, Glòria Garrabou. *Unravelling inclusion body myositis using a patient-derived fibroblast model*. Journal of Cachexia, Sarcopenia and Muscle. 2023; doi:10.1002/jcsm.13178. IF: 8.9; D1 (JCR): "Geriatrics & Gerontology".

ARTICLE 2:

Judith Cantó-Santos, Laura Valls-Roca, Ester Tobías, Francesc Josep García-García, Mariona Guitart-Mampel, Félix Andújar-Sánchez, Anna Esteve-Codina, Beatriz Martín-Mur, Joan Padrosa, Raquel Aránega, Emma Peruga, Irene Madrigal, Paula Segalés, Carmen García-Ruiz, Pedro J. Moreno-Lozano, José César Milisenda, Ana Sevilla, Josep M. Grau-Junyent, Glòria Garrabou. *Modelling inclusion body myositis using human pluripotent stem cell-derived skeletal myotubes*. Submitted to: Journal of Cachexia, Sarcopenia and Muscle. IF: 8.9; D1 (JCR): "Geriatrics & Gerontology".

ARTICLE 3:

Marc Catalan-Garcia, Francesc Josep García-García, Pedro J Moreno-Lozano, Gema Alcarraz-Vizan, Adria Tort-Merino, José César Milisenda, **Judith Cantó-Santos**, Tamara Barcos-Rodriguez, Francesc Cardellach, Albert Llado, Anna Novials, Gloria Garrabou, Josep M Grau-Junyent. *Mitochondrial Dysfunction: A Common Hallmark Underlying Comorbidity between sIBM and Other Degenerative and Age-Related Diseases*. Journal of clinical medicine. 2020; 9;1446. doi:10.3390/jcm9051446. IF: 4.2; Q1 (JCR): "Medicine, General & Internal".

ARTICLE 4:

Judith Cantó-Santos, Laura Valls-Roca, Ester Tobías, Clara Oliva, Francesc Josep García-García, Mariona Guitart-Mampel, Félix Andújar-Sánchez, Anna Esteve-Codina, Beatriz Martín-Mur, Joan Padrosa, Raquel Aránega, Pedro J. Moreno-Lozano, José César Milisenda, Rafael Artuch, Josep M. Grau-Junyent, Glòria Garrabou. *Integrated multi-omics analysis to infer molecular players in Inclusion body myositis*. Under review in Antioxidants. IF: 7.0; D1 (JCR): "Chemistry, Medicinal".

SUPPLEMETARY MANUSCRIPT I:

Judith Cantó-Santos, Josep M. Grau-Junyent and Glòria Garrabou. *The Impact of Mitochondrial Deficiencies in Neuromuscular Diseases*. Antioxidants. 2020; 9, 964; doi:10.3390/antiox9100964. IF: 6.3; D1 (JCR): "Chemistry, Medicinal".

SUMMARY OF THE THESIS

A summary in Catalan of this doctoral thesis is presented below.

A continuació es presenta un resum d'aquesta tesi doctoral en català.

Títol: Nous models cel·lulars per a la identificació de biomarcadors i dianes terapèutiques en a la Miositis per cossos d'inclusió

Introducció:

La Miositis per cossos d'inclusió (IBM) és una malaltia minoritària inflamatòria que afecta als músculs proximals i distals i causa debilitat muscular de forma progressiva. Debuta a partir dels 50 anys i els primers símptomes solen aparèixer als quàdriceps i als flexors dels dits. Es diagnostica a partir de les troballes histopatològigues inflamatòries, degeneratives i mitocondrials en la biòpsia muscular. Aquestes troballes són: a nivell inflamatori, infiltració de limfòcits T CD8+ en les fibres musculars i expressió anormal del complex major d'histocompatibilitat tipus I. A nivell degeneratiu, aparició de vacuoles ribetejades al citoplasma, formades per proteïnes acumulades mal plegades i a causa de l'autofàgia alterada o insuficient. A nivell mitocondrial, s'aprecien fibres vermelles esfilagarçades (RRF), fibres COX negatives i algunes SDH positives.

La IBM va ser considerada la forma esporàdica (sIBM) de les miopaties per cossos d'inclusió, malalties musculars amb base genètica que presenten alguns trets comuns, com les vacuoles ribetejades, però no presenten inflamació. Per això, els termes sIBM i IBM s'han utilitzat indistintament en diversos estudis.

Per a poder estudiar l'etiologia de les malalties, moltes vegades es fan servir models de la malaltia, que poden ser cel·lulars, animals, computacionals, etc. i que ajuden a obtenir evidencia de l'etiologia, evolució o tractaments efectius per a una determinada malaltia. En el cas de la IBM, l'etiologia no es coneix i no hi ha models validats de malaltia, biomarcadors ni tractaments efectius.

Hipòtesi:

La hipòtesi d'aquesta tesi és que nous models cel·lulars derivats de pacients amb IBM recapitularan els trets moleculars principals del teixit diana, el múscul, i podran contribuir a validar nous models de malaltia, a conèixer l'etiologia i identificar biomarcadors per al diagnòstic i pronòstic de la IBM.

Objectius:

Validar un model de fibroblasts derivats de pacients amb IBM i un model de cèl·lules musculars derivades de cèl·lules mare pluripotents induïdes (iPSC) prèviament obtingudes dels fibroblasts dels pacients amb IBM. En aquests models es determinarà la presència d'alteracions transcriptòmiques i funcionals (inflamatòries, degeneratives i mitocondrials) per comprovar si recapitulen els trets del teixit diana (múscul). Amb el model de fibroblasts, també s'avaluarà la comorbiditat amb altres malalties (com l'Alzheimer i la Diabetis mellitus tipus 2) i s'identificaran biomarcadors mitjançant anàlisi multi-òmics.

Principals resultats:

Els fibroblasts derivats de pacients amb IBM recapitulaven trets inflamatoris, degeneratius i mitocondrials com els del teixit diana de la malaltia, el múscul. Respecte a l'expressió gènica, els fibroblasts amb IBM tenien un perfil distintiu, amb gens relacionats amb la inflamació, mitocondri, regulació del cicle cel·lular i metabolisme. Funcionalment, els fibroblasts derivats d'IBM mostraven un augment en la secreció de citocines inflamatòries; una reducció de l'activitat de l'autofàgia, amb menys quantitat d'intermediaris proteics i menys formació d'autofagosomes. Al mitocondri, mostraven menys quantitat de mtDNA, uns nivells inferiors de respiració mitocondrial, de potencial de membrana mitocondrial, d'elongació dels mitocondris i d'activitats enzimàtiques respecte als controls, més estrés oxidatiu, capacitat antioxidant i un perfil incrementat d'àcids orgànics. Tot açò confirmava que els fibroblasts podien ser un bon model de malaltia pel que fa a la IBM, i tal vegada podrien exportar-se com a model d'altres malalties musculars.

Les cèl·lules musculars derivades d'iPSC, originades a partir de fibroblasts, es van desenvolupar com a model per tal d'obtenir mioblasts mitjançant una metodologia no invasiva. Els resultats que es van obtenir a nivell d'expressió gènica eren canvis miopàtics i en la contracció muscular, en relació amb la clínica de la IBM. Funcionalment, no hi havia alteracions inflamatòries. L'autofàgia estava reduïda amb menys formació d'intermediaris proteics del procés. L'activitat mitocondrial estava conservada a pel que fa a la respiració i capacitat antioxidant, però les activitats enzimàtiques del complex IV de la MRC i la citrat sintasa (marcador del número de mitocondris) i la producció de lactat estaven augmentades, senyalant certa alteració en la funció mitocondrial. Per tal d'observar inflamació o canvis més pronunciats, aquests miotubs es podrien estimular amb agents estressants (químics, mecànics o d'envelliment) per a induir un fenotip més propi d'IBM i simular l'envelliment muscular característic dels pacients amb IBM.

Amb els fibroblasts derivats d'IBM es va voler comprovar si compartien trets moleculars i clínics amb l'Alzheimer o amb la Diabetis mellitus tipus 2, ja que totes tres presenten disfunció mitocondrial. Amb l'Alzheimer es va veure que la IBM no presenta comorbiditat, malgrat ser ambdues malalties degeneratives. Amb la diabetis, es va veure que els fibroblasts derivats d'IBM mostraven un patró pre-diabètic, amb canvis en el metabolisme de la glucosa. Aquesta desregulació podria estar causada per l'estil de vida, degut a una reducció de la mobilitat en els pacients amb IBM, entre d'altres factors.

Per tal d'identificar possibles variacions en el metabolisme dels pacients amb IBM, es va comparar el perfil d'àcids orgànics en fibroblasts vs. en orina, i els gens diferencialment expressats relacionats amb el metabolisme al múscul. Es va observar que els alts nivells d'àcid piroglutàmic i àcid oròtic a la orina estaven relacionats amb un augment del glutatió i de la síntesi de pirimidines, en concret orotidina, al plasma i a la orina, respectivament; i amb els gens L2HGDH, IDH2, OPLAH i ASL, diferencialment expressats al múscul. Per tant, d'una banda els canvis en els metabòlits a nivell sistèmic en la IBM, i d'altra, la identificació de biomarcadors en fluids derivats de pacients, poden ajudar a entendre millor la etiologia o facilitar el diagnòstic d'aquests pacients.

Conclusions:

Les conclusions d'aquesta tesi són que els models cel·lulars derivats de pacients amb IBM constitueixen una eina raonable per a investigar la seva etiologia, identificar biomarcadors i avaluar comorbiditats amb altres malalties. A més, s'ha manifestat el paper rellevant del metabolisme i el mitocondri en la IBM, i potser en altres malalties musculars. Malgrat no hi ha simptomatologia clínica fora del múscul, molecularment s'han trobat alteracions fora del teixit diana, senyalant que algunes troballes poden ser sistèmiques. La identificació de gens amb un patró d'expressió gènica alterat pot ajudar a identificar gens reguladors i vies de senyalització afectades que aportin informació sobre la fisiopatologia de la IBM.

INTRODUCTION

CHAPTER 1: Inclusion body myositis

1. Neuromuscular diseases: definition and classification

Neuromuscular diseases (NMDs) are a group of rare disorders caused by damage or impairment of various parts of the nervous and muscular systems, including the lower motor neurons of the spinal cord, peripheral nerves, neuromuscular junctions, or skeletal muscles. This damage leads to symptoms such as muscular weakness and atrophy, difficulty swallowing and breathing, and potential heart failure (1).

With over 500 genes implicated in the pathogenesis of NMDs, these disorders can present a wide range of symptoms and clinical heterogeneity (2). Their prevalence ranges from 1 to 10 per 100,000 population (3), and their diversity often leads to delays in diagnosis, typically taking 7 years, with 30% of diagnoses never achieved (1). This is partly due to misdiagnosis and a lack of non-invasive diagnostic and prognostic biomarkers. Although disease models and effective treatments are scarce, recent studies have focused on depicting the etiology of these disorders (4). Advances in genome sequencing and genetic analysis have enabled the diagnosis of monogenic NMDs, and a better understanding of the genome could help to characterize complex disease inheritance and etiology. This could eventually aid in the identification of effective treatments for NMDs using precision medicine (1).

NMDs are currently classified into 7 main groups: muscular dystrophies, neuromuscular junction diseases, motor neuron diseases, peripheral nerve diseases, mitochondrial myopathies, muscle channelopathies, and myopathies. In this article, we will focus on idiopathic inflammatory myopathies (IIM), which are characterized by inflammation in the muscles leading to muscle weakness (1). A comprehensive classification of NMDs into each group is provided in the review at the supplementary manuscript I.

2. Idiopathic inflammatory myopathies

IIM, also known as myositis, are a heterogeneous group of disorders characterized by chronic muscle inflammation that presents with a range of clinical symptoms, responses to treatment, and prognoses. While muscle weakness, low endurance, and myalgia are common, these disorders often display extramuscular manifestations such as skin rash, arthritis, interstitial lung disease and heart involvement, highlighting the systemic inflammatory nature of these conditions (5).

Initially, polymyositis (PM) was the overarching term used to describe these conditions. In 1863, a subgroup of the disease with a skin rash was identified and named dermatomyositis (DM). However, it wasn't until the 1950s that a clinical definition for PM and DM was proposed. As research progressed, IIM was further classified into subgroups based on clinical and histopathological manifestations of muscle tissue (Table 1), including DM (both juvenile and adult onset), PM, inclusion body myositis (IBM), and amyopathic DM (ADM) (5). More recently, new subgroups of IIM with distinct clinical manifestations and muscle histopathological features have been identified based on myositis-specific autoantibodies, such as antisynthetase syndrome (ASyS) in the 1990s and immune-mediated necrotizing myopathy (IMNM) in 2006. Additionally, suggested subgroups of IIM include cancer-associated myositis and overlap myositis (myositis that coexists with another autoimmune disorder). Diagnosing IIM and its subgroups requires a combination of clinical symptoms and signs,

such as muscle biopsy features, magnetic resonance imaging (MRI) patterns, serological assessment (autoantibodies), and serum levels of muscle enzymes (Table 1) (5).

Table 1. Classification of the idiopathic inflammatory myopathies (IIM) according to their histopathological features. MAC: membrane attack complex (Lundberg, I *et al.* 2021) (5).

Myositis subtype	Muscle fibres and tissue	Inflammatory cell infiltrates	MHC I expression	MAC depositions	Other specific findings
Dermatomyositis	Perifascicular atrophy, reduced number of capillaries	Perivascular, perimysial, T cells, B cells, macrophages, plasmacytoid dendritic cells	Perifascicular fibres	Small blood vessels	Sarcoplasmic MxA expression
Polymyositis	Degeneration, necrosis, regeneration	Endomysial inflammatory infiltrate with T cells often surrounding and/or invading non-necrotic muscle fibres	Diffuse distribution	No specific findings	Absence of rimmed vacuoles
Immune-mediated necrotizing myopathy	Necrotic fibres with scattered distribution, different stages of necrosis and myophagocytosis and regeneration, endomysial fibrosis and proliferation	Macrophage predominant, paucilymphocytic infiltrates	Diffuse distribution, sometimes only faint	Sarcolemmal and/or on small blood vessels	No specific findings
Antisynthetase syndrome	Oedematous and/or fragmented perimysium that stains with alkaline phosphatase, sometimes perifascicular myofibre necrosis	Scattered perimysial $CD68^+$, $CD4^+$, $CD8^+$ cells	Perifascicular predominance	Fibres adjacent to the perimysium, sarcolemmal on non-necrotic fibres	Myonuclear actin filament inclusions in electron microscopy, absence of MxA expression
Inclusion body myositis	Rimmed vacuoles, ragged red fibres, cytochrome oxidase-negative fibres, groups of atrophic fibres	Endomysial inflammatory infiltrate with mainly $CD8^+$ cells surrounding and/or invading non-necrotic muscle fibres	Diffuse distribution	No specific findings	TDP43, p62 aggregates, 15–18 nm filaments in electron microscopy

Instead of targeting specific pathogenic pathways, current treatment for IIM typically involves high doses of glucocorticoids in combination with other immunosuppressive drugs. However, the inclusion of heterogeneous patient populations in past clinical trials has led to highly variable response rates (6). To improve the power of clinical trials and identify effective treatments for the different forms of inflammatory myopathies, the current classification of IIM and the discovery of myositis-specific autoantibodies should aid in defining more homogeneous patient populations (6).

Despite these improvements, transformative changes in the treatment of inflammatory myopathies will likely require a deep understanding of disease mechanisms to reveal novel therapeutic targets (6). As our understanding of inflammatory myopathy disease mechanisms expands, we can expect the identification of additional therapeutic targets and the development of new therapeutic approaches.

3. Inclusion body myositis

3.1. Introduction, clinical features, epidemiology & comorbidities

IBM is a progressive muscle disease affecting proximal and distal muscles with an asymmetrical pattern (Figure 1). The onset is at 50 years old and is more common in males (2:1) (7). The prevalence varies across geographic populations, estimated at 1-10 per million (8) but raises to 50-180 per million in the population over 50 years old (7).

Before being classified as IIM, it was within the group of inclusion body myopathies, muscular genetic diseases with features including rimmed vacuoles, but without inflammation(9,10). Previously, IBM was considered the sporadic (due to absent or unknown genetic basis) form of inclusion body myopathies. The term sporadic IBM (sIBM) and IBM have been applied synonymously in several studies(10). However, in this thesis, we will refer to it as IBM.

The initial symptoms of IBM arise in quadriceps and finger flexors (Figure 1), with patients experiencing difficulties climbing stairs and grasping objects with their hands. Dysphagia is common and affects 64% of the patients (Figure 1) (8). The most disabling features in IBM are the need for wheelchair assistance after 15 years of disease onset, severe dysphagia and respiratory function impairment. Despite extensive research, the cause of IBM is still not fully understood, and there are currently no effective treatments or biomarkers available.

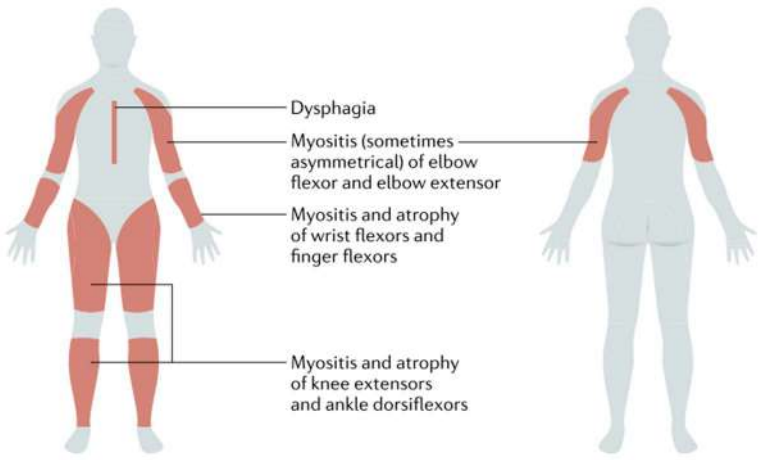

Figure 1. Pattern of muscle involvement in Inclusion body myositis (IBM). The hallmarks of muscle manifestations in IBM are in quadriceps and forearm muscles, leading to muscle weakness. >60% of IBM patients develop dysphagia. (Lundberg, I *et al.* 2021) (5).

The clinical course is typically chronic, with a progression lasting from 5-20 years, although some patients experience periods of stability lasting from 4-12 years (11). Several studies attempted to measure the progression in IBM patients, being the quantitative muscle testing (QMT) and IBM functional rating scale (IBMFRS) the most common indicators. IBMFRS was the first functional scale developed exclusively for IBM, ranging from 0 (disability) to 40 (normal behavior)(12). It correlates well with lower extremity functions. However, most of the former studies focused on lower extremity functions or walking/ambulation as an outcome measure, but insufficient attention was paid to upper extremity functions and related disability. A more recent study has developed a new IBM Patient-Reported Outcome with modified measurements for upper extremity function (13), displaying a better correlation with grip and pinch strength than the IBMFRS (13,14).

Clinically meaningful scales are essential in measuring disease progression and the impact of treatments on slowing disease progression, especially in diseases without conventional laboratory markers of disease activity (12). The lack of validated outcome measures for disease severity is a barrier to therapeutic trials in rare diseases such as IBM.

IBM is also associated with various comorbidities, including peripheral neuropathy (2.7 times more than general population), Sjogren's syndrome (6.2 times more), haematologic malignancy (3.9 times more) and T-cell large granular lymphocytic leukemia (58% of the total IBM patients, only found in IBM population)(8,11). On the contrary, the frequency of neurodegenerative disorders and solid cancers was similar to the control population. Compared to population controls, patients with IBM have lower survival, they die 3 years younger on average (8). The most common causes of death were respiratory failure or pneumonia (44.4%), cancer (14.8%), and old age and medical comorbidities (14.8%) in IBM group (8).

3.2. Diagnosis

The diagnosis is made after clinical observations and muscle histopathology studies. The updated diagnostic features for IBM were included in the classification criteria for adult and juvenile IIM in the 2017 European League Against Rheumatism/ American College of Rheumatology (EULAR/ACR) (15). However, most of the studies published so far still follow the 2011 European Neuromuscular Centre (ENMC) guidelines (8,14,16) (Table 2).

Table 2. The 2011 European Neuromuscular Centre (ENMC) guidelines for IBM diagnosis (Rose MR *et al.,* 2011) (16)

Clinical and laboratory features	Classification	Pathological features
Duration >12 months Age at onset >45 years Knee extension weakness ⩾ hip flexion weakness and/or Finger flexion weakness > shoulder abduction weakness sCK no greater than 15×ULN	Clinico-pathologically defined IBM	All of the following: Endomysial inflammatory infiltrate Rimmed vacuoles Protein accumulation* or 15–18 nm filaments
Duration >12 months Age at onset >45 years Knee extension weakness ⩾ hip flexion weakness and Finger flexion weakness > shoulder abduction weakness sCK no greater than 15×ULN	Clinically defined IBM	One or more, but not all, of: Endomysial inflammatory infiltrate Up-regulation of MHC class I Rimmed vacuoles Protein accumulation* or 15–18 nm filaments
Duration >12 months Age at onset >45 years Knee extension weakness ⩾ hip flexion weakness or Finger flexion weakness > shoulder abduction weakness sCK no greater than 15×ULN	Probable IBM	One or more, but not all, of: Endomysial inflammatory infiltrate Up-regulation of MHC class I Rimmed vacuoles Protein accumulation* or 15–18 nm filaments

*Protein accumulation referred to p62, TDP-43, etc.

Although weakness in quadriceps and finger flexors give a clue about IBM diagnosis, the definitive diagnosis is given after a muscle biopsy, based on inflammatory, degenerative and mitochondrial features in the muscle histopathology (6,17). At inflammatory level, we highlighted the presence of endomysial inflammatory infiltrates invading muscle fibers and triggering an overexpression of major histocompatibility complex I (MHC-I). Rimmed vacuoles formed by aggregation of unfolded proteins comprising transactive response DNA-binding protein 43 (TDP-43), p62, p-Tau, b-amyloid, etc. and insufficient autophagy lead to the deposition of proteins inside muscle fibers.

Mitochondrial alterations are present in cytochrome c oxidase deficient (COX-) fibers (absence of complex IV from the mitochondrial respiratory chain (MRC)), associated with multiple mitochondrial DNA deletions, succinate dehydrogenase positive (SDH+) fibers, and ragged-red fibers (6,17). All these features (Figure 2) might not be present at the time of diagnosis in a single muscle biopsy, what delays IBM diagnosis or leads to misdiagnosis.

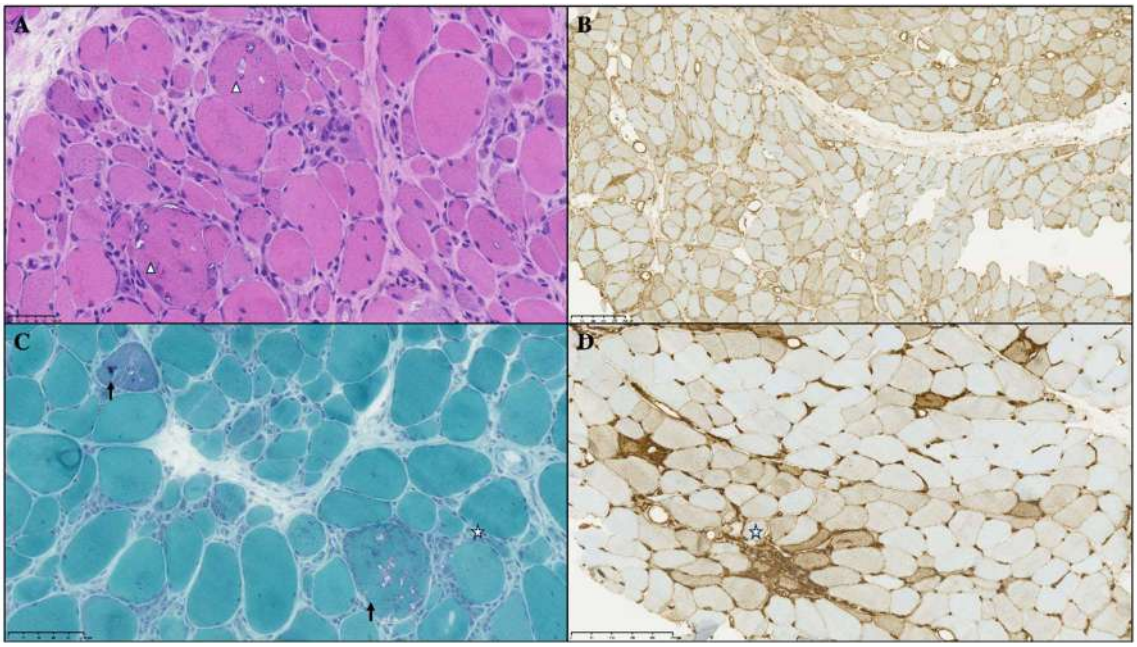

Figure 2. Pathological findings in Inclusion Body Myositis (IBM) muscle histopathology. A) Marked variability in fiber size. Some rimmed vacuoles can be seen (head of arrow). H&E on frozen tissue. B) Universal positivity of the MHC class I antigens. IHQ on frozen tissue. C) Some rimmed vacuoles (arrows) together with endomisial mononuclear cells are present (asterisc). Gomori's TCR on frozen tissue. D) Focal positivity of the MHC class II antigens can clearly be observed. Inflammatory reaction is also present (star) IHQ on frozen tissue. Images at 40X from the Muscle Unit at the Hospital Clinic of Barcelona.

The presence of rimmed vacuoles previously mislead the classification of IBM in the same group as vacuolar myopathies, also called hereditary inclusion body myopathies (10,11). However, these disease group do not display inflammation nor the clinically distinct pattern of IBM, they are monogenic diseases caused by valosin-containing protein (VCP), laminin subunit alpha-2 (LAMA2), glucosamine (UDP-N-Acetyl)-2-Epimerase/N-Acetylmannosamine kinase

(GNE), myosin heavy chain 2 (MYH2), or other genes and their onset is at younger ages (10,11,18).

3.3. Pathogenesis

The trigger of IBM pathogenesis has generated a strong debate, with claims supporting a degenerative vs. an autoimmune disease (10,19–21). Recent studies advocate for an inflammatory origin (7,11,19). In this section we revise the inflammatory, degenerative and mitochondrial features of IBM pathogenesis.

3.3.1. Inflammation

The inflammatory pattern of muscles in IBM is characterized by the infiltration of highly differentiated highly cytotoxic CD8+ T cells in muscle (Figure 2) (22). These cells express CD57+ and KLRG1 receptor and are resistant to apoptosis (23). The inflammatory stimuli that trigger the T cell infiltration is still unknown. After the CD8+ T cell invasion, macrophages, plasma cells and myeloid dendritic cells move to the site of muscle infiltration, increasing the inflammatory state of the muscle in IBM (Figure 3) (7,11). The clonal expansion of immune cells promotes the release of cytotoxic, proinflammatory cytokines and chemokines.

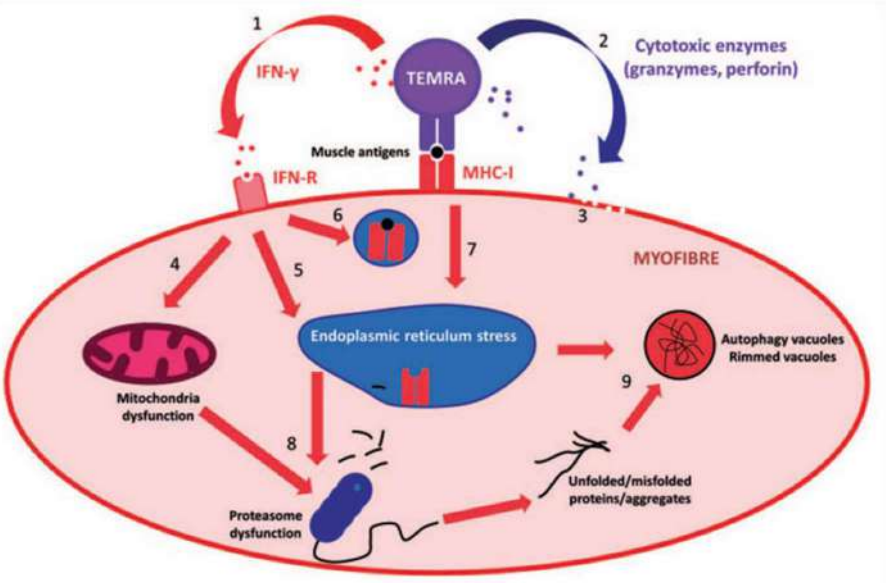

Figure 3. Pathogenesis of Inclusion Body Myositis (IBM) considering an inflammatory origin. Highly differentiated and cytotoxic CD8+ T effector cells (TEMRA) are activated by an unknown trigger and release IFNγ and cytotoxic enzymes that induce myofiber damage. IFNγ triggers mitochondrial dysfunction, endoplasmic reticulum (ER) stress and MHC-I upregulation, the last increasing the ER stress. Mitochondrial dysfunction and ER stress impair proteasome function, endorsing the appearance of misfolded proteins and rimmed vacuoles (degeneration) (Greenberg, 2020) (10).

This autoimmune environment promotes the transformation of CD20+ B cells in the muscle of IBM patients into CD138+ plasma cells, which trigger the production of autoantibodies (7). 60% of IBM patients contain the circulating autoantibody cytosolic 5'-nucleotidase 1A (cN1A), also found in other autoimmune diseases (24,25).

Among the cytokines and chemokines released, the levels of chemokine (C-X-C motif) ligand 9 (CXCL9) and C-C motif chemokine 5 (CCL5) are remarkably increased, as a result of T cell activation and interferon gamma (IFNγ) production (Figure 3) (11,26). The expression of IFNγ-related genes is higher in myofibers invaded by CD8+ T cells. IFNγ also promotes the upregulation of MHC-I in muscle fibers. Moreover, tumor necrosis factor alpha (TNFα) reduces the amount of microRNAs involved in muscle differentiation (miRNA-1, miRNA-133a, miRNA-133b), which are related to both inflammation and degeneration (7).

3.3.2. Degeneration

Abnormal expression of MHC-I in muscle fibers contributes to endoplasmic reticulum (ER) stress (Figure 3). In these conditions, rimmed vacuoles are formed, containing b-amyloid peptides, sarcoplasmic p62, microtubule-associated protein light chain 3 (LC3), VCP and TDP-43, etc. (Figure 3) (8,27). These aggregates accumulate as a result of an overloaded degradation system, ubiquitin-proteasome system and dysfunctional autophagy (28).

Briefly, autophagy is an essential self-eating process that cells perform to allow degradation of old or damaged intracellular components, including soluble proteins, aggregated proteins, organelles, macromolecular complexes, and foreign bodies (29). Autophagy is an evolutionary conserved process and has been

associated with multiple human diseases. In IBM, autophagy is partially impaired and rimmed vacuoles accumulate (28,30).

The accumulation of rimmed vacuoles triggers the activation of the unfolded protein response (UPR)(31). This response promotes the upregulation of chaperones to compensate the unfolded protein deposits and the increase in the transcription of cytokines, MHC-I, etc., endorsing the inflammatory environment.

3.3.3. Mitochondria

Mitochondrial dysfunction in IBM muscles is associated with the presence of ragged-red, COX- and SDH+ fibers (Figure 3), as seen in mitochondrial diseases. Ragged-red fibers increase the number of mitochondria around myofibers to compensate the dysfunctional ones, some of which do not get recycled due to insufficient autophagy and mitophagy (6,17).

Mitochondrial damage increases with the pro-inflammatory cytokine release (IL1β, TNFα) due to the CD8+ T cells infiltration in IBM muscles (Figure 2 and Figure 3)(7). The presence of cytokines increases the levels of the reactive oxygen and nitrogen species (ROS and RNS), incrementing the oxidative stress, and consequently the ER stress (Figure 3). This leads to an increased mitochondrial permeability, potentially opening the mitochondrial membrane pore (MMP) and facilitating an uncontrolled transport of substances across the membrane (7).

The opening of the MMP endorses a dysfunctional MRC, also affected by an accumulation of mtDNA mutations, mtDNA depletion (32) and large mtDNA deletions (30). In COX- fibers we also find a downregulation of MRC complex I (33).

Damaged mitochondria are not properly recycled due to insufficient autophagy and mitophagy (30), contributing to the mitochondrial dysfunction. Consequently, mitochondrial damage and chronic inflammation accelerate muscle fiber atrophy and muscle aging in IBM muscles (7,30).

3.4. Genetic studies in IBM and biomarkers

Although IBM is an idiopathic disease with unknown causal gene, multiple genetic variants have been identified as risk factors that contribute to its pathogenesis. The most strongly associated region with IBM is the human leukocyte antigen (HLA) region, specifically the HLA-DRB103:01 variant, which has independent associations with HLA-DRB101:01 and HLA-DRB113:01 (11). Heterozygotes with the HLA-DRB103:01-HLA-DRB101:01 and HLA-DRB103:01-HLA-DRB1*13:01 genotypes were found in higher frequencies than expected in IBM cases (7,34).

Another genetic variant associated with IBM is a frameshift mutation (rs333) in the C–C chemokine receptor type 5 (CCR5) on chromosome 3 p21.31 (34–36). CCR5 binds pro-inflammatory chemokines, and a non-functional or reduced expression of CCR5 may inhibit T cell migration into muscle fibers (7).

In the mtDNA, an increased prevalence of somatic large mtDNA deletions and duplications associated with a higher heteroplasmy level in IBM muscle were reported. Additionally, there was an increased number of mtDNA mutations and a reduction in mtDNA copy number variations. COX-fibers, which are associated with T-lymphocyte infiltration and muscle fiber atrophy, have larger mtDNA deletions, displaying an accelerated mitochondrial muscle aging (7).

Two genotypes of the apolipoprotein E (APOE) gene, involved in lipid transport, e3/e3 and e4, are associated with IBM. APOE genotype e3/e3 revealed a later disease onset, while the e4 allele was found in higher frequency in males with IBM (7,37). Furthermore, a variant in a very long poly-T repeat allele of the mitochondrial protein translocase of the outer mitochondrial membrane 40 (TOMM40) was associated with a later age of disease onset, particularly in individuals with APOE genotype e3/e3 (4 years of onset delay) (7).

Rare missense variants in the FYVE and coiled-coil domain autophagy adaptor 1 (FYCO1) and in the VCP and sequestosome 1 (SQSTM1) (p62) were also identified in individuals with IBM, supporting the involvement of altered protein

homeostasis and autophagy in IBM pathogenesis. In addition, the prevalence of 47, XXY males and 47, XXX females were particularly high in IBM (7).

Understanding the genetic variants associated with IBM can help identify diagnostic and prognostic biomarkers for the disease. Biomarkers can be identified not only at the DNA level but also at the RNA, protein, or metabolite level. Biomarkers can be used to predict and monitor diseases and their response to treatment, which can make drug discovery and trials easier, as current treatments for IBM lack reliable and monitorable clinical outcome measures (38).

3.5. Treatment strategies and clinical trials

IBM has been shown to be refractory to immunotherapy (5), including immunosuppressive and immunomodulatory treatments (7). One hypothesis is that delayed diagnosis leads to treatment starting at advanced disease stages marked by degeneration, fiber atrophy, and fibrosis, where anti-inflammatory effects may be insufficient (7).

Double-blinded randomized clinical trials in IBM have been limited. Currently, there are 19 clinical trials in IBM in active or recruiting phase (39). We will explain some of them in this section.

Myodegeneration has recently become a target in clinical trials (e.g., arimoclomol, bimagrumab, follistatin, oxandrolone, and rapamycin), consistent with its possible involvement in IBM pathophysiology (40). Arimoclomol is an activator of chaperones, which was supposed to induce protein degradation and reduce the levels of oxidative stress in IBM. However, the trial failed (31). Rapamycin is currently in a phase III clinical trial (NCT04789070). Rapamycin inhibits AMPK, a protein kinase that regulates several intracellular processes, including survival, protein synthesis, and autophagy (5).

Targeting inflammation, a phase 1 trial is directed to suppress T CD8+ KLRG1+ cells, with ABC008 drug, a humanized monoclonal antibody (mAb) specific for KLRG1 (NCT04659031) (7). They are currently recruiting for the phase II/III (39).

The recent innovation in the gene and cell therapies area has also reached IBM treatment approaches. There are 3 clinical trials based on advanced therapy medicinal products (ATMPs) (41).

One trial used follistatin, a myostatin antagonist, and was based on quadriceps injections of follistatin integrated in adeno-associated virus (AAV) vectors. It improved the 6-minute walk distance and increased muscle fiber diameter, while decreasing fibrosis and inflammation in IBM patients (31,42).

To increase muscle fiber, a second approach is based on stem cell injections in the muscle (7). Adipose-derived stem/stromal cells have exhibited immunomodulatory and angiogenic regenerative properties and may help to control muscle inflammation and rebuild damaged muscle in IBM. Thus, their use is being explored in two independent phase I trials (NCT05032131; NCT04975841) (40).

Regardless of the clinical trials ongoing, supportive care, including physical therapy, speech/swallowing therapy, nutritional support, and education on falls prevention, remains the cornerstone of IBM management. Assistive devices may improve functional ability, and botulinum toxin injections, esophageal dilation, or cricopharyngeal myotomy may lead to symptomatic improvement of dysphagia (40). Exercise is currently the only treatment that consistently shows a varied degree of benefit in IBM, although the optimal exercise program has yet to be determined (5).

Patient associations, such as Share4rare (43), Cure IBM (44), and the Myositis association (45), as well as international clinical consortiums like ERN Euro-NMD (46), are strong advocates for new treatment options in IBM.

CHAPTER 2: Disease models

Disease models are animal, cells or computational models, among others, that manifest all or some of the pathological mechanisms observed in a specific human disease. Disease models enable the understanding of the disease onset, evolution and molecular mechanisms and the development of potential therapies to treat them (47,48). In this section, we briefly describe some of the animal and cell models useful for biomedical research.

1. Animal models

Animal models have played a crucial role in advancing biomedical research (49). As humans are the ultimate target audience of medical research, findings from human studies hold greater potential for direct application than those obtained from animal models (50). However, animal models offer several benefits, including reproducibility, controlled environmental conditions, access to relevant tissues, precise phenotyping, the potential for an unlimited number of biological replicates, and the ability to follow up on experimental hypotheses (50). Moreover, mammalian genomes are highly evolutionary conserved. Thus, animal models could be useful as human disease models and as a tool to study disease mechanisms in different tissues and cell types (51) . Nonetheless, animal models also have limitations, such as being limited to a single genetic background in some gene-specific models, failing to replicate complex human diseases, and making it challenging to test certain human disease manifestations (50). In the following sections, we will review both animal and cell models and highlight their contributions to biomedical research (Table 3).

Table 3. Disease models for biomedical research, and specifically, muscle diseases. Among them, there are 2D models like myoblasts and pluripotent stem cells; 3D models like organoids; microfluidic devices as muscle-on-a-chip; mouse and other animal models and computational models. Multiple variables must be considered to choose the model of interest to prove a specific hypothesis (Speciale A, *et al.* 2020)(49)

Models.	Myoblasts	Stem Cells Derived Cultures	Organoids	Muscle-on-a-Chip	Mouse Models	Other Animal Models	Computational Models
Parameter							
Production complexity	Low	Medium, depends on protocol	Medium/High	High, requires engineered chambers	High	High/Medium	Medium/High
On-platform assay	Easy access to readouts, individual cell analyses possible	Medium difficulty, individual cell analyses possible	Medium/High difficulty, analyses possible at the tissue level	Medium/High, organ function analyses possible	Low difficulty, analyses possible both at cellular and tissue levels	Low difficulty, analyses possible both at cellular and tissue levels	Can account for contributions only of known variables
Duration of experiments	Minutes to days	Days to weeks	Days to weeks	Days to weeks, depends on platform design	Weeks to months	Days to weeks	Days
Variability and clinical relevance	Low variability and relevance	High variability and relevance	High variability and relevance	Low variability, high relevance	Low variability, high relevance	Low variability, moderate relevance	Low variability but requires in vivo confirmation
Level of control over variables	High	Medium/Low	Low	High	High/Medium	High/Medium	High
Biodistribution and toxicology studies	Useful for initial toxicology	Useful for initial toxicology	Useful for initial toxicology and limited biodistribution studies	Useful for initial toxicology and limited biodistribution studies	Useful for toxicology, biodistribution and life span assays	Useful for toxicology and life span assays	Useful to predict outcomes
High throughput feasibility	High	Medium/High	Medium/High, depends on tissues	Medium, depends on platform design	Low	High	High
Precision medicine potential	Low, easy to manipulate but homogenous cultures	High, takes into account individual variability	High, depends on tissues and is subject to model validation	High, allows high level of control and personalization	High, depends on model availability	Medium/High, easy to manipulate but low translational relevance	High when used in combination with in vitro/vivo methods

1.1. Mice models

Among animal models in biomedical research, mice have been extensively used for being a cost-effective model, due to their size, handling and control of the environment and inbreeding strains. However, mice are smaller than humans, with a shorter lifespan and 1% of human genes are not present in their genome, especially in non-coding, promoter or splicing regions (49).

To adjust mouse models to recapitulate human diseases, humanization of mice by genetic or engrafting tissue approaches are being developed. Genetic mouse models have allowed to examine the effects of a mutation at a system level (49). Tissue xenografts in mice has allowed the mimicking of a human pathological tissue in a model to study their etiology and progression (52). Moreover, combining mouse strains is appropriate to tackle the risks of a lack of reproducibility in the results (Table 3). Considering genetic, tissue, and strain variability in mouse models are essential to improve the reproducibility of the results in these models to improve the understanding of human diseases and test new therapeutic interventions (49).

In IBM, three murine models have been claimed as "IBM models"(53): the MCK-AβPP model, the VCP-mutant model and the IBM xenograft model (19).

The MCK-AβPP transgenic mouse model consists of the C57BL6/SJL transgenic mouse strain that carries the human amyloid beta precursor protein (AβPP) cDNA transgene, under control of the muscle creatine kinase (MCK) gene promoter, resulting in over-expression of AβPP in skeletal muscle (54). This model failed to produce specific histological features of IBM (53).

The VCP mutant mice, was based on VCP mutations from the genetic disease inclusion body myopathy. It was confused with IBM because of its degenerative features and reported to endorse the arimoclomol use in IBM to tackle protein accumulation and heat shock response (52,53,55). However, this model lacks the inflammatory component crucial to IBM (14,53).

The IBM mouse xenograft model was recently developed with the transplantation of human muscle biopsies from IBM patients into nude mice (52). Xenograft

models derived from patients' samples have been already developed to test cancer and personalized medicine treatments, among others (56). Xenografts have recently been used to study genetic disorders of skeletal muscle, and whole muscle xenografts have been successfully used to model facioscapulohumeral muscular dystrophy (FSHD) and test potential therapies (56). Thus, the aim here was to determine if human muscle xenografts could also be used to model IBM, being an idiopathic, late-onset, inflammatory muscle disease (14).

The IBM xenograft mimic the inflammatory and degenerative hallmarks of IBM, including endomysial inflammation, invasion of myofibers by CD3+ T cells, COX-fibers, and/ MyoKD or rimmed vacuoles. The model was treated with CD3 monoclonal antibodies (OKT3), which significantly eliminated muscle inflammation (depleted T cells) but did not affect the degenerative pathology (52). However, we cannot determine whether inflammatory or degenerative changes are primary in IBM. Remarkably, these xenografts reproduce the genetic and epigenetic background of human diseases, not possible in other animal models, and are postulated as *in vivo* models for understanding disease progression and testing new potential therapies (14).

1.2. Other animal models

Alongside with mice, other animal models like *Drosophila melanogaster*, zebrafish and *Caenorhabditis Elegans (C. elegans)* have been useful in deciphering disease mechanisms (Table 3). Here we highlight some of the contributions of these models to human disease pathology.

The fruit fly, *Drosophila melanogaster*, can be used as a model to study human NMDs due to its neural circuits, multinucleated muscle cells, and neuromuscular junctions, even their complexity is lower than in humans. Genetic mutations in *Drosophila* can help to understand the function of specific proteins at the synapse of the neuromuscular junction and the development of muscular dystrophy over time (49).

Zebrafish (*Danio rerio*) has also become a valuable organism for studying NMDs genetic disorders (57). About 70% of human genes have at least one zebrafish orthologue (58), and mutant zebrafish lines have been created to model common human myopathies. The transparency of zebrafish embryos, external development, and ease of genetic manipulation make it an ideal model for high-throughput drug screening in a whole-organism context. The zebrafish model has also provided insight into the functional aspects of disease pathogenesis for several muscle conditions, including RYR1-related myopathies, which have been linked to oxidative stress through the study of relatively relaxed (ryr) mutants (59).

Lastly, *Caenorhabditis elegans*, a nematode with a fully sequenced genome and 40% of human disease genes having a nematode ortholog, is a valuable model to investigate various human physiological and pathological mechanisms, including Duchenne muscular dystrophy (DMD) (60).

2. Cellular models

2.1. Fibroblasts

Fibroblasts are a cell type involved in the formation of connective tissue, to support and connect other tissues and organs in the body (61). They are essential cells in the homeostatic balance of tissue function (62) by maintaining the structure of tissues through the secretion of collagen proteins. They also participate in wound healing processes.

They are widely used in biomedical research because they are easily grown in lab from a skin punch biopsy in patients, from which genetic and biochemical analysis are performed (61). In addition, fibroblasts can be reprogrammed to become other cell types, through trans-differentiation approaches (e.g., myofibroblasts, expressing MyoD gene (63)) or reprogramming of induced pluripotent stem cells (iPSCs) to obtain pluripotent cells that can be derived to every cell type, like neurons or muscle cells) (64). These approaches allow the study of disease etiology and test potential treatments. Currently, mitochondrial and neurodegenerative diseases are being diagnosed with the use of fibroblasts, including mitochondrial myopathy, encephalopathy, lactic acidosis, and stroke-like episodes (MELAS) and Leigh syndrome (65) among mitochondrial diseases and Alzheimer (AD) and Parkinson disease (PD) among neurodegenerative ones (66). These cells are being validated as a model in other diseases. In the following section, we explain the use of fibroblast as a model for several diseases.

PD, a neurodegenerative disease affecting dopaminergic neurons in the brain, has benefited from the use of fibroblasts, which avoids the need to perform diagnosis and pathological study in the target tissue, in the brain, which is invasive and difficult to access. The fibroblast model for PD was presented in 2012 with their benefits and drawbacks as a model (66). From there onwards, other studies examining the mitochondrial, autophagic and transcriptional alterations of fibroblasts with PD disease have been published (67–69).

Amyotrophic lateral sclerosis (ALS) and frontotemporal dementia (FTD), a motor neuron and a brain disorder disease, respectively, share the most common genetic cause, an intronic hexanucleotide repeat expansion (G4C2) in the C9orf72

gene (70). The impact of this gene in bioenergetics, autophagy, RNA metabolism and mitochondrial dysfunction, among others, has been examined with the use of fibroblasts from C9orf72 patients (70,71).

In addition to neurological disorders, human dermal fibroblasts are being tested in psychiatric disorders, like major depressive disorder (MDD) (72). In this study, they use fibroblasts as a potential model to study the biological mechanisms behind MDD and the antidepressant drug (ADD) response. MDD is the second cause of disability worldwide but the efficacy of ADD treatment is inadequate. Moreover, the etiopathology of MDD and the mechanisms of action of ADD are highly unknown (72).

Fibroblasts have also been involved in identifying the cause of new disorders. This was the case of congenital autophagy deficient ATG7 syndrome (73). In this study, mechanistic experiments in multiple samples including fibroblasts, allowed the detection of a deleterious, recessive variants in human ATG7, a core autophagy-related gene encoding a protein that is essential to autophagy (73). This was a breakthrough, as impaired autophagy is found in a broad range of complex human diseases, but congenital autophagy disorders are rare (73).

Furthermore, fibroblasts were used as a model to measure the impact of external stimuli, like pollutants, cytotoxic agents, mechanical stress, etc. In Park *et al.* (74), they used fibroblasts to test the impact of air pollution on autophagy and skin aging, by analyzing particulate matter in air. In Nadalutti *et al.* (75), they examine the cytotoxic effect of formaldehyde, a biological aldehyde generated inside cells after DNA and protein demethylation, amino acid and one carbon metabolism, and lipid peroxidation. Formaldehyde accumulation is linked to mitochondrial dysfunction and DNA damage. In Weider *et al.* (76), fibroblasts were used as a model to study periodontal stress, including bite force or orthodontic tooth movement.

Alongside to biomedical research, fibroblasts have been effective to understand comparative physiology (77). The comparison of fibroblasts from different species (human, mice, rat, seals, camel, rhinos) displayed relationships between the temperature of the habitat and oxygen consumption of the species and their fibroblasts (77). Although the use of fibroblasts to compare among species might

be a reductionist approach, fibroblasts may display fidelity to whole animal physiological phenotypes, facilitating their study (77).

2.2. Myoblasts derived from iPSCs

The discovery of iPSCs was a breakthrough in biomedical research and specifically, in disease modeling. In 2006, murine adult fibroblasts were successfully reprogrammed by introducing only four transcription factors (Oct3/4, Sox2, c-Myc and Klf4) into the cells using retroviral vectors (Figure 4) (78). The reprogrammed cells, called iPSCs, revealed a pluripotency state found only in embryonic stem cells, as well as similar morphology, cell growth rate, and expression of embryonic stem cells genes.

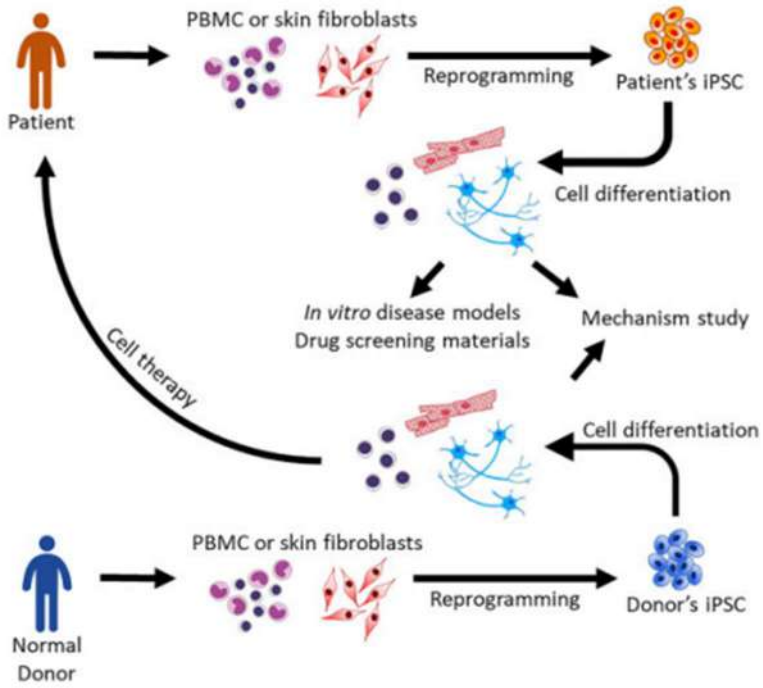

Figure 4. Application of patient-derived induced pluripotent stem cells (iPSCs). Skin fibroblasts or peripheral blood mononuclear cells (PBMCs) from patients can be reprogrammed using Oct3/4, Sox2, c-Myc and Klf4 into iPSCs. iPSCs can differentiate into the cell type of interest in a specific disease, to be used as disease models for understanding their pathophysiology and for drug screening. Moreover, reprogramming skin fibroblasts or PMBCs from healthy individuals into iPSCs allow the potential introduction of healthy cells into the patients, for cell transplantation therapy, currently being tested in clinical trials (Chang C *et al.* 2018) (79)

Only 1 year later, in 2007, human adult fibroblasts were effectively reprogrammed to become pluripotent using the same four factors (Figure 4) (80). Lately, due to the integrative nature of retroviral vectors, there is interest in reprogramming by using non-integrative methods, such as adenovirus, episomal vectors, Sendai virus, synthetic mRNAs and recombinant proteins (81). Besides, distinct types of somatic cells like fibroblasts, urine cells and blood cells have been reprogrammed successfully (49).

The main advantages of iPSCs are that they are an infinite pool of cells who do not enter senescence, as they maintain pluripotency; and they can be obtained from patients' cells and derived to any cell type of interest (Table 3, Figure 4). Different iPSCs models have already been developed for a wide variety of disorders, like neurological diseases, optical atrophies, mitochondriopathies and even psychiatric disorders (64). The possibility to derive iPSCs into every cell type, including the ones with difficult access to the target tissue, like neurons and muscle cells, explains the variety of diseases that applied iPSC to obtain the cell type of the target tissue. However, the efficiency of conversion and differentiation to/from iPSCs is moderately low and heterogeneous, there is a high variability within samples, and they can display morphological and chromosomal aberrations. In addition, complex diseases without a clear genetic background, with low penetrance, late onset or with an unknown affected cellular phenotype, are much more complicated to model using iPSCs technology (64).

The obtaining of myoblasts derived from iPSCs has been accomplished by several methods. The first one is based on the overexpression of myogenic transcription factors in the iPSCs, generally MyoD, Pax3 and Pax7, using integrative vectors such as lentivirus (82). This method is effective, but integrative vectors can trigger genotoxicity. The other alternative is based on the supplementation with defined factors for a myogenic induction in iPSCs, trying to mimic the embryonic development (83). Although it may have a lower efficiency, this approach is safer and allows the use of the differentiated cells for therapeutic applications (64). The differentiation protocols in muscle cells are effective. Indeed, skeletal muscle fibers derived from iPSCs preferentially express myosin heavy-chain isoforms associated with slow and oxidative muscles, but no longer express developmental myosins, thus indicating postnatal composition (84).

One study describing the differentiation of iPSCs to fused myotubes using growth factors in cell culture was performed by Caron *et al.* (85), who described iPSCs-derived skeletal muscle cell model of FSHD. They developed a monolayer system to differentiate iPSCs into mature skeletal muscle cells within 26 days and 3 stages, from iPSCs to myogenic progenitors, then myoblasts and finally myotubes, without cell sorting or genetic manipulation. They validated the approach through gene expression and functional profiles, revealing a different pattern in FSHD vs. control differentiated skeletal muscle cells. Another study by Moretti *et al.* (86), used the same method to differentiate iPSCs to skeletal muscle cells with DMD.

In IBM, the development of iPSCs and further derivation to muscle cells may be a useful approach to obtain the cell type of the target tissue, as muscle biopsy material is limited and myoblasts, explained in the next section, become senescent after limited rounds of division.

2.3. Myoblasts

Myoblasts are obtained from muscle biopsies from humans or animal models. The satellite cells (myogenic progenitors) isolated from the tissue, grow and expand along several rounds of division, until they reach confluence and start to fuse. Human-derived myoblasts have a slower growth rate and flatter morphology than the mice myoblasts, so their contraction rate is weaker in response to electrical stimulation (49). Myoblasts have been extensively used in NMDs (Table 3) and muscular disorders, including IBM (49,87–89). Due to its limited division rounds before reaching senescence, several studies have used immortalized myoblasts to examine disease mechanisms and test potential therapies (49).

One study using human derived myoblasts in IBM was based on the inhibition of the autophagy process *in vitro* to mimic the degenerative changes in IBM, such as vacuolization, reduced activity of lysosomal enzymes, increased Ab42 oligomers and y-secretase activity (89). Then, sodium phenylbutyrate, an active chemical chaperone approved in urea cycle disorders that mimics the function of

molecular chaperones to prevent protein aggregation (90), was applied to the myoblasts. The effects were that lysosomal activity increased, Aβ42 oligomers and γ-secretase activity decreased, and muscle-fiber vacuolization was not observed (89). Phenylbutyrate went into clinical trials in IBM, completed in 2022, but no results were posted yet (90).

Myoblasts have been obtained not only from human patients, but also from animal models. In one study, primary rat myoblast cultures were either transfected with AβPP or exposed to inflammatory cytokines, which led to the formation of cytoplasmic inclusion bodies, a hallmark of IBM, containing AβPP, ubiquitin, and TDP-43 among other proteins (91). MHC-I expression and pro-apoptotic protein caspase-3 were also increased. In these myoblasts, they tested the effect of arimoclomol, before it was used in a clinical trial. The main finding was that using rat myoblast cultures, up-regulation of the heat shock response with arimoclomol reduced key pathological markers of IBM *in vitro* (91).

Another study based on DMD compared the primary myoblasts with iPSC-induced myoblasts at gene expression and functional level (88). They found that myoblasts derived from iPSCs recapitulated the skeletal myogenesis developmental process and the disease hallmarks characteristic of DMD, revealing that both myoblasts' sources were equivalent for disease modeling in DMD (88).

2.4. 3D models: skeletal muscle organoids and muscle-on-a-chip

Cell disease models in 2D cultures are evolving towards 3D systems that could better reflect the cell-to-cell interaction, extracellular matrix exchanges, and 3D tissue architecture (49). Here we explain organoids, organ-on-a-chip and organ constructs among 3D models (Table 3).

An organoid is a self-organized 3D tissue that is typically derived from stem cells (pluripotent, fetal or adult), and which mimics the key functional, structural and biological complexity of an organ (Table 3) (92). Thus, organoids are becoming a

tool to model human development and organogenesis, disease etiology, injury and regeneration. Organoids from brain, retina, kidney, liver, stomach, lung, gut, heart or muscle have been developed so far (93), displaying the potential to model human disease in multiple organs and tissues. The physiological structure of organoids could be useful to test new therapeutic approaches before their clinical translation. However, their scalability and maturity need to improve, as they mostly resemble fetal rather than adult tissue, and their reproducibility and production are limited (Table 3) (49).

Alongside with organoids, organ-on-a-chip are another model being develop to study disease states and biomechanical forces *in vitro* by using 3D printing, microfluidics and microfabrication engineering techniques (Table 3). The critical features of these devices are the 3D structure, the integration of several cell types in the chip, and the presence of biomechanical forces in the device, to reflect tissue physiology. Organ-on-a-chip of brain, gut, heart, kidney, blood-brain barriers and muscle have been developed, among others. For example, myotonic dystrophy type 1 (DM1) (94) have been modeled by skeletal muscle-on-a-chip.

The combination of multiple disease models in 3D was given the name “organ constructs”, complex 3D structures formed by cellular and non-cellular elements that recapitulate the components, architecture, functionality and pathophysiology of *in vivo* organs (95). A broad range of organ constructs are being generated to study development, model disease onset and evolution and generate tissue biobanks for regenerative medicine (95).

CHAPTER 3: Omics technologies, functional studies and their applications

Understanding the pathogenesis of a disease, identifying biomarkers or potential therapeutic targets and treatments are possible after performing experiments and analysis to respond to the hypothesis of interest (49,95).

There are multiple methodologies to test a hypothesis, mainly based on *in silico* vs. *in vivo* or *in vitro* approaches (49). *In silico* approaches are based on computational studies that are able to integrate multiple omics data and identify interactions in a holistic approach (Table 3). *In vitro* and *in vivo* studies are targeted, by performing functional studies with a specific aim (identify a protein, the expression of a particular gene, the activity of an enzyme, etc.)(50). In both approaches, the data is obtained from patients' samples or from animal models.

The integration of omics and functional studies allows to confirm or discard the hypothesis of interest, and eventually validate new disease models, describe the effect of new gene variants, identify therapeutic targets and test effective treatments. In the following section we explain the impact of omics (specifically, gene expression studies) and functional studies, to understand their role in biomedical research.

1. Omics technologies

The field of biomedical research has been transformed by high-throughput technologies, which led to the development of the systems biology field (50). This field integrates different omics data types, such as genomics, epigenomics, transcriptomics, proteomics, and metabolomics, to identify molecular patterns associated with disease (Figure 5) (50). Briefly, we will go through each of them and their main applications:

- Genomics: the aim is to find genetic variants associated with disease, response to treatment and disease progression. For instance, genome-wide association studies (GWAS) is a successful approach to identify thousands of genetic variants, called single-nucleotide polymorphisms (SNP), associated with complex diseases in human populations (Figure 5).

Whole exome-sequencing (WES) allows for the diagnosis of multiple mendelian rare diseases (96,97). Other genetic aberrations like copy number variants (CNV), loss of heterozygosity (LOH), or genomic rearrangements are identified with genomic tools.

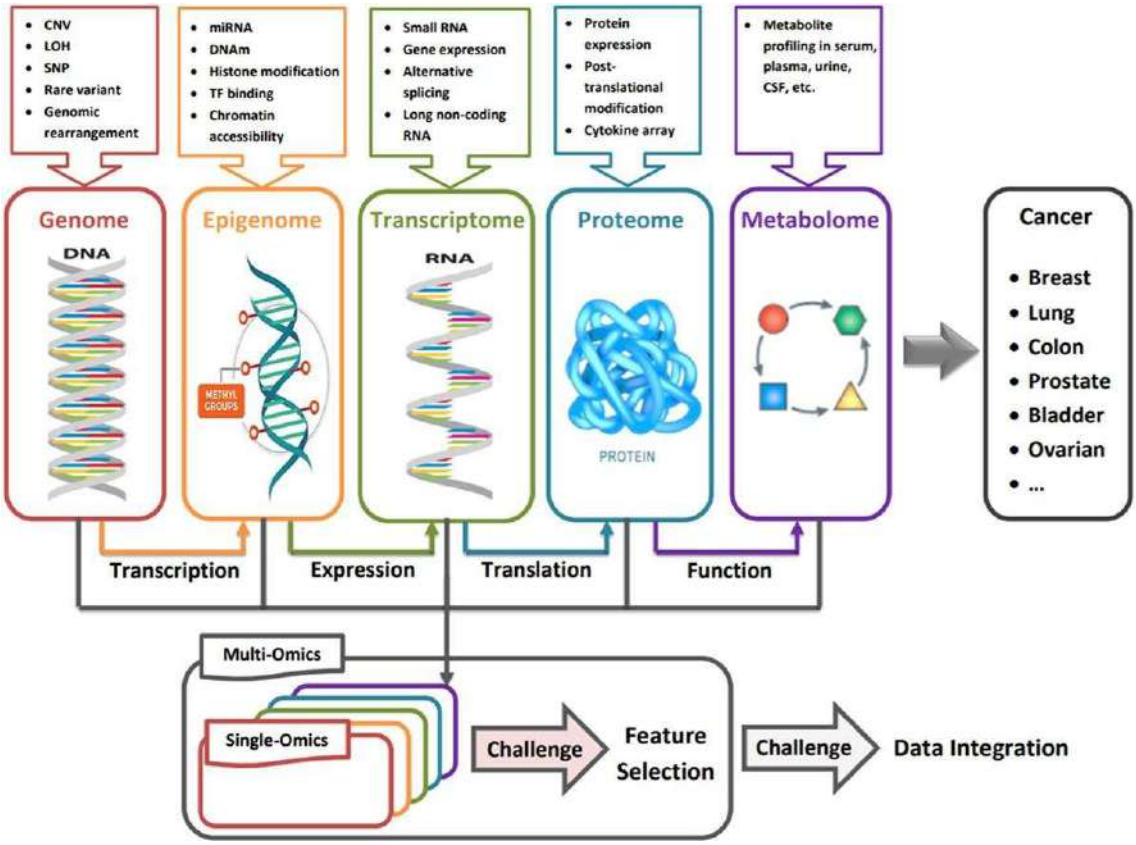

Figure 5. Multiple omics layers and their main targets. Single vs. multi-omics data analysis offer the possibility of identifying alterations at different molecular levels to unravel pathophysiological mechanisms or potential therapeutic targets. However, one of the bottlenecks of multi-omics analysis is the integration of data from different sources. These approaches have been widely applied to cancer research (Momeni, Z *et al.* 2020)(98).

- Epigenomics characterizes reversible modifications of DNA or DNA-associated proteins, such as DNA methylation or histone acetylation, which regulate gene transcription and cell fate, among other functions (Figure 5). These modifications have a genetic and an environmental influence and could be inherited by the offspring (99,100).

- Transcriptomics examines RNA levels genome-wide and sheds light on the protein-coding transcriptome, long non-coding RNAs, short RNAs, and circular RNAs (Figure 5). Dysregulation of these RNAs is associated with multiple diseases and they may be used as potential biomarkers or therapeutic targets (101–103).
- Proteomics quantifies peptide abundance, modification, and interaction (Figure 5). Post-translational modifications in proteins (proteolysis, glycosylation, phosphorylation, nitrosylation, and ubiquitination) are related to their function. Thus, these modifications are involved in intracellular signaling, enzyme activity, protein turnover and transport, and cell homeostasis (104).
- Metabolomics reveals the metabolic function and profile of small molecules like amino acids, fatty acids, carbohydrates, etc. often in fluid samples (Figure 5). An altered pattern of metabolites is usually associated with a disease (105).

Each type of omics data gives information about correlations or association between a common driver, that could be a molecule, process or pathway, between disease and control groups. To find the cause of a disease pattern, we often need the integration of different omics (106). This way we can identify the pathways linked to a disease and target the molecular "key drivers" in them (107). When these "key drivers" are identified, we need to test if they are causal or associated to the disease pattern. Thus, to relate a specific change to a specific phenotype, we need to rely on molecular studies *in vitro* and *in vivo*.

One example of these studies is related to genomics. In genome or exome sequencing, the identification of genetic variants of unknown significance (VUS) are common, as numerous gene variants are unknown in the human genome. VUS are genetic variants potentially causal of a disease but their function is unknown (50,108,109). To prove that a VUS is causal of a disease, there are different approaches at omics and functional level that aid to determine its function. They can be based on patients' samples or disease models. Some assays are based on metabolomics, transcriptomics, protein expression analysis, protein visualization and subcellular localization of molecules, mitochondrial respiratory chain activity, etc.

Sometimes, if we cannot determine the causal effect of a VUS, the omics data can be stored and reanalyzed later when more evidence is provided (50). This is one of the main advantages of omics datasets, their enduring availability. However, omics datasets stored in public repositories require standard terminology and methodology in all aspects of data collection and analysis, appropriate sample size, and control of sample processing and data acquisition to avoid batch effects and technical artifacts that can be confused with biological changes (110–112).

1.1. Transcriptomics studies

Transcriptomics data obtained through RNA seq is used to identify gene expression patterns. In this section, we will discuss examples where RNA seq was used to identify a causal variant of a disease or provide insights into disease pathogenesis.

As mentioned in the previous section, WES and whole genome sequencing (WGS) are applied in the diagnosis of Mendelian diseases. However, their diagnosis rate in rare diseases is comprised between 25-50% (97,113). Cummings *et al.* added RNA seq to the diagnosis pipeline of rare muscle diseases and diagnosed 17 out of 50 patients (97). This was supported by Gonorazky *et al.*, who diagnosed 9 out of 25 cases of monogenetic neuromuscular disorders by RNA seq (113). Both studies emphasized the importance of sequencing the disease target tissue and having a sufficient sample size to obtain robust results (97,113). Interestingly, Gonorazky *et al.* found that transcriptome in transdifferentiated myoblasts obtained from fibroblasts where adequately determining the transcriptomic profile of the target tissue (muscle) while this was not the case of blood transcriptome analysis (113).

The sample of origin is essential in the output of an RNA seq analysis. In one study they examined the expression pattern of the same sample type, fibroblasts, but in different organs, to examine tissue-specific expression by RNA seq (114). This way, gene expression studies are useful for comparing different models or tissues of the same disease, or also, the same sample type from different organs or tissues.

When comparing the expression of genes in different tissues, a valuable source is the Genotype-Tissue Expression (GTEx) database (115). GTEx is a consortium that made possible to study tissue-specific gene expression and regulation in 54 healthy tissues in 1000 healthy individuals.

In the field of IIMs, transcriptomic data alone can be used to identify a muscle biopsy sample from a patient with DM, ASyS, IMNM or IBM with over 90% accuracy (5). Amici *et al.* (116), studied gene expression changes across different myositis subtypes and generated a co-expression network of shared biological processes among IIM and distinctive disease processes. Briefly, upregulated pathways in IIM included muscle regeneration, cytokine-specific profiles, acute phase response and neutrophil degranulation. Focusing on each IIM, the specific pathways involved where: type 1 interferon signaling and titin for dermatomyositis, RNA processing for ASyS and vasculogenesis for IBM. This project shed light into the gene expression regulation in IIMs (14,116).

2. Functional studies

Despite the information given my multi-omics data (Figure 5) and molecular networks, the evidence of molecular alterations requires to be tested in functional studies, to prove they are causal or associated to a specific phenotype (50). There are endless examples of cases in which functional studies were applied to unveil the impact of genetic and molecular changes in a specific phenotype and their contribution to the diagnosis, prognosis and treatment selection (Figure 6). In this section we are going to present 4 cases in which functional studies were applied to prove 4 different hypotheses, sometimes combined with omics analysis (Figure 6). In the first case, the aim was to unveil the function and mechanism of the gene variant GLUD2, associated with early onset of PD (109). In the second case, ATG7 deleterious variants were proven to be the cause of a new disease (73). In the third case, the metabolic and lipid profile aid in stratifying patients of the same disease according to their molecular profile (117). In the fourth case, they validated a new model of disease (118).

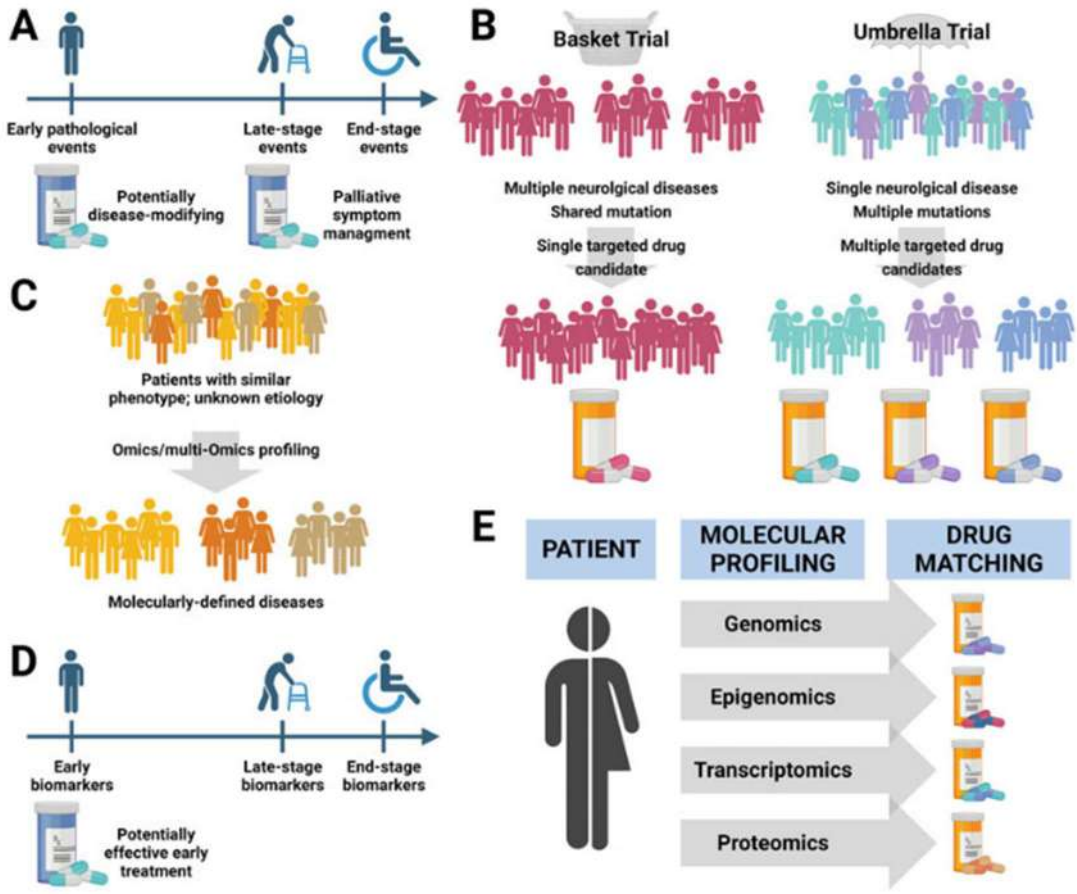

Figure 6. Applications of omics and functional studies to address neurological clinical needs. A) In longitudinal studies, the identification of early pathological changes (prior to symptom onset) to target upstream disease-modifying events rather than downstream palliative care events could aid in stopping or lowering down the disease progression. B) The use of omics profiling to stratify participants for clinical trials of targeted, mechanism-based drug candidates. Basket trials could involve participants with multiple diseases harboring the same actionable mutation, while umbrella trials could involve participants with a single disease harboring multiple actionable mutations. In both cases, participants are profiled and matched to a targeted drug candidate. C) Development of molecular-based diagnostic criteria and treatment selection to stratify patients with a similar phenotype, using omics profiling. D) Identification of biomarkers for early diagnostics and treatment, and for monitoring disease evolution. E) Precision medicine by matching a patient's omics profile with approved drugs. Overall, the aim of molecular and multi-omics profiling of patients is to aid in the diagnosis, disease monitoring and treatments selection for patients (Savelieff, MG *et al.* 2022)(119).

In the first case, GLUD2 is a glutamate dehydrogenase gene located in mitochondria and involved in recycling glutamate during neurotransmission. Specifically, it catalyzes the reversible oxidative deamination of glutamate to alpha-ketoglutarate (120). A rare gain-of-function variant of GLUD2 (T1492G) was associated with early onset in male PD patients; however, the function and underlying mechanism of this variant remained unknown. To unveil them, they generated AAV expressing GLUD2 and its mutant and injected the virus into the brain of untreated mice or 1-methyl-4-phenyl-1,2,3,6-tetrahydropyridine (MPTP)-induced PD mice model (121). In MPTP-induced PD mice, GLUD2 endorses movement deficits and dopaminergic neuron death and reduces glutamate transporters expression and function (109).

Once the function of GLUD2 was determined, GC-Q-TOF/MS-based metabolomics was performed to determine the mechanism of GLUD2 damage. They found that GLUD2 mutation damages mitochondrial function by decreasing SDH activity to impede the tricarboxylic acid cycle (TCA) in the brain of MPTP-induced PD mice (109). Thus, these mice showed a lower energetic metabolism and higher level of apoptosis. This is the mechanism of the variant in GLUD2 that may contribute to the disease onset of PD. This way, the function and mechanism of a genetic variant in GLUD2 was untangled with genetic modification tools, using viral vectors (AAV), mouse models (untreated and MPTP-induced PD mice) and metabolomics (109).

In the second case, they identified five families with ataxia and developmental delay and deleterious, biallelic ATG7 variants who have survived with a severe loss or complete absence of ATG7, an essential autophagy enzyme with unknown paralogue (73). The study revealed the clinical significance of dysfunctional autophagy in humans, responsible of the profound neurologic and developmental impairments of the patients (Figure 6C) (73). The experimental process was the following:

1. Exome sequencing from each family and computer modeling to predict variant pathogenicity.
2. Histochemical, enzyme-linked and immunostaining of skeletal muscle biopsy in one ATG7-deficient patient. Mild myopathic changes were found. ATG7 protein was undetectable in cultured myoblasts from that patient.
3. Cell studies with primary or immortalized patient-derived dermal fibroblasts where autophagy was induced and then blocked at different time-points. To analyze the autophagic flux, immunoblotting, immunofluorescence, long-lived protein degradation and electron microscopy were performed. ATG7 protein was undetectable or severely diminished in all patients.
4. Protein modeling in 3D models of homology between the wild-type and mutated ATG7 built from the crystal structure of the yeast Atg7–Atg3 and Atg7–Atg8 complexes. This was done in yeast because autophagy has been conserved through evolution and the ATG7 protein sequence is maintained across species.

After the mechanistic investigations in multiple models, the disease mechanism of severe loss or absence of ATG7 in human was revealed and is the following: recessive ATG7 variants, decrease ATG7 gene expression and ATG7 protein function is impaired. This decreases the lipidation of LC3 protein and promotes p62 accumulation. Less LC3-II formation diminishes autophagic cargo sequestration and altogether trigger a neurodevelopmental disorder with several symptoms. In this case, they also suggest two therapeutic approaches: one based on AAV for gene therapy that correct the amount of ATG7 loss; and the other

based on small molecules increasing autophagosome formation and degradation (73).

In the third case, the aim was to identify the plasma metabolomics and lipidomics signatures that underlie peripheral neuropathy (PN) in an observational study of individuals with average class 3 obesity (117). They compared obese participants with and without PN, matched for glycemic status, vs. lean non-neuropathic controls. The results revealed that plasma metabolomics and lipidomics differs in obese groups vs. lean group. Inside the obese groups, plasma metabolomics and lipidomics differ in the ones with and without PN, separating the obese group in two (117). Metabolic and complex lipid pathways can differentiate obese individuals with and without PN, independent of glycemic status, making this approach able to stratify patients of the same disease according to their molecular profile (Figure 6B, E) (117).

In the fourth case, they determine whether human skeletal muscle xenografts can be used to model IBM, as mentioned above in the mouse models' section. IBM mice xenografts revealed regeneration of human myofibers coupled with inflammatory and degenerative hallmarks of the disease (118). These hallmarks were endomysial infiltration of CD8+ T cells, MHC-I up-regulation, mitochondrial pathology with COX- fibers, rimmed vacuoles, p62-positive inclusions, nuclear clearance and cytoplasmic aggregation of TDP-43. This way they validated a new model of disease that can recapitulate the complex genetic and epigenetic abnormalities that exist in human disease (118).

HYPOTHESIS

The hypothesis of the project is that new cell models derived from IBM patients will recapitulate the main molecular hallmarks of the target tissue and will contribute to:

1. Validate new disease models for IBM.
2. Acquire knowledge of the etiopathology of the disease.
3. Identify biomarkers for an early diagnose and possible management of IBM.

OBJECTIVES

1. Validate human-derived dermal fibroblasts from inclusion body myositis (IBM) patients as a model for IBM identifying the presence of genetic and functional alterations (inflammatory, degenerative and mitochondrial changes) that recapitulate the features of the target tissue.

2. Validate skeletal muscle cells derived from iPSC obtained from fibroblasts from IBM patients as a model for IBM, identifying the presence of genetic and functional alterations (inflammatory, degenerative and mitochondrial changes) that recapitulate the features of the target tissue.

3. Evaluate the use of cell models derived from IBM patients (fibroblasts) to test the comorbidity of IBM and other age-related diseases (like Alzheimer disease and Diabetes mellitus type 2).

4. Evaluate the use of cell models derived from IBM patients (fibroblasts) to identify biomarkers through a multi-omics analysis.

RESULTS

MANUSCRIPT I:

Title: *Unravelling inclusion body myositis using a patient-derived fibroblast model*

Authors: Judith Cantó-Santos, Laura Valls-Roca, Ester Tobías, Francesc Josep García-García, Mariona Guitart-Mampel, Anna Esteve-Codina, Beatriz Martín-Mur, Mercedes Casado, Rafael Artuch, Estel Solsona-Vilarrasa, José Carlos Fernandez-Checa, Carmen García-Ruiz, Carles Rentero, Carlos Enrich, Pedro J. Moreno-Lozano, José César Milisenda, Francesc Cardellach, Josep M. Grau-Junyent, Glòria Garrabou.

Journal: Journal of Cachexia, Sarcopenia and Muscle. 2023; doi:10.1002/jcsm.13178.

IF: 8.9

ORIGINAL ARTICLE

Journal of Cachexia, Sarcopenia and Muscle (2023)
Published online in Wiley Online Library (wileyonlinelibrary.com) **DOI:** 10.1002/jcsm.13178

Unravelling inclusion body myositis using a patient-derived fibroblast model

Judith Cantó-Santos[1,2,3], Laura Valls-Roca[1,2,3], Ester Tobías[1,2,3], Francesc Josep García-García[1,2,3], Mariona Guitart-Mampel[1,2,3], Anna Esteve-Codina[4,5], Beatriz Martín-Mur[4], Mercedes Casado[3,6], Rafael Artuch[3,6], Estel Solsona-Vilarrasa[7,8], José Carlos Fernandez-Checa[7,8], Carmen García-Ruiz[7,8], Carles Rentero[9], Carlos Enrich[9], Pedro J. Moreno-Lozano[1,2,3], José César Milisenda[1,2,3], Francesc Cardellach[1,2,3], Josep M. Grau-Junyent[1,2,3]* & Glòria Garrabou[1,2,3]*

[1]*Muscle Research and Mitochondrial Function Lab, Centre de Recerca Biomèdica CELLEX - Institut d'Investigacions Biomèdiques August Pi i Sunyer (IDIBAPS) and Faculty of Medicine and Health Sciences, University of Barcelona, Barcelona, Spain;* [2]*Department of Internal Medicine, Hospital Clinic of Barcelona, Barcelona, Spain;* [3]*CIBERER—Spanish Biomedical Research Centre in Rare Diseases, Madrid, Spain;* [4]*CNAG-CRG, Centre for Genomic Regulation, Barcelona Institute of Science and Technology, Barcelona, Spain;* [5]*Universitat Pompeu Fabra (UPF), Barcelona, Spain;* [6]*Department of Clinical Biochemistry, Institut de Recerca Sant Joan de Déu; Esplugues de Llobregat, Barcelona, Spain;* [7]*Department of Cell Death and Proliferation, Institute of Biomedical Research of Barcelona (IIBB-CSIC), Liver Unit-HCB-IDIBAPS, Barcelona, Spain;* [8]*CIBEREHD-Spanish Biomedical Research Centre in Hepatic and Digestive Diseases, Madrid, Spain;* [9]*Department of Biomedicine, Cell Biology Unit, CELLEX-IDIBAPS, Faculty of Medicine and Health Sciences, University of Barcelona, Barcelona, Spain*

Abstract

Background Inclusion body myositis (IBM) is an inflammatory myopathy clinically characterized by proximal and distal muscle weakness, with inflammatory infiltrates, rimmed vacuoles and mitochondrial changes in muscle histopathology. There is scarce knowledge on IBM aetiology, and non-established biomarkers or effective treatments are available, partly due to the lack of validated disease models.

Methods We have performed transcriptomics and functional validation of IBM muscle pathological hallmarks in fibroblasts from IBM patients ($n = 14$) and healthy controls ($n = 12$), paired by age and sex. The results comprise an mRNA-seq, together with functional inflammatory, autophagy, mitochondrial and metabolic changes between patients and controls.

Results Gene expression profile of IBM vs control fibroblasts revealed 778 differentially expressed genes (P-value adj < 0.05) related to inflammation, mitochondria, cell cycle regulation and metabolism. Functionally, an increased inflammatory profile was observed in IBM fibroblasts with higher supernatant cytokine secretion (three-fold increase). Autophagy was reduced considering basal protein mediators (18.4% reduced), time-course autophagosome formation (LC3BII 39% reduced, P-value < 0.05), and autophagosome microscopic evaluation. Mitochondria displayed reduced genetic content (by 33.9%, P-value < 0.05) and function (30.2%-decrease in respiration, 45.6%-decline in enzymatic activity (P-value < 0.001), 14.3%-higher oxidative stress, 135.2%-increased antioxidant defence (P-value < 0.05), 11.6%-reduced mitochondrial membrane potential (P-value < 0.05) and 42.8%-reduced mitochondrial elongation (P-value < 0.05)). In accordance, at the metabolite level, organic acid showed a 1.8-fold change increase, with conserved amino acid profile. Correlating to disease evolution, oxidative stress and inflammation emerge as potential markers of prognosis.

Conclusions These findings confirm the presence of molecular disturbances in peripheral tissues from IBM patients and prompt patients' derived fibroblasts as a promising disease model, which may eventually be exported to other neuromuscular disorders. We additionally identify new molecular players in IBM associated with disease progression, setting the path to deepen in disease aetiology, in the identification of novel biomarkers or in the standardization of biomimetic platforms to assay new therapeutic strategies for preclinical studies.

Keywords Inclusion body myositis; Myopathy; Fibroblasts; Autophagy; Inflammation; Mitochondria

Received: 11 May 2022; Revised: 24 November 2022; Accepted: 2 January 2023
**Correspondence to: Josep M. Grau-Junyent and Glòria Garrabou, Muscle Research and Mitochondrial Function Lab CELLEX-IDIBAPS, Faculty of Medicine and Health Sciences, University of Barcelona, Internal Medicine Service, Hospital Clinic of Barcelona, 08036 Barcelona, Spain. Email: jmgrau@clinic.cat; garrabou@clinic.cat*
Josep M. Grau-Junyent and Glòria Garrabou are last signatory.

Introduction

Inclusion body myositis (IBM) is an inflammatory myopathy characterized by proximal and distal muscle weakness, inflammation, rimmed vacuoles and mitochondrial alterations in myofibres.[1] This rare disease (OMIM 147421) is the most common acquired muscle disease in patients over 50 years old.[2] Its prevalence ranges from 46 to 84 patients per million,[3,4] raising due to the aging of the population. The time from symptoms onset to diagnosis is delayed (around 4–5 years) with a high level of misdiagnosis, due to a lack of specialized diagnostic teams and non-invasive biomarkers. Despite the progression towards disability being slow, effective treatments are absent, leading to an unmet medical need.[1]

Scarce knowledge has been gathered about IBM aetiology. First characterized in 1978, it is currently categorized as an inflammatory myopathy (or myositis), together with polymyositis, dermatomyositis, immune-mediated necrotizing myopathy and non-specific myositis.[1] However, IBM was considered the sporadic form (sIBM) of inherited vacuolar myopathies (hIBM, caused by mutations in around 12 genes, mainly *VCP*), because both shared the presence of rimmed vacuoles. Inflammation is not present in vacuolar myopathies,[5,6] whereas it is prominent in IBM. This prompted the classification of IBM among inflammatory myopathies[2,5] and, currently, sIBM nomenclature is being moved to IBM.

The first symptoms appear in quadriceps and finger flexor muscles, leading to difficulties for climbing stairs and handling objects. In 60% of the cases, there is dysphagia and swallowing dysfunctions. The diagnosis is based on clinical and muscle histology studies, where inflammatory infiltrate, rimmed vacuoles and mitochondrial abnormalities must be present. Briefly, muscle biopsies show: (i) inflammation (CD8+ T cells, aberrant expression of MHC1 and endomysial mononuclear cell infiltrates in myofibres); (ii) degeneration (rimmed vacuoles, ubiquitin-positive inclusions and amyloid deposits) and (iii) mitochondrial abnormalities (cytochrome c oxidase negative fibres (COX-), succinate dehydrogenase positive cells (SDH+) and ragged-red fibres (RRF), corresponding to an increased number of abnormal mitochondria around myofibres).[1,2,6]

Currently, there is no treatment for IBM. Although being an inflammatory myopathy, corticosteroids have failed, and all trials with immunosuppressants, immunomodulating agents, TGFβ inhibitors and muscle growth factors have been ineffective. Intravenous immunoglobulin treatment has been useful to treat dysphagia, despite this, IBM patients are limited to physical therapy (with difficulties for some patients) and participation in clinical trials.[7]

Validated disease models for IBM could help to gain insight into the pathophysiology of this condition, improve diagnosis and test effective treatments. However, previous attempts to develop animal models (*MCK-βAPP* transgenic mice,[8] *VCP* mutant mice models,[9] and a cholesterol rabbit model[10]) revealed serious limitations, probably because they were mainly based on gene editing, and IBM is an acquired disease with poor (or merely unknown) genetic base. Consequently, most of the advances in IBM have been accomplished directly with samples from affected patients.[5] Previous studies from our group revealed some pathological muscle features in IBM lymphocytes[11] or alternative peripheral tissues,[12] suggesting that IBM hallmarks could be present besides the target tissue (muscle). Considering fibroblasts are proliferative cells, used to diagnose mitochondrial diseases and to model neurodegenerative diseases,[13–15] we tested their usefulness as a potential model to study IBM. Fibroblasts preserve genetic, epigenetic and environmental cues of affected patients, offering a low-cost maintaining platform to deepen in disease aetiology, discover novel biomarkers and assay new therapeutic strategies for preclinical studies.

In this article, we aim to report a detailed phenotyping of fibroblasts from IBM patients compared with age and sex-paired healthy controls (CTL), as a promising model for this disease. We offer the transcriptomic and functional assessment of this cell model together with the clinical and pathological data of included patients. Briefly, fibroblasts from IBM patients showed a clear deregulated transcriptomic pattern of 778 differentially expressed genes (DEGs) and a pathological inflammatory, degenerative and mitochondrial profile, resembling the target tissue of the disease. Additionally, the present findings prompt distinct molecular targets as relevant key players in IBM.

Methods

Study design and population

A case–control study was conducted in the Department of Internal Medicine from Hospital Clínic of Barcelona (Barcelona, Spain), including 14 patients and 12 healthy volunteers. IBM patients and healthy volunteers signed the informed consent (ethical code HCB/2015/0562). Additional information is provided in the Supporting Information.

Fibroblast culture

Fibroblasts were obtained from a skin biopsy from cases and controls. Cells were harvested and collected at 80% of confluence, and phenotyped at passages 3 to 10. Briefly, fibroblasts from both groups displayed similar morphology and size. Cell growth rate was slightly reduced in IBM fibroblasts (0.019 ± 0.002 vs. 0.024 ± 0.006), although non-significantly. Additional information is provided in the Supporting Information.

DOI: 10.1002/jcsm.13178

RNA extraction, mRNA library preparation and sequencing

Total RNA was isolated from cell lysates of three IBM and three CTL fibroblasts. Differential expression analysis was performed with DESeq2 v1.26.0 R package, and genes were considered differentially expressed with an adjusted *P*-value < 0.05 and absolute fold change $|FC| > 1.5$. A detailed description of mRNA libraries, sequencing and analysis is presented in the Supporting Information.

Inflammation: Bio-Plex assay of secreted inflammatory cytokines

A Bio-plex assay (Bio-Plex Pro™ Human Cytokine 27-plex Assay #M500KCAF0Y) from Bio-Rad (Hercules, CA, USA) was performed to quantify 27 inflammatory cytokines secreted in the supernatant of IBM and CTL fibroblasts after 96 h in culture (undiluted samples) normalized by cell number.

Autophagy protein array

Cell lysates were obtained from IBM and CTL fibroblasts; 250–500 μg of protein per sample were loaded in the Ray Bio® C Series Human Autophagy Array 1 (Cat#: AAHATG-1-8, Ray Biotech, Inc., Atlanta, GA, USA), incubated overnight at 4°C and detected by chemiluminescence. Additional information is provided in Supporting Information.

Autophagy time-course

Autophagy flux in IBM versus CTL fibroblasts was measured in a time-course in basal conditions (0 h), and 4 h and 8 h after the addition of 0.1 μM bafilomycin A1 from *Streptomyces griseus* (Sigma-Aldrich® #B1793 SIGMA, Missouri, USA), and analysed through western blot analysis. Blots were probed against the anti- SQSTM1/p62 (Abcam #ab56416, Cambridge, UK) and anti-LC3B (Cell Signaling #2775S, Massachusetts, USA) antibodies. More information provided in the Supporting Information.

Immunocytochemistry for autophagosome characterization

Cells were seeded in a 16-well glass slide (Nunc™ #178599 Lab-Tek® Chamber Slide™, Austin, USA) at 37°C with 5% CO_2 for 24 h. Autophagosomes were stained with anti-LC3 pAB (MBL International® #PM036, Massachusetts, USA) and images were taken with a Zeiss LSM confocal microscope (63×). A detailed protocol is presented in the Supporting Information.

Mitochondrial respiration

Mitochondrial respiration was measured according to the oxygen consumption of the mitochondrial respiratory chain (MRC). The oxygen consumption rate was detected with the XF Cell Mito Stress Test™ (Seahorse-XF^{e}24-Analyser, Agilent Technologies), according to the manufacturer's protocol. Additional information is found in the Supporting Information.

MRC enzymatic activities: COX and citrate synthase (CS) activities

COX and CS enzymatic activities were assessed in 40 μg of total protein from each fibroblast sample according to standardized protocols,[15] at 37°C, and expressed as COX/CS ratio.

Oxidative stress

Oxidative stress was measured through lipid peroxidation (measuring malondialdehyde (MDA) and 4-hydroxyalkenal (HAE)) and total antioxidant capacity of the cell (TAC).[11] Reagents and protocols are provided in the Supporting Information.

Mitochondrial membrane potential

Mitochondrial membrane potential (MMP) was quantified with tetramethyl rhodamine methyl ester (TMRM) and detected with confocal microscopy, as the number of cells with active mitochondria per total number of cells.

mtDNA genome content

mtDNA content was evaluated with the fragments of the mitochondrially encoded 12S rRNA gene and the nuclear-encoded RNase-P gene, amplified by RT-PCR (Applied Biosystems). The relative mtDNA content was expressed as the ratio mtDNA 12S rRNA:nDNA RNase-P.

Mitochondrial elongation

Mitochondrial network was immunostained with TOMM20 (St Cruz Bio #sc-11415 (1:100)), imaged with a Zeiss confocal microscope (63×) and analysed with ImageJ software using a mitochondrial morphology macro to quantify mitochondrial elongation (also called aspect ratio: AR = major axis/minor axis, where a higher AR is linked to healthier mitochondria.[16]

DOI: 10.1002/jcsm.13178

Transmission electron microscopy (TEM)

Fibroblasts were fixed and incubated with 1% OsO_4 before being sectioned using Leica ultramicrotome (Leica Microsystems). Ultrathin sections (50–70 nm) were stained and observed using a TEM, JEOL JEM-1010 fitted with a Gatan Orius SC1000 (model 832) digital camera[17] to seek for abnormal organelle structures. Detailed information is presented in the Supporting Information.

Metabolite quantification

Organic acids were extracted in fibroblasts as previously reported.[18] The trimethylsilyl derivatives obtained were separated by gas chromatography (Agilent 7890A, Wilmington, DE, USA) and detected in a mass spectrometer (Agilent 5975C, Wilmington, DE, USA). Amino acids were quantified in fibroblasts by ultra-performance liquid chromatography coupled to tandem mass spectrometry, as previously reported.[19] Both measurements were normalized by protein content. Additional information is detailed in the Supporting Information.

Statistical analysis

Statistical analysis was performed with the Statistical Package for the Social Sciences software, version 25 (IBM SPSS Statistics; SPSS Inc) and GraphPad Prism 8 (GraphPad Software, San Diego, CA, USA). Results were expressed as mean ± SEM or in fold change between conditions, calculated as mean fold change ratio (and deviation) in IBM patients versus CTL fibroblasts, normalized by cell number or by protein content. Obtained data were compared between independent experiments using the non-parametric Mann–Whitney *U* test or Kruskal–Walli's test. Statistically significant results (P-value < 0.05) were highlighted along the manuscript. Additionally, borderline significant results were included according to their biological relevance for better understanding of the biological context.

Results

Clinical and epidemiological data

In this study, IBM patients belonged to Caucasian population between 40 and 83 years old (mean age 66.9 ± 3.6) following a 1:1.7 male to female ratio (n = 14). Control subjects also belonged to the Caucasian population (n = 12), from 35 to 86 years old (mean age 57.4 ± 4.6), following a 1:2.5 male to female ratio. According to the IBM functional rating scale (IBMFRS; ranges from 0 (inability)-40 (normal behaviour)[20]), the IBM cohort scored 25.1 ± 2.1, indicating moderate clinical severity. The average time from symptoms onset to diagnosis was 37 months; six patients showed stable IBM prognosis and eight of them had a progressive disease decline. This overview of clinical data is summarized in Table 1, together with patients' muscle biopsy features that aid in IBM diagnosis.

Transcriptomic phenotyping: Altered gene expression in IBM fibroblasts

RNA sequencing was performed in fibroblasts from IBM patients (n = 3) and genetically unrelated healthy subjects (n = 3). A principal component analysis (PCA) revealed IBM and healthy subjects clustered separately (*Figure* 1A), suggesting a differential gene expression pattern of disease, comprising 778 DEGs with P-value adj (FDR) < 0.05; of them, 457 were downregulated and 321 upregulated (*Table* S1). The top 50 DEGs are represented in the heatmap (*Figure* 1B). Among these DEGs, some are related to inflammation (MHC components like *CD59*; T-cell expansion genes like *CLEC2A*, *CLEC2B*, and *CLEC3B*, and others like *CSCS* and *TNFAIP6*); mitochondria (*PCK2*, *MTHFD2*, *GPAT2*, *ATP2B4*, and *CYP2U1*); and other processes like cell cycle regulation, metabolism of amino acids and derivatives, and so on. Gene names are found in *Table* S1.

These DEGs were clustered with a Gene Ontology enrichment analysis, where the most deregulated clusters were related to *cell communication*, *cell signalling* and *systems development*. Gene set enrichment analysis (GSEA) revealed 358 significantly altered pathways (P-value < 0.05), the top ones found in *Figure* 1C.

In addition to GSEA, DEGs were analysed using Ingenuity Pathway Analysis (IPA) software. IPA showed *tRNA charging* as the top canonical pathway, top networks related to *cell cycle*, *DNA replication*, *cell-to-cell* signalling, and *interaction*, similar to GSEA results, confirming the consistency of reported findings. Overall, these findings point out a clear deregulated transcriptomic profile in IBM fibroblasts and highlight significant pathways and molecular targets in IBM.

Functional phenotyping

Increased inflammatory profile in IBM fibroblasts

Inflammation is one of the hallmarks of IBM in muscle. To explore inflammation in IBM versus CTL fibroblasts, we performed an mRNA-seq and measured secreted cytokines in cell supernatants.

In the transcriptome, we found a differential inflammatory profile in IBM versus CTL fibroblasts. Briefly, we found 62

Table 1 Clinical data of the cohorts and features from IBM patients muscle's biopsies

Sample code (IBM)	Sex	Age	Time to symptoms diagnosis (months)	IBMFRS	Evolution	Rimmed vacuoles	Inflammation	MHC1	Auto Ab	CD57	Mitochondrial Changes
IBM01	F	67	26	16	Stability	+	+	NA	All −	Normal	No
IBM02	M	51	48	16	Progression	++	++	NA	All −	Increase	No
IBM03	M	48	48	31	Stability	+	+	NA	All −	NA	Yes
IBM04	F	81	26	17	Progression	+++	+	NA	All −	Normal	Yes+
IBM05	M	63	36	27	Progression	+	+++	Universal	All −	NA	Yes +
IBM06	M	77	48	28	Progression	+	+	Neg	All −	Increase	Yes
IBM07	F	61	36	23	Progression	+++	+++	Universal	All −	NA	Yes
IBM08	F	83	12	8	Progression	+	+++	NA	All −	T clonal	Yes +
IBM09	M	62	84	30	Progression	+++	++	Universal	All −	Increase	Yes
IBM10	M	78	12	28	Progression	+++	+++	+ Not universal	All −	NA	No
IBM11	F	80	24	33	Stability	+++	+	Universal	Ro +	Normal	Yes +
IBM12	M	71	36	30	Stability	+++	+++	Universal	Ro52 +	Increase	Yes
IBM13	M	75	72	32	Stability	+	++	Universal	All −	Reduced B normal CD57	Yes
IBM14	M	40	3	33	Stability	+++	++	Universal	All −	NA	Yes+
Sample code (CTL)	CTL01	CTL02	CTL03	CTL04	CTL05	CTL06	CTL07	CTL08	CTL09	CTL10	CTL11 CTL12
Sex	M	F	F	F	F	F	M	F	F	M	M M
Age	69	66	61	41	48	47	35	45	82	86	57 52

Summary	Fibroblasts (*n*)	Male/female ratio	Mean age (years)	Time to diagnose (months)	IBMFRS
IBM	14	0.6	66.9 ± 3.6	37	25.1 ± 2.1/40
CTL	12	0.4	57.4 ± 4.6		

Note: Data presented as mean ± SEM.
Abbreviations: Sex: F, female; M, male; IBMFRS, Inclusion Body Myositis Functional Rating Scale (from 0 to 40 points).[20] Rimmed vacuoles: from 0 to +++; Inflammation: from 0 to +++; MHC1: Major Histocompatibility Complex: Universal; NA: not available; + not universal: splattered pattern; Auto Ab: Autoantibodies: Myositis specific and associated auto antibodies include: Anti-Jo-1, anti-SRP, anti-Mi2, anti-TIF1gamma, anti-MDA5, anti-SAE, anti-NXP2 and anti-HMGCR (specific) and anti-PM/Scl, anti-Ro, anti-La, and anti-U1RNP (associated); Mitochondrial changes: Yes or No. Yes: RRF and/or COX neg. Yes + (strong alterations). No: no changes; Age and gender-paired distribution between cohorts (P = NS).

inflammatory-related genes (*Table* S2) related to MHC1, cytokines and IL receptors, NF-kB pathway, IFN genes and T-cell expansion genes, which were grouped in gene clusters (*Figure* 2A), all involved in IBM pathogenesis.

Considering cytokine secretion in fibroblast supernatants, we quantified 21 pro-inflammatory cytokines, grouped in chemokines (eotaxin, IP10, MCP1, MIP1a, MIP1b, RANTES, and IL8) and proinflammatory cytokines (GCSF, TNFa, GMCSF, IL7, IL4, IL13, IL17, IL1b, IL9, FGFb, IL1ra, IFNg, IL6, and VEGF). Cytokines drifted towards an upregulated three-fold expression in IBM patients (*Figure* 2B and *Table* S3). In particular, eotaxin (*CCL11*), involved in a chemotactic activity for eosinophils,[21] showed a statistically significant increase of 4.2 times in IBM versus CTL fibroblasts (P-value < 0.05, n = 13 IBM vs. 12 CTL), whereas GCSF (that regulate the production, differentiation, and function of granulocytes) showed a high 13.3-fold change ratio between groups (*Figure* 2B). These findings revealed a trend towards an increased inflammation in IBM fibroblasts at a transcriptomic and functional level, identifying relevant pathways and targets in this pathology.

Degenerative features and impaired autophagy in IBM fibroblasts

Rimmed vacuoles are another hallmark in the muscle of IBM patients, partly due to misfolded protein depots in the cytoplasm of muscle cells, caused by impaired or insufficient autophagy. Here, we examined autophagy in IBM versus CTL fibroblasts by mRNA-seq data and analysing target proteins at basal and time-course manners.

In the gene expression analysis, we found 37 DEGs related to autophagy (*Table* S2) affecting many steps of the signalling cascade (heat-shock proteins, stress-related factors, proteasome genes and regulators of the master *AMPK* gene), which were grouped in degenerative gene clusters (*Figure* 3A).

In the functional autophagy analysis, we assessed expression of 20 proteins at steady-state levels in IBM and CTL fibroblasts. The expression of autophagic proteins was 18.4% reduced in IBM (*Table* S4 and *Figure* 3B), leading towards a downregulation of the whole autophagic process. In particular, the following pathways were more affected[22]: *Receptor-mediated mitophagy* (ATG5, ATG12, LC3A, and LC3B),

DOI: 10.1002/jcsm.13178

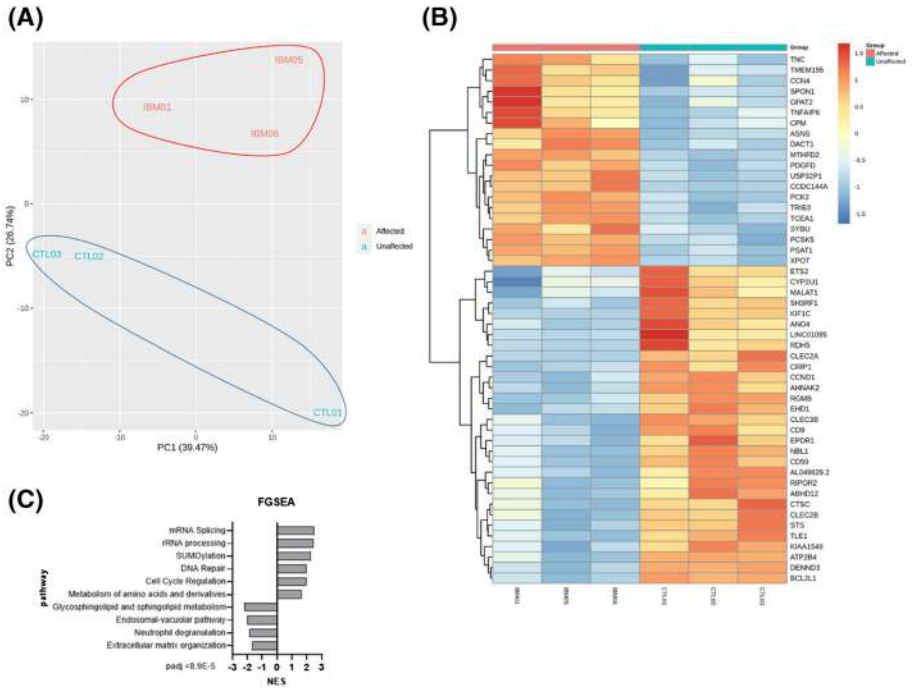

Figure 1 Transcriptome analysis of IBM and CTL fibroblasts (n = 3/group). (A) Principal component analysis (PCA) of affected (IBM) versus unaffected (CTL) subjects. (B) Heatmap of the top 50 differentially expressed genes (DEGs) obtained in a differential expression analysis between both cohorts. All DEGs are represented in *Table* S1. (C) Top pathways (with lowest *P*-value adj) after a functional gene set enrichment analysis (GSEA) and considering their normalized enrichment score (NES). PCA, heatmap and pathway analysis revealed a differential gene expression pattern in IBM patients, with DEGs and pathways related to inflammation, mitochondria and other processes like cell cycle regulation and metabolism of amino acids and derivatives.

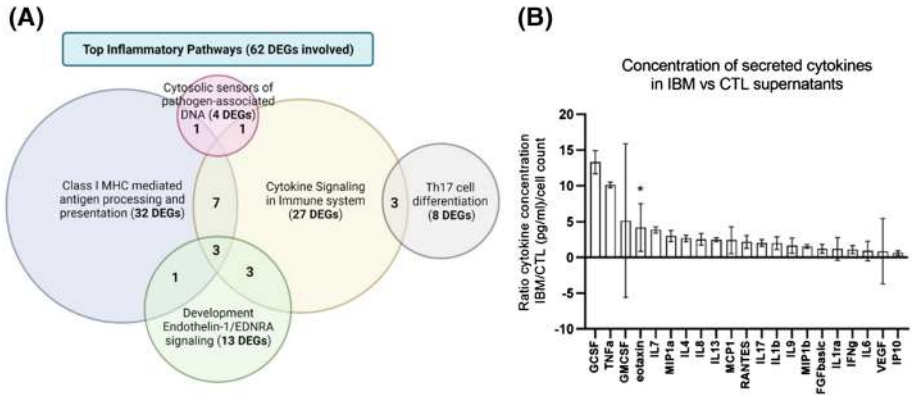

Figure 2 The inflammatory pattern of IBM and CTL fibroblasts. (A) Venn's diagram of the most affected inflammatory clusters and the number of differentially expressed genes (DEGs) involved. Some DEGs are involved in more than one cluster. The list of inflammatory DEGs is represented in *Table* S2. (B) Mean fold change ratio (and deviation) of secreted cytokines in IBM patients versus CTL fibroblasts, normalized by cell number (n = 13 IBM vs. 12 CTL; **P*-value < 0.05, Mann–Whitney *U* test) (ratio > 1: Higher concentration in IBM). The concentration of each cytokine and their full names are represented in *Table* S3. Briefly, an increased inflammatory profile is observed in IBM versus CTL fibroblasts, with differentially expressed genes (DEGs) related to MHC1, cytokines, interleukins, and so on and higher cytokine secretion in fibroblast supernatants.

PINK1-PRKN Mediated Mitophagy (ATG12, P62, LC3A, LC3B, and ATG5) and the super pathway *Macroautophagy* (ATG12, ATG7, Rheb, ATG4A, ATG13, Beclin, P62, GABARAP, LC3B, ATG5, ATG10, LC3A, ATG3, and ATG4B) that displayed a trend of 22.0%, 21.6%, and 17.5% reduction in IBM fibroblasts.

To evaluate if a decreased autophagic activity was due to the inactivation of the process or, to higher consumption of

DOI: 10.1002/jcsm.13178

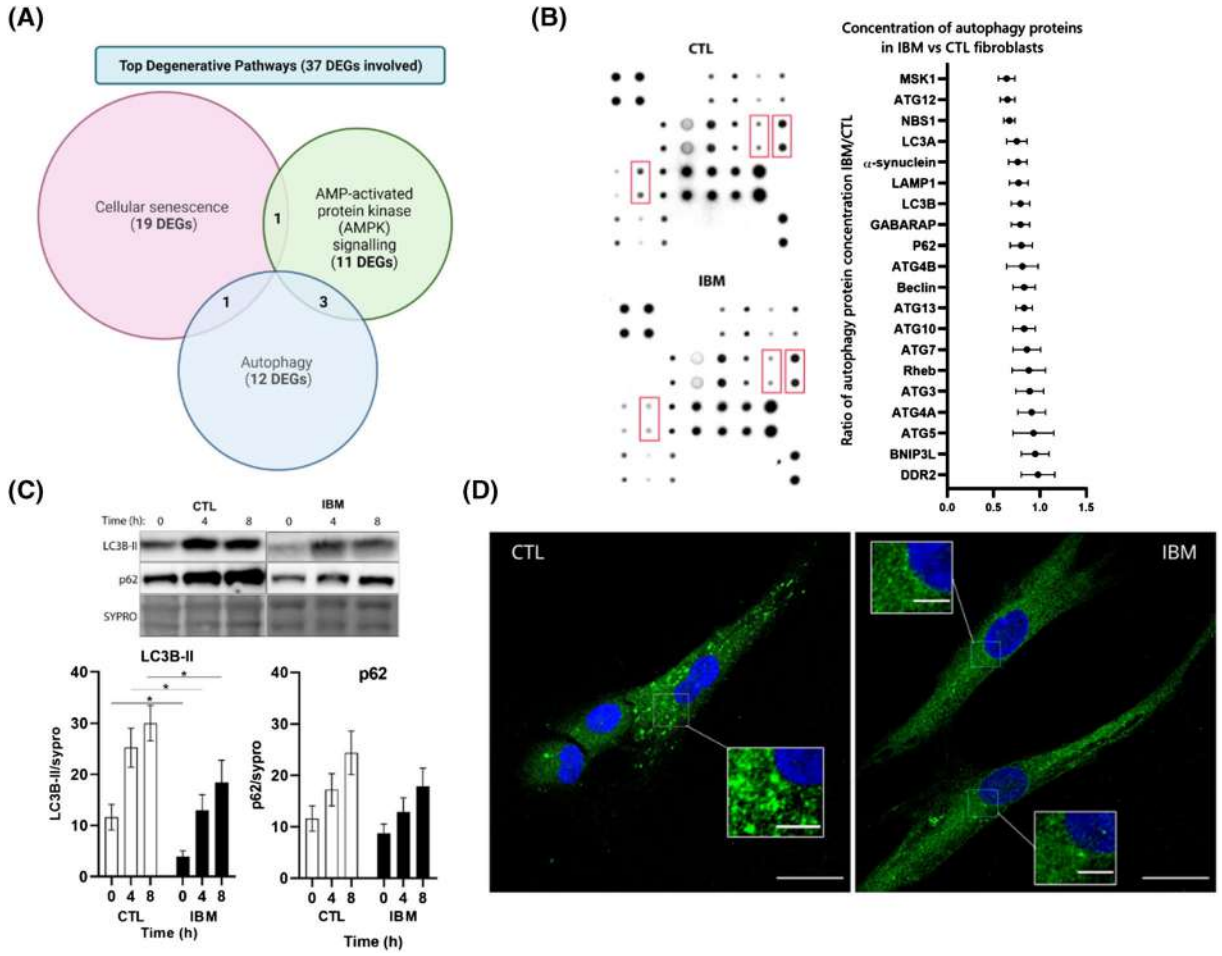

Figure 3 Autophagy in IBM versus CTL fibroblasts. (A) Venn's diagram of the most affected degenerative clusters and the number of differentially expressed genes (DEGs) involved. Some DEGs are involved in more than one cluster. The list of degenerative DEGs is represented in *Table* S2. (B) Representative images of two autophagy protein arrays of one inclusion body myositis (IBM) and one control (CTL) fibroblast and quantification of $n = 8$/group autophagy protein arrays. In red, differences in protein concentration (according to spot intensity) among IBM and CTL fibroblasts. In the graph, mean fold change ratio (and deviation) of autophagy proteins in IBM patients versus CTL fibroblasts, normalized by protein content (ratio < 1: Lower concentration in IBM). Each protein concentration is depicted in *Table* S4. (C) Representative images and graphs of an autophagy time-course (at basal, 4 h and 8 h under bafilomycin A1 treatment) measured by western blot between IBM ($n = 13$) and CTL ($n = 12$) fibroblasts. Results: Mean ± SEM, $n = 13$ IBM versus 11 CTL; Kruskal–Wallis test, $^*P$-value < 0.05. SQSTM1/p62: Autophagy substrate, LC3BII: Autophagy receptor, lipidated form, sypro: Total protein content. (D) Representative images of autophagosome accumulation in IBM versus CTL fibroblasts treated with bafilomycin A1 (100 nM) for 6 h obtained by confocal microscope (LC3B in green; nuclei in blue with DAPI, scale 25 μM (inserts 5 μM)). Briefly, autophagy is impaired in terms of differentially expressed genes (DEGs) and decreased expression of basal protein mediators, time-course autophagosome formation, and microscopic evaluation.

mediators caused by a higher autophagic rate, we performed a time-course experiment that blocked the process. As observed in *Figure* 3C, flux rate of both LC3BII and p62 effectors at 4 h and 8 h after bafilomycin A1 treatment was non-significantly reduced between cohorts when normalized by basal levels. Interestingly, raw data non-normalized by basal expression showed significantly reduced levels of LC3B-II marker at 4 h and 8 h after treatment in IBM fibroblasts (44.4% and 33.6% reduced in IBM, P-value < 0.05), suggesting a lower autophagic performance in the IBM cohort. Overall, a decreased autophagic activity could lead to insufficient cell recycling and accumulation of damaged components in the cytoplasm, increasing the endoplasmic reticulum stress and compromising the homeostatic balance within cells. In the case of p62 expression, we also found a slight reduction in IBM fibroblasts (24.9%, 19.0%, and 20.6% reduced).

To visualize the proportion of autophagic vesicles between cohorts, we performed immunostaining of LC3B after 6 h under bafilomycin A1 treatment (*Figure* 3D). The results revealed a lower accumulation of autophagosomes in IBM fibroblasts. These findings manifested a deregulated autophagic and degenerative profile in IBM fibroblasts, prompting relevant pathways and targets in this disease.

DOI: 10.1002/jcsm.13178

Mitochondrial abnormalities increased oxidative status in IBM fibroblasts

The third hallmark of IBM in muscle are mitochondrial alterations. In muscle biopsies, there is an increased number of mitochondria across myofibres (creating RRF) and increased complex II expression (SDH+ fibres), probably as an attempt to compensate dysfunctional mitochondria, evidenced as decreased complex IV expression (COX-fibres).[6,11,23,24] These are features of primary mitochondrial diseases. We aimed to examine the mitochondrial state of IBM versus CTL fibroblasts by analysing mitochondrial deregulated genes, and by functional assessment of bioenergetic and metabolic performance.

Regarding mitochondrial gene expression, we found 42 mitochondrial DEGs compiled in the Mitocarta (version 3.0),[25] in *Table* S2. Among them, some DEGs were encoded in the mitochondrial genome (NADH:CoQ oxidoreductase subunits, COX and ATP synthase), others related to the MRC function but encoded in the nuclear genome; and tricarboxylic acid cycle (TCA) enzymes. Also, some DEGs were stress-related or peroxisomal genes. These genes were grouped in gene clusters (*Figure* 4A).

At functional level, we measured the respiratory profile of IBM and CTL fibroblasts to quantify the oxygen consumption rate (*Figure* 4B). IBM fibroblasts leaned towards a decreased respiratory pattern (*Figure* 4B), especially at basal and maximal respiration levels (28.6% and 31.8% reduced in IBM), suggesting a trend towards less active MRC activity.

These results were supported at the enzymatic level by a 45.6% COX significant decrease, as seen in muscle, normalized by CS activity (P-value < 0.001) (*Figure* 4C). Moreover, CS activity shifted towards a 44.6% increase in IBM fibroblasts, leading to an increased mitochondrial mass to compensate for COX reduction, as seen in RRF from IBM muscles.

To assess if MRC downward is correlated to oxidative stress and antioxidant levels, lipid peroxidation markers like MDA and HAE were measured in cell lysates (*Figure* 4D). Lipid peroxidation tended to increase a 14.3% in IBM versus CTL fibroblasts, suggesting a trend towards higher oxidative stress in IBM cells; coupled with a 135.2% significant increased level of antioxidant defences (TAC) in IBM (P-value < 0.05) (*Figure* 4D). Moreover, in the mRNA-seq we found aldehyde dehydrogenases (*ALDH1L2*, *ALDH1B1*, *ALDH4A1*, and *ALDH18A1*), enzymes involved in lipid peroxidation, and some antioxidant enzymes (*CBR3*, *CYB5R3*, *ETHE1*, *PRXL2A*, and *SQOR*), among the DEGs between IBM and CTL fibroblasts.

Mitochondrial dysfunction is usually linked to the depolarization of MMP, that was significantly decreased by 11.6% in IBM fibroblasts (P-value < 0.05) (*Figure* 4E). MMP depolarization may result in impaired proton pumping, leading to the opening of the mitochondrial membrane pore, and potential activation of apoptosis.

mtDNA genome content was significantly decreased by 33.9% in IBM fibroblasts (*Figure* 4F; P-value < 0.05), as previously observed in IBM muscle[11] and in accordance to abnormal mitochondrial morphology, either externally (showing a significant 42.8%-reduced mitochondrial elongation, *Figure* 4F, *Figure* 5A), and internally (at subcellular level) (*Figure* 5B). Briefly, using TEM ultrastructural visualization, 76.2% of IBM fibroblasts revealed abnormal mitochondria (61.9% of them with altered cristae and 42.2% with a round shape, associated with unhealthier mitochondria), compared with 25.1% of CTL fibroblasts with abnormal mitochondria (of which 7.9% had altered cristae and 17.2% a round shape). At mRNA level, we found three DEGs related to mitochondrial dynamics (BCL2L1, FKBP8, and MGARP), all downregulated.

Overall, these findings highlight a mitochondrial impairment in IBM fibroblasts and identify contributing pathways and key players in disease.

Targeted metabolites characterization

To examine if mitochondrial dysfunction was linked to metabolic misbalances beyond the MRC, we measured DEGs and metabolite levels related to organic acids and amino acids in IBM and CTL fibroblasts.

At gene expression level, we observed 10 DEGs involved in organic acids and amino acids metabolism (in *Table* S5). Briefly, increased lactic acid and alanine are related to *MT-ND5*, *MT-CO2*, and *MT-ATP6*, components of the MRC and related to the TCA cycle. *ETHE1* is also linked to increased alanine, ethylmalonic and methyl succinic, and related to the *SQOR* gene. *PSAT1* and *GPX3*, albeit not being mitochondrial genes, are directly related to mitochondrial metabolism, involved in serine and glycine biosynthesis and pyroglutamic acid metabolism, respectively.

At functional level, organic acids showed a 1.8-fold change increase in IBM, suggesting deregulation of intermediary metabolism. The most relevant organic acids were: lactic acid (biomarker of mitochondrial diseases); succinic acid (part of MRC complex II, increased in SDH+ fibres in muscle); pyroglutamic acid (involved in glutathione synthesis); sebacic acid (involved in the electron transfer from the β-oxidation pathway to MRC complex II) and above all, 2OH-glutaric acid (TCA cycle component which accumulates in case of mitochondrial defect), that were significantly deregulated (*Figure* 6A and *Table* S6). These components or derivatives of the TCA cycle are related to amino acids or fatty acid metabolism and their increase is frequently linked to MRC dysfunction. Regarding amino acids levels, no relevant differences were observed between IBM and CTL fibroblasts (*Figure* 6B and *Table* S7).

Metabolic reprogramming in IBM fibroblasts supports mitochondrial dysfunction beyond the MRC, and unravels the main pathways and targets involved in IBM.

Association of molecular phenotype and disease progression

Phenotyping IBM vs CTL fibroblasts has revealed an overall differential gene expression and functional profile, especially

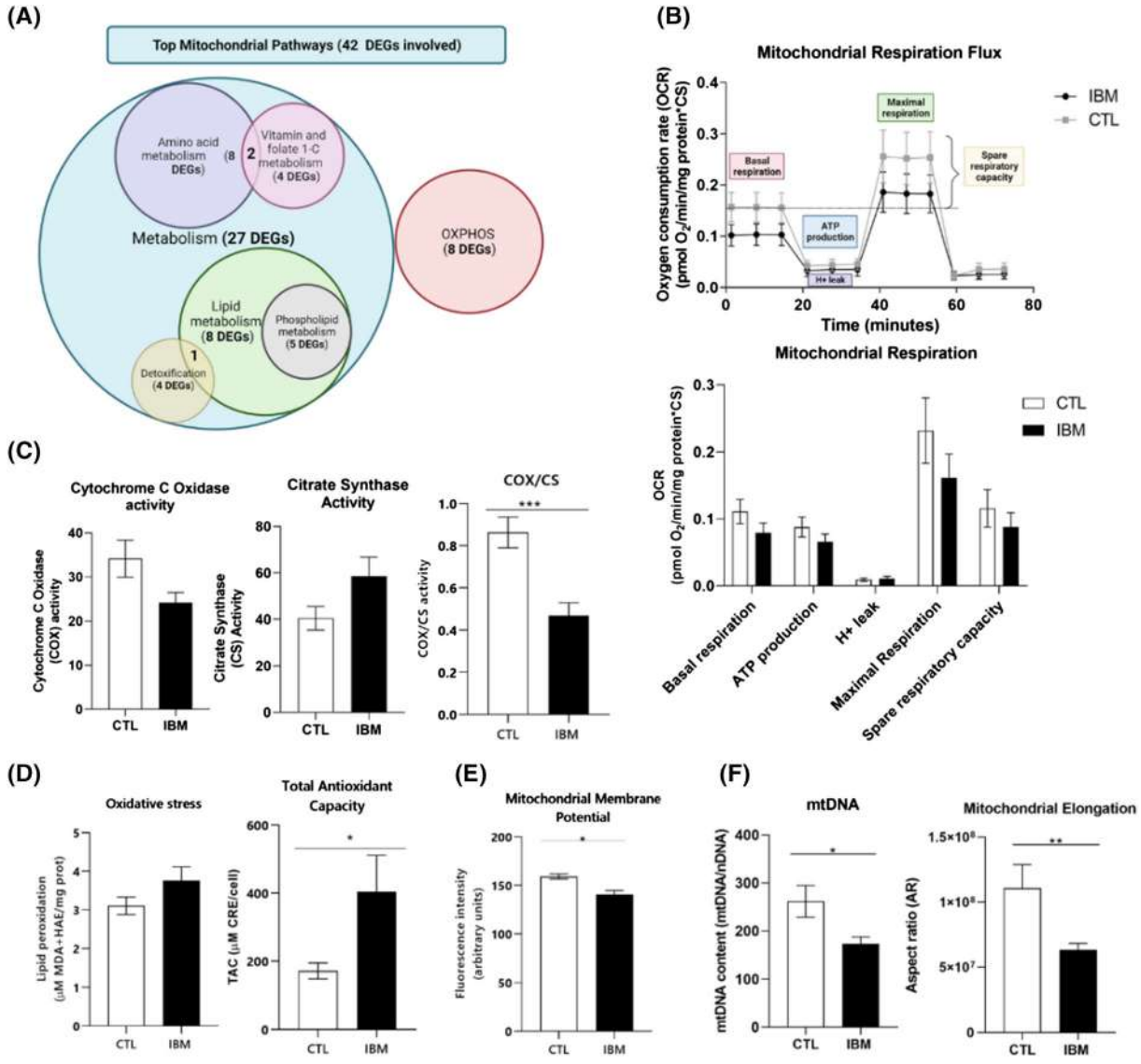

Figure 4 Mitochondrial profile in IBM versus CTL fibroblasts. (A) Venn's diagram of the most affected mitochondrial clusters and the number of differentially expressed genes (DEGs) involved. Many DEGs are involved in more than one cluster. The list of mitochondrial DEGs is represented in *Table* S2. (B) Mitochondrial respiratory flux and rates of IBM versus CTL fibroblasts. Each sample was seeded in quadruplicate per condition (n = 10/group, Mann–Whitney U test). OCR = oxygen consumption rate. Respiratory control ratios were normalized by total protein content and by citrate synthase (CS) activity as a marker of mitochondrial content. (C) Cytochrome C oxidase (COX), citrate synthase (CS) and COX per CS activity (COX/CS ratio, as a marker of complex IV from the mitochondrial respiratory chain (MRC) per mitochondrial mass (n = 10/group, P-value < 0.001, Mann–Whitney U test), normalized by protein content. (D) Oxidative stress measured through lipid peroxidation in IBM versus CTL fibroblasts normalized by total protein content (n = 9 IBM vs. 8 CTL, Mann–Whitney U test) (MDA: Malondialdehyde; HAE: Hydroxialkenal); coupled to Total antioxidant capacity (TAC) expressed as µM CRE (copper reducing equivalents) per total cell number (n = 11 IBM vs. 4 CTL, P-value < 0.05, Mann–Whitney U test). (E) Mitochondrial membrane potential (MMP) measured with TMRM + Arimoclomol in IBM versus CTL fibroblasts (n = 4/group, P-value < 0.05, Mann–Whitney U test). The results were expressed as mean ± SEM (*$P < 0.05$). (F) mtDNA genome content in IBM versus CTL fibroblasts expressed as the ratio of mtDNA 12S rRNA:nDNA RNase-P (mitochondrial vs. nuclear encoded gene) (n = 9 IBM vs. 8 CTL, P-value < 0.05, Mann–Whitney U test) and mitochondrial elongation (represented by the aspect ratio) in IBM versus CTL fibroblasts (n = 3/group, P-value < 0.05, Mann–Whitney U test). Briefly, mitochondrial performance is disturbed in IBM versus CTL fibroblasts in terms of genetic content, differentially expressed genes (DEGs) and functionality (reduced respiratory profile, marked COX/CS decline, higher oxidative stress and antioxidant defence activation, reduced MMP and mitochondrial elongation).

considering inflammation, degeneration and mitochondrial function. Interestingly, this pattern seems to differ slightly depending on disease evolution.

As observed in Table 1, six patients showed stable IBM prognosis whereas eight followed a progressive disease decline. The correlation of molecular and clinical data yielded

DOI: 10.1002/jcsm.13178

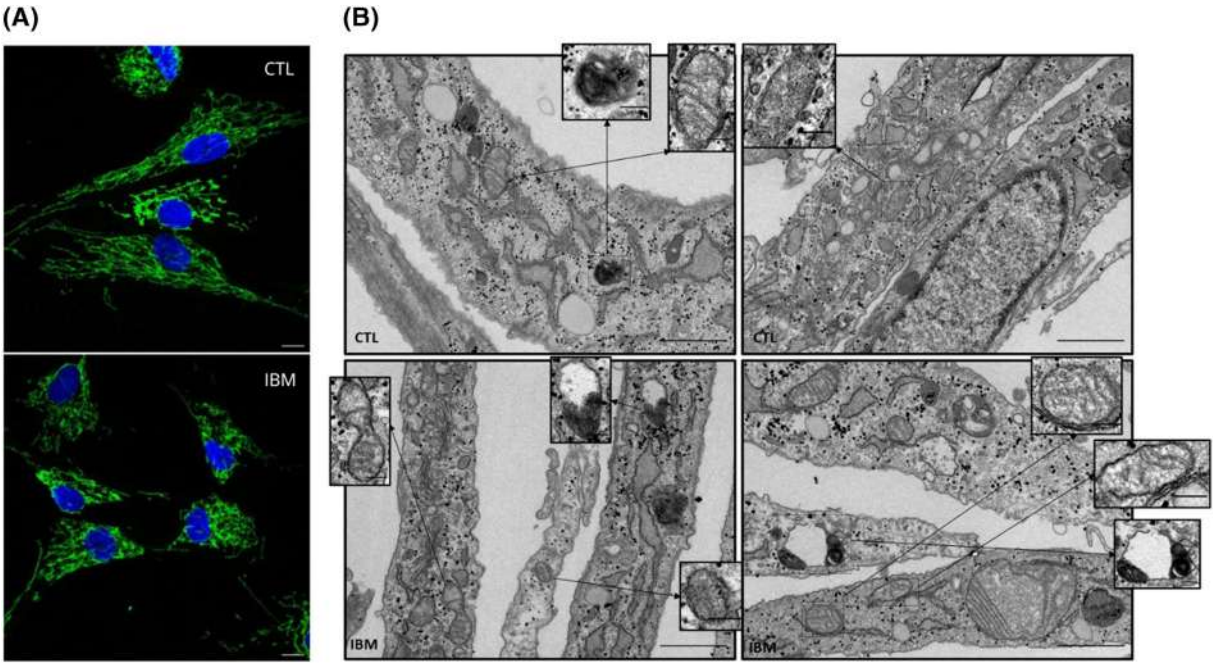

Figure 5 Mitochondrial morphology in IBM versus CTL fibroblasts. (A) Mitochondrial network in a representative image of IBM versus CTL fibroblasts obtained by confocal microscope (TOMM20 in green; nuclei in blue with DAPI, scale 10 μM) displaying reduced mitochondrial elongation in IBM (associated to poor mitochondrial health). (B) Transmission electron microscopy (TEM) images of IBM versus CTL fibroblasts. In IBM fibroblasts, some mitochondria lacked cristae (see inserts) presenting a discontinuous cristae distribution. Also, increased mitochondrial fission (see insert) could explain the smaller and more circular shape of these organelles associated with unhealthier mitochondria. Additionally, the presence of impaired autophagosome-lysosome structures in IBM patients (see inserts) might be a result of incomplete autophagy. Briefly, these findings highlight a mitochondrial impairment in IBM fibroblasts. Magnification: 30 000×, scale 1 μm for each picture and 0.2 μm for inserts.

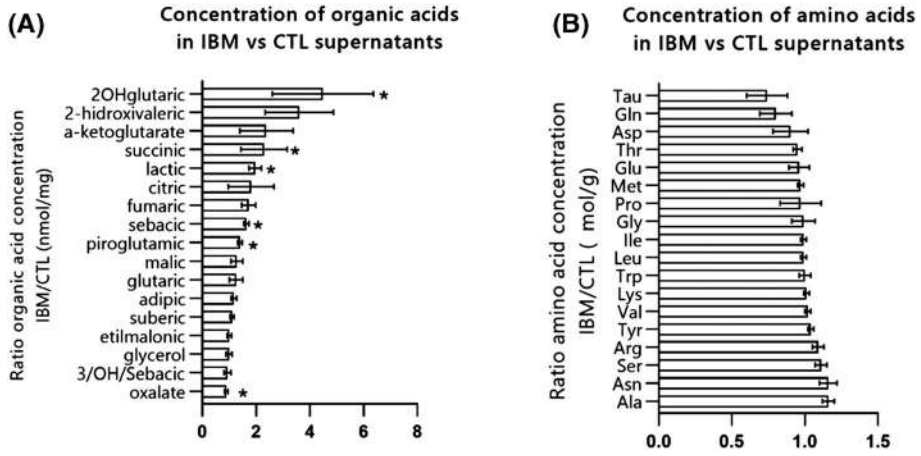

Figure 6 Metabolites concentration in IBM versus CTL fibroblasts. (A) Mean fold change ratio (and deviation) of organic acids in IBM patients versus CTL fibroblasts, normalized by protein content (n = 11 IBM vs. 10 CTL, *P-value < 0.05, Mann–Whitney U test) (ratio > 1: Higher concentration in IBM). The raw data of each organic acid concentration is represented in *Table* S6. (B) Mean fold change ratio (and deviation) of amino acids IBM patients versus CTL fibroblasts, normalized by protein content (n = 11 IBM vs. 10 CTL, Mann–Whitney U test) (ratio > 1: Higher concentration in IBM; ratio < 1: Lower concentration in IBM). The raw data of each amino acid concentration is represented in *Table* S7. Briefly, organic acid levels showed a general increase in IBM, suggesting deregulation of intermediary metabolism related to mitochondrial dysfunction, whereas no relevant differences in amino acid levels were observed between IBM and CTL fibroblasts.

to the association of increased pro-inflammatory and organic acids signature in stable IBM (*Table* S8 and *Figure* 7). Contrarily, progressive IBM showed increased oxidative stress and antioxidant capacity. Together, stable and progressive IBM present an evident decrease in LC3BII time-course and COX/CS with respect to CTLs.[26]

DOI: 10.1002/jcsm.13178

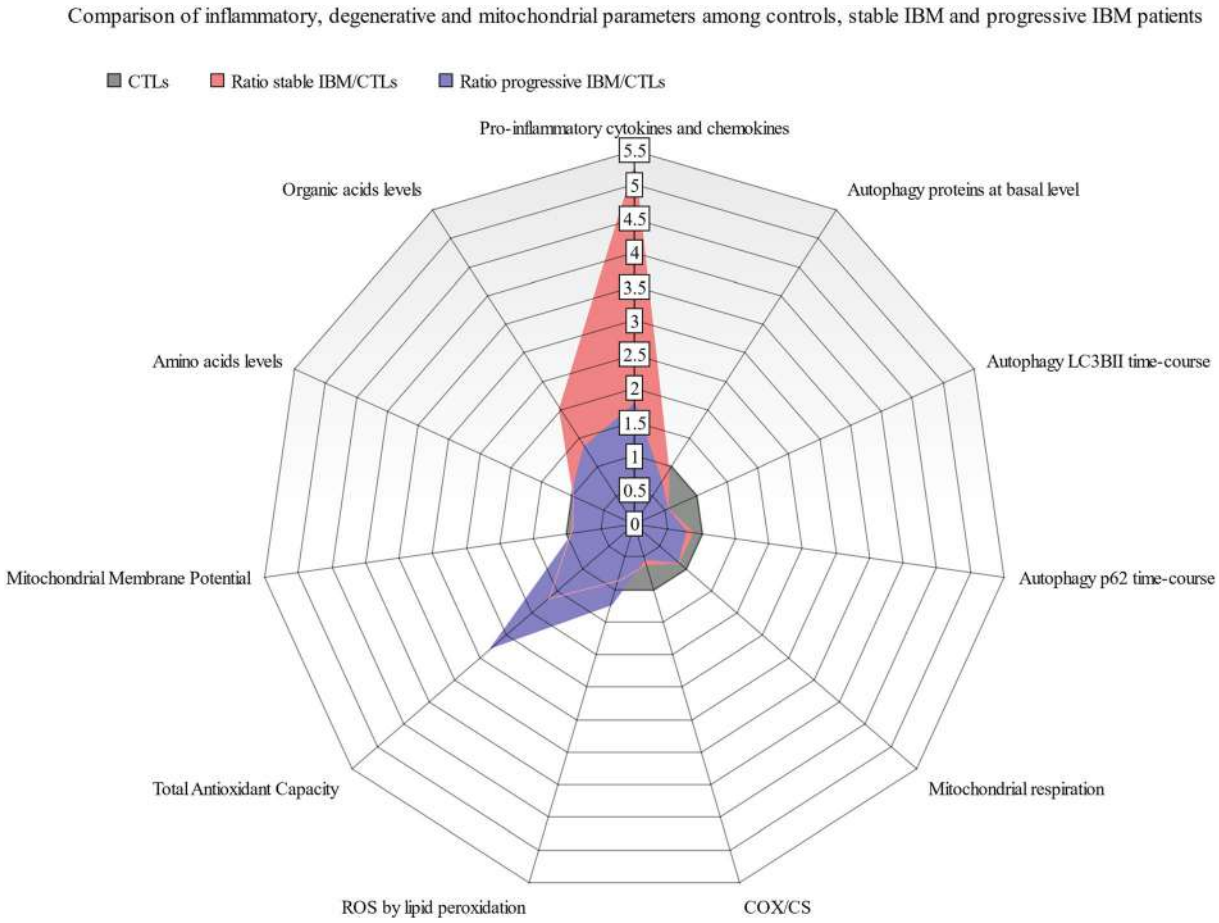

Figure 7 Comparison of inflammatory, degenerative and mitochondrial parameters among controls (CTLs), IBM patients with stable evolution (stable IBM) and IBM patients with disease progression (progressive IBM). Ratios between IBM (stable or progressive) and control fibroblasts were measured to compare inflammatory, degenerative and mitochondrial parameters among the three groups (*Table* S8). Briefly, stable IBM showed an increased pro-inflammatory and organic acids signature compared with progressive IBM and controls. Progressive IBM showed increased oxidative stress (ROS) and antioxidant capacity. Together, IBM stable and progressive present an evident decrease in LC3BII time-course (autophagy marker) and COX/CS (cytochrome c oxidase related to citrate synthase, a marker of mitochondrial mass) with respect to CTLs (ratio $>$ 1: Higher concentration in IBM; ratio $<$ 1: Lower concentration in IBM).

The presence of common and differential molecular profile between stable and progressive IBM patients could help in understanding disease pathogenesis and become potential markers of prognosis.

Discussion

Here we reported the validation of fibroblasts as a disease model for untangling IBM and identifying novel pathogenic molecular players. Briefly, we observed transcriptomic and functional inflammatory, degenerative and mitochondrial changes in IBM fibroblasts, which resemble the alterations found in the target tissue, in muscle.

Previous studies analysed IBM transcriptome[27,28] at muscular and blood level, but this is the first IBM RNA-seq in fibroblasts. Here we found 778 DEGs, supporting a clear pathological pattern of gene expression in IBM.

At the inflammatory level, IBM fibroblast transcriptome revealed altered inflammatory genes resembling muscle features, including MHC1 (*HLA* genes) and *IFN* genes. These alterations were found in an IBM deep neural network model.[29,30] At the functional scale, cytokines secretion in IBM fibroblasts was increased. Previous studies in IBM muscle detected CD8+ T cell-secreted cytokines and chemokines related to IFN-ɣ genes (*CXCL9*, *CXCL10*, *CCL5*, and *CCL18*) and others, including *TNF*, *IL7*, *IL15*, *IL16*, and *IL32*,[1,26] some of which were also detected in the sera of IBM patients.[26] Although fibroblasts are not part of the immune system, these results partially mimic the inflammation of IBM muscles.

Regarding degeneration in IBM, impaired autophagy and disturbed proteostasis have been described in muscle.[24] Some degenerative markers like TDP43, p62, and LC3 show

DOI: 10.1002/jcsm.13178

an aberrant expression in IBM muscle.[5,31] Herein, we found impaired autophagy at gene and functional level, with lower production of autophagy proteins and deficient formation of autophagosomes in IBM fibroblasts, leading to insufficient recycling needs and deposition of cargos within the cell. This phenotype is remarkable in fibroblasts, as their high turnover avoids debris accumulation. In contrast, muscle is a post-mitotic tissue that accumulates cell debris, forming rimmed vacuoles in IBM, where autophagic deficiencies are more evident.

Related to deficient macroautophagy and mitophagy in IBM, there is a lower turnover of mitochondria, leading to bioenergetic deficits and cell damage due to oxidative stress generation.[24,32] The deficient mitochondrial profile observed in IBM fibroblasts revealed altered gene expression, impaired respiratory capacity, increased oxidative stress and mitochondrial mass (CS), reduced MMP, COX activity, mtDNA content and mitochondrial elongation, all previously seen in muscle tissue[11,13,24] and in mitochondrial myopathies,[13,33] suggesting that IBM slightly behaves as a mitochondrial disease.

Metabolic reprogramming could be linked to mitochondrial dysfunction, as proposed in IBM blood metabolomes[33] and primary mitochondrial diseases. Many pathways and genes related to the IBM blood metabolome are altered in IBM fibroblasts. Buzkova *et al*. demonstrated that IBM blood metabolome clustered more accurately with mitochondrial myopathies than neuromuscular diseases,[33] prompting a higher mitochondrial implication in IBM than previously thought. The current results in fibroblasts support previous findings.

Interestingly, these pathological features of IBM fibroblasts and muscle (inflammation, degeneration and mitochondrial dysfunction), resemble standard physiologic aging, including decreased muscle strength,[23] supporting that IBM involves an accelerated muscle aging.

Considering IBM evolution, it revealed that progressive IBM (22.1 ± 2.7 IBMFRS) is associated to higher imbalances in oxidant and antioxidant capacities whereas stable IBM (29.2 ± 2.7 IBMFRS) is associated to higher inflammatory profile. This increased inflammation could be a protective mechanism in the stable IBM, as these patients perform better at a clinical scale (higher IBMFRS). Considering these findings, oxidative stress and inflammation emerge as potential markers of prognosis.

Overall, this is the first attempt to suggest fibroblasts as a model of IBM pathogenesis, scarcely tested as a model in neuromuscular diseases.[12,34] So far, most of the pathological mechanisms in IBM have been discovered in cells and tissue samples from patients. However, although preclinical and omic studies help in understanding disease pathogenesis, the gap in translation to clinical research remains elusive.[35] Currently in IBM, 16 clinical trials are active,[36] in which most treatments were discovered or tested in cell models (e.g. phenylbutyrate in *in vitro* muscle fibres[37]), suggesting the relevance of disease models in regulatory settings. In this sense, fibroblasts emerge as a promising model of IBM to discover new targets and perform screening of biomarkers and potential therapies.

Nevertheless, there are some limitations in the present study. First, our limited sample size, mainly due to IBM being a rare disease, even though for a reference unit like ours. In addition, even fibroblasts are associated to cost-effective maintenance conditions, other cell models, closer to the target tissue, might better reflect IBM pathogenesis. This may be the case of myotubes differentiated from induced pluripotent stem cells, which avoid the invasiveness of a muscle biopsy, but may offer a closer approach to muscle behaviour. However, they require complex protocols, rending fibroblasts to a cost-effective cell model.

Despite these contingencies, in the present study we validated fibroblasts as a disease model for IBM, showing IBM alterations are present beyond the target tissue of the disease. This model could be exported to other myositis or neuromuscular diseases. Additionally, we unveil numerous pathways and specific molecules that emerge as relevant key players in disease aetiology or evolution, for further evaluation as candidate biomarkers or therapeutic targets.

Acknowledgements

We acknowledge the contribution of patients and their families, collaborating to expand the state-of-the-art in rare diseases. We also appreciate the support given by the Advanced Optical Microscopy department of the University of Barcelona. All authors of this manuscript certify that they comply with the ethical guidelines for authorship and publishing in the *Journal of Cachexia, Sarcopenia and Muscle*.[38]

Funding

This study was supported by Instituto de Salud Carlos III (ISCIII-FEDER, grants PI18/00498, PI18/00451 and PI21/00935) and co-funded by the European Union. Additionally, JC-S is supported by the APIF Programme (University of Barcelona), FJG-G by the CIBERER (ISCIII-FEDER), MG-M by CD21/00019 (ISCIII- FSE+), CR by the Serra Húnter Programme (Generalitat de Catalunya), RA by Torrons Vicens, JCF-C by PID2019-111669RB-I00, CG-R by PID2020-115055RB-I00 and AE-C by PT17/0009/0019 (ISCIII-MINECO-FEDER).

Conflict of interest

The authors declare that they have no conflict of interest.

Online supplementary material

Additional supporting information may be found online in the Supporting Information section at the end of the article.

References

1. Greenberg SA. Inclusion body myositis: clinical features and pathogenesis. *Nat Rev Rheumatol* 2019;**15**:257–272.
2. Weihl CC. Sporadic Inclusion Body Myositis and Other Rimmed Vacuolar Myopathies. *CONTINUUM Lifelong Learn Neurol* 2019; **25**:1586–1598.
3. Callan A, Capkun G, Vasanthaprasad V, Freitas R, Needham M. A Systematic Review and Meta-Analysis of Prevalence Studies of Sporadic Inclusion Body Myositis. *J Neuromuscul Dis* 2017;**4**:127–137.
4. Keshishian A, Greenberg SA, Agashivala N, Baser O, Johnson K. Health care costs and comorbidities for patients with inclusion body myositis. *Curr Med Res Opin* 2018; **34**:1679–1685.
5. Greenberg SA. Pathogenesis of inclusion body myositis. *Curr Opin Rheumatol* 2020; **32**:542–547.
6. Catalán M, Selva-O'Callaghan A, Grau JM. Diagnosis and classification of sporadic inclusion body myositis (sIBM). *Autoimmun Rev* 2014;**13**:363–366.
7. Dalakas MC. Inflammatory myopathies: update on diagnosis, pathogenesis and therapies, and COVID-19-related implications. *Acta Myologica* 2020;**39**:289–301.
8. Sugarman MC, Yamasaki TR, Oddo S, Echegoyen JC, Murphy MP, Golde TE, et al. Inclusion body myositis-like phenotype induced by transgenic overexpression of βAPP in skeletal muscle. *Proc Natl Acad Sci U S A* 2002;**99**:6334–6339.
9. Ahmed M, Machado PM, Miller A, Spicer C, Herbelin L, He J, et al. Targeting protein homeostasis in sporadic inclusion body myositis. *Sci Transl Med* 2016; **8**:331ra41.
10. Chen X, Ghribi O, Geiger JD. Rabbits fed cholesterol-enriched diets exhibit pathological features of inclusion body myositis. *Am J Physiol Regul Integr Comp Physiol* 2008;**294**:829–835.
11. Catalán-García M, Garrabou G, Morén C, Guitart-Mampel M, Hernando A, Díaz-Ramos À, et al. Mitochondrial DNA disturbances and deregulated expression of oxidative phosphorylation and mitochondrial fusion proteins in sporadic inclusion body myositis. *Clin Sci* 2016;**130**: 1741–1751.
12. Katsetos CD, Koutzaki S, Melvin JJ. Mitochondrial dysfunction in neuromuscular disorders. *Semin Pediatr Neurol* 2013;**20**: 202–215.
13. de Paepe B. Sporadic inclusion body myositis: An acquired mitochondrial disease with extras. *Biomolecules MDPI AG* 2019;**9**:15.
14. Tokuyama T, Hirai A, Shiiba I, Ito N, Matsuno K, Takeda K, et al. Mitochondrial Dynamics Regulation in Skin Fibroblasts from Mitochondrial Disease Patients. *Biomolecules* 2020;**10**:450.
15. González-Casacuberta I, Juárez-Flores DL, Ezquerra M, Fucho R, Catalán-García M, Guitart-Mampel M, et al. Mitochondrial and autophagic alterations in skin fibroblasts from Parkinson disease patients with Parkin mutations. *Aging* 2019;**11**: 3750–3767.
16. GitHub - MariaCalvo-UB/MitochondrialMorphologyAnalysis_Folder.ijm: This macro segments cells and mitochondria network, and measures mitochondria network area and morphology cell by cell.
17. Meneses-Salas E, García-Melero A, Kanerva K, Blanco-Muñoz P, Morales-Paytuvi F, Bonjoch J, et al. Annexin A6 modulates TBC1D15/Rab7/StARD3 axis to control endosomal cholesterol export in NPC1 cells. *Cell Mol Life Sci* 2020;**77**: 2839–2857.
18. Hoffmann GF, Feyh P. *Organic Acid Analysis. In: Physician's Guide to the Laboratory Diagnosis of Metabolic Diseases*. Berlin, Heidelberg: Springer Berlin Heidelberg; 2003. p 27–44.
19. Casado M, Sierra C, Batllori M, Artuch R, Ormazabal A. A targeted metabolomic procedure for amino acid analysis in different biological specimens by ultra-high-performance liquid chromatography–tandem mass spectrometry. *Metabolomics* 2018; **14**:76.
20. Jackson CE, Barohn RJ, Gronseth G, Pandya S, Herbelin L, The Muscle Study Group (MSG). Inclusion body myositis functional rating scale: A reliable and valid measure of disease severity. *Muscle Nerve* 2008;**37**: 473–476.
21. Safran M, Dalah I, Alexander J, Rosen N, Iny Stein T, Shmoish M, et al. GeneCards Version 3: the human gene integrator. *Database (Oxford)* 2010;**2010**:baq020.
22. Reactome|Pathway Browser. https://reactome.org/PathwayBrowser/ (accessed December 15, 2021).
23. Joshi PR, Vetterke M, Hauburger A, Tacik P, Stoltenburg G, Hanisch F. Functional relevance of mitochondrial abnormalities in sporadic inclusion body myositis. *J Clin Neurosci* 2014;**21**:1959–1963.
24. Askanas V, Engel WK, Nogalska A. Sporadic inclusion-body myositis: A degenerative muscle disease associated with aging, impaired muscle protein homeostasis and abnormal mitophagy. *Biochim Biophys Acta Mol Basis Dis* 2015; **1852**:633–643.
25. Rath S, Sharma R, Gupta R, Ast T, Chan C, Durham TJ, et al. MitoCarta3.0: An updated mitochondrial proteome now with sub-organelle localization and pathway annotations. *Nucleic Acids Res* 2021;**49**: D1541–D1547.
26. Badrising UA, Tsonaka R, Hiller M, Niks EH, Evangelista T, Lochmüller H, et al. Cytokine Profiling of Serum Allows Monitoring of Disease Progression in Inclusion Body Myositis. *J Neuromuscul Dis* 2017;**4**: 327–335.
27. Pinal-Fernandez I, Casal-Dominguez M, Derfoul A, Pak K, Plotz P, Miller FW, et al. Identification of distinctive interferon gene signatures in different types of myositis. *Neurology* 2019;**93**:E1193–E1204.
28. Amici DR, Pinal-Fernandez I, Mázala DAG, Lloyd TE, Corse AM, Christopher-Stine L, et al. Calcium dysregulation, functional calpainopathy, and endoplasmic reticulum stress in sporadic inclusion body myositis. *Acta Neuropathol Commun* 2017;**5**:24.
29. deAndrés-Galiana EJ, Fernández-Ovies FJ, Cernea A, Fernández-Martínez JL, Kloczkowski A. Deep neural networks for phenotype prediction in rare diseases. In *Artificial Intelligence in Precision Health*. Elsevier; 2020. p 189–202.
30. Tadenev ALD, Burgess RW. Model validity for preclinical studies in precision medicine: precisely how precise do we need to be? *Mamm Genome* 2019;**30**:111–122.
31. Hiniker A, Daniels BH, Lee HS, Margeta M. Comparative utility of LC3, p62 and TDP-43 immunohistochemistry in differentiation of inclusion body myositis from polymyositis and related inflammatory myopathies. *Acta Neuropathol Commun* 2013; **1**:29.
32. Nogalska A, D'Agostino C, Engel WK, Cacciottolo M, Asada S, Mori K, et al. Activation of the Unfolded Protein Response in Sporadic Inclusion Body Myositis But Not in Hereditary GNE Inclusion Body Myopathy HHS Public Access. *J Neuropathol Exp Neurol* 2015;**74**:538–546.
33. Buzkova J, Nikkanen J, Ahola S, Hakonen AH, Sevastianova K, Hovinen T, et al. Metabolomes of mitochondrial diseases and inclusion body myositis patients: treatment targets and biomarkers. *EMBO Mol Med* 2018;**10**:1–15.
34. Kodavati M, Wang H, Hegde ML. Altered Mitochondrial Dynamics in Motor Neuron Disease: An Emerging Perspective. *Cell* 2020;**9**:1065.

35. Mak IWY, Evaniew N, Ghert M. Lost in translation: Animal models and clinical trials in cancer treatment. *Am J Transl Res* 2014;**6**:114–118.
36. Search of: Recruiting, Not yet recruiting, Active, not recruiting Studies |Interventional Studies|Inclusion Body Myositis - List Results - ClinicalTrials.gov. https://clinicaltrials.gov/ (accessed December 10, 2021).
37. Nogalska A, D'Agostino C, Engel WK, Askanas V. Sodium phenylbutyrate reverses lysosomal dysfunction and decreases amyloid-β42 in an in vitro-model of inclusion-body myositis. *Neurobiol Dis* 2014;**65**:93–101.
38. von Haehling S, Morley JE, Coats AJS, Anker SD. Ethical guidelines for publishing in the Journal of Cachexia, Sarcopenia and Muscle: update 2021. *J Cachexia Sarcopenia Muscle* 2021;**12**:2259–2261.

MANUSCRIPT II:

Title: *Modelling inclusion body myositis using human pluripotent stem cell-derived skeletal myotubes*

Authors: Judith Cantó-Santos, Laura Valls-Roca, Ester Tobías, Francesc Josep García-García, Mariona Guitart-Mampel, Félix Andújar-Sánchez, Anna Esteve-Codina, Beatriz Martín-Mur, Joan Padrosa, Raquel Aránega, Emma Peruga, Irene Madrigal, Paula Segalés, Carmen García-Ruiz, Pedro J. Moreno-Lozano, José César Milisenda, Ana Sevilla, Josep M. Grau-Junyent, Glòria Garrabou.

Journal: Submitted to the Journal of Cachexia, Sarcopenia and Muscle.

IF: 8.9

Research article

Modelling inclusion body myositis using human pluripotent stem cell-derived skeletal myotubes

Judith Cantó-Santos[1,2,3], Laura Valls-Roca[1,2,3], Ester Tobías[1,2,3], Francesc Josep García-García[1,2,3], Mariona Guitart-Mampel[1,2,3], Félix Andújar-Sánchez[1,2,3], Anna Esteve-Codina[4,5], Beatriz Martín-Mur[4], Joan Padrosa[1,2,3], Raquel Aránega[1,2,3], Emma Peruga[6], Irene Madrigal[3,6], Paula Segalés[7,8], Carmen García-Ruiz[7,8], José Carlos Fernandez-Checa[7,8], Pedro J. Moreno-Lozano[1,2,3], José César Milisenda[1,2,3,*], Ana Sevilla[9,*], Josep M. Grau-Junyent[1,2,3], Glòria Garrabou[1,2,3,*]

[1]Inherited Metabolic Disorders and Muscular Diseases Research Group, Institut d'Investigacions Biomèdiques August Pi i Sunyer (IDIBAPS) and Faculty of Medicine and Health Sciences, University of Barcelona, Barcelona, Spain
[2]Department of Internal Medicine, Hospital Clinic of Barcelona, Barcelona, Spain
[3]CIBERER— Spanish Biomedical Research Centre in Rare Diseases - ISCIII, Madrid, Spain
[4]CNAG-CRG, Centre for Genomic Regulation, Barcelona Institute of Science and Technology, Barcelona, Spain
[5]Universitat Pompeu Fabra (UPF), Barcelona, Spain
[6]Biochemistry and Molecular Genetics Department, Hospital Clinic of Barcelona, 08036 Barcelona, Spain
[7]Department of Cell Death and Proliferation, Institute of Biomedical Research of Barcelona (IIBB-CSIC), Liver Unit-HCB-IDIBAPS, Barcelona, Spain
[8]CIBEREHD-Spanish Biomedical Research Centre in Hepatic and Digestive Diseases, Madrid, Spain
[9]Departament de Biologia Cel·lular, Fisiologia i Immunologia, Facultat de Biologia, Universitat de Barcelona, Barcelona, Spain

*Correspondence to: jcmilise@clinic.cat; garrabou@clinic.cat, anasevilla@ub.edu

Running title: IBM iPSC-derived myotubes

Summary: Transcriptomic and functional validation of iPSC-derived myotubes from IBM patients reveals that this model partially recapitulates the main hallmarks of the disease.

Keywords: Inclusion body myositis (IBM), iPSC, myotubes, inflammation, autophagy, mitochondria, RNA-seq

ABSTRACT

Inclusion body myositis (IBM) is a degenerative inflammatory myopathy that clinically displays proximal and distal muscle weakness. At histopathological level, the muscle of IBM patients reveals inflammatory infiltrates, rimmed vacuoles and mitochondrial changes. IBM etiology is still unknown and there is a lack of validated disease models, biomarkers and effective treatments for this disease. In this study we developed a cell model based on derived myotubes from induced pluripotent stem cells (iPSCs) derived from IBM patients vs. age and sex-paired controls (n=4 per group). In this model, we evaluated untargeted gene expression profile by an mRNA-seq and targeted functional pattern of inflammation, degeneration and mitochondrial function. The gene expression profile revealed 875 differentially expressed genes (DEGs) (654 upregulated and 221 downregulated) related to myopathy features and muscle contraction alterations, mimicking some clinical symptoms. Of them, only 1 DEG was related to inflammation, 15 to autophagy and 21 to mitochondrial metabolism. Accordingly, at functional level, inflammation was conserved between cohorts, autophagy slightly altered (with lower production of autophagy mediators) and mitochondrial function was greatly found dysfunctional (with conserved respiratory profile and antioxidant capacity, but lower citrate synthase/cytochrome c oxidase ratio (COX/CS) and significantly higher lactate secretion). These preliminary findings validate the use of iPSC-myotubes as a model of IBM that may better reproduce the hallmarks of the disease after stress or toxic stimulation, ideally in bigger cohorts, and with potential crosstalk with immune mediators.

INTRODUCTION

Inclusion body myositis (IBM) is a degenerative inflammatory myopathy that clinically displays proximal and distal muscle weakness. At histopathological level, the muscle of IBM patients reveals inflammatory infiltrates, rimmed vacuoles and mitochondrial changes [1]. IBM belongs to the idiopathic inflammatory myopathies (IIM) group, formed by heterogeneous, systemic autoimmune diseases with muscles or skin as a primary target [2]. Although many IIM are treated with corticoids and immune-suppressants and there are many clinical trials ongoing, there is no treatment available for IBM [3]. Indeed, IBM etiology is still unknown and there is a lack of validated disease models and biomarkers for this disease.

Clinical manifestations of IBM are predominantly found in muscle, appearing first in quadriceps and finger flexor muscles, leading to difficulties for climbing stairs and handling objects [4]. In 60% of the cases, there is dysphagia and consequent swallowing dysfunctions [2]. Muscle histology studies are required for ultimate diagnosis of this disease, where inflammatory infiltrate, rimmed vacuoles and mitochondrial abnormalities must be present [1]. Briefly, muscle biopsies show inflammatory CD8+ T cells, aberrant expression of MHC-I and endomysial mononuclear cell infiltrates in myofibers. In degeneration, they present rimmed vacuoles, ubiquitin-positive inclusions and amyloid deposits. In mitochondria, there are abnormal changes like cytochrome c oxidase negative fibers (COX-) corresponding to the complex IV from the mitochondrial respiratory chain (MRC), succinate dehydrogenase positive cells (SDH+) from complex II from the MRC, and ragged-red fibers (RRF), related to an increased number of abnormal mitochondria around myofibers [1,5,6]. The invasiveness of the target tissue poses difficulties to obtain enough quantity of muscle tissue for further molecular profiling and potential identification of biomarkers.

The discovery of induced pluripotent stem (iPSCs) cells in 2006 from mouse embryonic fibroblast [7] and the following year from adult human fibroblasts [8], allowed the reprogramming *in vitro* of a somatic differentiated cell back to their pluripotency state. This discovery prompted our ability to manipulate cell fate [9]. Moreover, it only required four defined transcription factors: the octamer-binding protein 3/4 (OCT3/4) (also known as POU5F1), SOX2, Krüppel-like factor 4 (KLF4) and MYC [7–9], collectively known as OSKM. On the path towards becoming iPSCs, somatic cells should not only achieve pluripotency, but also acquire the capacity to proliferate indefinitely, key for the self-renewal of iPSCs.

The history of cell reprogramming started around the 1960s. Before 1962, when the first successful example of somatic cell nuclear transfer (SCNT) was announced, scientists thought the differentiation of cells into a lineage was permanent [9]. Shortly after, embryo-derived stem cells, called embryonic stem cells (ES cells) were established *in vitro*, which were able to differentiate into other cell lineages. Together with transdifferentiation protocols, able to convert one somatic cell into a different somatic lineage bypassing the pluripotent state, ES paved the way for the discovery of iPSCs, which functionally resemble ES cells. iPSCs are potentially applied to many fields, including drug discovery, disease modelling and regenerative medicine [9,10].

In disease modeling, iPSCs allowed the scientific community to have access to every cell type from many biological samples using a suitable differentiation protocol. For our study, to obtain skeletal muscle cells, the differentiation protocols were either based on muscle gene overexpression or on the administration of growth factors to the iPSCs in culture. In an attempt to resemble the developmental conditions, we chose the growth

factors differentiation protocol. This way we generated differentiated IBM iPSC-myotubes to perform untargeted and targeted analysis (by OMICs and functional analysis, respectively) of IBM muscle hallmarks (inflammation, degeneration and mitochondrial alterations) in this model. The use of iPSCs in muscular diseases have been limited to Duchenne muscular dystrophy (DMD) [11–13] and Facioscapulohumeral muscular dystrophy (FSHD)[14], among others, but has not been applied to IBM.

The lack of validated disease models in IBM, coupled to the potential use of iPSCs to obtain muscle cells that could enable a closer approach to the target tissue, lead us to hypothesize that skeletal muscle cells derived from iPSCs cells could recapitulate the main molecular hallmarks of the target tissue (muscle) and could be used as a tool to understand the etiology, identify biomarkers and potential treatments for IBM.

RESULTS

Clinical and epidemiological data

The samples included in this study were 4 IBM and 4 healthy controls (CTL). All sources of patient-derived samples for iPSC-myotubes generation were fibroblasts except for CTL4 (peripheral blood mononuclear cells, PBMCs), and all were obtained after signing the corresponding informed consent approved by the ethical committee of our hospital. Both cohorts were paired by age and sex and belong to the white Caucasian population. The epidemiological data is found in Table 1.

Table 1. Sample inclusion from inclusion body myositis (IBM) and control (CTL) cohorts

Sample code	Gender	Age	Disease
IBM1	*Female*	*67*	*Inclusion Body Myositis*
IBM2	*Male*	*63*	
IBM3	*Female*	*83*	
IBM4	*Male*	*78*	
CTL1	*Male*	*69*	*Healthy Volunteer*
CTL2	*Female*	*61*	
CTL3	*Female*	*52*	
CTL4	*Male*	*40*	

Generation of iPSC and differentiation into myotubes

The outline of the experimental approach in this study is found in Fig. 1. It includes the reprogramming of fibroblasts (and 1 PBMC sample) into iPSCs, their differentiation into skeletal muscle cells and the phenotyping seeking for IBM hallmarks by mRNA-seq and functional studies.

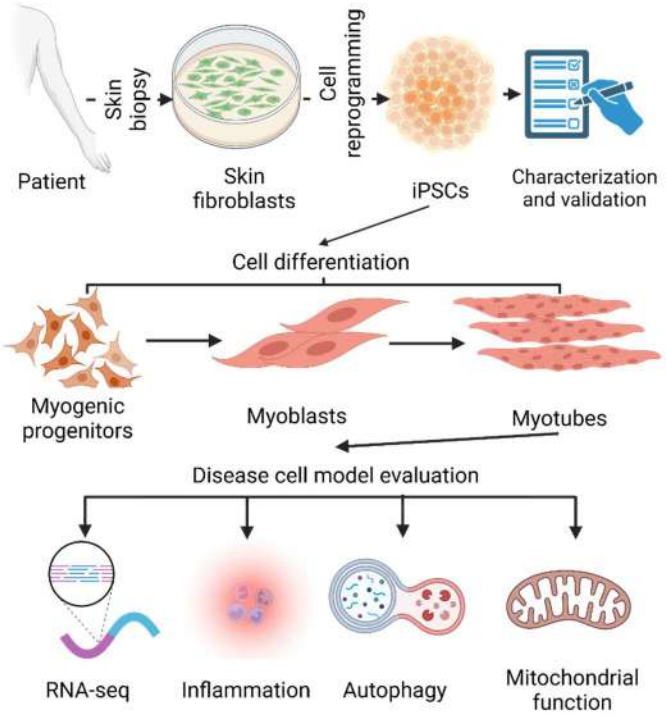

Figure 1. Flowchart: Obtaining iPSCs from fibroblasts and differentiation into muscle cells. First, a skin biopsy is taken from IBM patients and CTLs and fibroblasts grow. Fibroblasts are reprogrammed into iPSCs, which are characterized to validate their pluripotency. Afterwards, iPSCs are differentiated into muscle cells, from myogenic progenitors to myoblasts to myotubes. Differentiated myotubes are phenotyped at RNA-seq and functional level (inflammation, autophagy and mitochondrial function) to examine if they are an appropriate disease model for IBM. Abbreviations: iPSCs: induced pluripotent stem cells; IBM: inclusion body myositis; CTL: healthy individuals.

First, the obtaining of iPSCs from IBM and CTL fibroblasts (and 1 PBMC sample) was performed using the transgene-free mRNA Sendai virus approach. This viral vector contains OSKM factors, needed for activating the pluripotency status in the cell.

To characterize the newly formed iPSCs, we checked their pluripotency, embryoid body (EB) formation, G-band karyotype, short tandem repeat (STR) fingerprinting, mycoplasma absence and transgene clearance. Details of these data are found in Fig. 2, in the Methods section, in Supplementary Fig. 1 and 2, and Supplementary Tables 1, 2 and 3.

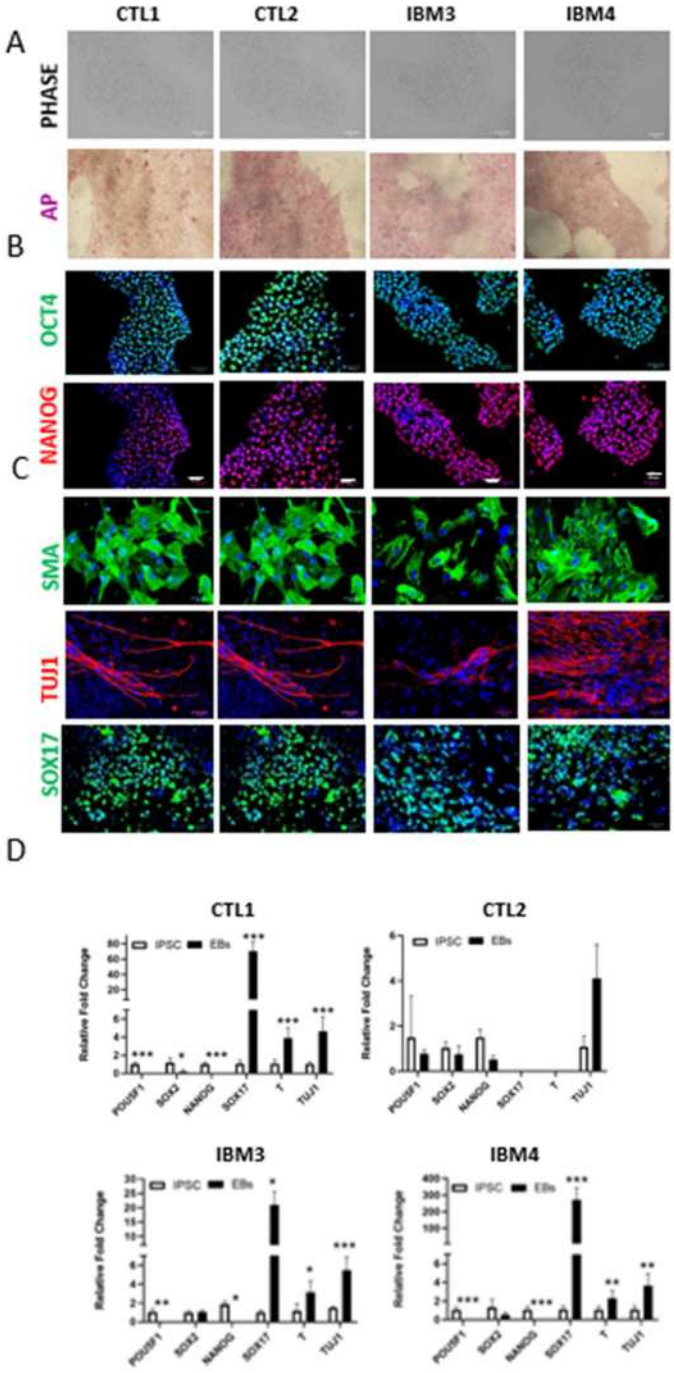

Figure 2. Characterization of 2 IBM and 2 CTLs iPSC lines. A) Phase contrast and alkaline phosphatase images. Scale bar 200 µM. B) Immunodetection of pluripotency markers Oct4 and Nanog. Scale bar: 200 mm. C) Expression of three germ layer markers by immunofluorescence analysis of *in vitro* Embryoid Bodies differentiation cell cultures using specific antibodies against the endodermal marker SOX17, mesodermal marker SMA, and ectodermal marker TUJ1. Nuclei were stained with DAPI. Scale bar: 100 mm. D) Expression levels of pluripotency (POU5F1, SOX2, NANOG) and early lineage markers (SOX17, T, TUJ1) determined by real-time PCR in the iPSC lines and in those same lines differentiated to embryoid bodies. The characterization of the other 2 IBM and 2 CTL lines is represented in Supplementary Figure 1.

All tests were successful for IBM vs. CTL samples with the exception of transgene clearance in IBM1 and IBM2, which kept the sendai virus, KOS and c-Myc vectors after multiple passages and temperature inactivation (39ºC) (Supplementary Fig. 1E). However, these 2 samples did not display aberrant gene expression or functional alterations, so they were included in the study. This event also happened to Mournetas *et al.* 2022 [12], that neither reported apparent consequences on cell phenotyping.

Once the iPSCs were validated, they were derived to skeletal muscle cells using small molecules and growth factors following a protocol validated by Caron *et al.* 2016 [14].

To ensure the successful obtaining of differentiated iPSC-myotubes we performed a qPCR with the following genes: MYOG, MYOD, Desmin and MHC-I (Fig. 3A) and immunofluorescence of sarcomeric anti-α-actinin (Fig. 3B) for all the samples. Although the expression of skeletal muscle markers and positive sarcomeric anti-α-actinin staining in myotubes revealed their muscle maturity.

A

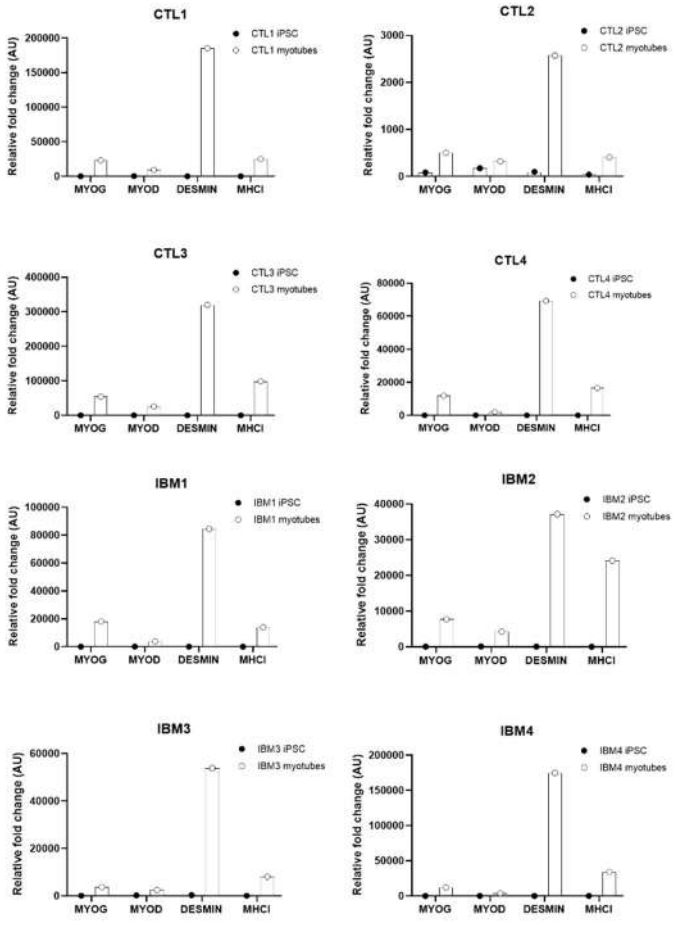

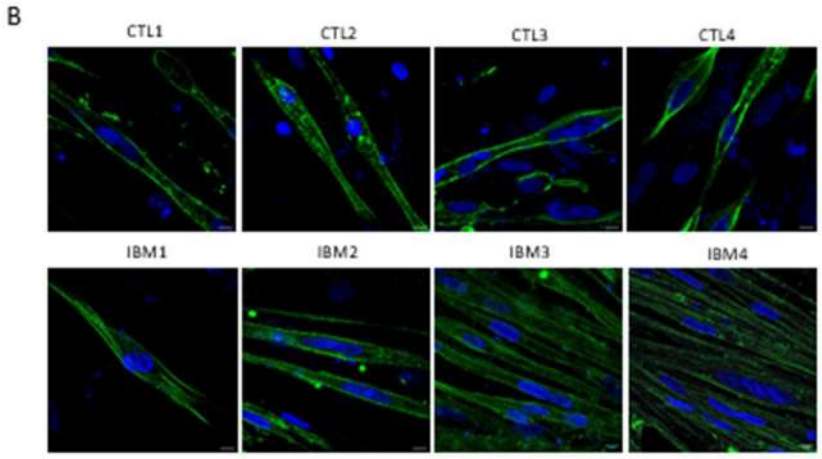

Figure 3. Characterization of iPSC-differentiated myotubes in IBM vs CTL lines. A) Expression levels of muscle markers (MYOG, MYOD, Desmin, MHCI) determined by real-time PCR in the iPSC lines and in those same lines differentiated to myotubes. B) Immunodetection of sarcomeric α.-actinin. Nuclei were stained with DAPI. Scale bar: 10 μm.

Gene expression profile of iPSC-myotubes in IBM vs. CTL samples

Once the *in vitro* model of iPSC-myotubes was successfully characterized, we started the phenotyping of IBM vs. CTL myotubes for IBM hallmarks. The first step was a mRNA-seq analysis. In the principal component analysis (PCA) we observed both cohorts separate according to PC1 (with the exception of IBM1) and PC2 (Fig. 4A), clustering patients apart from controls. In the heatmap, the top 50 genes with the most differential expression between IBM vs. CTLs were represented, 3 downregulated while 47 upregulated (Fig. 4B). The downregulated genes in the heatmap are MEIS1, required for hematopoiesis, megakaryocyte lineage development and vascular patterning and plays a crucial role in normal development; FAM131B, involved in MAPK signaling; and CD24, involved in the control of autoimmunity.

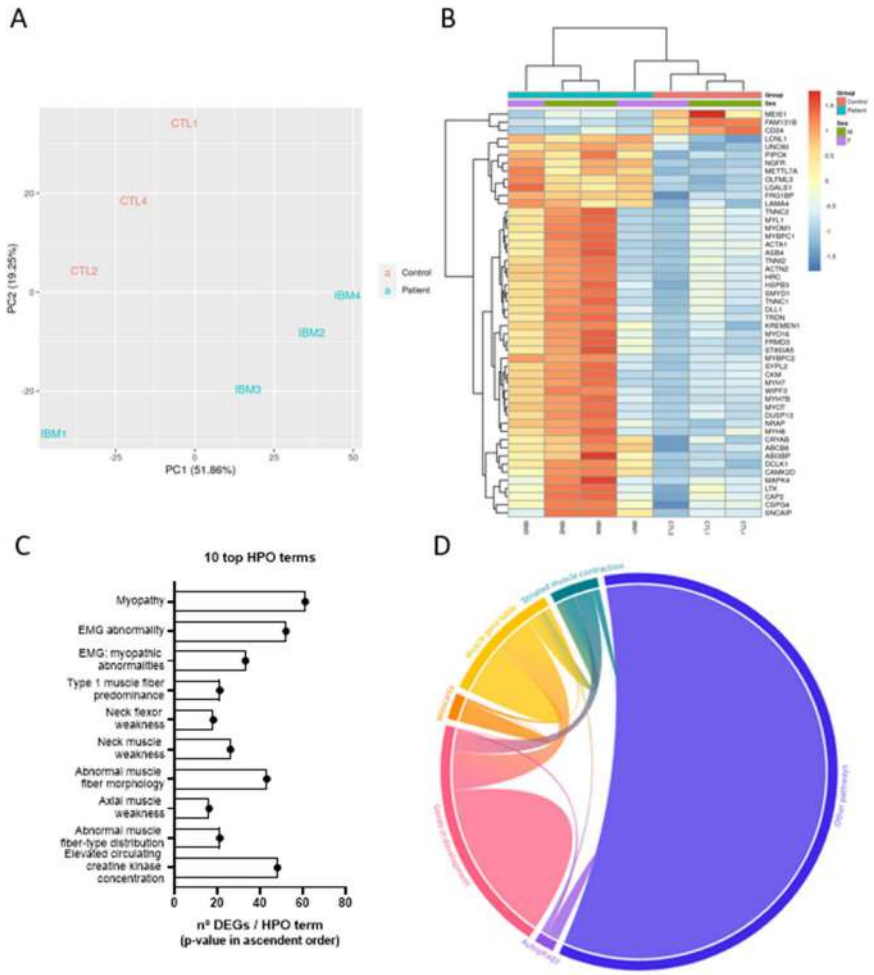

Figure 4. RNA-seq in differentiated myotubes from IBM vs CTL lines. A) Principal component analysis (PCA). B) Heatmap of the top 50 differentially expressed genes (DEGs) in IBM vs CTLs. C) Top 10 HPO terms. D) Chords diagram of the targeted RNA-seq analysis. Each pathway is represented in a different color.

The other 47 upregulated genes in the heatmap mainly belonged to the muscle function, development and cell function clusters (Fig. 4B). 20/50 top genes were related to muscle function, many of them related to muscle contraction, including troponins (TNNC1, TNNC2) and calcium regulation and sarcoplasmic reticulum related genes (TRDN, TNNI2, HRC)[15]. 4/20 muscle function genes were myopathy-related genes, like TNNI2, MYH7 (in myosin storage myopathy), MYOT (in limb-girdle muscular dystrophy and myofibrillar myopathies) and ACTA1 (nemaline myopathy and multiple congenital myopathies)[16]. MYH8, predominantly expressed in fetal skeletal muscle; and SMYD1, involved in myoblast and myotube differentiation, belong to the muscle function and development gene clusters. Developmental genes account for 10/50 top DEGs. 11/50 top DEGs are responsible for multiple cell functions including SNCAIP, although low expressed in muscle, it interacts with alpha-synuclein in neuronal tissue and may play a role in the formation of cytoplasmic inclusions and neurodegeneration [17].

In the total mRNA-seq, there were 875 DEGs with p-value adj <0.05 and |log2FC| ≥ 2 between IBM and CTL myotubes, 654 upregulated and 221 downregulated genes (Supplementary Table 4). In a gene ontology (GO) enrichment analysis, the muscle function and developmental gene clusters were the most represented in the mRNA-seq, in the biological process (BP), cell compartment (CC) and molecular function (MF) GO

database. In the human phenotype ontology (HPO), the top HPO terms were related to myopathy, including muscle weakness and abnormal muscle fibers (Fig. 4C). KEGG, Reactome and Wiki Pathways databases confirmed the findings related to altered muscle function.

All the DEGs, gene clusters and pathways related to myopathy and muscle functions display clinical manifestations of IBM. For instance, when we examined those DEGs present in the Muscle gene table of muscular diseases [18], we found 85 DEGs, including ACTN2, COL6A3 and MYOD1, causal genes of myopathies like distal myopathy, Bethlem myopathy and congenital myopathy, respectively. Also, as mentioned before in the heatmap, multiple DEGs were related to muscle contraction. Thus, we examined the striated muscle contraction pathway, containing 41 genes in the Pathcards database [19], and found that 26 out of 41 were deregulated in IBM vs. CTL iPSC-myotubes, confirming the altered muscle contraction in this cell model, by mRNA-seq. We did the same for developmental genes [20] and found 177 DEGs matching the list in the RNA data set. All DEGs from the above-mentioned pathways are found in Supplementary Table 5.

When we delved into the specific molecular and pathophysiological alterations of IBM in muscle, we performed a targeted search for the genes and pathways involved in inflammation, degeneration and mitochondria. The list of the DEGs involved in these functions is found in Supplementary Table 5 and in Fig. 4D.

We only found 1 DEG related to inflammation (IL11), revealing the absence of inflammation in the gene expression profile of these cells. In autophagy, we found 15 DEGs: 2 related to the amyloid precursor protein (APP) processing, PAWR and PSEN2, the first involved in the progression of age-related diseases and the second causal of an inherited form of Alzheimer's disease. BDNF, whose expression is reduced in Alzheimer's, Parkinson's, and Huntington's disease patients, is also downregulated in this IBM group. LMNA, upregulated, is required for normal development of peripheral nervous system and skeletal muscle and for muscle satellite cell proliferation. DEPTOR, negative regulator of mTORC signaling, and MAP1LC3C, involved in antibacterial autophagy, are also upregulated. Related to mitochondrial function, 21 DEGs matched the ones in the Mitocarta 3.0 [21], including ACADS, ACACB and HSD17B8, involved in fatty acids metabolism, CHCHD10, SMDT1 and COX6A2, involved in mitochondrial structure and function [21,22]. Specifically, CHCHD10 is part of the cristae structure, SMDT1 in a calcium channel in the mitochondrial inner membrane, and COX6A2 as the terminal enzyme of the MRC that catalyzes the electron transfer from cytochrome c to oxygen. PRXL2A, involved in redox regulation of the cell, and CKMT2, responsible for the transfer of high energy phosphate from mitochondria to creatinine (cytosolic carrier), are also among the DEGs related to the Mitocarta 3.0 [21].

Overall, we found a clear pattern of deregulated gene expression in IBM iPSC-myotubes with trends towards myopathy-related alterations in the mRNA-seq, revealing that the clinical symptoms of IBM are expressed in these myotubes. At molecular level, the impairment of degeneration and mitochondrial-related genes was present in this model, but inflammation was almost absent.

Similar Inflammatory Profile in IBM vs. CTL iPSC-myotubes

To examine the inflammatory profile in a functional test, we performed a cytokine protein array with 80 cytokines, containing inflammatory and regulatory cytokines, using the supernatant of myotubes 72h in culture. The secreted cytokines displayed an

upregulated pattern for 52.5% of the molecules in IBM (Fig. 5A), while 47.5% were reduced (Fig. 5B). The ratio of the mean IBM vs. mean CTL concentration per cytokine is displayed in Fig 5.

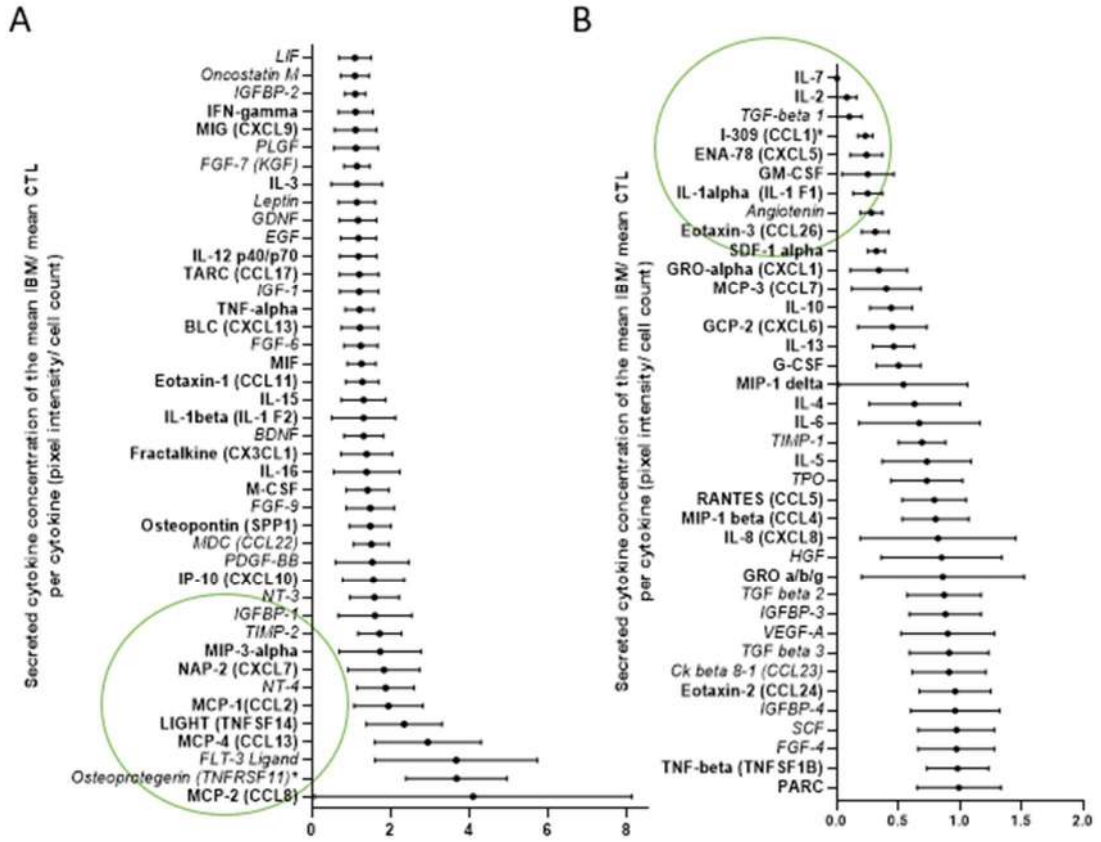

Figure 5. Secreted cytokines in the supernatant of IBM vs CTL differentiated myotubes. A) Upregulated cytokines, the top 10 ones are highlighted. B) Downregulated cytokines, the lowest 10 ones are highlighted. In bold, inflammatory cytokines, in italics, regulatory cytokines including the ones involved in development, differentiation and proliferation. *p-value<0.05.

Among the cytokines, 60% of them are inflammatory cytokines (mostly pro-inflammatory, except IL-4, which is anti-inflammatory); and 40% of them are related to development, growth or differentiation. We referred to the last type of cytokines as regulatory cytokines. In general, pro-inflammatory cytokines are in the top and the lowest expressed clusters (circled in Fig. 5), while regulatory cytokines appear more conserved. In numbers, 28.75% of inflammatory cytokines were 1.7-fold increased, and 31.25% of them reduced with a FC of 0.52. Regulatory cytokines, 23.75% were 1.46-fold increased and 16.25% of them reduced with a FC of 0.77. The top 10 increased cytokines are six inflammatory vs. four regulatory cytokines. Among the inflammatory ones, five are chemokines, MCP-2 (CCL8), MCP-4 (CCL13), MCP-1 (CCL2), NAP-2 (PPBP) and MIP-3α (CCL20), chemoattractants of different immune cell types and LIGHT (TNFSF14) cytokine, is involved in T-cell proliferation and IFNγ production [16]. The regulatory cytokines, Osteoprotegerin (TNFRSF11B) is involved in organogenesis, FLT-3 and NT-4 (NTF4) in cell differentiation and TIMP-2 in tissue homeostasis. The 10 lowest expressed cytokines, 8 of them are inflammatory vs. 2 regulatory cytokines. Among the inflammatory cytokines, IL-7, involved in T-cell survival; IL-2 in the proliferation of T and B lymphocytes, IL-1α in inflammatory and apoptotic response; SDF-1 (CXCL12) in inflammatory response and tissue homeostasis, GM-CSF (CSF2) in growth and

differentiation of hematopoietic precursor cells, and I-309 (CCL1), Eotaxin-3 (CCL26) and ENA-78 (CXCL5) in the recruitment of monocytes, eosinophils and basophils, and neutrophils, respectively. The regulatory cytokines Angiogenin (ANG) and TFG-b1, play a role in vascularization and cell proliferation and differentiation, respectively.

Despite cytokine secretion showed deregulated expression pattern in IBM patients and IBM is an inflammatory myopathy, no clear proinflammatory profile was observed. These molecular data confirmed the lack of inflammation at functional level in this *in vitro* model, previously observed by transcriptomic means.

Degeneration and Autophagic Changes in IBM vs. CTL iPSC-myotubes

The functional degenerative profile was analyzed by checking the activity of the autophagy process in iPSC-myotubes in basal vs. treated conditions (6h under bafilomycin A1 treatment). First, we checked the formation and accumulation of autophagosomes visually, through an immunofluorescence of LC3 marker. In basal conditions, it appeared a similar number of autophagosomes in IBM vs. CTL (accumulated green dots) (Fig. 6A), while at 6h under bafilomycin A1 treatment, slightly more autophagosomes were accumulated in the CTL cohort, suggesting that IBM might have some impairment that hampers the closure of autophagosomes and thus, the autophagic flux is reduced in IBM iPSC-myotubes.

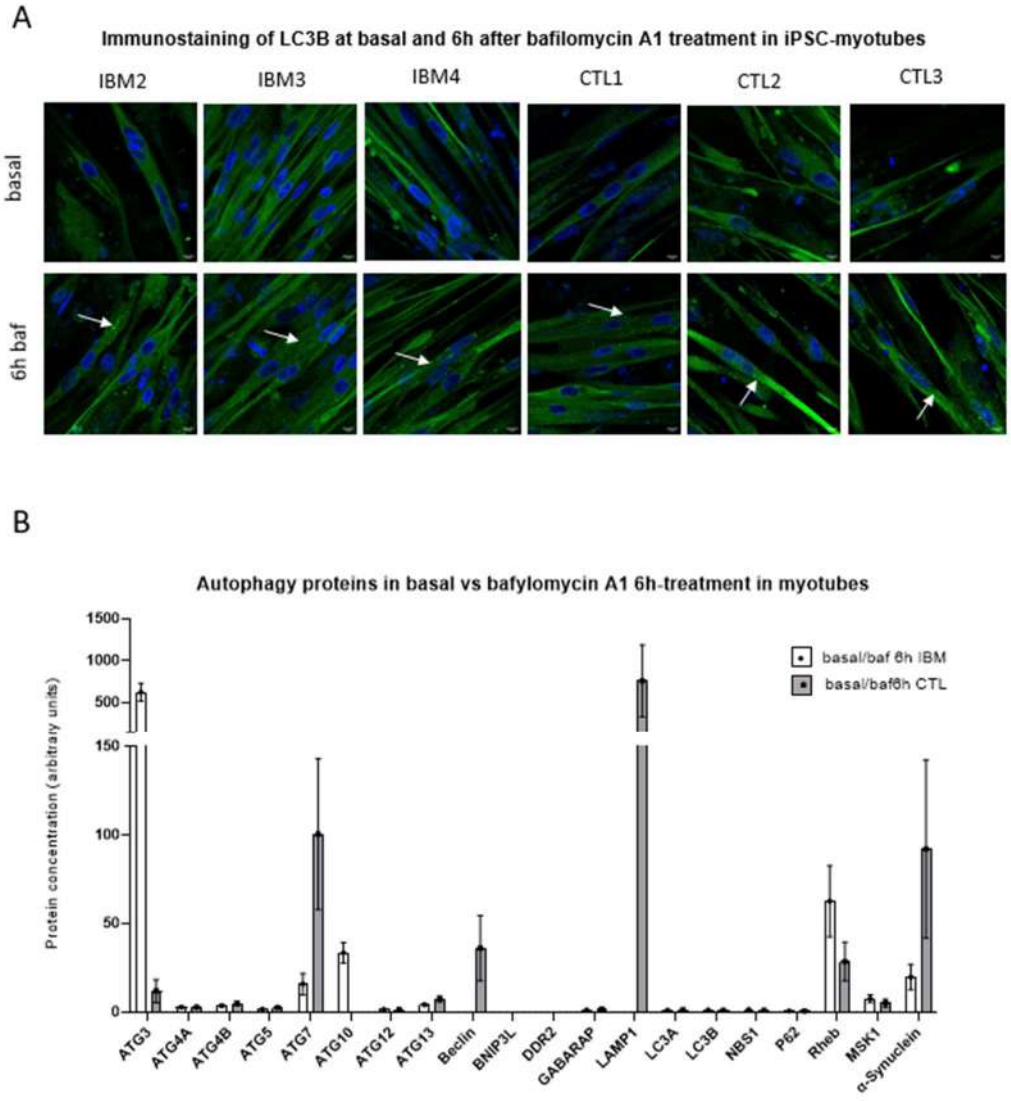

Figure 6. Autophagy profile in IBM vs CTL myotubes. A) Immunostaining of LC3 autophagosome marker at basal conditions vs. 6h-bafilomycin A1 treated myotubes. Arrows pointed the accumulated autophagosomes (green dots). Scale: 10 μM. B) Autophagy proteins concentration in basal vs. bafilomycin A1 treatment in IBM vs. CTL.

Later, we wanted to check the protein levels of an extended number of mediators regulating autophagosome formation and accumulation, so we performed an autophagy protein array with 20 mediators, in basal vs. treated conditions (6h under bafilomycin A1 treatment, as before). The representative graph (Fig. 6B) contains the ratio of basal vs. treated concentrations for each protein in the IBM vs. CTL cohorts. In IBM, the similar concentration of mediators before and after the blockage of the process displays a reduced autophagic flux, suggesting that autophagy is less active in IBM. In detail, ATG7, Beclin, LAMP1 and α-synuclein accumulation, observed in CTLs, are absent in IBM iPSC-myotubes. ATG7 promotes mitophagy, to decrease oxidative stress, and it is involved in glucose metabolism. Beclin is involved in the initiation of autophagy, endocytosis and inside mitochondria, in apoptosis. LAMP1 is involved in lysosome biogenesis. α -synuclein acts as a chaperone of the SNARE complex (vesicular transport of secretory components)[16,22]. In IBM, ATG3, ATG10 and Rheb are increased. ATG3 is involved in autophagy related cell death and mitochondrial homeostasis when bound to ATG12; Rheb activates mTORC1, which inhibits autophagy, and ATG10 participates in the autophagosome formation. This reveals that in IBM, the autophagosome formation process starts (high ATG10) but after that, the process is somewhere impaired or blocked, and apoptosis (ATG3) or mTORC pathway (Rheb, inhibits autophagy) reinforce the idea of autophagy not highly activated at later stages. In CTLs, basal autophagy is more active, and the difference is higher when the process is blocked by bafilomycin A1, also in mitochondria (ATG7, Beclin). A lower activity of basal autophagy is often linked to senescence, so IBM profile could suggest an accelerated aging phenotype in relation to autophagy, as previously observed by LC3-immunofluorescence staining of cells.

Mitochondrial function is altered in IBM vs. CTL iPSC-myotubes

The mitochondrial phenotype was first analyzed by measuring the oxygen consumption in the mitochondrial respiration. A Mito Stress test revealed similar respiratory profile in IBM vs. CTL myotubes (Fig. 7A). In detail, basal respiration, ATP production, H+ leak, coupling efficiency, maximal respiration and spare respiratory capacity were also similar between cohorts. In alignment with this results, oxidative stress, as a result of oxygen consumption or ROS detoxification, was also conserved in terms of antioxidant capacity (Fig. 7B). However, we found a significant lactate secretion on iPSC-myotubes (Fig. 7B) together with slightly reduced COX enzymatic activity from the MRC in IBM, along with the COX/CS ratio (Fig. 7C).

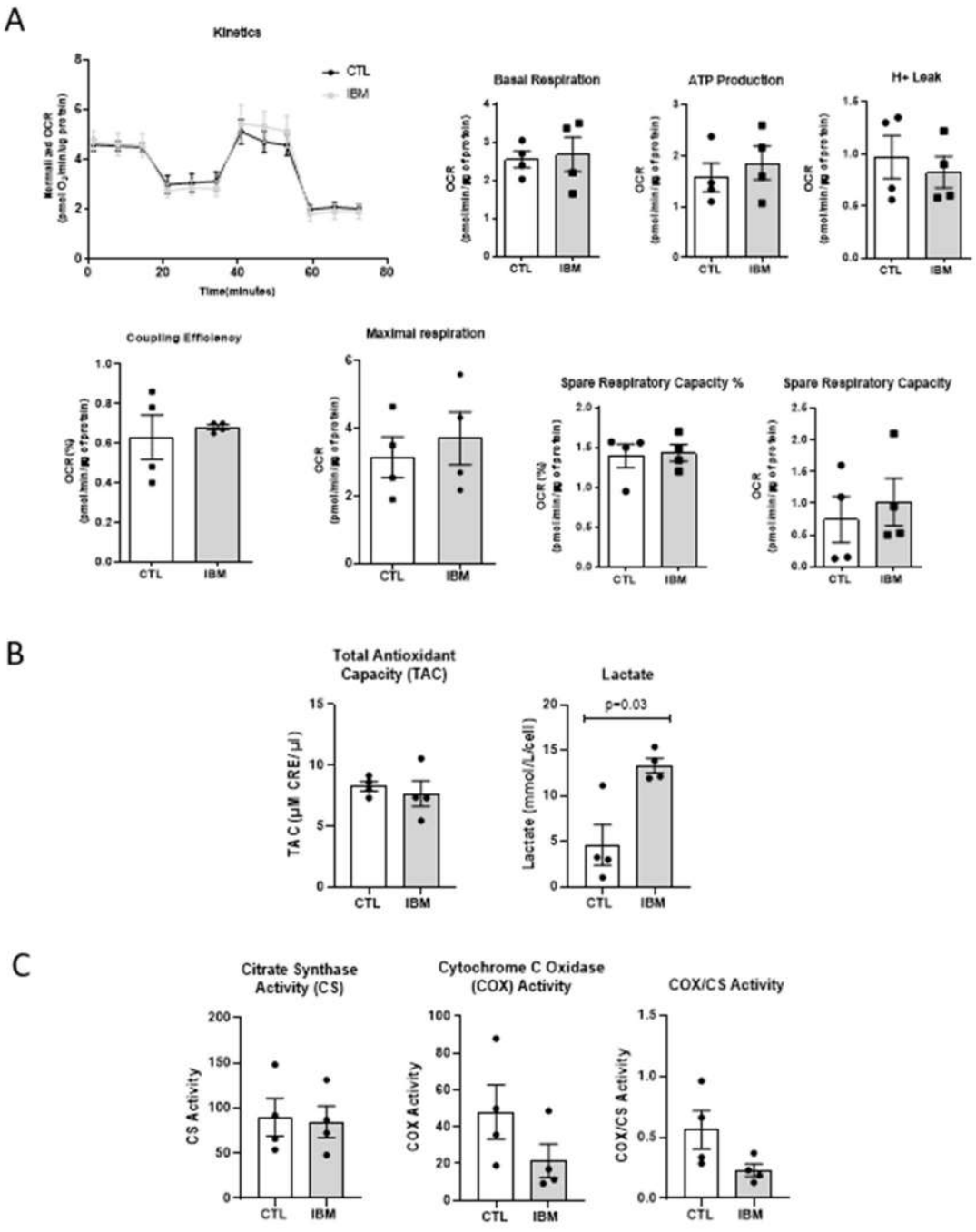

Figure 7. Mitochondrial profile in IBM vs. CTL myotubes. A) Mitochondrial respiration represented by kinetics, basal respiration, ATP production, H+ leak, coupling efficiency, maximal respiration and spare respiratory capacity in IBM vs. CTLs. B) Total antioxidant capacity (TAC) and lactate secretion in IBM vs. CTLs. C) Citrate synthase (CS) activity and cytochrome c oxidase activity (COX) and COX/CS ratio.

Despite we found no differences in the mitochondrial respiration profile or antioxidant defense, there is an overall mitochondrial dysfunction evident through decreased mitochondrial COX/CS activity and significantly increased lactate secretion.

MATERIALS AND METHODS

1. *Study design and sample inclusion*

A case-control study was conducted from 2018 to 2022, in the Department of Internal Medicine from Hospital Clínic of Barcelona (Barcelona, Spain), including 4 patients and 4 age and sex-paired healthy volunteers (Table 1). IBM patients were diagnosed according to clinical and pathological tests performed in our hospital, after fulfilling the criteria proposed by the European Neuromuscular Centre for IBM diagnosis [23]. IBM patients and healthy volunteers signed the informed consent previously approved by the Ethical Committee of our hospital (code HCB/2019/0558), and by the regional and national ethical committees.

2. *Generation of iPSC*

Cell Reprogramming

Fibroblasts derived from seven skin punch biopsy were cultured in 5 mM glucose DMEM supplemented with 10% FBS and 1% penicillin-streptomycin, at 37 ◦C, in a humidified 5% CO_2 air incubator (all from Gibco, Waltham, MA, USA). PBMCs were isolated from total blood using Lymphoprep™ (#07801, Stemcell, Vancouver, Canada) density gradient. Fibroblasts at passage 4 and PBMCs were transduced with Cytotune_iPS 2.0 Sendai Reprogramming kit (A16518, ThermoFisher Scientific, Waltham, MA, USA) following manufacturer's instructions. Isolated iPSCs were cultured on Geltrex (A1413202, Gibco, Waltham, MA, USA) coated 6-well plates in mTeSR1 (85850, StemCell Technologies, Vancouver, BC, Canada). All the iPSC lines were passaged to passage 12 or higher with TrypLE Express (12604013, Gibco Waltham, MA, USA) for full characterization (Supplementary Table 1 and 2).

Pluripotency validation

Alkaline Phosphatase Staining Kit (Abcam 242286) was used to detect alkaline phosphatase activity. For immunofluorescence staining, iPSCs were fixed in 4% PFA for 15 min, permeabilized with 0.1% Triton X-100 (Sigma) for 15 min, blocked for 1 hour in 1% BSA-DPBS, and incubated overnight at 4ºC with the respective primary antibodies against OCT4 and NANOG (Supplementary Table 3). Alexa Fluor 488 or 555-conjugated secondary antibodies (Fisher Scientific) were used to visualize the immunoreactivity and DAPI for cell nuclei (Life Technologies). Cells were imaged under the Zoe Fluorescent Cell Imager (Bio-Rad). qRT-PCR reaction was performed on the iCycler (Bio-Rad), Fast SYBR Green Master Mix (Bio-Rad) and specific primers (Supplementary Table 3) were used to quantify the expression of endogenous OCT4, SOX2, and NANOG, which were normalized with GAPDH as an internal control and relative fold change with respect to the iPSCs.

Three germ layer differentiation

Differentiation of the three germ layers was demonstrated by using the EB assay. For spontaneous differentiation through EB formation, iPSCs derived cells were dissociated by TrypLE™ Express (Gibco) treatment and 40,000 cells per well were transferred to low attachment 96-well plates (Costar, Corning) in Knockout DMEM supplemented with 20% Knockout serum replacement, non-essential amino acids, L-glutamine, penicillin/streptomycin (all from Thermo Fisher Scientific) and b-mercaptoethanol (Sigma-Aldrich) and 10 μM of thiazovivin or Rock inhibitor (S1049, Selleck, Houston, TX, USA). Cell aggregates (EBs) were cultured for a total of 16 days with media exchanges every other day. EBs were manually harvested at day 16. mRNA from the collected EBs

was extracted using the RNeasy Micro kit (Qiagen). 1µg of RNA was reverse transcribed with the High-Capacity cDNA Reverse transcription kit (Applied Biosystems). Diluted cDNA was used for gene expression analysis by qPCR (see Supplementary Table 3 for oligo sequences).

In parallel, some EBs were transferred, after 8 days in suspension culture, to geltrex-coated plates and cultured in the same medium for another 8 days for immunostaining of the three lineage markers. Immunohistochemistry analysis of the EBs showed the presence of SOX17 (endoderm), TUJ1 (ectoderm) and SMA (mesoderm) markers (Fig. 2C, Supplementary Fig. 1C). Gene expression assay of the EBs also showed high expression levels of the endoderm marker (SOX17), ectoderm marker (TUJ1) and mesoderm marker (T) with respect to the undifferentiated state which presented high expression of the pluripotency genes (POU5F1, NANOG and SOX2) (Fig. 2D and Supplementary Fig. 1D).

FACS analysis

Pluripotency was analyzed by flow cytometry for the expression of SSEA-4, SSEA-3, TRA 1-60 and TRA 1-81 (Supplementary Fig. 2A). Cells were dissociated with TrypLE express (Gibco) and incubated with the antibodies at 4 °C for 20 min. After two washes, cells were acquired on a FACS Canto II flow cytometer equipped with FACS Diva analysis software (Becton Dickinson, San Jose, CA, USA).

DNA Fingerprinting analysis (STR analysis)

DNA Fingerprinting analysis was assessed at 16 independent markers from highly polymorphic STR sequences of DNA (CSF1PO, D2S1338, D3S1358, D5S818, D7S820, D8S1179, D13S317, D16S539, D18S51, D19S433, D21S11, FGA, TH01, TPOX, vWA, AMEL (Amelogenin, gender marker) using AmpFlSTR® Identifiler® Plus PCR Amplification Kit and GeneMapper ID software (Applied Biosystems) in fibroblasts and PBMCs (before reprogramming) and iPSCs (Supplementary Table 2).

Transgene-free confirmation

Total RNA from cells were extracted from iPSCs with RNeasy Mini Kit (Qiagen), and reversely transcribed to single strand cDNA with High-Capacity cDNA Reverse Transcription Kit (Applied Biosystems). The cDNA was diluted 1:10 and amplified by PCR with MyFi DNA Polymerase (Bioline) under specific primers against OSKM factors (primers sequences in Supplementary Table 3).

Mycoplasma detection

Endpoint PCR using mycoplasma specific primers (in Supplementary Table 3) and iPSC cell culture supernatants was used to detect absence of mycoplasma contamination.

Karyotype analysis

Karyotype of the reprogrammed iPSCs lines was done by the Inborn Errors of Metabolism Service from the Clinical Biochemistry Institute (Hospital Clinic of Barcelona) around passage 15. Twenty G-banded metaphase cells per sample were analysed by cytogenetic analysis. All cells demonstrated a normal female or male karyotype (Supplementary Fig. 2B).

3. Obtaining iPSC-myotubes

iPSC differentiation to myotubes using growth factors

iPSCs skeletal muscle differentiation was performed in a 5% CO_2 incubator, by using the commercially available Genea Biocells skeletal muscle differentiation kit (SKM-KIT, San Diego, CA, USA), following manufacturer's protocol [14]. Briefly, iPSCs were plated at 5000 cells/cm^2 onto collagen I-coated plates (#5005-100mL, Advanced BioMatrix, Carlsbad, CA, USA) and maintained for 7 days in skeletal muscle induction medium (SKM01). At day 7, cells were dissociated with 0.05% TrypLE Express (12604013, Gibco Waltham, MA, USA), plated at 5000 cells/cm^2 onto collagen I-coated plates, and maintained for 7 days in skeletal myoblast medium (SKM02). After 14 days of differentiation, cells were attained and incubated in myotube fusion medium for 7 days (SKM03+). At day 7, characterization and functional experiments were performed. The differentiation protocol was performed 3 times in each sample.

Characterization of differentiated myotubes with qPCR and immunofluorescence of muscle-associated markers

Myoblasts were seeded in a 96-well glass slide (Greiner BioOne Cell Star Uclear #655090, Nürtingen, Germany) coated with collagen type I (#5005-100mL, Advanced BioMatrix, Carlsbad, CA, USA) for 7 days with myoblast media (SKM02) plus 7 days with myotube fusion media (SKM03+) for cell differentiation at 37ºC with 5% CO_2. Myoblasts were stained with a monoclonal sarcomeric anti-α-actinin (A7811 Millipore Sigma, Burlington, MA, USA) and Alexa Fluor 488 donkey anti-mouse IgG antibody (Invitrogen A-21202, Life Sciences Europe, NL), counterstaining with DAPI. Images were obtained with a Zeis LSM 880 laser scanning confocal system using a 63X oil immersion objective.

GoTaq® qPCR Master Mix (A6001, Madison, WI, USA) and specific primers (Supplementary Table 3) were used to quantify the expression of desmin, myoD, myoG, and MHC-I at day 7 in myotubes, normalized with GAPDH as an internal control.

4. Phenotyping iPSC-myotubes for IBM muscle hallmarks

RNA extraction and mRNA library preparation and sequencing

Total RNA was isolated from cell lysates (2 million of cells) of 4 IBM and 4 CTL myotubes using RNeasy Mini Kit (Qiagen, Hilden, Germany), according to the manufacturer's protocol. Total RNA content was assessed through Quawell UV-Vis Spectrophotometer Q5000. Concentrations were adjusted to 100 ng/uL in RNase-free water. The quality control of the total RNA was done using the Qubit® RNA HS Assay (Life Technologies) and RNA 6000 Nano Assay on a Bioanalyzer 2100 (Agilent, Santa Clara, CA, USA). The RNASeq libraries were prepared using the TruSeq®Stranded mRNA LT Sample Prep Kit. 500ng of total RNA were enriched for the mRNA fraction and fragmented. Strand-specificity was achieved by the second-strand cDNA incorporating dUTPs instead of dTTPs. Adenylation of the 3' blunt-ends double stranded cDNA and ligation to previously added Illumina platform adaptors (with unique dual indexes and unique molecular identifiers) (Integrated DNA Technologies). The ligation product was enriched with 15 PCR cycles and the final library was validated on an Agilent 2100 Bioanalyzer with the DNA 7500 assay. The libraries were sequenced on HiSeq 4000 (Illumina) with a read length of 2x51bp using the HiSeq 4000 SBS kit (Illumina). Primary data analysis, image analysis, base calling and quality scoring of the run were processed using the

manufacturer's software Real Time Analysis (RTA 2.7.7) followed by generation FASTQ sequence files.

RNA-seq data processing and analysis

RNA-seq reads were mapped against human reference genome (GRCh38) using STAR software version 2.5.3a [24] with ENCODE parameters. Annotated genes were quantified using human GENCODE annotation file version 34 with RSEM v1.3.0 [25] and default parameters. Differential expression analysis was performed with DESeq2 v1.26.0 R package [26] using a Wald test to compare affected and control groups, adjusting for sex in the model. Genes were considered differentially expressed with an adjusted p-value < 0.05 and absolute fold change |FC| > 1.5. A Gene Ontology enrichment analysis was generated with the significant genes using gProfileR v.07.0 [27]. Additionally, a GSEA was performed with a list of pre-ranked genes by the Wald statistic, using fgsea R package v1.12.0 [28] and the Reactome pathways database. PCA plot was generated with regularized log transformed (rlog) counts, considering only the top 500 most variable genes. Heatmap plot also represents rlog counts to show scaled expression of the top 50 DEGs. These plots were generated using ggplot2 v0.1.8 [29] and pheatmap R packages, respectively. The Pathcards database [30], Gene a la Cart [16], Mitocarta 3.0 [21], Muscle gene table [31], Autophagy [32] and development [20] gene lists were used to relate DEGs to the pathways of interest.

Inflammatory cytokine array

Cell culture supernatants of myotubes at day 7 after 72h in culture were loaded in the Human Cytokine Antibody Array C5 (AAH-CYT-5-8, RayBio® C-Series, Atlanta, GA, USA), for detecting 80 human cytokines. Supernatants were incubated overnight at 4ºC and detected by chemiluminescence, using the Image Quant TL Software (GE Healthcare), and calculated by AAH-CYT-5-8 analysis tools provided by RayBiotech, Inc. (Atlanta, USA). The results were normalized by the cell count in each supernatant.

Immunofluorescence for autophagosome characterization

Myoblasts were seeded in a 96-well glass slide (Greiner BioOne Cell Star Uclear #655090, Nürtingen, Germany) coated with collagen type I (#5005-100mL, Advanced BioMatrix, Carlsbad, CA, USA) for 7 days with myoblast media (SKM02) plus 7 days with myotube fusion media (SKM03+) for cell differentiation at 37ºC with 5% CO_2. In some samples, degradation of autophagolysosomes was blocked by adding 100nM bafilomycin A1 from Streptomyces griseus (Sigma-Aldrich® #B1793 SIGMA, Missouri, USA) for 6 hours vs. untreated samples (basal conditions). Autophagosomes were stained with anti-LC3 pAB (MBL International® #PM036, Massachusets, USA) and donkey anti-rabbit Alexa Fluor® 488 IgG antibody (Life Technologies Europe, NL), counterstaining with DAPI. Images were obtained with a Zeiss LSM 880 laser scanning confocal system using a 63X oil immersion objective.

Autophagy protein array

Two cell lysates were obtained from each IBM and CTL myoblast sample. One lysate was obtained under basal conditions and the other at 6h under 10nm bafilomycin A1 (B1793, Sigma, Burlignton, MA, USA) treatment at 37ºC. Each lysate (250 µg of protein) was loaded in the RayBio® C Series Human Autophagy Array 1 (Cat#: AAHATG-1-8, RayBiotech, Inc., Atlanta, GA, USA), incubated overnight at 4ºC and detected by chemiluminescence, using the Image Quant TL Software (GE Healthcare), and calculated by AAH-ATG-1 analysis tools provided by RayBiotech, Inc. (Atlanta, USA).

Mitochondrial Respiration

Mitochondrial respiration was measured according to the oxygen consumption of the MRC. The oxygen consumption rate was detected with the XF Cell Mito Stress Test™ (Seahorse-XFe24-Analyzer, Agilent Technologies), according to the manufacturer's protocol and normalized by the protein content of each sample.

Total Antioxidant Capacity (TAC)

TAC was measured in 100 µL of myotube supernatant (at day 7) after 72h in culture using an OxiSelect™ Total Antioxidant Capacity Assay kit (Cell Biolabs Inc., San Diego, CA, USA) by spectrophotometry at 490 nm and normalized by cell count (µM CRE (Copper Reducing Equivalents)).

MRC Enzymatic Activities: COX and CS function

COX and CS enzymatic activities were measured spectrophotometrically in 40 µg of total protein from each myotube sample according to standardized protocols[33], at 37ºC.

Lactate secretion

Lactate quantifications were performed in 100 µL of myotube supernatant (at day 7) after 72h in culture using the epoc® Blood Analysis System (epoc System Software version 3.32.0, Siemens Healthineers Global, Erlangen, Germany). The lactate concentration was normalized by cell count (mmols/L/cell).

5. Statistical analysis

Statistical analysis was performed with the Statistical Package for the Social Sciences software, version 27 (IBM SPSS Statistics; SPSS Inc) and GraphPad Prism 9 (GraphPad Software, San Diego, CA, USA). Results were expressed as mean ± SEM or in fold change between conditions. Obtained data were compared between independent experiments using the non-parametric Mann-Whitney U test or Kruskal-Wallis test. The signification threshold was set at p-value < 0.05.

DISCUSSION

In this study, our aim was to model IBM using an *in vitro* model of myotubes differentiated from iPSCs. The phenotyping of IBM iPSC-myotubes did not fully replicate all the characteristic features observed in the target tissue, in muscle, but recapitulated some of the main hallmarks, reinforcing the value of this model as a platform to study and test novel insights in IBM. The key point about developing this model was to obtain the same cell type as the target tissue: myotubes. To characterize to what extent iPSC-myotubes recapitulated the IBM muscle features, here we evaluated the reprogramming, differentiation, and phenotyping processes to identify the strengths and limitations of this model to aid in studying IBM pathophysiology *in vitro.*

Firstly, the reprogramming of fibroblasts (or other primary cells) to iPSCs has some limitations. The efficiency of reprogramming can vary, resulting in incomplete pluripotency in iPSCs [9]. In such cases, the cell population becomes heterogeneous, with distinct differentiation potentials [34,35]. This heterogeneity makes it challenging to standardize human pluripotent stem cells in culture (PSCs, both iPSCs and ES cells) [34,35]. Nevertheless, significant progress has been made in improving the quality of iPSCs and enhancing the efficiency of generating fully reprogrammed cells.

Reprogramming cells to pluripotency is a powerful tool that allows the generation of multiple iPSC clones from an individual [9].

Secondly, when selecting a stem cell-based model for studying human diseases, several criteria should be considered [10]. iPSC-based models are appropriate for diseases resulting from a single gene (monogenic disorders), exhibiting high penetrance, early onset during development, and a clear cellular phenotype. In such cases, iPSCs successfully display the disease phenotype *in vitro*. On the contrary, for diseases caused by multiple genes (complex disorders), displaying low penetrance, late onset, or involving aberrant morphogenesis in target organs, modeling them using PSCs is more challenging [10]. However, successful modeling of human diseases from all three classes using PSCs has been reported [10]. Examples include monogenic diseases such as Lesch–Nyhan disease [36] and fragile X syndrome [37] , chromosomal diseases such as Down syndrome [38], and complex disorders such as Turner syndrome [39], autism spectrum disorder (ASD) [40] and schizophrenia [41]. These advancements have been particularly promising for complex diseases that are difficult to diagnose prenatally or reproduce through gene editing. These cases are now modelled by reprogramming patient cells into iPSCs or SCNT-ES cells [10].

Thirdly, in terms of differentiation protocols for generating muscle cells, we selected a protocol based on growth factors to mimic the developmental stage. This approach avoids genotoxicity when transforming iPSC into muscle cells. This strategy was effective to obtain functional myotubes in IBM vs. CTL groups within a time-efficient period (around 21 days in culture). However, their survival time in culture was limited to 7-10 days, which may have been insufficient to accumulate additional alterations in the IBM cohort. Indeed, in other cell types, longer differentiation protocols can be used to obtain some mature cell types, including neurons and hepatocytes [10].

Despite that, we successfully differentiated iPSCs from IBM and CTLs into myotubes, as confirmed by the expression of skeletal muscle markers such as sarcomeric α-actinin, myoD, myoG, MHC-I, and desmin. Moreover, we characterized iPSC-myotubes in an untargeted vs. targeted approach, and found that in the gene expression profile, myopathy-related hallmarks pop-up, revealing that clinical alterations were displayed in these IBM myotubes, together with mitochondrial dysfunction and partial autophagic alterations. However, inflammation was absent in the cell model.

The absence of inflammation could be due to the lack of crosstalk mediated by T-cells within myofibers. To address this, a co-culture with IBM lymphocytes or an induction of stress by bacterial toxins (like lipopolysaccharides), could reinforce the inflammatory response in IBM iPSC-myotubes.

In autophagy, some blockage of the process was revealed at gene expression and functional level. The lower accumulation of autophagy proteins in IBM vs. CTLs when the process was blocked suggested that IBM cells may not be synthesizing enough autophagy mediators, and eventually blocking the process.

In mitochondria, mitochondrial respiration and antioxidant defense appeared mostly adequate, but reduced COX/CS activity in IBM and significantly increased lactate levels uncovered mitochondrial dysfunction. Lower COX/CS activity recapitulates this hallmark from the muscle of IBM patients. Considering lactate, it is the molecular marker of non-mitochondrial respiration and the clinical marker of mitochondrial disease. Significantly higher concentration of lactate secretion in the supernatant of IBM iPSC-myotubes revealed that mitochondrial dysfunction is present in this cell model and, IBM myotubes

might need extra source of energy from the anaerobic glycolysis, producing lactate on the process.

A limitation of this study is the limited sample size of n=4 samples per group, given that this is a proof-of-concept study and IBM is a rare disease. Despite that, this is the first attempt to model IBM using iPSCs differentiated myotubes, which reflect some myopathic, autophagic and mitochondrial alterations from this disease. In addition, iPSC-myotubes derived from IBM patients' samples, so they maintain multiple genetic, epigenetic and environmental cues and they are the cell type of the target tissue. The drawbacks are that the cost-effectiveness of the model is high, with complex handling protocols, and time-consuming and expensive experiments. In addition, it lacks inflammation, a key hallmark in IBM. To tackle inflammation and endorse a more degenerative and aged phenotype in IBM iPSC-myotubes, several stimuli could be induced. Indeed, stressors such as hydrogen peroxide, MG-132 and concanamycin A were used to induce ageing-like features of Parkinson disease in iPSC models [10,42]. Another approach is based on expressing aging-related genes, like progerin, a truncated version of the lamin A protein involved in Hutchinson–Gilford progeria syndrome of premature aging [10]. In a study involving Parkinson disease iPSC-derived neurons [43], markers associated with cellular ageing, such as nuclear morphology, heterochromatin markers and DNA damage, disappeared in iPSC-derived neurons, but reappeared when progerin was ectopically expressed in these cells, recapitulating cellular ageing [10]. A similar approach could be applied to our IBM iPSC-myotubes.

The application of iPSCs to *in vitro* disease modeling in various cell types has been widely embraced in the scientific community, as it enables access to invasive tissues through a non-invasive approach [44]. To overcome the limitations of iPSC disease modeling, integrated cell culture systems such as co-cultures or organs 'on-a-chip' designs, could facilitate the interconnection of tissues in a physiologically relevant manner [45,46]. These approaches could bring us closer to achieving more accurate physiological disease models [44], which may be adequate for modeling IBM.

Overall, this proof-of-concept study of IBM iPSC-myotubes revealed that they recapitulate myopathy, mitochondrial and autophagic alterations, and could be a useful model for better understanding IBM pathophysiology, for the identification of biomarkers or as drug screening platforms for potential treatments.

Acknowledgements

We acknowledge the contribution of patients and their families, collaborating to expand the state-of-the-art in rare diseases. We also appreciate the support given by the Advanced Optical Microscopy department of the University of Barcelona.

Funding

This study was supported by Instituto de Salud Carlos III (ISCIII-FEDER, grant PI21/ 00935) and co-funded by the European Union. Additionally, FJG-G is supported by the CIBERER (ISCIII-FEDER), MG-M by CD21/00019 (ISCIII- FSE+).

Conflict of interest

The authors declare that they have no conflict of interest.

REFERENCES

1. Greenberg, S.A. Inclusion Body Myositis: Clinical Features and Pathogenesis. *Nat Rev Rheumatol* **2019**, *15*, 257–272, doi:10.1038/s41584-019-0186-x.

2. Lundberg, I.E.; Fujimoto, M.; Vencovsky, J.; Aggarwal, R.; Holmqvist, M.; Christopher-Stine, L.; Mammen, A.L.; Miller, F.W. Idiopathic Inflammatory Myopathies. *Nat Rev Dis Primers* **2021**, *7*, 1–22, doi:10.1038/s41572-021-00321-x.

3. Cantó-Santos, J.; Valls-Roca, L.; Tobías, E.; García-García, F.J.; Guitart-Mampel, M.; Esteve-Codina, A.; Martín-Mur, B.; Casado, M.; Artuch, R.; Solsona-Vilarrasa, E.; et al. Unravelling Inclusion Body Myositis Using a Patient-derived Fibroblast Model. *J Cachexia Sarcopenia Muscle* **2023**, doi:10.1002/jcsm.13178.

4. Selva-O'callaghan, A.; Pinal-Fernandez, I.; Trallero-Araguás, E.; Milisenda, J.C.; Grau-Junyent, M.; Mammen, A.L. Classification and Management of Adult Inflammatory Myopathies. *Lancet Neurol* **2018**, *17*, 816–828, doi:10.1016/S1474-4422(18)30254-0.

5. Weihl, C.C.; Mammen, A.L. Sporadic Inclusion Body Myositis - a Myodegenerative Disease or an Inflammatory Myopathy. *Neuropathol Appl Neurobiol* **2017**, *43*, 82–91, doi:10.1111/nan.12384.

6. Catalán, M.; Selva-O'Callaghan, A.; Grau, J.M. Diagnosis and Classification of Sporadic Inclusion Body Myositis (SIBM). *Autoimmun Rev* **2014**, *13*, 363–366, doi:10.1016/j.autrev.2014.01.016.

7. Takahashi, K.; Yamanaka, S. Induction of Pluripotent Stem Cells from Mouse Embryonic and Adult Fibroblast Cultures by Defined Factors. *Cell* **2006**, *126*, 663–676, doi:10.1016/J.CELL.2006.07.024.

8. Takahashi, K.; Tanabe, K.; Ohnuki, M.; Narita, M.; Ichisaka, T.; Tomoda, K.; Yamanaka, S. Induction of Pluripotent Stem Cells from Adult Human Fibroblasts by Defined Factors. *Cell* **2007**, *131*, 861–872, doi:10.1016/J.CELL.2007.11.019.

9. Takahashi, K.; Yamanaka, S. A Decade of Transcription Factor-Mediated Reprogramming to Pluripotency. *Nat Rev Mol Cell Biol* **2016**, *17*, 183–193, doi:10.1038/nrm.2016.8.

10. Avior, Y.; Sagi, I.; Benvenisty, N. Pluripotent Stem Cells in Disease Modelling and Drug Discovery. *Nat Rev Mol Cell Biol* **2016**, *17*, 170–182, doi:10.1038/nrm.2015.27.

11. Chal, J.; Oginuma, M.; Al Tanoury, Z.; Gobert, B.; Sumara, O.; Hick, A.; Bousson, F.; Zidouni, Y.; Mursch, C.; Moncuquet, P.; et al. Differentiation of Pluripotent Stem Cells to Muscle Fiber to Model Duchenne Muscular Dystrophy. *Nat Biotechnol* **2015**, *33*, 962–969, doi:10.1038/nbt.3297.

12. Mournetas, V.; Massouridès, E.; Dupont, J.B.; Kornobis, E.; Polvèche, H.; Jarrige, M.; Dorval, A.R.L.; Gosselin, M.R.F.; Manousopoulou, A.; Garbis, S.D.; et al. Myogenesis Modelled by Human Pluripotent Stem Cells: A Multi-Omic Study of Duchenne Myopathy Early Onset. *J Cachexia Sarcopenia Muscle* **2021**, *12*, 209–232, doi:10.1002/JCSM.12665.

13. Moretti, A.; Fonteyne, L.; Giesert, F.; Hoppmann, P.; Meier, A.B.; Bozoglu, T.; Baehr, A.; Schneider, C.M.; Sinnecker, D.; Klett, K.; et al. Somatic Gene Editing Ameliorates Skeletal and Cardiac Muscle Failure in Pig and Human Models of Duchenne Muscular Dystrophy. *Nature Medicine 2020 26:2* **2020**, *26*, 207–214, doi:10.1038/S41591-019-0738-2.

14. Caron, L.; Kher, D.; Lee, K.L.; McKernan, R.; Dumevska, B.; Hidalgo, A.; Li, J.; Yang, H.; Main, H.; Ferri, G.; et al. A Human Pluripotent Stem Cell Model of Facioscapulohumeral Muscular Dystrophy-Affected Skeletal Muscles. *Stem Cells Transl Med* **2016**, *5*, 1145–1161, doi:10.5966/sctm.2015-0224.

15. RefSeq: NCBI Reference Sequence Database. Available online: https://www.ncbi.nlm.nih.gov/refseq/ (accessed on 30 May 2023).

16. GeneALaCart - GeneCards Batch Queries. Available online: https://genealacart.genecards.org/ (accessed on 29 May 2023).

17. GTEX. Available online: https://gtexportal.org/home/ (accessed on 10 March 2023).

18. GeneTable. Available online: https://www.musclegenetable.fr/index.html (accessed on 27 May 2023).

19. PathCards: Pathways Integration. Available online: https://pathcards.genecards.org/ (accessed on 27 May 2023).

20. Yi, H.; Xue, L.; Guo, M.-X.; Ma, J.; Zeng, Y.; Wang, W.; Cai, J.-Y.; Hu, H.-M.; Shu, H.-B.; Shi, Y.-B.; et al. Gene Expression Atlas for Human Embryogenesis. *The FASEB Journal* **2010**, *24*, 3341, doi:10.1096/FJ.10-158782.

21. Rath, S.; Sharma, R.; Gupta, R.; Ast, T.; Chan, C.; Durham, T.J.; Goodman, R.P.; Grabarek, Z.; Haas, M.E.; Hung, W.H.W.; et al. MitoCarta3.0: An Updated Mitochondrial Proteome Now with Sub-Organelle Localization and Pathway Annotations. *Nucleic Acids Res* **2021**, *49*, D1541–D1547, doi:10.1093/nar/gkaa1011.

22. The Human Protein Atlas. Available online: https://www.proteinatlas.org/ (accessed on 30 May 2023).

23. MR, R. 188th ENMC International Workshop: Inclusion Body Myositis, 2-4 December 2011, Naarden, The Netherlands. *Neuromuscul Disord* **2013**, *23*, 1044–1055, doi:10.1016/J.NMD.2013.08.007.

24. Dobin, A.; Davis, C.A.; Schlesinger, F.; Drenkow, J.; Zaleski, C.; Jha, S.; Batut, P.; Chaisson, M.; Gingeras, T.R. STAR: Ultrafast Universal RNA-Seq Aligner. *Bioinformatics* **2013**, *29*, 15–21, doi:10.1093/BIOINFORMATICS/BTS635.

25. Li, B.; Dewey, C.N. RSEM: Accurate Transcript Quantification from RNA-Seq Data with or without a Reference Genome. *BMC Bioinformatics 2011 12:1* **2011**, *12*, 1–16, doi:10.1186/1471-2105-12-323.

26. Love, M.I.; Huber, W.; Anders, S. Moderated Estimation of Fold Change and Dispersion for RNA-Seq Data with DESeq2. *Genome Biology 2014 15:12* **2014**, *15*, 1–21, doi:10.1186/S13059-014-0550-8.

27. Reimand, J.; Kull, M.; Peterson, H.; Hansen, J.; Vilo, J. G:Profiler—a Web-Based Toolset for Functional Profiling of Gene Lists from Large-Scale Experiments. *Nucleic Acids Res* **2007**, *35*, W193–W200, doi:10.1093/NAR/GKM226.

28. Korotkevich, G.; Sukhov, V.; Budin, N.; Shpak, B.; Artyomov, M.; Sergushichev, A. Fast Gene Set Enrichment Analysis. **2016**, doi:10.1101/060012.

29. Wickham, H. *Ggplot2: Elegant Graphics for Data Analysis*; New York: Springer-Verlag, 2009;

30. Belinky, F.; Nativ, N.; Stelzer, G.; Zimmerman, S.; Stein, T.I.; Safran, M.; Lancet, D. PathCards: Multi-Source Consolidation of Human Biological Pathways. *Database* **2015**, *2015*, 1–13, doi:10.1093/database/bav006.

31. GeneTable. Available online: https://www.musclegenetable.fr/index.html (accessed on 29 May 2023).

32. Bordi, M.; De Cegli, R.; Testa, B.; Nixon, R.A.; Ballabio, A.; Cecconi, F. A Gene Toolbox for Monitoring Autophagy Transcription. *Cell Death & Disease 2021 12:11* **2021**, *12*, 1–7, doi:10.1038/s41419-021-04121-9.

33. Catalán-García, M.; Oria Garrabou, G.; Morén, C.; Guitart-Mampel, M.; Hernando, A.; Angels Díaz-Ramos, `; González-Casacuberta, I.; Juárez, D.-L.; Bañó, M.; Enrich-Bengoa, J.; et al. Mitochondrial DNA Disturbances and Deregulated Expression of Oxidative Phosphorylation and Mitochondrial Fusion Proteins in Sporadic Inclusion Body Myositis. *Clin Sci* **2016**, *130*, 1741–1751, doi:10.1042/CS20160080.

34. Narsinh, K.H.; Sun, N.; Sanchez-Freire, V.; Lee, A.S.; Almeida, P.; Hu, S.; Jan, T.; Wilson, K.D.; Leong, D.; Rosenberg, J.; et al. Single Cell Transcriptional Profiling Reveals Heterogeneity of Human Induced Pluripotent Stem Cells. *J Clin Invest* **2011**, *121*, doi:10.1172/JCI44635DS1.

35. Hough, S.R.; Thornton, M.; Mason, E.; Mar, J.C.; Wells, C.A.; Pera, M.F. Stem Cell Reports Ar Ticle Single-Cell Gene Expression Profiles Define Self-Renewing, Pluripotent, and Lineage Primed States of Human Pluripotent Stem Cells. *Stem Cell Reports* **2014**, *2*, 881–895, doi:10.1016/j.stemcr.2014.04.014.

36. Urbach, A.; Schuldiner, M.; Benvenisty, N. Modeling for Lesch-Nyhan Disease by Gene Targeting in Human Embryonic Stem Cells. *Stem Cells* **2004**, *22*, 635–641, doi:10.1634/stemcells.22-4-635.

37. Eiges, R.; Urbach, A.; Malcov, M.; Frumkin, T.; Schwartz, T.; Amit, A.; Yaron, Y.; Eden, A.; Yanuka, O.; Benvenisty, N.; et al. Cell Stem Cell Developmental Study of Fragile X Syndrome Using Human Embryonic Stem Cells Derived from Preimplantation Genetically Diagnosed Embryos., doi:10.1016/j.stem.2007.09.001.

38. Briggs, J.A.; Sun, J.; Shepherd, J.; Ovchinnikov, D.A.; Chung, T.-L.; Nayler, S.P.; Kao, L.-P.; Morrow, C.A.; Thakar, N.Y.; Soo, S.-Y.; et al. Integration-Free Induced Pluripotent Stem Cells Model Genetic and Neural Developmental Features of Down Syndrome Etiology EMBRYONIC STEM CELLS/INDUCED PLURIPOTENT STEM CELLS Integration-Free Induced Pluripotent Stem Cells Model Genetic and Neural Developmental Features of Down Syndrome Etiology., doi:10.1002/stem.1297.

39. Li, W.; Wang, X.; Fan, W.; Zhao, P.; Chan, Y.-C.; Chen, S.; Zhang, S.; Guo, X.; Zhang, Y.; Li, Y.; et al. Modeling Abnormal Early Development with Induced Pluripotent Stem Cells from Aneuploid Syndromes., doi:10.1093/hmg/ddr435.

40. DeRosa, B.A.; Van Baaren, J.M.; Dubey, G.K.; Lee, J.M.; Cuccaro, M.L.; Vance, J.M.; Pericak-Vance, M.A.; Dykxhoorn, D.M. Derivation of Autism Spectrum Disorder-Specific Induced Pluripotent Stem Cells from Peripheral Blood Mononuclear Cells. *Neurosci Lett* **2012**, *516*, 9, doi:10.1016/J.NEULET.2012.02.086.

41. Brennand, K.J.; Simone, A.; Jou, J.; Gelboin-Burkhart, C.; Tran, N.; Sangar, S.; Li, Y.; Mu, Y.; Chen, G.; Yu, D.; et al. Modelling Schizophrenia Using Human Induced Pluripotent Stem Cells. *Nature 2011 473:7346* **2011**, *473*, 221–225, doi:10.1038/NATURE09915.

42. Cooper, O.; Seo, H.; Andrabi, S.; Guardia-Laguarta, C.; Graziotto, J.; Sundberg, M.; McLean, J.R.; Carrillo-Reid, L.; Xie, Z.; Osborn, T.; et al. Pharmacological Rescue of Mitochondrial Deficits in IPSC-Derived Neural Cells from Patients with

Familial Parkinson's Disease. *Sci Transl Med* **2012**, *4*, doi:10.1126/SCITRANSLMED.3003985.

43. Miller, J.D.; Ganat, Y.M.; Kishinevsky, S.; Bowman, R.L.; Liu, B.; Tu, E.Y.; Mandal, P.K.; Vera, E.; Shim, J.W.; Kriks, S.; et al. Human IPSC-Based Modeling of Late-Onset Disease via Progerin-Induced Aging. *Cell Stem Cell* **2013**, *13*, 691–705, doi:10.1016/j.stem.2013.11.006.

44. Chal, J.; Al Tanoury, Z.; Hestin, M.; Gobert, B.; Aivio, S.; Hick, A.; Cherrier, T.; Nesmith, A.P.; Parker, K.K.; Pourquié, O. Generation of Human Muscle Fibers and Satellite-like Cells from Human Pluripotent Stem Cells in Vitro. *Nat Protoc* **2016**, *11*, 1833–1850, doi:10.1038/nprot.2016.110.

45. Demestre, M.; Orth, M.; Föhr, K.J.; Achberger, K.; Ludolph, A.C.; Liebau, S.; Boeckers, T.M. Formation and Characterisation of Neuromuscular Junctions between HiPSC Derived Motoneurons and Myotubes. *Stem Cell Res* **2015**, *15*, 328–336, doi:10.1016/J.SCR.2015.07.005.

46. Benam, K.H.; Dauth, S.; Hassell, B.; Herland, A.; Jain, A.; Jang, K.J.; Karalis, K.; Kim, H.J.; MacQueen, L.; Mahmoodian, R.; et al. Engineered In Vitro Disease Models. *https://doi.org/10.1146/annurev-pathol-012414-040418* **2015**, *10*, 195–262, doi:10.1146/ANNUREV-PATHOL-012414-040418.

SUPPLEMENTARY MATERIALS

Supplementary Tables

Supplementary Table 1. Characterization and validation of iPSC lines

Supplementary Table 2. Short tandem repeat (STR) fingerprinting of IBM and CTL fibroblasts (1 PBMCs) and iPSC samples

Supplementary Table 3. Reagents details

Supplementary Table 4. Differentially expressed genes (DEGs) from the mRNA-seq of inclusion body myositis (IBM) and control (CTL) myotubes.

Supplementary Table 5. Differentially expressed genes (DEGs) associated to each pathway and represented in Fig. 4D.

Supplementary Figures

Supplementary Figure 1. Characterization of 2 IBM and 2 CTLs iPSC lines. A) Phase contrast and alkaline phosphatase images. Scale bar X um. B) Immunodetection of pluripotency markers Oct4 and Nanog. Scale bar: 200 mm. C) Expression of three germ layer markers by immunofluorescence analysis of *in vitro* Embryoid Bodies differentiation cell cultures using specific antibodies against the endodermal marker SOX17, mesodermal marker SMA, and ectodermal marker TUJ1. Nuclei were stained with DAPI. Scale bar: 100 mm. D) Expression levels of pluripotency (POU5F1, SOX2, NANOG) and early lineage markers (SOX17, T, TUJ1) determined by real-time PCR in the iPSC lines and in those same lines differentiated to embryoid bodies. E) Transgene clearance of pluripotency factors and mycoplasma-free iPSC lines.

Supplementary Figure 2. A) Analysis of the pluripotent cell surface markers SSEA-4, TRA 1-60 and TRA 1-81 by flow cytometry in 4 IBM and 4 CTL iPSC lines. B) Karyotypes of IBM and CTL iPSC lines.

MANUSCRIPT III:

Title: *Mitochondrial Dysfunction: A Common Hallmark Underlying Comorbidity between sIBM and Other Degenerative and Age-Related Diseases*

Authors: Marc Catalan-Garcia, Francesc Josep García-García, Pedro J Moreno-Lozano, Gema Alcarraz-Vizan, Adria Tort-Merino, José César Milisenda, Judith Cantó-Santos, Tamara Barcos-Rodriguez, Francesc Cardellach, Albert Llado, Anna Novials, Gloria Garrabou, Josep M Grau-Junyent.

Journal: Journal of clinical medicine. 2020; 9;1446. doi:10.3390/jcm9051446.

IF: 4.2

Journal of
Clinical Medicine

MDPI

Article

Mitochondrial Dysfunction: A Common Hallmark Underlying Comorbidity between sIBM and Other Degenerative and Age-Related Diseases

Marc Catalán-García [1,2,3,†], Francesc Josep García-García [1,2,3,†], Pedro J. Moreno-Lozano [1,2,3,†], Gema Alcarraz-Vizán [4,5], Adrià Tort-Merino [6], José César Milisenda [1,2,3], Judith Cantó-Santos [1,2,3], Tamara Barcos-Rodríguez [1,2,3], Francesc Cardellach [1,2,3], Albert Lladó [6,*], Anna Novials [4,5,*], Glòria Garrabou [1,2,3,*] and Josep M. Grau-Junyent [1,2,3]

1 Muscle Research and Mitochondrial Function Laboratory, CELLEX-IDIBAPS, Faculty of Medicine, University of Barcelona, 08036 Barcelona, Spain; marccatalangarcia@gmail.com (M.C.-G.); fjgarcia@ub.edu (F.J.G.-G.); pjmoreno@clinic.cat (P.J.M.-L.); jcmilise@clinic.cat (J.C.M.); jcanto@clinic.cat (J.C.-S.); barcos@clinic.cat (T.B.-R.); fcardell@clinic.cat (F.C.); jmgrau@clinic.cat (J.M.G.-J.)
2 Internal Medicine Department, Hospital Clinic of Barcelona, 08036 Barcelona, Spain
3 CIBERER—Spanish Biomedical Research Centre in Rare Diseases, 28029 Madrid, Spain
4 Diabetes and Obesity Laboratory Research, Institut d'Investigacions Biomèdiques August Pi I Sunyer (IDIBAPS), 08036 Barcelona, Spain; alcarraz@clinic.cat
5 CIBERDEM—Spanish Biomedical Research Centre in Diabetes and Associated Metabolic Disorders, 28029 Madrid, Spain
6 Alzheimer's Disease and Other Cognitive Disorders Unit, Hospital Clínic and Institut d'Investigacions Biomèdiques August Pi I Sunyer (IDIBAPS), 08036 Barcelona, Spain; atort@clinic.cat
* Correspondence: allado@clinic.cat (A.L.); anovials@clinic.cat (A.N.); garrabou@clinic.cat (G.G.); Tel.: +34-932275400 (ext. 2907) (G.G.)
† All are considered first authors.

Received: 31 March 2020; Accepted: 5 May 2020; Published: 13 May 2020

Abstract: Sporadic inclusion body myositis (sIBM) is an inflammatory myopathy associated, among others, with mitochondrial dysfunction. Similar molecular features are found in Alzheimer's disease (AD) and Type 2 Diabetes Mellitus (T2DM), underlying potential comorbidity. This study aims to evaluate common clinical and molecular hallmarks among sIBM, AD, and T2DM. Comorbidity with AD was assessed in n = 14 sIBM patients by performing neuropsychological and cognitive tests, cranial magnetic resonance imaging, AD cerebrospinal fluid biomarkers (levels of amyloid beta, total tau, and phosphorylated tau at threonine-181), and genetic apolipoprotein E genotyping. In the same sIBM cohort, comorbidity with T2DM was assessed by collecting anthropometric measures and performing an oral glucose tolerance test and insulin determinations. Results were compared to the standard population and other myositis (n = 7 dermatomyositis and n = 7 polymyositis). Mitochondrial contribution into disease was tested by measurement of oxidative/anaerobic and oxidant/antioxidant balances, respiration fluxes, and enzymatic activities in sIBM fibroblasts subjected to different glucose levels. Comorbidity of sIBM with AD was not detected. Clinically, sIBM patients showed signs of misbalanced glucose homeostasis, similar to other myositis. Such misbalance was further confirmed at the molecular level by the metabolic inability of sIBM fibroblasts to adapt to different glucose conditions. Under the standard condition, sIBM fibroblasts showed decreased respiration (0.71 ± 0.08 vs. 1.06 ± 0.04 nmols O_2/min; p = 0.024) and increased anaerobic metabolism (5.76 ± 0.52 vs. 3.79 ± 0.35 mM lactate; p = 0.052). Moreover, when glucose conditions were changed, sIBM fibroblasts presented decreased fold change in mitochondrial enzymatic activities (−12.13 ± 21.86 vs. 199.22 ± 62.52 cytochrome c oxidase/citrate synthase ratio; p = 0.017) and increased oxidative stress per mitochondrial activity (203.76 ± 82.77 vs. −69.55 ± 21.00; p = 0.047), underlying scarce metabolic plasticity. These findings do not demonstrate higher prevalence of AD in sIBM patients, but evidences of prediabetogenic conditions were found. Glucose deregulation in myositis

suggests the contribution of lifestyle conditions, such as restricted mobility. Additionally, molecular evidences from sIBM fibroblasts confirm that mitochondrial dysfunction may play a role. Monitoring T2DM development and mitochondrial contribution to disease in myositis patients could set a path for novel therapeutic options.

Keywords: sIBM 1; Alzheimer 2; T2DM 3; mitochondria 4; comorbidity 5; myositis 6

1. Introduction

Inflammatory myopathies are a heterogenic group of diseases characterized by a progressive symmetric weakness and inflammatory infiltrates within the skeletal muscle [1,2]. Regarding their distinct clinicopathological features, inflammatory myopathies can be classified in four main subtypes: dermatomyositis (DM), polymyositis (PM), necrotizing autoimmune myopathies (NAM), and sporadic inclusion body myositis (sIBM) [3].

The former, sIBM, is the unique inflammatory myopathy associated with the accumulation of misfolded proteins and ageing [2]. With a male:female ratio of 3:1, it is considered a rare disease (ORPHA611) and its prevalence varies from 4.7 per million in the Netherlands [4] to 50 per million in South Australia [5]. In fact, these rates continue to increase, probably due to improved diagnostic protocols and increased ageing of the population, making it the most frequent myopathy in individuals over their 50s, at least in some countries.

In stark contrast with other myositis, sIBM patients show asymmetrical wasting of proximal and distal muscles, in particular quadriceps and finger flexors, leading to difficulty in performing tasks requiring these muscles such as lifting objects or climbing stairs, among others. In addition, neck extensors and pharyngeal involvement may cause dropped head or dysphagia, respectively, affecting 60% of patients over time [2,5].

At the moment, muscle biopsy remains the definitive diagnostic procedure for sIBM [6]. At the histopathological level, the combination of inflammatory changes (CD8+ T-cell infiltrate and expression of class I major histocompatibility complex antigens -MHC-I- in muscle cells), degenerative features (rimmed vacuoles and intra-cellular protein aggregates) [7], and mitochondrial changes (COX-/SDH+ cells and ragged-red-fibbers) are specific and required for sIBM diagnosis [8]. Although knowledge about the molecular hallmarks of the disease is increasing every day, sIBM is still a disease without an effective treatment. Moreover, the aetiology of this progressive degenerative disorder of the skeletal muscles remains unknown [2].

Interestingly, the presence of inflammation, protein depots, and mitochondrial failure seems not to be exclusive for sIBM and, in the last few years, growing evidence has supported the deregulation of these pathways in other chronic and age-related neurodegenerative or metabolic disorders. Among them, the deregulation of mitochondrial function and associated cell consequences has been speculated as the major molecular hallmark underlying a number of these disorders, since mitochondrial dysfunction can trigger, by its own, from bioenergetic failure and oxidative stress production to protein accumulation, inflammation, and cell death [9], features that are present in most of these degenerative age-related disorders.

In physiologic conditions, mitochondria are essential for cell survival, playing a central role in calcium homeostasis, bioenergetics, metabolism, and cell respiration. In pathological conditions, they are indeed the main organelle involved in triggering apoptosis and producing reactive oxygen species (ROS).

Thus, mitochondrial homeostasis and balance is fundamental for cell function, especially in highly energetic and dependent tissues (including muscle, central nervous system, lymphoid organs, or glands), where its dysfunction may become evident much earlier.

Despite the fact that pathological mitochondrial evidence is frequently observed in muscle biopsies from sIBM patients, mitochondrial abnormalities in this disease have scarcely been assessed at a molecular level [10,11]. Our group described, for the first time, mitochondrial DNA alterations in sIBM muscle. Furthermore, down-regulated activity of mitochondrial respiratory chain (MRC) has been found, not only restricted to muscle, also in other peripheral tissues, such as blood [12].

Interestingly, mitochondrial abnormalities, energy failure, respiratory chain impairment, and generation of ROS have also been described in brain aging related to neural loss and synaptic alteration [13]. Moreover, the accumulation of a variety of proteins such as β-amyloid, phospho-Tau, p62, TDP43, and caveolin, among others, and consequent inflammation in the muscle of sIBM patients is like those observed in the brains of patients with neurodegenerative disorders, such as Alzheimer's disease (AD). For all these common molecular hallmarks, growing support is given to a potential shared pathophysiology between sIBM and AD [14,15]. In fact, sIBM is also known as the "muscle Alzheimer's disease" due to these common deregulations. However, as far as we know, neither epidemiological nor molecular studies have been conducted so far to corroborate or discard the comorbidity between these two disorders.

Alzheimer's disease is the commonest cause of dementia, with huge implications for individuals and large sociosanitary and economic associated burdens currently affecting 50 million people. AD is the single biggest cause of dementia, accounting for 50%–75%, and is primarily a condition of later life, roughly doubling in prevalence every 5 years after age 65 [16]. Dementia is the major cause of dependence, disability, and mortality. In the coming years, the largest increase in dementia prevalence is expected to affect 152 million by 2050, which indeed shows patterns of association with cardiovascular disease, hypertension, and diabetes [17]. Consequently, any data that may support comorbidity with alternative diseases may be of help to guide assistance and improve the quality of life in these patients.

Similarly to sIBM and AD, the accumulation of proteins and inflammation has also been described as a trigger of type 2 diabetes mellitus (T2DM). In fact, the presence of amyloid deposits within the pancreatic islets is a pathophysiological hallmark of T2DM [18]. Moreover, mitochondrial dysfunction concerning bioenergetics alterations, respiratory chain disability, and ROS production in T2DM has also been widely described in different tissues [19,20].

T2DM is one of the most prevalent and chronic metabolic disorders worldwide. It is characterized by the presence of hyperglycaemia caused by different alterations converging in the development of insulin resistance accompanied by relative to severe insulin deficiency secretion [21]. This disease is associated with being overweight in 90% of cases, a family history of T2DM in 75%–90% of cases, and poor insulin production. It was estimated that in 2017 there were 451 million people with diabetes worldwide. These figures were expected to increase to 693 million by 2045. Currently, approximately 5 million deaths worldwide were attributable to diabetes [22] and its frequency is expected to increase on account of extensive diagnosis and aging of the population in developed countries.

The link between AD and T2DM is clearly established in literature [23,24]. However, despite the fact that there are common molecular mechanisms that are also shared with sIBM, the comorbidity between T2DM and sIBM has not yet been clarified.

In this study, we aim to evaluate sIBM patients at two levels to assess clinical and molecular comorbidity between sIBM, AD, and T2DM. From a clinical point of view, we will evaluate the neurological and metabolic status in a cohort of sIBM patients to determine the comorbidity between sIBM and AD or T2DM, respectively. In addition, we aim to include a cohort of patients with inflammatory myopathies other than sIBM, such as DM and PM, to evaluate differential or common deregulation with diseases that clinically overlap with sIBM. From a molecular point of view, we aim to evaluate common molecular hallmarks between these degenerative and age-related diseases, focusing our interest on the mitochondrial homeostasis of sIBM fibroblasts that will be subjected to different pathophysiological conditions.

2. Experimental Section

2.1. Study Population

The sIBM cases were diagnosed by clinical and pathological tests in the Department of Internal Medicine from the Hospital Clínic of Barcelona (Barcelona, Spain). All the patients fulfilled the criteria proposed by the European Neuromuscular Centre for sIBM diagnosis [25]. Exclusion criteria were: age < 40 years, family history of hereditary mitochondrial disease and HIV infection, or drug abuse. A cohort of 14 patients was consequently included after signing the informed consent previously approved by the Ethical Committee of our institution (code HCB/2015/0562). Then, 10 underwent neurological evaluation and 8 (not necessarily the same participants) underwent T2DM and mitochondrial testing, depending on their possibilities to endure invasive or uncomfortable tests such as magnetic resonance imaging (MRI), lumbar puncture, or biopsy performance.

On inclusion, sIBM patients completed the IBMFRS (inclusion body myositis functional rating scale), a validated disease-specific functional rating scale to assess disease severity. Epidemiological and clinical data (age, gender, and ethnicity) were also recruited.

2.1.1. Biopsy Performance

Muscles biopsies were performed for diagnostic purposes indicated for muscle weakness or raised creatine kinase (CK) levels. Surgical muscle biopsies were obtained by trained physicians and the samples were processed routinely in the laboratory as described elsewhere [26].

2.1.2. Histological Studies

Fresh samples were frozen in cooled isopentane, sectioned by cryotome at −30 °C, and stained and reacted with different reagents for diagnostic purposes: haematoxylin and eosin, modified Gomori's trichrome, non-specific esterase, periodic acid-Schiff stain, Oil Red O, acid and alkaline phosphatase, NADH, COX, SDH, and ATPase at pH 4.3, 4.6 and 9.4, as reported elsewhere [26]. In addition, some immunohistochemistry reactions such as MHC-I as well as p62 were performed. In parallel, blood samples or cerebrospinal fluid (CSF) from sIBM patients were collected, when indicated, for analytic purposes.

2.1.3. Control Population

According to the standards for diagnosis, results of clinical evaluation for T2DM and AD in sIBM patients were compared to age bracket control data from individuals free of disease or, alternatively, with a cohort of patients with inflammatory myopathies other than sIBM, such as DM (n = 7) and PM (n = 7). This second cohort was prospectively included in parallel to sIBM patients to evaluate differential or common deregulation with diseases that clinically overlap with sIBM. These patients were also diagnosed at the Department of Internal Medicine from the Hospital Clinic of Barcelona (Barcelona, Spain) following the current established clinical and pathological criteria [3]. Experimental studies for mitochondrial evaluation were performed in the same cohort of sIBM patients and compared to healthy control volunteers (C; n = 5), who were prospectively included.

2.2. Neurological Evaluation of sIBM Patients

This part of the study included neuropsychological and cognitive tests, cranial MRI, AD biomarkers in CSF (amyloid beta or Aß42 levels, total tau, and phosphorylated tau at threonine-181 content), and apolipoprotein E (APOE) genotype.

2.2.1. Clinical, Psychological, and Cognitive Assessment

Participants were evaluated by a trained neurologist with a comprehensive neuropsychological battery of tests. Clinical diagnosis was established following the current clinical criteria for mild cognitive impairment (MCI) [27] and dementia due to AD [28].

The neuropsychological battery of tests encompassed five cognitive domains. The memory domain included the Free and Cued Selective Reminding Test [29], the landscape test [30], and the Rey–Osterrieth complex figure [31]. The language domain comprised of the Boston Naming Test [32] and a semantic fluency task [33]. The praxis domain contained a copy of the Rey–Osterrieth complex figure and the ideomotor subtest of the Western Aphasia Battery [34]. The visual perception domain included the object decision, number location, and incomplete letters subtests of the Visual Object and Space Perception battery [35]. The executive functions domain consisted of the Trail Making Test [36], the Stroop Test [37], the Symbol Digit Modalities Test [38], and the Digit Span test of the Wechsler Adult Intelligence Scale [39]. Global cognition was assessed with the Mini Mental State Evaluation (MMSE) [40]. Premorbid intelligence was assessed with the Spanish word accentuation test [41]. Cognitive reserve was evaluated with the cognitive reserve questionnaire [42]. Finally, anxiety and depression levels were measured with the Hospital Anxiety and Depression Scale.

2.2.2. Image Acquisition

For each participant, a T1-weighted, high-resolution, MPRAGE structural MRI scan (echo time (TE) 2.98 ms, repetition time (TR) 2300 ms, inversion time 900 ms, flip angle 9°, bandwidth 240 Hz/pixel, matrix 256 × 256, 240 axial slices, isometric voxel size 1⁄4 1.0 mm^3) was acquired at the IDIBAPS's Imaging core facilities with a 3T whole-body MRI scanner (Siemens Magnetom Trio; Hospital Clinic, Barcelona, Spain).

For all subjects, global cortical atrophy (GCA), medial temporal lobe atrophy (MTL), and white matter integrity (Fazekas) scores were obtained by a trained radiologist.

2.2.3. Determination of AD CSF Biomarkers and Apolipoprotein E (APOE) Genotype

Subjects underwent a lumbar puncture between 9 a.m. and 12 p.m. In the extraction, 10 mL of CSF was collected. The samples were centrifuged and stored in polypropylene tubes at –80 °C within the first hour after extraction. CSF Aß42 levels, total tau (tau), and phosphorylated tau at threonine-181 (ptau) were measured by enzyme-linked immunosorbent assay kits (Innogenetics, Ghent, Belgium). The following cut off points were considered: (a) Aß42 ≤ 550 pg/mL, (b) tau ≥ 385 pg/mL, and (c) ptau ≥ 65 pg/mL.

Genomic DNA was extracted from the peripheral blood of probands using the QIAamp DNAblood minikit (Qiagen AG, Basel, Switzerland). APOE genotyping was performed by polymerase chain reaction amplification and HhaI restriction enzyme digestion.

2.3. T2DM Evaluation of sIBM Patients

2.3.1. Oral Glucose Tolerance Test (OGTT) Procedures

Procedures for the 2h-OGTT required previous fasting after midnight, to obtain baseline fasting glucose level, and further administration of the oral glucose load (75 g) within a 5 min period. Blood specimens to determine the plasma glucose level were subsequently drawn at 30, 60, 90, and 120 min, timed from the beginning of the glucose load. Patients were established as having impaired fasting glucose (IFG; if the venous plasma glucose level was greater than 100 and less than 126 mg/dL) or having impaired glucose tolerance (IGT; if the 120-min venous plasma glucose value fell between 140 and 200 mg/dL). Criteria for new-onset T2DM was a fasting plasma glucose level greater than 126 mg/dL or 120-min venous plasma glucose level greater than 200 mg/dL on the OGTT.

2.3.2. Medical Records Data

The following data were collected from medical records: circulating baseline levels of insulin (mU/L) and glycated haemoglobin, HbA1c (%). Homeostatic model assessment of insulin resistance (HOMA-IR) was calculated to determine the insulin resistance as: (basal insulin level in μU/mL × basal glucose level in mmol/L)/22.5. Anthropometric and physical examination data concerning weight and height were also recruited to calculate body mass index (BMI; calculated as weight in kilograms divided by the square of the height in meters).

2.4. Mitochondrial Characterization in sIBM Patients

2.4.1. Fibroblasts Culture

Fibroblasts were obtained by a skin punch biopsy. Cells were grown in 25 mM glucose Dulbecco's Modified Eagle's medium (DMEM from Gibco, Life Technologies, Burlington, ON, Canada) supplemented with 10% heat-inactivated foetal bovine serum and 1% penicillin-streptomycin at 37 °C in a humidified 5% CO_2 air incubator until 80% optimal confluence was reached. Fibroblasts were harvested with 2.5% trypsin (Gibco, Life Technologies, Burlington, ON, Canada) and centrifuged at 500 g for 8 min. All functional assays were performed in cells between passages 5 and 10.

To test fibroblast response to pro-diabetogenic in vitro conditions, cells were cultured under different glucose conditions: high glucose (HG: 25 mM) and low glucose (LG: 5 mM) DMEM media 10 days prior the experiment, mimicking the glucose deregulation observed in T2DM.

Expected response to 10 days glucose decrease (from HG to LG) should promote mitochondrial activation to enhance energetic output. To evaluate mitochondria activation in front of glucose reduction, we tested oxidative vs. anaerobic metabolism and oxidant/antioxidant balance, together with mitochondrial respiration and enzymatic activities.

2.4.2. Mitochondrial Respiration

Mitochondrial respiration is the result of oxygen consumption by the MRC. It was measured in 1 million cells by high-resolution respirometry using Oroboros™ Oxygraph-2K® technology (Innsbruck, Austria) in non-permeabilized fibroblasts, following the manufacturer's protocols [43]. Two measures were obtained: one of them is considered a sign of proper mitochondrial function and is calculated as the ratio between the basal respiration flux (standard oxygen consumption) in respect to the maximal respiration capacity (by adding the uncoupler CCCP). In parallel, proton leak was secondarily measured (by adding oligomycin) as a sign of inefficient and unhealthy MRC activity. Results were expressed relative to cell count and were expressed as nmols/min.

2.4.3. Lactate Production

Lactate measures were performed in 100 μL of fresh supernatant fibroblast culture using the epoc® Blood Analysis System, epoc System Software version 3.32.0 (Siemens Healthineers Global, Erlangen, Germany), normalized by cell count and expressed as mmols/L.

2.4.4. Total Antioxidant Capacity

Total Antioxidant Capacity (TAC) was measured in 100 μL of cell supernatant using an OxiSelect™ Total Antioxidant Capacity Assay kit (Cell Biolabs Inc., San Diego, CA, USA) by spectrophotometry (absorption maximum at 490 nm), normalized by cell count and expressed as μM CRE (Copper Reducing Equivalents).

2.4.5. MRC Enzymatic Activity

Cytochrome c oxidase (COX) function was assessed in 40 μg of total protein from each fibroblast sample according to standardized protocols [44] and normalized by mitochondrial content, measured

as citrate synthase (CS) enzymatic activity. CS is a mitochondrial enzyme from the Krebs cycle and is widely considered to be a reliable marker of mitochondrial amount. Both enzymatic activities were measured by spectrophotometry, using internal controls, and were expressed as the ratio between COX vs. CS function.

2.4.6. Oxidative Stress Assay

Lipid peroxidation (an indicator of oxidative damage produced by ROS to cellular lipid compounds) was quantified in 150 µg of protein from a fibroblast sample using the OxysResearch™ LPO-586™ kit (Deltaclon, Portland, OR, USA) through the spectrophotometric measurement of malondialdehyde and 4-hidroxyalkenal, both of which are products of fatty acid peroxide decomposition. Lipid peroxidation was normalized by COX/CS activity as a measure of oxidative stress production per mitochondrial activity.

2.5. Statistics

Results were expressed as mean ± standard error of the mean (SEM) or in fold change between conditions (HG vs. LG). Statistical analysis was performed after filtering for outliers to evaluate differential phenotypes depending on group-assignment (patients or controls) by using the non-parametric independent sample Mann-Whitney U test. The signification threshold was set at $p < 0.05$.

3. Results

3.1. Clinical DATA

The sIBM patients included in this study corresponded to $n = 14$ subjects aged between 48 and 90 (mean age 67.70 ± 3.84 years), 9:5 male to female ratio, and all white Caucasian. According to the design of the study, no statistical differences were observed in regards to age, gender, or ethnicity between sIBM patients and the control cohorts. Specifically, PM patients presented a mean age of 69.57 ± 5.39 years and a 1:6 male to female ratio, DM subjects a mean age of 66.67 ± 3.20 years and a 2:5 male to female ratio, and healthy control volunteers aged 57.12 ± 5.38 years and presented a 1:4 male to female ratio, all white Caucasian, according to sIBM demographic characteristics.

At the time of inclusion, the sIBM patient cohort scored 22.00 ± 2.37 out of 40 with the IBMFRS test, indicating moderate-to-advanced sIBM clinical severity.

3.2. Neurological Evaluation of sIBM Patients

3.2.1. Patient Characteristics

Ten sIBM patients underwent the neurological assessment. Education level ranged between 7 and 18 years and the cognitive reserve questionnaire scored 7 to 18 points. Demographics of the cognitive study are shown in Table 1.

3.2.2. Clinical and Neuropsychological Assessment

Eight out of the ten subjects that underwent clinical and neuropsychological evaluation were cognitively impaired. From those, 5 were diagnosed with MCI and 3 with dementia (two of them were diagnosed as AD).

Three subjects presented symptoms of anxiety and/or depression. MMSE ranged between 6 and 29 (maximum MMSE score in health is 30 points) and the neuropsychological profile of the study subjects was heterogeneous, although most of them showed an amnestic pattern (verbal and/or visual memory decline).

Table 1. Demographic characteristics of sIBM patients included in the cognitive study.

	Case 1	Case 2	Case 3	Case 4	Case 5	Case 6	Case 7	Case 8	Case 9	Case 10
Demographics										
Gender	♂	♀	♂	♂	♀	♂	♂	♀	♀	♂
Age	68.9	72.4	77.4	48.9	67.3	63.0	66.8	81.6	90.5	62.2
Years of education	9	8	18	12	8	11	17	11	7	11
CRQ	11	-	21	12	12	16	18	14	9	21
Cognitive data										
Clinical diagnosis	MCI	AD	AD	Control	MCI	Control	MCI	MCI	Dementia	MCI
HADS anxiety/depression	0/4	-	3/3	9/5	6/16	4/1	4/3	9/10	4/5	3/1
MMSE	28/30	19/30	23/30	29/30	26/30	27/30	29/30	24/30	6/30	29/30
Neuropsychological profile	Amnestic (mild)	Global deterioration	Global deterioration	Cognitively normal	Amnestic (mild)	Cognitively normal	Amnestic (mild)	Amnestic (mild)	Severe global deterioration	Amnestic (mild)
MRI data										
GCA scale (0–3)	2	1	2	0	1	0	1	-	-	1
MTA score (0–4)	2	3	3	0	1	0	0	-	-	1
Fazekas scale (0–3)	3	1	2	1	1	1	1	-	-	1
Biological & CSF data										
APOE genotype	ε4/3 †	-	ε3/3	-	ε3/2	ε3/3	-	-	-	ε3/3
$A\beta_{42}$	519.1	-	434.0	-	907.0	634.6	-	-	-	1059.0
Tau	217.9	-	-	-	163.0	136.2	-	-	-	225.0
pTau	40.7	-	182.2	-	39.0	29.6	-	-	-	42.0

Null cognitive impairment was observed in sIBM patients when compared to age bracket control data. Key. CRQ: Cognitive Reserve Questionnaire; HADS: Hospital Anxiety & Depression Scale; MMSE: MiniMental State Examination (20 to 24 score suggests mild dementia, 13 to 20 moderate dementia, and less than 12 indicates severe dementia); GCA: Global Cortical Atrophy; MTA: Medial Temporal lobe Atrophy score (score 0: no atrophy; score 1: only widening of choroid fissure; score 2: also widening of temporal horn of lateral ventricle; score 3: moderate loss of hippocampal volume; score 4: severe volume loss of hippocampus); Fazekas: Fazekas scale for white matter lesions (score 0: none or single punctate white matter hyperintensities; score 1: multiple punctate lesions; score 2: beginning confluency of lesions – bridging; score 3: large confluent lesions); APOE: Apolipoprotein E; CSF: cerebrospinal fluid; $A\beta_{42}$: Amyloid-beta isoform 42; Tau: total tau; pTau: phosphorylated tau. † APOE ε4 carrier.

Despite reported disturbances in the clinical and neuropsychological assessment, no higher incidence of dementia or AD was detected in sIBM patients when the results were compared to the prevalence of dementia in Europe [45]. See clinical and neuropsychological data of the Neurological study in Table 1.

3.2.3. MRI Data

Eight sIBM subjects underwent the magnetic resonance scan. Medial temporal lobe atrophy (MTL score > 1) was found in 3 subjects (maximum pathological score is 4 points) and all individuals presented different levels of white matter deterioration, including two subjects with a Fazekas score ≥ 2 (maximum pathological score is 3) (see Table 1).

However, MTL score > 1 was also found in controls in previous studies [46]. Furthermore, in our study, 1 out of 2 subjects with MTL >1 had normal AD CSF biomarkers, thus excluding AD [27]. Consequently, we concluded that MRI analysis of sIBM patients reported no higher incidence of AD.

3.2.4. AD CSF Biomarkers and APOE Genotype

Five subjects completed the CSF testing for AD biomarkers and APOE genotype. CSF biomarker levels were positive for AD in one case and, additionally, one subject was an APOE ε4 carrier. From the 3 dementia cases, one presented a typical AD CSF profile, another received a clinical diagnosis of AD without biological confirmation, and the last one presented advanced dementia at 90 years. None of the MCI had a typical AD CSF biomarker pattern, although one subject presented reduced levels of CSF $A\beta_{42}$ with normal CSF tau and phosphor-tau levels (amyloidosis alone; data regarding AD CSF biomarkers and APOE genotype is shown in Table 1).

We found only 1 out of 5 patients with typical AD CSF biomarkers and this percentage is very similar to the frequencies of brain amyloidosis found in individuals with normal cognitive function at similar ages [47].

Considering the diagnostic criteria stablished by the National Institute on Aging-Alzheimer's Association workgroups [27], neither CSF biomarkers nor APOE genotyping stand for higher prevalence of AD in sIBM patients when compared with age bracket control data.

3.3. T2DM Evaluation of sIBM Patients

The OGTT was performed to $n = 8$ sIBM patients with respect to the normality ranges of age bracket control data [48]. When basal glucose level was measured, 38% (3/8) of patients showed disturbances: 25% (2/8) were in the prediabetic range (plasma glucose level greater than 100 and less than 126 mg/dL), while the other 13% (1/8) were considered as T2DM patients (Figure 1).

The 2 h venous plasma glucose level in the sIBM cohort ($n = 7$) showed alterations in 42% (3/7) of the patients, while 14% (1/7) were in the prediabetic range (the plasma glucose level fell between 140 and 200 mg/dL) and the remaining 28% (2/7) felt into the T2DM category (glucose level greater than 200 mg/dL). Moreover, medical records in blood tests from the sIBM population ($n = 8$) showed increased HbA1c % in 50% (4/8) of these patients (HbA1c greater than 5.7). Finally, when HOMA-IR was assessed in the sIBM cohort ($n = 7$), 14% (1/7) of the patients were close to insulin resistance values (HOMA-IR > 5; Figure 1).

With respect to the age bracket control data [48], all evaluated sIBM patients presented one or more deregulated parameter of glucose metabolism, suggesting a prediabetogenic state. Moreover, when sIBM subjects were compared with respect to other patients presenting with alternative myopathies (DM and PM), similar deregulation of glucose parameters was observed, as shown in Figure 1 and Table 2.

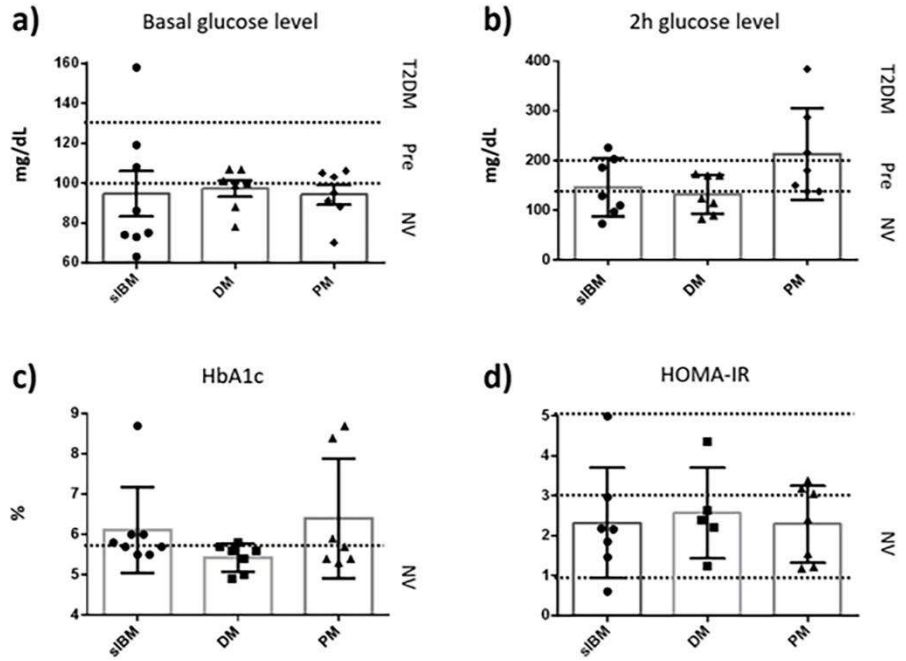

Figure 1. Type 2 Diabetes Mellitus (T2DM) markers analyzed in different myositis populations suggesting frequent alteration in most of the biomarkers when compared to age bracket control data: (**a**) Basal glucose levels; (**b**) Two hours glucose level; (**c**) HbA1c % of glycated haemoglobin; and (**d**) HOMA-IR: Homeostatic model assessment of insulin resistance (normal value 1–3; insulin resistance is consistent with greater than 5 HOMA-IR values). Key: sIBM: sporadic Inclusion Body Myositis; DM: Dermatomyositis; PM: Polymyositis.; Pre: Prediabetic; NV: Normal values.

Specifically, the basal glucose level was also determined in a cohort of patients with DM (n = 7) and PM (n = 7) showing prediabetic state values in 43% (3/7) of cases from both populations. The 2 h venous plasma glucose level in the DM population was greater in 43% (3/7) of patients, which is considered suggestive of a prediabetic state, while the PM cohort showed altered values in 71% (5/7) of patients, 28% (2/7) were considered as in a prediabetic state, and the other 43% (3/7) were consistent with T2DM. Medical data records from blood tests of DM and PM populations also showed altered HbA1c profiles in both cohorts. Particularly, 14% (1/7) of DM and 43% (3/7) of PM had greater values compared to age bracket control data (HbA1c < 5.7%) [48]. Finally, the HOMA-IR calculation showed that 14% (1/7) of the DM cohort and 43% (3/7) of the PM population showed greater HOMA-IR ratio than age bracket control ranges, however the obtained data is under the insulin resistance values (HOMA-IR > 5).

Considering the T2DM definition stratified by age from the American College of Endocrinology [49], the alteration of T2DM biomarkers in sIBM patients (and in the rest of the studied cohorts as PM and DM) is consistent with a prediabetic condition, eventually demonstrating the clinical comorbidity between these diseases.

3.4. Mitochondrial Characterization in sIBM Patients

Under standard conditions (see Figure 2), sIBM fibroblasts showed significantly decreased basal to maximal respiration (0.71 ± 0.08 vs. 1.06 ± 0.04 nmols/min; p = 0.024), increased anaerobic metabolism (5.76 ± 0.52 vs. 3.79 ± 0.35 mM lacate; p = 0.052), and TAC levels (403.89 ± 107.02 vs. 171.73 ± 23.17 μM CRE; p = 0.006), reflecting the mitochondrial dysfunction characteristic of the target tissue of the disease (muscle).

Table 2. Type 2 Diabetes Mellitus (T2DM) markers in different myositis populations.

	Glu 0 h	Glu 2 h	Ins	Hb1Ac	HOMA-IR	BMI
sIBM1	•					•
sIBM2		•				•
sIBM3						•
sIBM4				•		•
sIBM5	•			•	•	
sIBM6		•		•		
sIBM7	•			•		•
sIBM8		•				•
DM1					•	•
DM2		•				•
DM3	•					•
DM4	•	•				
DM5						•
DM6	•					
DM7		•		•		•
PM1		•		•	•	•
PM2		•				
PM3	•	•		•		
PM4	•	•			•	
PM5		•		•	•	•
PM6	•	•				
PM7		•				

The black spot in one patient for a specific parameter indicates an altered value with respect to bracket control data. These findings suggesting a prediabetogenic state for most of the patients and the deregulation of one or more parameters of the glucose metabolism in all studied myositis. Key: Glu 0 h: basal glucose level; Glu 2 h: venous plasma glucose level at 2 h after the oral glucose tolerance test (OGTT); Ins: basal insuline levels; Hb1Ac: glycated haemoglobin; HOMA-IR: Homeostatic model assessment of insulin resistance; BMI: body mass index, calculated as body weight in kg divided by height in m^2 and considered altered >25; sIBM: sporadic inclusion myositis; PM: polymyositis; DM: dermatomyositis.

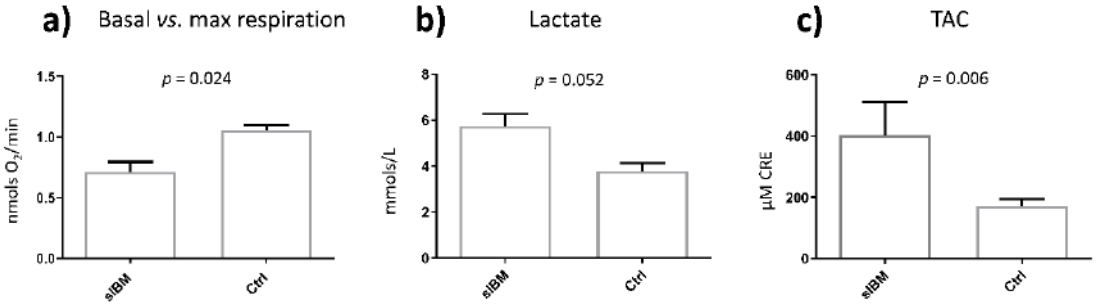

Figure 2. Mitochondrial characterization at standard conditions demonstrated deregulated mitochondrial function in sIBM fibroblasts when compared to healthy controls. (**a**) Oxygen consumption expressed as a ratio of basal respiration vs. max. respiration; (**b**) Lactate secretion expressed in mmols/L and (**c**) TAC (Total Antioxidant Capacity) expressed as µM CRE, Copper Reducing Equivalents. (**b**,**c**) measurements were normalized by total cell amount. sIBM: sporadic inclusion myositis; Ctrl: Healthy controls.

Cells increase mitochondrial activity in response to the decrease of glucose levels, probably as an attempt to maximize the energetic output in case of glucose restriction. Such activation was observed in control fibroblasts when subjected to glucose changing conditions (HG vs. LG) in terms of respiration. Under high glucose concentration, the mitochondrial respiration rate was low, indicating decreased oxygen consumption and high anaerobic metabolism. When the glucose concentration was diminished, oxygen consumption increased, indicating the activation of the aerobic (mitochondrial) metabolism (Supplementary Figure S1).

Contrarily, when sIBM fibroblasts were subjected to glucose decrease to evaluate mitochondrial contribution to sIBM-T2DM comorbidity, such activation was not observed. Specifically, sIBM fibroblasts vs. controls showed decreased fold change basal to maximal respiration (1.65 ± 15.74 vs. 34.88 ± 58.02) and enzymatic activities (−12.13 ± 21.86 vs. 199.22 ± 62.52 COX/CS ratio; $p = 0.017$). Additionally, a lack of mitochondrial activation in sIBM fibroblasts was accompanied by increased fold change proton leak (92.29 ± 73.89 vs. 6.16 ± 83.05) and oxidative stress per mitochondrial activity (203.76 ± 82.77 vs. −69.55 ± 21.00; $p = 0.047$) (Figure 3).

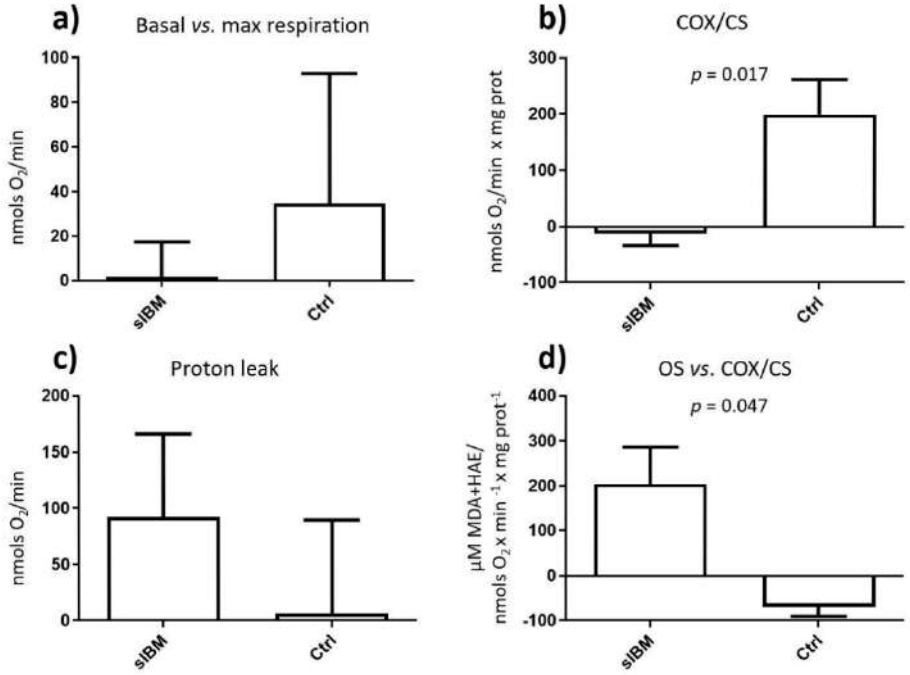

Figure 3. Mitochondrial characterization after glucose changing conditions demonstrating the inability of sIBM fibroblasts to adapt to different glucose conditions when compared to heathy controls. Fold change adaptation from HG (high glucose) to LG (low glucose) for (**a**) Basal respiration vs. max respiration, (**b**) Enzymatic activities (cytochrome c oxidase/citrate synthase; COX/CS), (**c**) Proton leak, (**d**) Oxidative stress (OS) per mitochondrial activity (COX/CS). sIBM: sporadic inclusion myositis; Ctrl: Healthy controls.

Glucose misbalance manifested at a clinical level in sIBM patients was further confirmed in vitro by the inability of sIBM fibroblasts to adapt to different glucose conditions, thus underlying the clinical and molecular comorbidity between sIBM and T2DM.

4. Discussion

Despite medical literature postulating potential comorbidity of sIBM with AD and T2DM, scarce data and epidemiological studies (if any) had been conducted to date to evaluate such overlap. Before our investigation, none of the sIBM patients had been diagnosed of T2DM or AD. In the present

study, and regardless of the small sample size herein tested, we found null comorbidity between sIBM and AD, but trends towards comorbidity between sIBM and T2DM.

Despite sIBM having been described as "Alzheimer in muscle" and both disorders sharing some pathophysiological mechanisms [14,15,50,51], the present outputs suggest that AD pathology is not more frequent in sIBM patients than in the age-paired population. These findings suggest that despite both diseases sharing common molecular pathways (including mitochondrial dysfunction, protein deposition, and inflammation, among others), such disorders present different regulatory mechanisms and/or the disease is specific, in each case, to a different target tissue.

Interestingly, partial comorbidity between sIBM and T2DM has been demonstrated in this work. Clinically, the metabolic deregulation in sIBM patients is characterized by the initial impairment of glucose metabolism compared with age bracket control data. Despite the fact that only a few of them could be concomitantly diagnosed by sIBM and T2DM, most of the sIBM patients showed clear signs of a prediabetogenic condition that underlie the comorbidity between both diseases.

Such coexistence of T2DM in sIBM patients could be due to common etiological links between both disorders. Previous literature describes similar mitochondrial alterations in T2DM and sIBM [5,20,52,53].

At a molecular level, the mitochondrial characterization of fibroblasts from sIBM patients under standard conditions of the present study demonstrate increased anaerobic metabolism and antioxidant capacity at the detriment of mitochondrial oxygen consumption. These results suggest that mitochondrial dysfunction is present in sIBM patients and is not only restricted to the target tissue of the disease (muscle), but may also extend to peripheric alternative tissues, including fibroblasts, as previously demonstrated in the case of blood cells [12]. These findings validate fibroblasts as a cell model for the study of sIBM, as previously demonstrated in cases of neurodegenerative and metabolic diseases including AD and T2DM [54–57].

Moreover, we used these fibroblasts to evaluate mitochondrial contribution into sIBM-T2DM comorbidity by exposing sIBM fibroblasts to different glucose conditions. That way, we observed that control fibroblasts showed full mitochondrial plasticity to adapt to different glucose environments, whilst sIBM fibroblasts were mitochondrially unable to adapt its metabolism. Particularly, sIBM fibroblasts were unable to increase their mitochondrial function in terms of respiration and MRC enzymatic activities in front of changes in glucose bioavailability. Mitochondrial dysfunction in sIBM fibroblasts may lead to reduced bioenergetics and consequent cell compromise. In fact, such metabolic stiffness leads sIBM fibroblasts to increased proton leak and oxidative stress, frequently associated with cell damage [58,59] and disease [9].

To our knowledge, there are no clinical or molecular evidences supporting the preferential affection of muscle tissue in sIBM or the particular targeting of certain muscles (greater in finger flexors and quadriceps), but there is probably a molecular rationale underlying such differential targeting and mitochondria (among others) may stand behind this.

Overall, these data demonstrate that mitochondrial dysfunction limit sIBM cell adaption to changing glucose metabolism, being a source of cell damage and the potential pathophysiological link between sIBM and T2DM. These molecular data confirm clinical comorbidity between both disorders, pointing out sIBM as a new population of underdiagnosed T2DM patients. T2DM is a silent infradiagnosed disease and any clue for emerging groups of risks may account for the reduction of further associated consequences. Interestingly, partial deregulated glucose metabolism was also found in other myositis as PM and DM, thus suggesting common lifestyle cues' contribution in observed comorbidity.

Probably, both mitochondrial deregulation and lifestyle habits (such as restricted mobility) may be conditioning the manifestation of metabolic disorders such as T2DM in sIBM patients. Due to its idiosyncrasy, myositis are a group of disorders characterized by weakness and wasting of the muscle and consequently low physical activity or a sedentary lifestyle. This situation is associated with the development of several chronic diseases including T2DM. Additionally, due to skeletal muscle

contribution to glucose homeostasis and muscle wasting on account of low patient activity, in a kind of vicious circle, glucose metabolism deregulation may be the final fate of a sedentary lifestyle, in this case, triggered by myositis and mitochondrial dysfunction.

Consequently, some general recommendations may be added in the clinical follow-up of patients with myopathy to prevent or manage potential T2DM development in accordance with international standards [60]. They are based on the control of risk factors for T2DM and metabolic syndrome development, including the avoidance of sedentarism and obesity through the performance of exercise (quite restricted in most cases of patients with myositis), but also dietetic control (reduction of caloric intake in cases of obesity, especially carbohydrates).

Some limitations must be acknowledged in the present work. The reduced number of patients included in the study may be the major downfall. Of note, due to the low prevalence of sIBM disorder (considered a rare disease), the study of bigger cohorts is often hampered but recommended. Additionally, further studies are warranted to provide more in-depth understanding of the deregulated pathways underlying glucose impairment in sIBM patients and whether the lipid profile and other features characteristic of the metabolic syndrome are affected in sIBM, even myositis in general, to establish a better correlation between these disorders and the metabolic syndrome. Similarly, the parallel inclusion of fibroblasts from PM or DM patients would have been of interest to deepen the knowledge of common and specific molecular patterns shared among these disorders that clinically overlap.

5. Conclusions

In summary, the conclusions of the present work stand for null comorbidity between sIBM and AD but partial comorbidity between sIBM and T2DM through the impairment of glucose homeostasis, mitochondrial function, and probably lifestyle conditions. Although further investigation is needed to validate this pilot study, these findings provide better knowledge of sIBM complications.

On account that effective treatment for sIBM is not yet available, this should be a red flag and the monitorization of the prediabetic state in myositis patients to avoid potential complications in clinical practice associated with the management of both diseases should be considered, thus contributing to improving the quality of life of patients with inflammatory myopathies.

Supplementary Materials: The following are available online at http://www.mdpi.com/2077-0383/9/5/1446/s1, Figure S1: Mitochondrial respiratory activation of control fibroblasts when glucose levels are reduced from HG to LG.

Author Contributions: Conceptualization, F.J.G.-G., G.A.-V., F.C., A.L., A.N., G.G., and J.M.G.-J.; Data curation, F.J.G.-G., G.A.-V., A.T.-M., and G.G.; Formal analysis, F.J.G.-G., G.A.-V., A.T.-M., and G.G.; Funding acquisition, F.C., A.L., A.N., G.G., and J.M.G.-J.; Investigation, M.C.-G., P.J.M.-L., G.A.-V., A.T.-M., J.C.M., J.C.-S., and T.B.-R.; Methodology, F.J.G.-G., G.A.-V., A.T.-M., and G.G.; Project administration, G.G.; Resources, F.J.G.-G., G.A.-V., and A.T.-M.; Software, F.J.G.-G.; Supervision, A.L., A.N., G.G., and J.M.G.-J.; Validation, M.C.-G., F.J.G.-G., P.J.M.-L., G.A.-V., A.T.-M., J.C.M., J.C.-S., T.B.-R., F.C., A.L., A.N., G.G., and J.M.G.-J.; Visualization, F.J.G.-G., P.J.M.-L., G.A.-V., A.T.-M., J.C.M., J.C.-S., T.B.-R., F.C., A.L., A.N., G.G., and J.M.G.-J.; Writing—original draft, F.J.G.-G. and G.G.; Writing—review & editing, M.C.-G., F.J.G.-G., P.J.M.-L., G.A.-V., A.T.-M., J.C.M., J.C.-S., T.B.-R., F.C., A.L., A.N., G.G., and J.M.G.-J. All authors have read and agreed to the published version of the manuscript.

Funding: The funders had no role in the study design, data collection and interpretation, or the decision to submit the work for publication, but contributed to support staff and material resources. This work was supported by funds from the Integrated Projects of Excellence PIE14/00061 and the Fondo de Investigaciones Sanitarias of the Instituto de Salud Carlos III (ISCIII) (grant numbers PI1800498 and PI1800451), the Centro de Investigación Biomédica en Red de Enfermedades Raras (CIBERER), all initiatives of ISCIII and FEDER, as well as Fundació Privada Cellex and Suports a Grups de Recerca (grant code 2017 SGR 893) and CERCA programs from the Generalitat de Catalunya. Dr. Albert Lladó (PERIS SLT008/18/00061) received funding from the Departament de Salut de la Generalitat de Catalunya.

Acknowledgments: We are in debt to all the patients that authorized their participation in the present study and the clinical staff and families that take care of their management.

Conflicts of Interest: The authors declare no conflict of interest.

References

1. Dalakas, M.C. Inflammatory Muscle Diseases. *N. Engl. J. Med.* **2015**, *372*, 1734–1747. [CrossRef] [PubMed]
2. Needham, M.; Corbett, A.; Day, T.; Christiansen, F.; Fabian, V.; Mastaglia, F.L. Prevalence of sporadic inclusion body myositis and factors contributing to delayed diagnosis. *J. Clin. Neurosci.* **2008**, *15*, 1350–1353. [CrossRef] [PubMed]
3. Schmidt, J. Current Classification and Management of Inflammatory Myopathies. *J. Neuromuscul. Dis.* **2018**, *5*, 109–129. [CrossRef] [PubMed]
4. Badrising, U.A.; Maat-Schieman, M.; Van Duinen, S.G.; Breedveld, F.; Van Doorn, P.; Van Engelen, B.; Van Den Hoogen, F.; Hoogendijk, J.; Höweler, C.; De Jager, A.; et al. Epidemiology of inclusion body myositis in the Netherlands: A nationwide study. *Neurology* **2000**, *55*, 1385–1387. [CrossRef] [PubMed]
5. Tan, J.A.; Roberts-Thomson, P.J.; Blumbergs, P.; Hakendorf, P.; Cox, S.R.; Limaye, V. Incidence and prevalence of idiopathic inflammatory myopathies in South Australia: A 30-year epidemiologic study of histology-proven cases. *Int. J. Rheum. Dis.* **2013**, *16*, 331–338. [CrossRef]
6. Vattemi, G.; Mirabella, M.; Guglielmi, V.; Lucchini, M.; Tomelleri, G.; Ghirardello, A.; Doria, A. Muscle biopsy features of idiopathic inflammatory myopathies and differential diagnosis. *Autoimmun. Highlights* **2014**, *5*, 77–85. [CrossRef]
7. De Paepe, B. Sporadic Inclusion Body Myositis: An Acquired Mitochondrial Disease with Extras. *Biomolecules* **2019**, *9*, 15. [CrossRef]
8. Catalán, M.; Selva-O'Callaghan, A.; Grau, J.M. Diagnosis and classification of sporadic inclusion body myositis (sIBM). *Autoimmun. Rev.* **2014**, *13*, 363–366. [CrossRef]
9. Akhter, F.; Chen, D.; Yan, S.F.; Yan, S.S. Mitochondrial Perturbation in Alzheimer's Disease and Diabetes. *Prog. Mol. Biol. Transl. Sci.* **2017**, *146*, 341–361. [CrossRef]
10. Bhatt, P.S.; Tzoulis, C.; Balafkan, N.; Miletic, H.; Tran, G.T.T.; Sanaker, P.S.; Bindoff, L.A. Mitochondrial DNA depletion in sporadic inclusion body myositis. *Neuromuscul. Disord.* **2019**, *29*, 242–246. [CrossRef]
11. Rygiel, K.A.; Miller, J.; Grady, J.P.; Rocha, M.C.; Taylor, R.W.; Turnbull, D.M. Mitochondrial and inflammatory changes in sporadic inclusion body myositis. *Neuropathol. Appl. Neurobiol.* **2015**, *41*, 288–303. [CrossRef]
12. Catalán-García, M.; Garrabou, G.; Morén, C.; Guitart-Mampel, M.; Hernando, A.; Díaz-Ramos, À.; González-Casacuberta, I.; Juárez, D.L.; Bañó, M.; Enrich-Bengoa, J.; et al. Mitochondrial DNA disturbances and deregulated expression of oxidative phosphorylation and mitochondrial fusion proteins in sporadic inclusion body myositis. *Clin. Sci.* **2016**, *130*, 1741–1751. [CrossRef] [PubMed]
13. Swerdlow, R.H. Mitochondria and Mitochondrial Cascades in Alzheimer's Disease. *J. Alzheimer's Dis.* **2018**, *62*, 1403–1416. [CrossRef] [PubMed]
14. Murphy, M.P.; Golde, T.E. Inclusion-body myositis and Alzheimer disease: Two sides of the same coin, or different currencies altogether? *Neurology* **2006**, *66*, S65–S68. [CrossRef] [PubMed]
15. Askanas, V.; Engel, W.K. Inclusion-Body Myositis: Newest Concepts of Pathogenesis and Relation to Aging and Alzheimer Disease. *J. Neuropathol. Exp. Neurol.* **2001**, *60*, 1–14. [CrossRef]
16. Lane, C.A.; Hardy, J.; Schott, J.M. Alzheimer's disease. *Eur. J. Neurol.* **2018**, *25*, 59–70. [CrossRef]
17. Patterson, C. *World Alzheimer Report 2018—The State of the Art of Dementia Research: New Frontiers*; Alzheimer's Disease International (ADI): London, UK, 2018; pp. 32–36.
18. Westermark, P.; Grimelius, L. The pancreatic islet cells in insular amyloidosis in human diabetic and non-diabetic adults. *Acta Pathol. Microbiol. Scand. Sect. A Pathol.* **2009**, *81A*, 291–300. [CrossRef]
19. Hesselink, M.K.C.; Schrauwen-Hinderling, V.; Schrauwen, P. Skeletal muscle mitochondria as a target to prevent or treat type 2 diabetes mellitus. *Nat. Rev. Endocrinol.* **2016**, *12*, 633–645. [CrossRef]
20. Pinti, M.V.; Fink, G.K.; Hathaway, Q.A.; Durr, A.J.; Kunovac, A.; Hollander, J.M. Mitochondrial dysfunction in type 2 diabetes mellitus: An organ-based analysis. *Am. J. Physiol. - Endocrinol. Metab.* **2019**, *316*, E268–E285. [CrossRef]
21. Kerner, W.; Brückel, J. Definition, Classification and Diagnosis of Diabetes Mellitus. *Exp. Clin. Endocrinol. Diabetes* **2014**, *122*, 384–386. [CrossRef]
22. Cho, N.H.; Shaw, J.E.; Karuranga, S.; Huang, Y.; da Rocha Fernandes, J.D.; Ohlrogge, A.W.; Malanda, B. IDF Diabetes Atlas: Global estimates of diabetes prevalence for 2017 and projections for 2045. *Diabetes Res. Clin. Pract.* **2018**. [CrossRef] [PubMed]

23. Pruzin, J.J.; Nelson, P.T.; Abner, E.L.; Arvanitakis, Z. Review: Relationship of type 2 diabetes to human brain pathology. *Neuropathol. Appl. Neurobiol.* **2018**, *44*, 347–362. [CrossRef] [PubMed]
24. Bharadwaj, P.; Wijesekara, N.; Liyanapathirana, M.; Newsholme, P.; Ittner, L.; Fraser, P.; Verdile, G. The Link between Type 2 Diabetes and Neurodegeneration: Roles for Amyloid-β, Amylin, and Tau Proteins. *J. Alzheimer's Dis.* **2017**, *59*, 421–432. [CrossRef] [PubMed]
25. Rose, M.R. 188th ENMC International Workshop: Inclusion Body Myositis, 2-4 December 2011, Naarden, The Netherlands. *Neuromuscul. Disord.* **2013**, *23*, 1044–1055. [CrossRef] [PubMed]
26. Dubowitz, V.; Sewry, C.; Oldfors, A.; Lane, R.J.M. *Muscle Biopsy: A Practical Approach/Victor Dubowitz, Caroline A. Sewry, Anders Oldfors; with Contribution on Toxic and Drug-Induced Myopathies by Russell Lane*, 4th ed.; Saunders Elsevier: Oxford, UK, 2013; ISBN 9780702050305.
27. Albert, M.S.; DeKosky, S.T.; Dickson, D.; Dubois, B.; Feldman, H.H.; Fox, N.C.; Gamst, A.; Holtzman, D.M.; Jagust, W.J.; Petersen, R.C.; et al. The Diagnosis of Mild Cognitive Impairment due to Alzheimer's Disease: Recommendations from the National Institute on Aging-Alzheimer's Association Workgroups on Diagnostic Guidelines for Alzheimer's Disease. *Focus (Madison)* **2013**, *11*, 96–106. [CrossRef]
28. McKhann, G.M.; Knopman, D.S.; Chertkow, H.; Hyman, B.T.; Jack, C.R.; Kawas, C.H.; Klunk, W.E.; Koroshetz, W.J.; Manly, J.J.; Mayeux, R.; et al. The diagnosis of dementia due to Alzheimer's disease: Recommendations from the National Institute on Aging-Alzheimer's Association workgroups on diagnostic guidelines for Alzheimer's disease. *Alzheimer's Dement.* **2011**, *7*, 263–269. [CrossRef]
29. Grober, E.; Buschke, H.; Korey, S.R. Genuine Memory Deficits in Dementia. *Dev. Neuropsychol.* **1987**, *3*, 13–36. [CrossRef]
30. Valls-Pedret, C.; Olives, J.; Bosch, B.; Caprile, C.; Castellví, M.; Molinuevo, J.L.; Rami, L. Landscape test for assessing visual memory in Alzheimer's disease. *Rev. Neurol.* **2011**, *53*, 1–7. [CrossRef]
31. Peña-Casanova, J.; Quiñones-Úbeda, S.; Gramunt-Fombuena, N.; Quintana-Aparicio, M.; Aguilar, M.; Badenes, D.; Cerulla, N.; Molinuevo, J.L.; Ruiz, E.; Robles, A.; et al. Spanish Multicenter Normative Studies (NEURONORMA Project): Norms for Verbal Fluency Tests. *Arch. Clin. Neuropsychol.* **2009**, *24*, 395–411. [CrossRef]
32. Roth, C. Boston Naming Test. In *Encyclopedia of Clinical Neuropsychology*; Kreutzer, J.S., DeLuca, J., Caplan, B., Eds.; Springer New York: New York, NY, USA, 2011; pp. 430–433. ISBN 978-0-387-79948-3. [CrossRef]
33. Roth, C. Boston Diagnostic Aphasia Examination. In *Encyclopedia of Clinical Neuropsychology*; Kreutzer, J.S., DeLuca, J., Caplan, B., Eds.; Springer New York: New York, NY, USA, 2011; pp. 428–430. ISBN 978-0-387-79948-3. [CrossRef]
34. Turkstra, L.S. Western Aphasia Battery. In *Encyclopedia of Clinical Neuropsychology*; Kreutzer, J., DeLuca, J., Caplan, B., Eds.; Springer International Publishing: Cham, Germany, 2018; pp. 1–3. ISBN 978-3-319-56782-2. [CrossRef]
35. Warrington, E.K.; James, M.; Thames Valley Test Company. *The Visual Object and Space Perception Battery*; Thames Valley Test Company: Bury St. Edmunds, UK, 1991; ISBN 9780951432273.
36. Reitan, R.M.; Wolfson, D. Category Test and Trail Making Test as Measures of Frontal Lobe Functions. *Clin. Neuropsychol.* **1995**, *9*, 50–56. [CrossRef]
37. Stroop, J.R. Studies of interference in serial verbal reactions. *J. Exp. Psychol.* **1935**, *18*, 643–662. [CrossRef]
38. Smith, A. The symbol-digit modalites test: A neuropsychologic test for economic screening of learning and other cerebral disorders. *Learn. Disord.* **1968**, *3*, 83–91.
39. Wechsler, D. *Wechsler Adult Intelligence Scale–Fourth Edition (WAIS–IV)*; Pearson, Ed.; Pearson Assessment: San Antonio, TX, USA, 2008.
40. Folstein, M.F.; Folstein, S.E.; McHugh, P.R. "Mini-mental state". A practical method for grading the cognitive state of patients for the clinician. *J. Psychiatr. Res.* **1975**, *12*, 189–198. [CrossRef]
41. Gomar, J.J.; Ortiz-Gil, J.; McKenna, P.J.; Salvador, R.; Sans-Sansa, B.; Sarró, S.; Guerrero, A.; Pomarol-Clotet, E. Validation of the Word Accentuation Test (TAP) as a means of estimating premorbid IQ in Spanish speakers. *Schizophr. Res.* **2011**, *128*, 175–176. [CrossRef]
42. Rami, L.; Valls-Pedret, C.; Bartrés-Faz, D.; Caprile, C.; Solé-Padullés, C.; Castellvi, M.; Olives, J.; Bosch, B.; Molinuevo, J.L. Cognitive reserve questionnaire. Scores obtained in a healthy elderly population and in one with Alzheimer's disease. *Rev. Neurol.* **2011**, *52*, 195–201. [CrossRef]

43. Pesta, D.; Gnaiger, E. High-resolution respirometry: OXPHOS protocols for human cells and permeabilized fibers from small biopsies of human muscle. *Methods Mol. Biol.* **2012**, *810*, 25–58. [CrossRef]
44. Medja, F.; Allouche, S.; Frachon, P.; Jardel, C.; Malgat, M.; de Camaret, B.M.; Slama, A.; Lunardi, J.; Mazat, J.P.; Lombès, A. Development and implementation of standardized respiratory chain spectrophotometric assays for clinical diagnosis. *Mitochondrion* **2009**, *9*, 331–339. [CrossRef]
45. Bacigalupo, I.; Mayer, F.; Lacorte, E.; Di Pucchio, A.; Marzolini, F.; Canevelli, M.; Di Fiandra, T.; Vanacore, N. A Systematic Review and Meta-Analysis on the Prevalence of Dementia in Europe: Estimates from the Highest-Quality Studies Adopting the DSM IV Diagnostic Criteria. *J. Alzheimer's Dis.* **2018**, *66*, 1471–1481. [CrossRef]
46. Pereira, J.B.; Cavallin, L.; Spulber, G.; Aguilar, C.; Mecocci, P.; Vellas, B.; Tsolaki, M.; Kłoszewska, I.; Soininen, H.; Spenger, C.; et al. Influence of age, disease onset and *ApoE4* on visual medial temporal lobe atrophy cut-offs. *J. Intern. Med.* **2014**, *275*, 317–330. [CrossRef]
47. Jack, C.R.; Wiste, H.J.; Weigand, S.D.; Rocca, W.A.; Knopman, D.S.; Mielke, M.M.; Lowe, V.J.; Senjem, M.L.; Gunter, J.L.; Preboske, G.M.; et al. Age-specific population frequencies of cerebral β-amyloidosis and neurodegeneration among people with normal cognitive function aged 50-89 years: A cross-sectional study. *Lancet Neurol.* **2014**, *13*, 997–1005. [CrossRef]
48. Soriguer, F.; Goday, A.; Bosch-Comas, A.; Bordiú, E.; Calle-Pascual, A.; Carmena, R.; Casamitjana, R.; Castaño, L.; Castell, C.; Catalá, M.; et al. Prevalence of diabetes mellitus and impaired glucose regulation in Spain: The Di@bet.es Study. *Diabetologia* **2012**, *55*, 88–93. [CrossRef] [PubMed]
49. Handelsman, Y.; Bloomgarden, Z.T.; Grunberger, G.; Umpierrez, G.; Zimmerman, R.S.; Bailey, T.S.; Blonde, L.; Bray, G.A.; Jay Cohen, A.; Dagogo-Jack, S.; et al. American association of clinical endocrinologists and American college of endocrinology - Clinical practice guidelines for developing a diabetes mellitus comprehensive care plan - 2015 -. *Endocr. Pract.* **2015**, *21*, 413–437. [CrossRef] [PubMed]
50. Dalakas, M.C. The spectrum of inflammatory myopathies: Dermatomyositis, polymyositis, necrotizing myositis, and inclusion-body myositis. In *Acquired Neuromuscular Disorders: Pathogenesis, Diagnosis and Treatment*; Springer International Publishing: Berlin/Heidelberg, Germany, 2016; pp. 83–98. ISBN 9783319295145. [CrossRef]
51. Tripoli, A.; Marasco, E.; Cometi, L.; De Stefano, L.; Marcucci, E.; Furini, F.; Barsotti, S.; Cavagna, L. One year in review 2019: Idiopathic inflammatory myopathies. *Clin. Exp. Rheumatol.* **2020**, *38*, 1–10. [PubMed]
52. Limaye, V.S.; Lester, S.; Blumbergs, P.; Roberts-Thomson, P.J. Idiopathic inflammatory myositis is associated with a high incidence of hypertension and diabetes mellitus. *Int. J. Rheum. Dis.* **2010**, *13*, 132–137. [CrossRef]
53. Ramírez, S.; Gómez-Valadés, A.G.; Schneeberger, M.; Varela, L.; Haddad-Tóvolli, R.; Altirriba, J.; Noguera, E.; Drougard, A.; Flores-Martínez, Á.; Imbernón, M.; et al. Mitochondrial Dynamics Mediated by Mitofusin 1 Is Required for POMC Neuron Glucose-Sensing and Insulin Release Control. *Cell Metab.* **2017**, *25*, 1390–1399.e6. [CrossRef]
54. González-Casacuberta, I.; Juárez-Flores, D.L.; Ezquerra, M.; Fucho, R.; Catalán-García, M.; Guitart-Mampel, M.; Tobías, E.; García-Ruiz, C.; Fernández-Checa, J.C.; Tolosa, E.; et al. Mitochondrial and autophagic alterations in skin fibroblasts from Parkinson disease patients with Parkin mutations. *Aging (Albany NY)* **2019**, *11*, 3750–3767. [CrossRef]
55. Auburger, G.; Klinkenberg, M.; Drost, J.; Marcus, K.; Morales-Gordo, B.; Kunz, W.S.; Brandt, U.; Broccoli, V.; Reichmann, H.; Gispert, S.; et al. Primary skin fibroblasts as a model of Parkinson's disease. *Mol. Neurobiol.* **2012**, *46*, 20–27. [CrossRef]
56. Ramamoorthy, M.; Sykora, P.; Scheibye-Knudsen, M.; Dunn, C.; Kasmer, C.; Zhang, Y.; Becker, K.G.; Croteau, D.L.; Bohr, V.A. Sporadic Alzheimer disease fibroblasts display an oxidative stress phenotype. *Free Radic. Biol. Med.* **2012**, *53*, 1371–1380. [CrossRef]
57. Lerman, O.Z.; Galiano, R.D.; Armour, M.; Levine, J.P.; Gurtner, G.C. Cellular dysfunction in the diabetic fibroblast: Impairment in migration, vascular endothelial growth factor production, and response to hypoxia. *Am. J. Pathol.* **2003**, *162*, 303–312. [CrossRef]
58. Yu, T.; Robotham, J.L.; Yoon, Y. Increased production of reactive oxygen species in hyperglycemic conditions requires dynamic change of mitochondrial morphology. *Proc. Natl. Acad. Sci. USA* **2006**, *103*, 2653–2658. [CrossRef]

59. Lustbader, J.W.; Cirilli, M.; Lin, C.; Xu, H.W.; Takuma, K.; Wang, N.; Caspersen, C.; Chen, X.; Pollak, S.; Chaney, M.; et al. ABAD Directly Links Aβ to Mitochondrial Toxicity in Alzheimer's Disease. *Science (80-)* **2004**, *304*, 448–452. [CrossRef] [PubMed]
60. Johnson, E.L.; Feldman, H.; Butts, A.; Chamberlain, J.; Collins, B.; Doyle-Delgado, K.; Dugan, J.; Leal, S.; Rhinehart, A.S.; Shubrook, J.H.; et al. Standards of medical care in diabetes—2020 abridged for primary care providers. *Clin. Diabetes* **2020**, *38*, 10–38. [CrossRef]

MANUSCRIPT IV:

Title: *Integrated multi-omics analysis to infer molecular players in Inclusion body myositis*

Authors: Judith Cantó-Santos, Laura Valls-Roca, Ester Tobías, Clara Oliva, Francesc Josep García-García, Mariona Guitart-Mampel, Félix Andújar-Sánchez, Anna Esteve-Codina, Beatriz Martín-Mur, Joan Padrosa, Raquel Aránega, Pedro J. Moreno-Lozano, José César Milisenda, Rafael Artuch, Josep M. Grau-Junyent, Glòria Garrabou.

Journal: Under review in Antioxidants.

IF: 7.0

antioxidants

MDPI

Article

Integrated multi-omics analysis to infer molecular players in Inclusion body myositis

Judith Cantó-Santos[1,2,3], Laura Valls-Roca[1,2,3], Ester Tobías[1,2,3], Clara Oliva[4], Francesc Josep García-García[1,2,3], Mariona Guitart-Mampel[1,2,3], Félix Andújar-Sánchez[1,2,3], Anna Esteve-Codina[5,6], Beatriz Martín-Mur[4], Joan Padrosa[1,2,3], Raquel Aránega[1,2,3], Pedro J. Moreno-Lozano[1,2,3], José César Milisenda[1,2,3*], Rafael Artuch[4], Josep M. Grau-Junyent[1,2,3*], Glòria Garrabou[1,2,3,*]

[1] Inherited Metabolic Disorders and Muscular Diseases Research Group, Institut d'Investigacions Biomèdiques August Pi i Sunyer (IDIBAPS) and Faculty of Medicine and Health Sciences, University of Barcelona, Barcelona, Spain; jcanto@recerca.clinic.cat (J.C.-S.); lvalls@recerca.clinic.cat (L.V.-R.); etobi-asb@clinic.cat (E.T.); fjgarcia@recerca.clinic.cat (F.J.G.-G.); mguitart@recerca.clinic.cat (M.G.-M.); fandujsa7@alumnes.ub.edu (F.A.-S.); padrosa@clinic.cat (J.P.); aranega@clinic.cat (R.AR.); pjmoreno@clinic.cat (P.J.M.-L.); jcmilise@clinic.cat (J.C.M.); jmgrau@clinic.cat (J.M.G.); garrabou@clinic.cat (G.G.)

[2] Department of Internal Medicine, Hospital Clinic of Barcelona, Barcelona, Spain

[3] CIBERER— Spanish Biomedical Research Centre in Rare Diseases - ISCIII, Madrid, Spain

[4] Department of Clinical Biochemistry, Institut de Recerca Sant Joan de Déu; Esplugues de Llobregat, Barcelona, Spain; clara.olivam@sjd.es (C.O.); rartuch@sjdhospitalbarcelona.org (R.A.)

[5] CNAG-CRG, Centre for Genomic Regulation, Barcelona Institute of Science and Technology, Barcelona, Spain; anna.esteve@cnag.crg.eu (A.E.-C.); beatriz.martin@cnag.crg.eu (B.M.-M.)

[6] Universitat Pompeu Fabra (UPF), Barcelona, Spain

[*] Correspondence: garrabou@clinic.cat, jmgrau@clinic.cat and jcmilise@clinic.cat

Abstract: Inclusion body myositis (IBM) is an acquired inflammatory myopathy affecting proximal and distal muscles leading to weakness in patients over 50s. Diagnosis is based on clinical and histological findings in muscle related to inflammation, degeneration and mitochondria. In IBM, a shortage of validated disease models, lack of biomarkers and effective treatments lead to an unmet medical need. To overcome these hurdles, we performed an omics analysis of multiple samples from IBM patients (saliva, fibroblasts, urine, plasma and muscle) to gain insight into the pathophysiology of IBM. Degeneration was evident by the presence of amyloid ß peptide 1-42 (Aβ1-42) in the saliva of IBM patients. Metabolic disarrangements in IBM were manifested by an imbalanced organic acid profile in fibroblasts and urine. Specifically, abnormal levels of L-pyroglutamic and orotic acid were supported by abnormal expression of related metabolites in plasma and urine (glutathione and pyrimidines) and aberrant expression of upstream gene regulators (L2HGDH, IDH2, OPLAH and ASL) in muscle. Combined levels of L-pyroglutamic and orotic acid displayed an outstanding biomarker signature in urine with 100% sensitivity and specificity. The confirmation of systemic metabolic disarrangements in IBM and the identification of novel biomarkers unveil novel insights that require validation in larger cohorts.

Keywords: Inclusion body myositis (IBM), metabolism, organic acids, nucleotides, biomarker

Citation: Lastname, F.; Lastname, F.; Lastname, F. Title. *Antioxidants* **2022**, *11*, x. https://doi.org/10.3390/xxxxx

Academic Editor: Firstname Lastname

Received: date
Accepted: date
Published: date

Publisher's Note: MDPI stays neutral with regard to jurisdictional claims in published maps and institutional affiliations.

1. Introduction

IBM is an acquired inflammatory myopathy (IM) affecting patients over 50 years old, which prevalence ranges from 50-180 per million [1,2]. The first symptoms arise in the quadriceps and finger flexors, with complications in climbing stairs and grasping objects. These symptoms evolve towards proximal and distal muscle weakness that eventually impairs ambulation within 10-15 years from the disease onset. Moreover, 60% of the patients are also affected by dysphagia [3,4]. Diagnosis is based on clinical and histological

findings at inflammatory, degenerative and mitochondrial levels. Inflammation is triggered by the infiltration of CD8+ cytotoxic T-cells in myofibers and the upregulation of major histocompatibility complex I (MHC-I). Degeneration is presented in the form of rimmed vacuoles and the inclusion of TDP43, p62 and amyloid protein deposits. In mitochondria, ragged-red fibers, complex IV (COX negative) from the mitochondrial respiratory chain (MRC) and complex II (SDH positive) fibers are displayed, also present in primary mitochondrial diseases and mitochondrial myopathies [1,5–7].

IBM-related inflammation is critical in the disease and is the reason it groups within IMs such as dermatomyositis, polymyositis, anti-synthetase syndrome, necrotizing myopathy and non-specific myositis. Indeed, apoptosis-resistant highly differentiated and cytotoxic CD8+ T cells (with KLRG1 receptor) might trigger the onset of IBM [1,3,8], yet is in doubt whether the trigger is inflammatory or degenerative. However, inflammatory treatments, effective for other IMs, like immunosuppressants and immunomodulatory treatments, are ineffective for IBM. Ongoing clinical trials in IBM include a monoclonal antibody against the KLRG1 receptor to deplete the highly differentiated and cytotoxic CD8+ T cells (clinical trial code: NCT04659031), rapamycin (previously approved to prevent rejection in organ transplantation and to treat certain types of cancer) that blocks effector T cells while preserving T regulatory cells and inducing autophagy (NCT04789070), and even stem cell muscle injections (NCT04975841)[1].

Considering mitochondrial damage in IBM, it has been speculated that could be the result of pro-inflammatory cytokine release (IL-1β, TNF-α, etc.) that would increase oxidative, nitrosative and endoplasmic reticulum stress. Such lesions may endanger mitochondrial membrane permeability and transport, leading to a dysfunctional MRC that would accumulate mtDNA mutations [1,3,9]. Dysfunctional mitochondria may be aggravated by insufficient autophagy and specifically mitophagy, further increasing inflammation by mitochondrial damage. All this contributes to a positive feedback loop that may eventually trigger muscle fiber atrophy and accelerated muscle aging [1,6]. To avoid or reduce the lesions produced by increased oxidative stress, several antioxidant defense systems are activated, including superoxide dismutases (SOD) and glutathione (GSH) redox systems [10]. An increase in GSH, catalyzed by the GSH peroxidases (GPX) enzymes, is usually associated to higher production of oxidants and electrophiles in cells [11,12]. Consequently, the lack of sufficient GSH antioxidant activity may aggravate the outcome of the disease [10–12]. Thus, some GSH analogs have been tested as therapeutics, while decreasing GSH activity has been proven effective as an anti-tumor target, making tumors more susceptible to chemotherapy or radiotherapy[11]. None of these antioxidant therapies, neither metabolic strategies, have been ever tested in IBM, despite IBM displays pathological traits of mitochondrial function and despite some metabolic disorders often show muscle involvement.

Targeting treatment efficacy could be eased in the presence of validated IBM disease models. So far, most of the pathophysiology of IBM has been revealed from biological samples from the target tissue (muscle histopathology studies, RNA-seq, etc.) or peripheral tissues (blood RNA-seq and metabolomes, lymphocytes, and fibroblasts model validation) [5,7,13,14]. A mice xenograft, containing IBM muscle biopsies[15], became a breakthrough in the field to allow *in vivo* evaluation of disease pathophysiology. The major contribution of this model has been the finding that rimmed vacuoles resist after mice xenografts were treated with anti-CD3+, which reduced CD8+ T cells and impairs MHC-I upregulation, supporting the idea that new treatments should target degeneration to treat muscle weakness. Another relevant model of IBM was developed and validated by our group [13] using patients' derived fibroblasts, that recapitulated the main hallmarks of the target tissue of the disease (inflammatory, degenerative and metabolic muscle imbalances). Mitochondrial impaired function in IBM fibroblasts was similar to that of primary mitochondrial diseases[7,16] and was present in a peripheral tissue out of muscle, confirming molecular disturbances at systemic level. A relevant finding of the study was an abnormal organic acid profile in fibroblasts associated with MRC dysfunction and oxidative stress. This alteration

uncovered the potential use of metabolites and fibroblasts to identify biomarkers needed to monitor disease progression. However, neither that nor other studies have screened those markers in non-invasive fluids of IBM patients.

The same study highlighted the usefulness of omics technology to seek novel molecular players in disease that may emerge as surrogate biomarkers or therapeutic targets. Indeed, the identification of genetic variants, proteins, or metabolites associated with disease onset and progression in several diseases has been acquired on account of the development of unbiased, high-throughput omics technologies [17]. These analyses provide massive amounts of data from a small quantity of biological material and a reduced number of measurements. In addition, omics can be combined (e.g., RNA-seq, target metabolome, WES, etc.) and integrated to obtain a broad view of disease pathophysiology [17].

Thus, in the present article, we aimed to identify novel target molecules and pathways in IBM that may be validated as non-invasive biomarkers, especially focusing on the mitochondrial and metabolic profile of the disease by performing an omics analysis (targeted metabolome and RNA seq) of different biological samples from IBM patients (saliva, urine, plasma, fibroblasts and muscle).

2. Materials and Methods

2.1. Study design

A case-control study was conducted from 2018 to 2022, in the Department of Internal Medicine at Hospital Clínic of Barcelona (Barcelona, Spain). IBM patients were diagnosed according to clinical and pathological tests performed in our hospital, after fulfilling the criteria proposed by the European Neuromuscular Centre for IBM diagnosis [18]. Exclusion criteria were: age <40 years old, family history of hereditary mitochondrial disease; comorbidities and concomitant infections or drug abuse. IBM patients participating in the study signed the informed consent previously approved by the Ethical Committee of our hospital (code HCB/2017/0808). CTL were collected from healthy volunteers, age and gender-paired to IBM patients, after excluding any comorbidity or pathological process, and signed the corresponding informed consent.

2.2. Sample collection

Saliva samples were passively collected (no stimulation) in sterile plastic containers, adding 0.5 mg sodium azide (Sigma #S2002, Saint Louis, MO, USA) and 0.5 mg thioflavin S (Sigma #T1892, Saint Louis, MO, USA), to prevent bacterial growth and Aß42 aggregation, respectively [19–21]. 9 IBM cases and 5 CTL were collected. Samples were immediately frozen at -80ºC until used.

Fibroblasts were obtained from a skin punch biopsy from 14 cases and 12 controls. Cells were grown in 25 mM glucose DMEM supplemented with 10% FBS and 1% penicillin-streptomycin, at 37ºC, in a humidified 5% CO_2 air incubator (all from Gibco, Waltham, MA, USA). Cells were harvested and collected by trypsin (Gibco, Waltham, MA, USA), at 80% of confluence, and characterized at passages 3 to 10.

Urine was collected from 6 cases and 6 controls, and organic acid and nucleotide content was analyzed and normalized by creatinine levels.

Plasma was collected from 12 patients and 12 controls and used to determine GPX activity.

Muscle biopsies were performed for diagnostic purposes [22,23]. Leftover biopsy material from 5 IBM patients and 6 CTL (defined as individuals without histological myopathic alterations) were included in this study for mRNA seq study.

2.3. Aß1-42 detection

To detect Aß1-42 in saliva, 50 µl per sample was added to an enzyme-linked immunosorbent assay (ELISA) plate, per duplicate (Biomatik #EKU02331, Ontario, Canada) following the manufacturer's protocol.

2.4. Metabolite quantification

Total protein amount in fibroblasts samples were quantified using a bicinchoninic acid protein assay (BCA) (Thermo Scientific #23255, MA, USA), and 5 mg/ml were resuspended in 200 µL pf PBS and centrifuged (1500g; 10 min) to collect the supernatant. Urine samples were normalized by creatinine content. Organic acids were extracted with ethyl acetate and diethyl ether and derived with bis(trimethylsilyl) trifluoro-acetamide, as previously reported [24]. The trimethylsilyl derivatives obtained were separated by gas chromatography (Agilent 7890A, Wilmington, DE, USA) and detected in a mass spectrometer (Agilent 5975C, Wilmington, DE, USA). The results were expressed as m/z ratio.

2.5. Glutathione peroxidase (GPX) activity assay

To quantify the GPX activity, 10 µl of plasma per sample was used in an enzymatic assay (MAK437, Sigma-Aldrich, Saint Louis, MO, USA), following the manufacturer's protocol.

2.6. RNA extraction and mRNA library preparation and sequencing

Total RNA was isolated from the muscle by tissue homogenization (OMNI Tissue) with (Roche #11667165001, Basel, Switzerland) and isopropanol (Sigma #190764, Saint Louis, MO, USA) precipitation protocols. Total content was assessed through Quawell UV-VIS Spectrophotometer Q5000. Concentrations were adjusted to 100 ng/µl in RNase-free water. The quality control of the total RNA was done using the Qubit RNA HS Assay (Life Technologies) and RNA 6000 Nano Assay on a Bioanalyzer 2100 (Agilent, Santa Clara, CA, USA). The RNA-seq libraries were prepared using the TruSeq Stranded mRNA LT Sample Prep Kit. Briefly, total RNA (500ng) was enriched for the mRNA fraction and fragmented. Strand-specificity was achieved by the second-strand cDNA incorporating dUTPs instead of dTTPs. The blunt-ended double stranded cDNA was 3'adenyIated and Illumina platform compatible adaptors with unique dual indexes and unique molecular identifiers (Integrated DNA Technologies) were ligated. The ligation product was enriched with 15 PCR cycles and the final library was validated on an Agilent 2100 Bioanalyzer with the DNA 7500 assay. The libraries were sequenced on 4000 (Illumina) with a read length of 2x51bp using the HiSeq 4000 SBS kit (Illumina). Primary data analysis, image analysis, base calling and quality scoring of the run were processed using the manufacturer's software Real Time Analysis (RTA 2.7.7) followed by the generation of FASTQ sequence files.

2.7. RNA-seq data processing and analysis

RNA-seq reads were mapped against the human reference genome (GRCh38) using STAR software version 2.5.3a [25] with ENCODE parameters. Annotated genes were quantified using human GENCODE annotation file version 34 with RSEM v1.3.0 [26] and default parameters. Differential expression analysis was performed with DESeq2 V1.26.0 R package [27] using a Wald test to compare affected and control groups, adjusting for sex in the model. Genes were considered differentially expressed with an adjusted p-value <0.05 and absolute fold change $|FC| > 1.5$. Differentially expressed genes (DEGs) were filtered according to the ones found in Mitocarta 3.0 [28], and specifically, to the Metabolism pathway. In the Metaboanalyst platform two analysis were performed: a Joint pathway analysis and Network analysis, both combining transcriptomics and targeted metabolomics lists with their fold values [29].

2.8. Statistical analysis

Statistical analysis was performed with the Statistical Package for the Social Sciences software, version 27 (IBM SPSS Statistics; SPSS Inc) and GraphPad Prism 9 (GraphPad Software, San Diego. CA, USA). Results were expressed as mean ± SEM or in FC between conditions, normalized by creatinine or protein load. Obtained data were compared between independent experiments using the non-parametric Mann-Whitney U test or

KruskaI-Wallis's test. Receiver Operating Characteristic (ROC) curves and the area under the ROC curve (AUC) were examined to check biomarker performance. AUC ranges from 0 to 1, where values > 0.7 reflect good biomarker performance. Sensitivity and specificity values were determined with a binary logistic regression analysis using Wald test method. The signification threshold was set at p-value < 0.05.

3. Results

3.1. Clinical and epidemiological data

In this study, the cohort of IBM patients was composed of white Caucasian population ranging from 40 to 83 years old, while controls (CTL; healthy individuals at the time of inclusion) were from the same population and ranged from 38 to 79 years old. Both cohorts were paired by age and sex. The number of samples per cohort, male vs. female ratio, and mean age in each cohort can be found in Table 1.

Table 1. Clinical and epidemiological data of the cohorts involved in the study

Sample type	Summary	Num samples (n)	Male/ Female Ratio	Mean age (years)
Fibroblasts	IBM	14	0.6	66.9±3.6
	CTL	12	0.4	57.4 ± 4.6
Urine	IBM	6	0.5	70.8± 3.7
	CTL	6	0.5	71.2± 3.4
Muscle	IBM	5	0.40	62.6±6.4
	CTL	6	0.67	44.6±4.7
Saliva	IBM	9	0.44	67.2± 4.7
	CTL	5	0.6	57.0 ±5.9
Plasma	IBM	12	0.6	63.7 ± 3.5
	CTL	12	0.6	75.3 ± 0.9

Data presented as mean ± SEM. Abbreviations: IBM: Inclusion Body Myositis patients. CTL: healthy individuals; Age and gender-paired distribution between cohorts.

3. 2. Degeneration markers: Aβ1-42 concentration was higher in IBM samples

The presence of amyloid β in rimmed vacuoles and protein depots of muscle tissue from IBM patients has been recently questioned [30]. Despite this long-standing belief is currently in controversy, we previously confirmed altered levels of amyloidogenic degenerative markers in plasma from IBM patients (including BACE-1 and PS-1[31]) and decided to evaluate the presence of Aβ1-42 (linked to β- and ɣ-secretase enzymes) in a fluid that could be easily accessible: saliva samples from IBM patients vs. CTL. Interestingly, Aβ1-42 displayed trends towards higher concentration in the IBM cohort (43.7±12.5 vs. 13.3±6.7, p-value=0.15) (Figure 1a) and significant 66.70% and 50.00% sensitivity and specificity scores as a surrogate marker of disease, with a high AUC of 0.78 ± 0.13 (p-value=0.12) (Figure 1b and Table S1). Although these results should be validated in bigger size cohorts, Aβ1-42 emerges as a promising marker to potentially discriminate between cohorts.

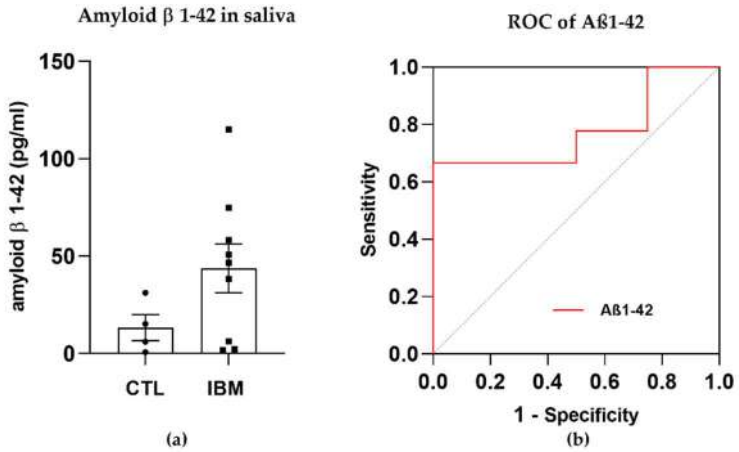

Figure 1. Amyloid β peptide 1-42 (Aβ1-42) in saliva samples. (a) Bar graphs of the concentration of Aβ1-42 in inclusion body myositis (IBM) vs control (CTL) samples. (b) Receiver Operating Characteristic (ROC) curve and area under the ROC curve (AUC) of Aß1-42 (AUC= 0.78 ± 0.13. p-value=0 .12). Sensitivity and specificity scores of 66.70% and 50.00%. respectively. Higher Aβ1-42 concentration and high AUC scores in IBM suggested it could aid to discriminate between cohorts.

3.3. Mitochondrial alterations

3. 3. 1. Organic acids profile increased in IBM fibroblasts

Targeted metabolome characterization of organic acids in fibroblasts represented by FC between IBM and CTL fibroblasts revealed higher concentration in IBM in Figure 2a. Such aberrant profile suggests altered intermediary metabolism potentially related to MRC dysfunction. Among them, we focused on L-pyroglutamic and 2-hydroxy glutaric acids (4.6 ± 0.6 vs. 3.0 ± 0.1, p-value=0.04 and 0.2±0.1 vs. 0.03±0.01, p-value=0.01, respectively) (Figure 2b), linked to GSH synthesis and tricarboxylic acid cycle (TCA) cycle, respectively. These organic acids may also be detected in non-invasive fluids as urine. Their ROC curves were significant in both cases. L-pyroglutamic acid showed AUC=0.76±0.12 (p-value=0.04) accompanied by significant 72.7% sensitivity and 80% specificity values; and 2-hydroxy glutaric acid showed high AUC=0.84±0.09 for (p-value=0.01), with 72.70% and 77.80% sensitivity and specificity values (Figure 2c and Table S1). Thus, the next step was to evaluate the signature of organic acids in other peripheral samples of IBM patients that may be used as a liquid biopsy for evaluation of disease. To promote non-invasive sample profiling, we decided to examine the organic acids in urine.

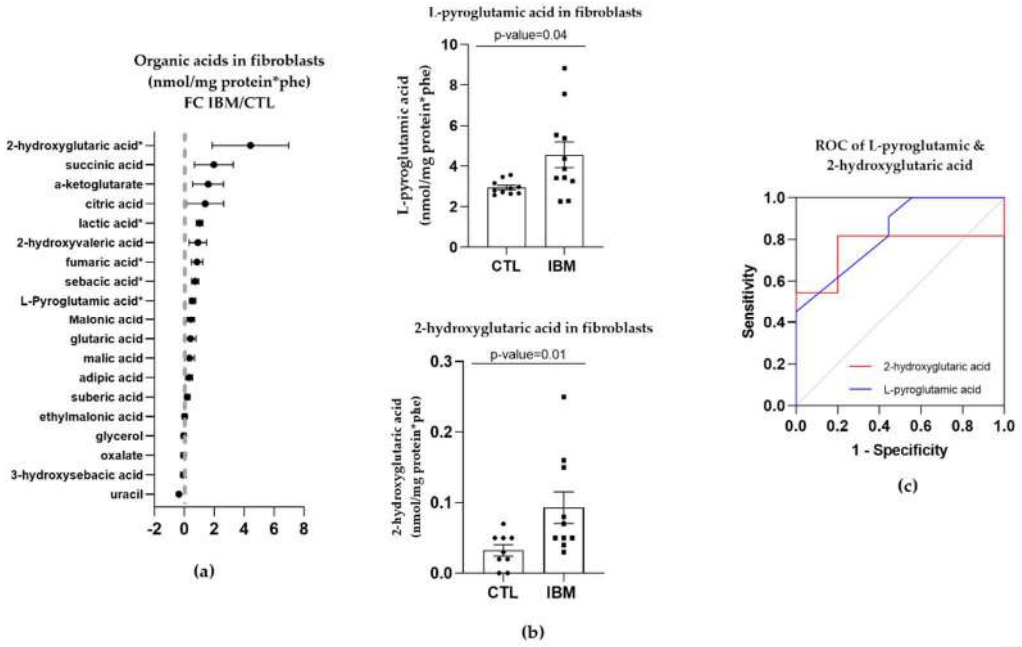

Figure 2. Organic acids profile in inclusion body myositis (IBM) vs. controls (CTL) fibroblasts (n=11 vs 10). (a) Fold change (FC) of the concentration of organic acids in IBM vs CTL fibroblasts (*p-value<0.05). (b) Bar graph of L-pyroglutamic and 2-hydroxyvaleric acids (p-value <0.05). (c) Receiver Operating Characteristic (ROC) curve and area under the ROC curve (AUC) of L-pyroglutamic (AUC=0.79 ± 0.12. p-value=0.03) and 2-hydroxyvaleric acids (AUC=0.84 ± 0.09. p-value=0.01). Their sensitivity and specificity values are 72.7% and 80% for L-pyroglutamic acid and 72.70% and 77.80% for 2-hydroxy glutaric acid. All the organic acids had an increased concentration in IBM vs CTL fibroblasts, being L-pyroglutamic and 2-hydroxy glutaric acids the most remarkable, the first linked to glutathione synthesis and the second to TCA cycle.

3. 3. 2. Organic acids profiling in urine reveals altered metabolism in IBM

In the urine of IBM patients, roughly half of the organic acids presented an upregulation and half a reduction, observed in Figure 3a. The most relevant organic acids were L-pyroglutamic (as in fibroblasts; 17.0 ± 9.1 vs. 7.0 ± 1.7, p-value=0.48) and orotic acid (6.1 ± 1.8 vs. 1.7 ± 0.5, p-value=0.01, Figure 3b), linked to GSH synthesis and pyrimidine biosynthetic pathway, respectively. Their ROC curves presented an AUC = 0.64±0.17 (p-value= 0.42, with 50% sensitivity and 83.3% specificity) for L-pyroglutamic acid and AUC = 0.94±0.07 (p-value=0.01) in orotic acid, with 100% sensitivity and 83.3% specificity scores (Figure 3c and Table S1). These sensitivity and specificity values increased to the 100% when L-pyroglutamic and orotic acid were tested combined. The presence of altered organic acids in urine supported the imbalanced organic acid profile in fibroblasts and targets L-pyroglutamic and orotic acid as potential fluid biomarkers in disease.

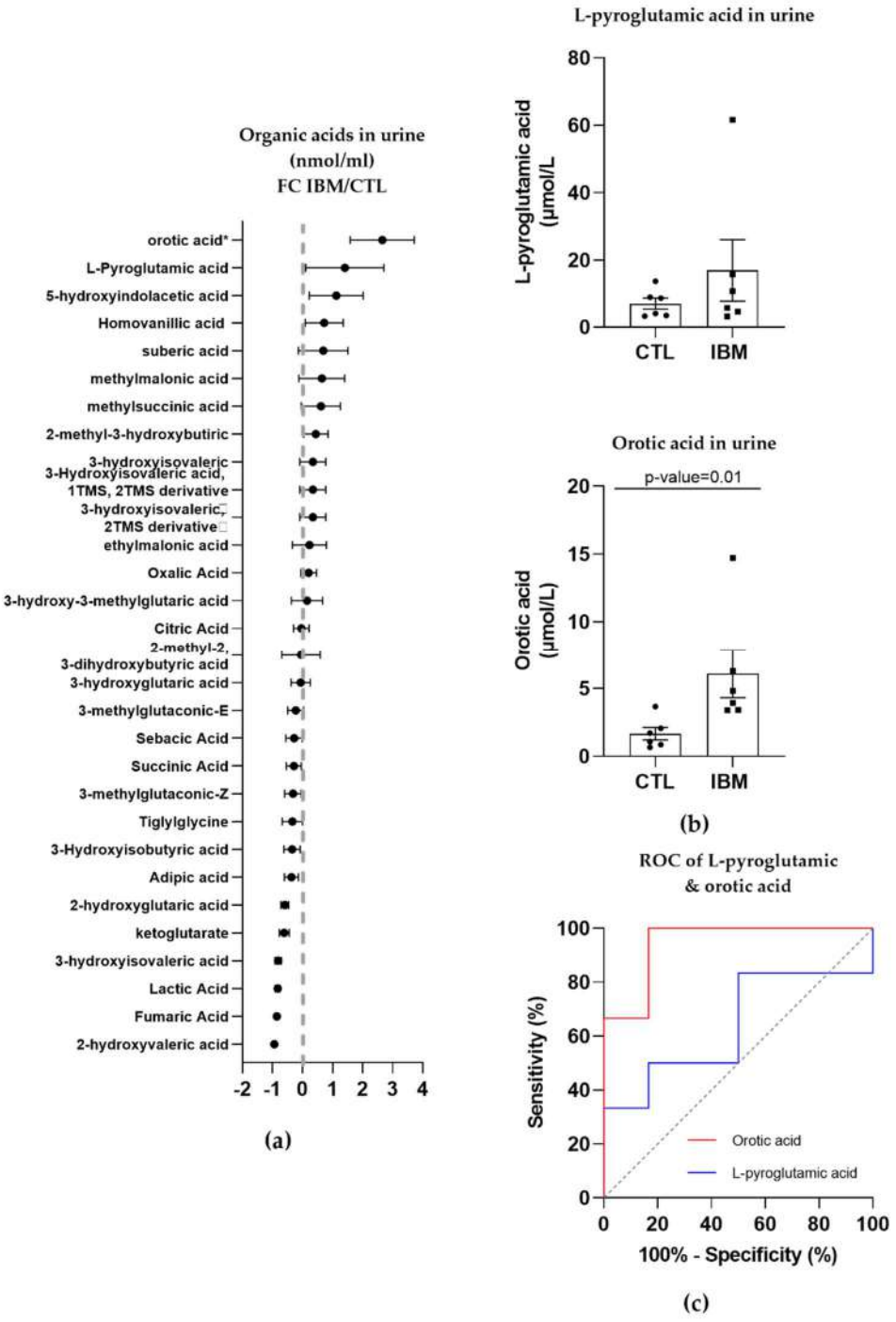

Figure 3. Organic acids profile in the urine of inclusion body myositis (IBM) vs. control (CTL) samples (n=6/group). (a) Fold change (FC) of the concentration of organic acids in the urine of lBM vs CTLs. (b) Bar graphs of L-pyroglutamic and orotic acids (p-value <0.05). (c) Receiver operating Characteristic (ROC) curve and area under the ROC curve (AUC) of L-pyroglutamic (AUC=0.64 ± 0.17. p-value=0.42) and orotic acids (AUC=0.94 ± 0.07. p-value=0.01). Their sensitivity and specificity values are 50.0% and 83.3% for L-pyroglutamic acid and 100.0% and 83.3% for orotic acid, but 100% sensitivity and specificity when both acids were tested together. The presence of altered organic acids in urine supported the imbalanced organic acid profile in fibroblasts and targets L-pyroglutamic and orotic acid as potential fluid biomarkers.

3. 3. 2. 1. Metabolites related to organic acids

3. 3. 2. 1. 1. Nucleotide synthesis precursors increased in the urine of IBM patients

As orotic acid plays a role in the pyrimidine biosynthetic pathway, we evaluated the nucleotide metabolism in urine in IBM vs. CTLs samples. Briefly, almost all pyrimidines and purines had a higher concentration in IBM in urine (Figure 4a), with orotidine and pseudo uridine being statistically significant (1.0 ± 0.2 vs 0.5 ± 0.1, p-value=0.03, and 39.1 ± 6.8 vs. 13.2 ± 2.3, p-value=0.01, respectively). These two metabolites are linked to the pyrimidine biosynthesis pathway; orotidine being the product of orotic acid plus 5-phosphoribosyl-1-pyrophosphate (PRPP) catalyzed by uridine monophosphate synthetase (UMPS) in its orotate phosphoribosyl transferase activity; and pseudo uridine being the product of orotidine catalyzed by UMPS in its orotidine-5′-phosphate decarboxylase (OMP decarboxylase) activity [32].

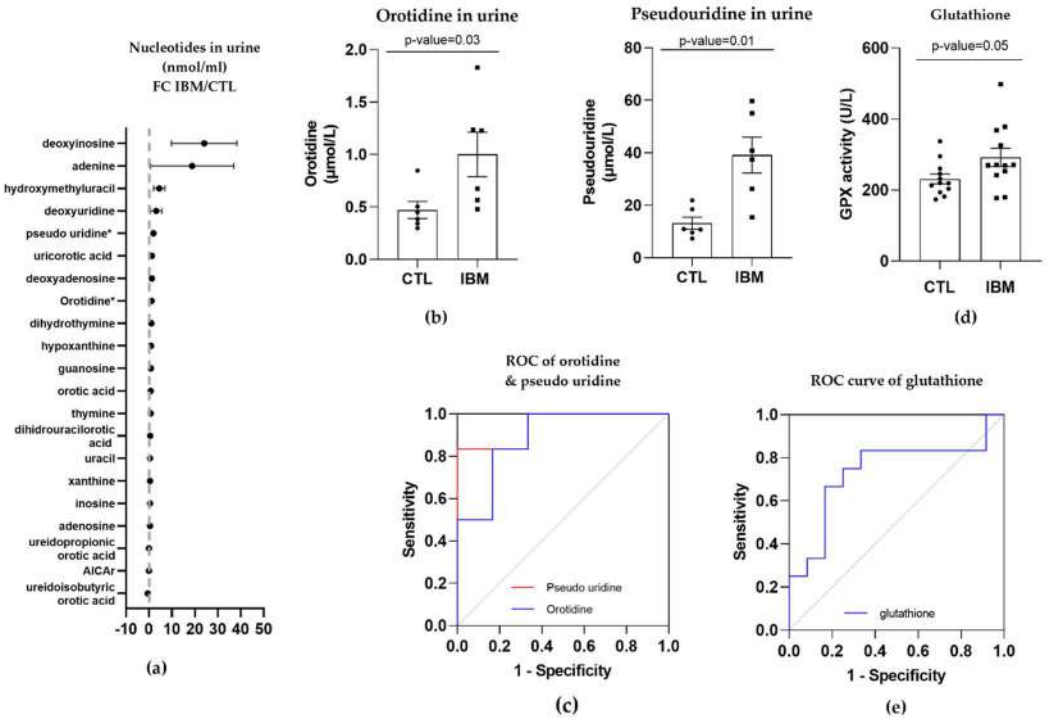

Figure 4. Nucleotides in urine and glutathione in plasma of inclusion body myositis (IBM) vs. control (CTL) samples (n=6/group). (a) Fold change (FC) of the concentration of nucleotides in urine of IBM vs CTLs. (b) Bar graphs of orotidine and pseudo uridine (p-value <0-05). (c) Receiver Operating Characteristic (ROC) curve and area under the ROC curve (AUC) of orotidine (AUC=0.89 ± 0.10. p-value=0.02) and pseudo uridine (AUC=0.94 ± 0.07. p-value=0.01). Their sensitivity and specificity values are 66.7% and 83.3% for orotidine and 83.3% for both in pseudo uridine. (d) Glutathione peroxidase (GPX) activity in IBM vs CTL plasma samples (p-value=0.05). (e) Receiver Operating Characteristic (ROC) curve and area under the ROC curve (AUC) of GPX (AUC=0.74 ± 0.11, p-value=0.05), with 66.7% sensitivity and 75.0% specificity. Almost all nucleotides had a higher concentration in IBM in urine, with orotidine and pseudo uridine being statistically significant, supporting the altered orotic acid biosynthesis previously observed. GPX activity was also higher in IBM, endorsing an increased glutathione redox system activity linked to oxidative stress.

The quantification of these two pyrimidines (Figure 4b) and the evaluation of their ROC curves displayed an AUC= 0.89 ± 0.10 (p-value=0.02) for orotidine, with 66.7% sensitivity and 83.3% specificity; and AUC=0.94±0.07 (p-value=0.01) for pseudo uridine, with 83.3% sensitivity and specificity (Figure 4c and Table S1), supporting the altered orotic acid biosynthesis previously observed.

3. 3. 2. 1. 2. GPX activity levels in plasma

The increase in L-pyroglutamic acid in fibroblasts and urine, could be potentially linked to GSH metabolism. Thus, we examined the activity of GPX to investigate the antioxidant defense system activity in the plasma of IBM vs CTLs.

The GPX activity was increased in IBM samples (292.0±25.9 vs. 231.4±13.7, p-value=0.05, Figure 4d) and significant 66.7% and 75.0% sensitivity and specificity scores, with high AUC of 0.74 ± 0.11 (p-value=0.05) (Figure 4e and Table S1). This assay revealed a higher activity in IBM, potentially needed to compensate for an increase in oxidative stress, previously described to contribute to neuromuscular diseases physiopathology [33].

3. 3. 2. 2. Metabolic-upstream related genes in the IBM muscle transcriptome

All metabolic disarrangements leaded to the identification of target metabolites related to nucleotide, TCA and glutathione system in different samples of IBM patients (Figure 5), that scored high values of specificity and sensibility (Table S1). Thus, the detection of target metabolites in fibroblasts and urine interrogates whether these pathways could be altered in the target tissue of the disease (muscle). Therefore, we filtered the genes related to metabolism among the DEGs of the muscle transcriptome between IBM and CTL muscles and we observed a larger number of DEGs from IBM patients related to metabolism. Specifically, from the 418 DEGs in IBM patients related to mitochondria [28], 197 were linked to metabolism [28], 32 were upregulated and 165 downregulated (Table S2). The top upregulated DEGs are OXCT2, KMO, MTHFD1L, CYP27B1, AIFM3, in descendant order; whereas the most downregulated DEGs are ACOT11, ALDH6A1, BCO2, GPT2, SLC25A30, in ascendant order. In depth, OXCT2 is involved in ketone body catabolism; KMO in tryptophan metabolism; MTHFD1L in purine biosynthesis; CYP27B1 in calcium homeostasis and AIFM3 in apoptosis; while ACOT11 plays a role in fatty acids and CoA metabolism; ALDH6A1 valine and pyrimidine catabolic pathways; BCO2 in vitamin A biosynthesis; GPT2 in pyruvate metabolism and SLC25A30 in mitochondrial membrane transport. These data supported functional metabolic deregulation at genetic level and confirmed the relevance of metabolic deregulation in disease.

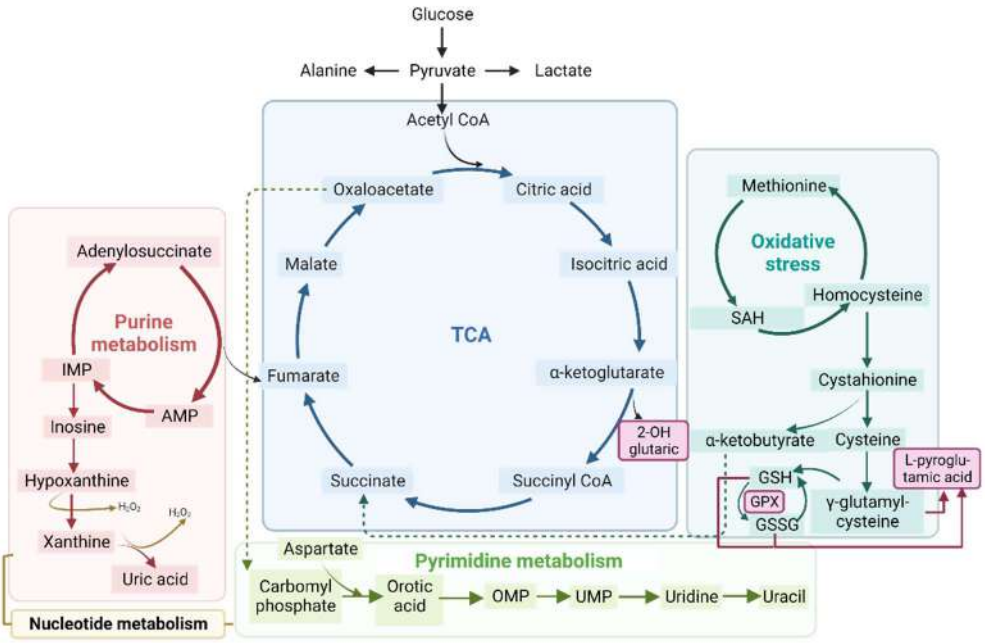

Figure 5. Schematic representation of the tricarboxylic acid cycle (TCA) (in blue), purine (in red) and pyrimidine (in green) metabolism (both part of the nucleotide metabolism) and oxidative stress (in turquoise). All of them are related to the metabolic profile examined in the organic acids, nucleotides and RNA seq analysis. Abbreviations: IMP: inosine monophosphate; AMP: adenosine monophosphate; OMP: orotate monophosphate; UMP: uridine 5'-monophosphate; SAH: S-adenosylhomocysteine; GSH: glutathione; GSSG: glutathione disulfide; GPX: glutathione peroxidase.

Specifically, these 197 metabolism-related genes were clustered in 9 Mito Pathways [28], which are carbohydrate, lipid, amino acid, nucleotide, vitamin, and sulfur metabolism, detoxification, electron carriers and metals and cofactors, represented in Figure 6. Among them, the top affected Mito Pathways were carbohydrate metabolism with a 56.8% of DEGs involved (42/74 DEGs in common) and metals and cofactors with a 52.8% (65/123 DEGs matched) [28] (Table S3). In all pathways, more DEGs were downregulated than upregulated. In addition, some genes were involved in more than one pathway, as seen in Figure 6, revealing how the metabolism is interconnected and every alteration could be directly or indirectly linked to a specific dysfunction.

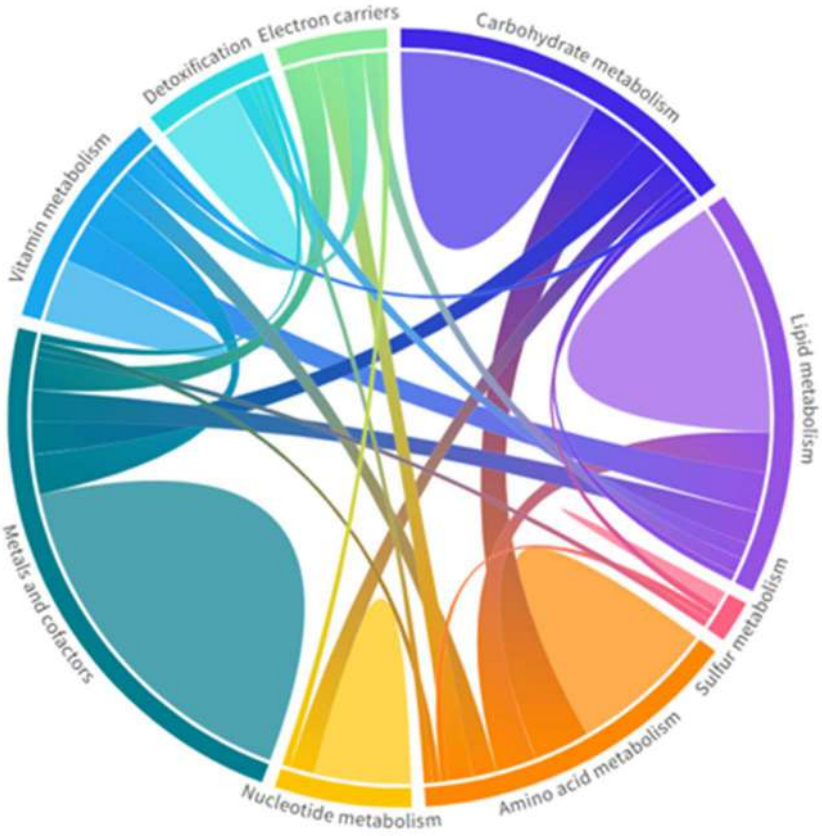

Figure 6. Metabolic pathways in the muscle RNA-seq of inclusion body myositis (IBM) vs controls (CTL). Each pathway is represented with a different color with the genes unique to that pathway (domes) and the interactions of genes across pathways (chords). Wider domes and chords represent a higher number of genes. Among them, *carbohydrate metabolism* and *metals and cofactors* with a 56.8% and 52.8% of DEGs involved were the most affected metabolic pathways (Table S2). Overall, these data supported functional metabolic deregulation at gene expression level and confirmed the relevance of metabolic deregulation in disease.

3. 4. Gene-metabolites interaction: potential interactome framework for IBM samples

To reveal whether metabolic DEGs may be related to deregulated organic acid profile in urine and potentially biomarkers of disease, we linked the previously relevant organic acids in fibroblasts and urine to their respective DEGs at the muscle level, represented in Figure 7. In brief, 2-hydroxy glutaric acid, increased in fibroblasts, was linked to L-2 and D-2-hydroxy glutaric aciduria genes (L2HGDH and IDH2), that were downregulated in muscle, as expected, and in common to primary 2-Hydroxy glutaric aciduria disease (ORPHA:19) [34]. In the case of L-pyroglutamic acid, increased in fibroblasts and urine, was linked to the 5-Oxoprolinase ATP-Hydrolyzing (OPLAH) gene, accordingly downregulated in muscle, as in primary 5-Oxoprolinuria disease (ORPHA:289846) [34,35]. Downregulated OPLAH is related to GSH defects in muscle, which leads to an increased concentration of L-pyroglutamic acid in urine. Regarding orotic acid, increased in urine, is associated with Argininosuccinate Lyase (ASL) gene, upregulated in muscle, as expected and in common to primary Argininosuccinic aciduria disorder (ORPHA:23) [34]. ASL is part of the urea cycle, but also plays a role in fumarate and arginine synthesis in muscle. All these multi-omics and interactome connection between metabolites and genes confirmed the metabolic dysregulation in IBM.

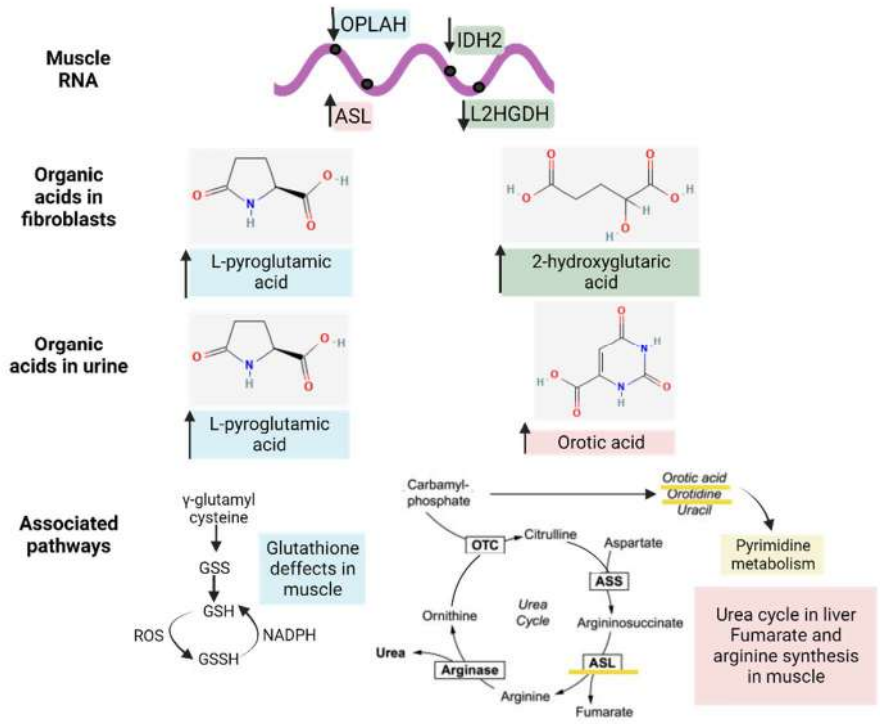

Figure 7. Interactome of the metabolic differentially expressed genes (DEGs) in muscle related to the significantly altered organic acids pattern (in fibroblasts and urine) and their associated pathways. In different colors (blue, green and pink) the upstream (genes) and downstream (organic acids and nucleotides) effectors of each pathway.

In parallel to the associations in Figure 7, we also performed a Metaboanalyst analysis [29] combining DEGs related to metabolism in muscle vs. organic acids and nucleotides in urine. This approach allows to identify interactions by connecting gene expression to metabolite data. Concisely, when compared against DEGs in metabolism, 10 pathways in organic acids and 7 in nucleotides were statistically significant (FDR < 0.05). All 7 pathways enriched in nucleotide analysis were also enriched in organic acids, being the TCA cycle the most relevant pathway (represented in Figure 5), followed by Valine, leucine and isoleucine degradation, Propanoate metabolism and Pyruvate metabolism (Table S4). In the network enrichment analysis, the TCA cycle was the most enriched network followed by Alanine, aspartate and glutamate metabolism (FDR < 0.05) in metabolic DEGs combined with organic acids; while Purine metabolism and Pyrimidine metabolism were the significantly enriched networks (FDR<0.05) in metabolic DEGs combined with nucleotides (Table S4). In short, the data reinforced the interconnection of all affected metabolic pathways and the relevance of metabolic changes in disease.

4. Discussion

The discovery of biomarkers linked to diagnosis or prognosis in IBM is scarce despite the development of omics technologies and high-throughput screenings of several samples and patients [17]. In IBM, the major advances in biomarker identification include the description of HLA haplotypes HLA-DRB1*03:01, HLA-DRB1*01:01 and HLA-DRB1*13:01 [1,36], the last two being IBM-specific alleles; the discovery of IBM specific CD8+ KLRG1+ T cells [8,37]; NT5c1A autoantibody in the sera of IBM patients [38,39]; cadherin 1 (CDH1) overexpressed in IBM muscle [40]; and type I and γ interferon pathways (detected at transcriptomic and proteomic level) [41], that supported the immune

interaction between immune cells and myofibers in IBM. Of note, none of the previous biomarker signatures are related to the degenerative or mitochondrial changes in IBM and none of them are real-time measures that may be evaluated in liquid biopsy to reflect disease evolution or prognosis.

This study aimed to perform multi-omics profiling through high throughput analysis of numerous biological samples from IBM patients to infer novel target molecules with a differential profile in disease. We first explored Aβ1-42 measurement in IBM saliva that yielded to relevant but non-significant conclusions that should be better explored in studies with larger cohorts. Interestingly, previous findings of our group depicting aberrant levels of BACE1 and PSN1 proteins in plasma of IBM patients may confirm the systemic affection of disease and implication of amyloidogenesis in IBM [31].

Later, the fact that IBM mitochondrial alterations resemble mitochondrial primary and secondary diseases [5,7,13,16], leaded us to analyze the metabolic profile in IBM samples, first in fibroblasts and then in urine. Briefly, the targeted metabolic profile of IBM fibroblasts displayed a higher expression of organic acids in IBM, with L-pyroglutamic and 2-hydroxy glutaric acid, the latter closely related with the TCA cycle, as the most remarkable ones. When the organic acid profile was examined in urine and more metabolites were detected, L-pyroglutamic acid and orotic acid emerged as surrogate biomarkers of disease. Orotic acid can be increased in different metabolic conditions involving urea cycle disorders and pyrimidine biosynthesis defects. Carriers of these conditions may display subtle orotic acid increments in urine, but considering that these are rare diseases, it is unlike that our cohort of IBM patients harbor variants in genes relates with these metabolic pathways. Pyroglutamic acid excretion in urine can increase due to genetic but also environmental conditions [35,42], such as special diets, drug treatments, prematurity or malnutrition). Although we did not rule out the presence of these factors in our cohort of patients, the increased pyroglutamic acid values also in fibroblasts, that it should not be influenced by environmental conditions, strongly support the feasibility of this surrogate for the study of IBM patients. To understand these organic acid alterations in disease, we determined GSH content and nucleotide levels in urine, due to their association to L-pyroglutamic acid and orotic acid metabolism, respectively. GPX activity was increased in IBM plasma samples, suggesting a need to counterbalance oxidative stress in IBM [13,33]. Specifically, GPX catalyzes the following reaction: GSH + H_2O_2 → GSSG + H_2O (where GSSG is GSH disulfide) to maintain redox cell homeostasis by attracting free radicals to reduced GSH and convert them into GSSG and H_2O. Related to orotic acid, orotidine and pseudo uridine, from the pyrimidine biosynthetic pathway, were increased in IBM samples in urine. These findings reinforce the metabolic and oxidant component of IBM, probably present also in other IMs [33].

When the metabolic profile was linked to the metabolic-related DEGs in RNA-seq in muscle, we observed a correlation between some DEGs and organic acids, confirming the value of L-pyroglutamic acid and orotic acid as potential biomarker signatures in IBM urine and the relevance of metabolism in disease. Specifically, the interactome analysis revealed the following Mito pathways affected in disease: carbohydrate, lipid, amino acid, nucleotide, vitamin, and sulfur metabolism, detoxification, electron carriers and metals and cofactors. In addition to Mito pathways, the Metaboanalyst combining metabolic DEGs in muscle, with organic acids and nucleotides in urine revealed that the TCA cycle, Valine, leucine and isoleucine degradation, Propanoate metabolism and Pyruvate metabolism were the most enriched pathways, endorsing the mitochondrial and metabolic role in the muscle DEGs.

Previously, other studies also found increased nucleotide synthesis precursors and altered pyrimidine and GSH metabolism among IBM pathway analysis [5], linked to L-pyroglutamic acid and orotic acid respectively, although it was in the blood from IBM patients. Indeed, the IBM pathway analysis in the blood metabolomes also resembles the Metaboanalyst pathway and network analysis that we observed in IBM in urine and muscle, supporting the RNA-seq to metabolome link in muscle vs. fluid samples (urine and

blood) and the robustness of the present findings. However, previous analyses were only conducted at transcriptomic level; this is the first study analyzing metabolites in non-invasive fluids of IBM patients.

Most of the biomarkers identified displayed high sensitivity and specificity scores and prompted the idea of potential support in diagnosis and follow-up by a non-invasive approach. However, we propose L-pyroglutamic combined to orotic acid as a surrogate biomarker of disease in urine, due to their highest sensitivity (100%) and specificity (100%) scores when tested together. Separately, L-pyroglutamic acid is a biomarker in Eosinophilic Esophagitis (in urine) and Glutathione Synthetase Deficiency (in urine and in blood) diseases. Chronically high levels of L-pyroglutamic acid are associated with several inborn errors of metabolism like 5-Oxoprolinuria, 5-oxoprolinase deficiency, Glutathione Synthetase Deficiency, Hakinsinuria and Propionic acidemia [43]. Similarly, orotic acid in urine is a biomarker of the following metabolic diseases: Ornithine Transcarbamylase Deficiency, N-Acetylglutamate Synthase Deficiency and Orotic Aciduria [44]. None of them have been associated with muscular diseases, thus avoiding potential overlap on clinical symptoms between these conditions. These results should be confirmed in a larger cohort, as well as validate its potential use as a prognostic marker in accordance with disease evolution.

Despite the novelty of these results and their translational relevance for clinical management, we should acknowledge some limitations. The main one is the small sample size of the study, mainly because IBM is a rare disease, with difficult access to biological samples. Interestingly, the intertwined and narrow relationship between the results obtained across the different analyses and tissues, made these findings stronger and validate the usefulness of multi-omics approaches to identify biomarkers in disease.

In detail, combining metabolite vs. RNA-seq profile (Fig. 7) revealed that L-pyroglutamic acid, increased in fibroblasts and urine, was linked to downregulated OPLAH gene, related to GSH defects in muscle and responsible for an increased concentration of L-pyroglutamic acid in urine [35]. Orotic acid, increased in urine, was associated with the ASL gene, part of the urea cycle, which is only metabolically completed in the liver, but also plays a role in fumarate and arginine synthesis in muscle. These associations should be confirmed in studies with larger cohorts, but these results display the emergent value of reported metabolites with high sensitivity and specificity scores, the potential support in diagnosis and follow-up of patient management, the systemic affection of this disease (previously thought to be restricted to muscle) and the relevance of metabolism in IBM (only thought to be minor and secondary). Whether these findings could guide future treatment strategies is still a matter of doubt, but the implication of metabolism and oxidative stress in IBM is now undeniable.

In future studies, the metabolic profiling of the same patients at different time points of the disease could contribute to a better understanding of disease evolution and the evaluation of reported biomarkers for disease prognosis, especially considering that IBM is a progressive disease but some patients experience little or no disease progression through periods of 4 to 12 years [3]. A better screening of IBM evolution could also aid in the stratification of patients, according to their progression rate and considering the hypothesis of IBM as a spectrum disorder [38]. Similarly, the use of these biomarkers in response to treatment efficacy could also yield to interesting conclusions.

In conclusion, multi-omics profiling is a powerful tool to reveal disease-specific metabolic dysregulation. By performing metabolic and RNA-seq profiling of fibroblasts, urine, plasma and muscle samples from IBM patients, we have identified potential biomarker signatures considering organic acids to gene expression associations. This preliminary study revealed promising metabolic fingerprints for examining disease progression and treatment efficacy.

5. Conclusions

- Metabolic dysregulation in IBM is present outside the target tissue (muscle), as seen with altered organic acids in fibroblasts and urine.
- Multi-omics profiling of patients' samples allows the evaluation of disease-associated phenotypes in an untargeted approach to potentially detect novel molecular players.
- The detection of L-pyroglutamic and orotic acids in urine displayed an outstanding biomarker signature, with 100% sensitivity and specificity.
- The validation of potential biomarkers in non-invasive samples like urine may eventually aid in the screening of patients' disease progression and treatment efficacy.

Supplementary Materials: The following supporting information can be downloaded at: www.mdpi.com/xxx/s1, Table S1: Biomarker performance values for target molecules; Table S2: Differentially expressed genes (DEGs) involved in metabolism (extracted from Mitocarta 3.0) from RNA-seq in the muscle of IBM patients (n=5) vs. CTL (n=6), Table S3: Metabolic Mito Pathways with the number of differentially expressed genes (DEGs) involved (from IBM muscle RNA-seq); Table S4: Metaboanalyst analysis combining metabolic differentially expressed genes (DEGs) in muscle RNA-seq with organic acids and nucleotides in urine. Significant pathways from pathway analysis and network enrichment analysis are represented in the table.

Author Contributions: Conceptualization, J.C.-S., R.A. and G.G; methodology, J.C.-S., L.V.-R., E.T., F.J.G.-G., M.G.-M., F.A.-S., J.P., R.AR., P.J.M.-L., J.C.M., J.M.G., G.G., C.O., R.A., A.E.-C., B.M.-M.; software, J.C.-S., J.P., C.O., R.A., A.E.-C., B.M.-M.; validation, J.C.-S., C.O., R.A., G.G.; formal analysis, J.C.-S., C.O., R.A., G.G.; investigation, J.C.-S., R.A., G.G.; resources, J.C.-S., L.V.-R., E.T., F.J.G.-G., M.G.-M., F.A.-S., J.P., R.AR., P.J.M.-L., J.C.M., J.M.G., G.G., C.O., R.A., A.E.-C., B.M.-M.; data curation, J.C.-S., C.O., R.A., A.E.-C., B.M.-M.; writing—original draft preparation, J.C.-S., G.G.; writing—review and editing, , J.C.-S., L.V.-R., E.T., F.J.G.-G., M.G.-M., F.A.-S., J.P., R.AR., P.J.M.-L., J.C.M., J.M.G., G.G., C.O., R.A., A.E.-C., B.M.-M.; visualization, J.C.-S., J.P., C.O., R.A., A.E.-C., B.M.-M.; supervision, J.C.M., J.M.G., G.G.; project administration, G.G.; funding acquisition, G.G. All authors have read and agreed to the published version of the manuscript.

Funding: This work was supported by Instituto de Salud de Carlos Ill (ISCIII-FEDER, P121/00935), and co-funded by the European Union. Additionally, FJG-G is supported by CIBERER (ISCIII-FEDER), RA by Torrons Vicens and Carmen de Torres grant from IRSJD and MG-M by CD21/00019 (ISCIII-FSE+).

Institutional Review Board Statement: The study was conducted in accordance with the Declaration of Helsinki and approved by the Ethical Committee of Clinical Investigation of the "Hospital Clínic de Barcelona" (protocol code HCB/2017/0808 approved on the 25/07/2018).

Informed Consent Statement: Informed consent was obtained from all subjects involved in the study. Written informed consent has been obtained from the patients to publish this paper.

Data Availability Statement: The data presented in this study are available in the article, supplementary material or on request from the corresponding authors.

Acknowledgments: We acknowledge the contribution of all patients and their families, always prone to collaborate and widen the state-of-the-art in rare diseases.

Conflicts of Interest: The authors declare no conflict of interest. The funders had no role in the design of the study; in the collection, analyses, or interpretation of data; in the writing of the manuscript, or in the decision to publish the results.

References

1. Nagy, S.; Khan, A.; Machado, P.M.; Houlden, H. Inclusion Body Myositis: From Genetics to Clinical Trials. *J Neurol* **2023**, *270*, 1787–1797, doi:10.1007/s00415-022-11459-3.

2. Callan, A.; Capkun, G.; Vasanthaprasad, V.; Freitas, R.; Needham, M. A Systematic Review and Meta-Analysis of Prevalence Studies of Sporadic Inclusion Body Myositis. *J Neuromuscul Dis* **2017**, *4*, 127–137, doi:10.3233/JND-160198.
3. Greenberg, S.A. Inclusion Body Myositis: Clinical Features and Pathogenesis. *Nat Rev Rheumatol* **2019**, *15*, 257–272, doi:10.1038/s41584-019-0186-x.
4. Naddaf, E.; Shelly, S.; Mandrekar, J.; Chamberlain, A.M.; Hoffman, E.M.; Ernste, F.C.; Liewluck, T. Survival and Associated Comorbidities in Inclusion Body Myositis. *Rheumatology (United Kingdom)* **2022**, *61*, 2016–2024, doi:10.1093/rheumatology/keab716.
5. Buzkova, J.; Nikkanen, J.; Ahola, S.; Hakonen, A.H.; Sevastianova, K.; Hovinen, T.; Yki-Järvinen, H.; Pietiläinen, K.H.; Lönnqvist, T.; Velagapudi, V.; et al. Metabolomes of Mitochondrial Diseases and Inclusion Body Myositis Patients: Treatment Targets and Biomarkers. *EMBO Mol Med* **2018**, *10*, 1–15, doi:10.15252/emmm.201809091.
6. Hedberg-Oldfors, C.; Lindgren, U.; Basu, S.; Visuttijai, K.; Lindberg, C.; Falkenberg, M.; Larsson Lekholm, E.; Oldfors, A. Mitochondrial DNA Variants in Inclusion Body Myositis Characterized by Deep Sequencing. *Brain Pathology* **2021**, *31*, doi:10.1111/BPA.12931.
7. Catalan-Garcia, M.; Garrabou, G.; Moren, C.; Guitart-Mampel, M.; Hernando, A.; Diaz-Ramos, A.; Gonzalez-Casacuberta, I.; Juarez, D.-L.; Bano, M.; Enrich-Bengoa, J.; et al. Mitochondrial DNA Disturbances and Deregulated Expression of Oxidative Phosphorylation and Mitochondrial Fusion Proteins in Sporadic Inclusion Body Myositis. *Clin Sci* **2016**, *130*, 1741–1751, doi:10.1042/CS20160080.
8. Greenberg, S.A.; Pinkus, J.L.; Kong, S.W.; Baecher-Allan, C.; Amato, A.A.; Dorfman, D.M. Highly Differentiated Cytotoxic T Cells in Inclusion Body Myositis. *Brain* **2019**, *142*, 2590–2604, doi:10.1093/brain/awz207.
9. Greenberg, S.A. Pathogenesis of Inclusion Body Myositis. *Curr Opin Rheumatol* **2020**, *32*, 542–547, doi:10.1097/BOR.0000000000000752.
10. Singh, R.J. Glutathione: A Marker and Antioxidant for Aging. *J Lab Clin Med* **2002**, *140*, 1, doi:10.1067/mlc.2002.129505.
11. Wu, J.H.; Batist, G. Glutathione and Glutathione Analogues; Therapeutic Potentials. *Biochimica et Biophysica Acta (BBA) - General Subjects* **2013**, *1830*, 3350–3353, doi:10.1016/j.bbagen.2012.11.016.
12. Forman, H.J.; Zhang, H.; Rinna, A. Glutathione: Overview of Its Protective Roles, Measurement, and Biosynthesis. *Mol Aspects Med* **2009**, *30*, 1–12, doi:10.1016/j.mam.2008.08.006.
13. Cantó-Santos, J.; Valls-Roca, L.; Tobías, E.; García-García, F.J.; Guitart-Mampel, M.; Esteve-Codina, A.; Martín-Mur, B.; Casado, M.; Artuch, R.; Solsona-Vilarrasa, E.; et al. Unravelling Inclusion Body Myositis Using a Patient-derived Fibroblast Model. *J Cachexia Sarcopenia Muscle* **2023**, doi:10.1002/jcsm.13178.
14. Amici, D.R.; Pinal-Fernandez, I.; Christopher-Stine, L.; Mammen, A.L.; Mendillo, M.L. A Network of Core and Subtype-Specific Gene Expression Programs in Myositis. *Acta Neuropathol* **2021**, *142*, 887–898, doi:10.1007/s00401-021-02365-5.
15. Britson, K.A.; Ling, J.P.; Braunstein, K.E.; Montagne, J.M.; Kastenschmidt, J.M.; Wilson, A.; Ikenaga, C.; Tsao, W.; Pinal-Fernandez, I.; Russell, K.A.; et al. Loss of TDP-43 Function and Rimmed Vacuoles Persist after T Cell Depletion in a Xenograft Model of Sporadic Inclusion Body Myositis. *Sci Transl Med* **2022**, *14*, 9196, doi:10.1126/scitranslmed.abi9196.
16. De Paepe, B. Sporadic Inclusion Body Myositis: An Acquired Mitochondrial Disease with Extras. *Biomolecules* **2019**, *9*, 15, doi:10.3390/biom9010015.
17. Hasin, Y.; Seldin, M.; Lusis, A. Multi-Omics Approaches to Disease. *Genome Biol* **2017**, *18*, 83, doi:10.1186/s13059-017-1215-1.
18. MR, R. 188th ENMC International Workshop: Inclusion Body Myositis, 2-4 December 2011, Naarden, The Netherlands. *Neuromuscul Disord* **2013**, *23*, 1044–1055, doi:10.1016/J.NMD.2013.08.007.
19. Bermejo-Pareja, F.; Antequera, D.; Vargas, T.; Molina, J.A.; Carro, E. Saliva Levels of Abeta1-42 as Potential Biomarker of Alzheimer's Disease: A Pilot Study. *BMC Neurol* **2010**, *10*, 108, doi:10.1186/1471-2377-10-108.

20. Lee, M.; Guo, J.P.; Kennedy, K.; Mcgeer, E.G.; McGeer, P.L. A Method for Diagnosing Alzheimer's Disease Based on Salivary Amyloid-β Protein 42 Levels. *Journal of Alzheimer's Disease* **2017**, *55*, 1175–1182, doi:10.3233/JAD-160748.
21. Sabbagh, M.N.; Shi, J.; Lee, M.; Arnold, L.; Al-Hasan, Y.; Heim, J.; McGeer, P. Salivary Beta Amyloid Protein Levels Are Detectable and Differentiate Patients with Alzheimer's Disease Dementia from Normal Controls: Preliminary Findings. *BMC Neurol* **2018**, *18*, 155, doi:10.1186/s12883-018-1160-y.
22. Catalán, M.; Selva-O'Callaghan, A.; Grau, J.M. Diagnosis and Classification of Sporadic Inclusion Body Myositis (SIBM). *Autoimmun Rev* **2014**, *13*, 363–366, doi:10.1016/j.autrev.2014.01.016.
23. Selva-O'callaghan, A.; Pinal-Fernandez, I.; Trallero-Araguás, E.; Milisenda, J.C.; Grau-Junyent, M.; Mammen, A.L. Classification and Management of Adult Inflammatory Myopathies. *Lancet Neurol* **2018**, *17*, 816–828, doi:10.1016/S1474-4422(18)30254-0.
24. Hoffmann, G.F.; Feyh, P. Organic Acid Analysis. In *Physician's Guide to the Laboratory Diagnosis of Metabolic Diseases*; Springer Berlin Heidelberg: Berlin, Heidelberg, 2003; pp. 27–44.
25. Dobin, A.; Davis, C.A.; Schlesinger, F.; Drenkow, J.; Zaleski, C.; Jha, S.; Batut, P.; Chaisson, M.; Gingeras, T.R. STAR: Ultrafast Universal RNA-Seq Aligner. *Bioinformatics* **2013**, *29*, 15–21, doi:10.1093/BIOINFORMATICS/BTS635.
26. Li, B.; Dewey, C.N. RSEM: Accurate Transcript Quantification from RNA-Seq Data with or without a Reference Genome. *BMC Bioinformatics 2011 12:1* **2011**, *12*, 1–16, doi:10.1186/1471-2105-12-323.
27. Love, M.I.; Huber, W.; Anders, S. Moderated Estimation of Fold Change and Dispersion for RNA-Seq Data with DESeq2. *Genome Biology 2014 15:12* **2014**, *15*, 1–21, doi:10.1186/S13059-014-0550-8.
28. Rath, S.; Sharma, R.; Gupta, R.; Ast, T.; Chan, C.; Durham, T.J.; Goodman, R.P.; Grabarek, Z.; Haas, M.E.; Hung, W.H.W.; et al. MitoCarta3.0: An Updated Mitochondrial Proteome Now with Sub-Organelle Localization and Pathway Annotations. *Nucleic Acids Res* **2021**, *49*, D1541–D1547, doi:10.1093/nar/gkaa1011.
29. Metaboanalyst. Available online: https://www.metaboanalyst.ca/ (accessed on 10 March 2023).
30. A.M. Snedden; K.A.B. Kellett; J.B. Lilleker; N.M. Hooper; H Chinoy. The Role of Protein Aggregation in the Pathogenesis of Inclusion Body Myositis. *Clin Exp Rheumatol* **2022**, *40*, 414–424.
31. Catalán-García, M.; Garrabou, G.; Morén, C.; Guitart-Mampel, M.; Gonzalez-Casacuberta, I.; Hernando, A.; Gallego-Escuredo, J.M.; Yubero, D.; Villarroya, F.; Montero, R.; et al. BACE-1, PS-1 and SAPPβ Levels Are Increased in Plasma from Sporadic Inclusion Body Myositis Patients: Surrogate Biomarkers among Inflammatory Myopathies. *Mol Med* **2016**, *21*, 817–823, doi:10.2119/molmed.2015.00168.
32. Lane, A.N.; Fan, T.W.M. Regulation of Mammalian Nucleotide Metabolism and Biosynthesis. *Nucleic Acids Res* **2015**, *43*, 2466–2485, doi:10.1093/nar/gkv047.
33. Cantó-Santos, J.; Grau-Junyent, J.M.; Garrabou, G. The Impact of Mitochondrial Deficiencies in Neuromuscular Diseases. *Antioxidants* **2020**, *9*, 964, doi:10.3390/antiox9100964.
34. Orphanet. Available online: https://www.orpha.net/ (accessed on 10 March 2023).
35. Calpena, E.; Casado, M.; Martínez-Rubio, D.; Nascimento, A.; Colomer, J.; Gargallo, E.; García-Cazorla, A.; Palau, F.; Artuch, R.; Espinós, C. 5-Oxoprolinuria in Heterozygous Patients for 5-Oxoprolinase (OPLAH) Missense Changes. *JIMD Rep* **2012**, *7*, 123–128, doi:10.1007/8904_2012_166.
36. Benveniste, O.; Stenzel, W.; Hilton-Jones, D.; Sandri, M.; Boyer, O.; M van Engelen, B.G. Amyloid Deposits and Inflammatory Infiltrates in Sporadic Inclusion Body Myositis: The Inflammatory Egg Comes before the Degenerative Chicken. *Acta Neuropathol* **2015**, *3*, 611–624, doi:10.1007/s00401-015-1384-5.
37. Goyal, N.A.; Coulis, G.; Duarte, J.; Farahat, P.K.; Mannaa, A.H.; Cauchii, J.; Irani, T.; Araujo, N.; Wang, L.; Wencel, M.; et al. Immunophenotyping of Inclusion Body Myositis Blood T and NK Cells. *Neurology* **2022**, *98*, e1374–e1383, doi:10.1212/WNL.0000000000200013.

38. Perez-Rosendahl, M.; Mozaffar, T. Inclusion Body Myositis: Evolving Concepts. *Curr Opin Neurol* **2022**, *35*, 604–610, doi:10.1097/WCO.0000000000001095.
39. Tawara, N.; Yamashita, S.; Zhang, X.; Korogi, M.; Zhang, Z.; Doki, T.; Matsuo, Y.; Nakane, S.; Maeda, Y.; Sugie, K.; et al. Pathomechanisms of Anti–Cytosolic 5′-Nucleotidase 1A Autoantibodies in Sporadic Inclusion Body Myositis. *Ann Neurol* **2017**, *81*, 512–525, doi:10.1002/ana.24919.
40. Ikenaga, C.; Date, H.; Kanagawa, M.; Mitsui, J.; Ishiura, H.; Yoshimura, J.; Pinal-Fernandez, I.; Mammen, A.L.; Lloyd, T.E.; Tsuji, S.; et al. Muscle Transcriptomics Shows Overexpression of Cadherin 1 in Inclusion Body Myositis. **2022**, doi:10.1002/ana.26304.
41. Pinal-Fernandez, I.; Casal-Dominguez, M.; Derfoul, A.; Pak, K.; Plotz, P.; Miller, F.W.; Milisenda, J.C.; Grau-Junyent, J.M.; Selva-O'Callaghan, A.; Paik, J.; et al. Identification of Distinctive Interferon Gene Signatures in Different Types of Myositis. *Neurology* **2019**, *93*, e1193–e1204, doi:10.1212/WNL.0000000000008128.
42. Liss, D.B.; Paden, M.S.; Schwarz, E.S.; Mullins, M.E. What Is the Clinical Significance of 5-Oxoproline (Pyroglutamic Acid) in High Anion Gap Metabolic Acidosis Following Paracetamol (Acetaminophen) Exposure? *Clin Toxicol* **2013**, *51*, 817–827, doi:10.3109/15563650.2013.844822.
43. L-Pyroglutamic Acid. Available online: https://pubchem.ncbi.nlm.nih.gov/compound/L-Pyroglutamic-acid (accessed on 24 June 2023).
44. Orotic Acid. Available online: https://pubchem.ncbi.nlm.nih.gov/ (accessed on 12 May 2023).

SUPPLEMETARY MANUSCRIPT I:

Title: *The Impact of Mitochondrial Deficiencies in Neuromuscular Diseases*

Authors: Judith Cantó-Santos, Josep M. Grau-Junyent and Glòria Garrabou

Journal: Antioxidants. 2020; 9, 964; doi:10.3390/antiox9100964.

IF: 6.3

antioxidants

MDPI

Review

The Impact of Mitochondrial Deficiencies in Neuromuscular Diseases

Judith Cantó-Santos [1,2,3], Josep M. Grau-Junyent [1,2,3] and Glòria Garrabou [1,2,3,*]

1 Muscle Research and Mitochondrial Function Laboratory, CELLEX-IDIBAPS, Faculty of Medicine, University of Barcelona, 08036 Barcelona, Spain; jcanto@clinic.cat (J.C.-S.); jmgrau@clinic.cat (J.M.G.-J.)
2 Internal Medicine Department, Hospital Clinic of Barcelona, 08036 Barcelona, Spain
3 CIBERER—Spanish Biomedical Research Centre in Rare Diseases, 28029 Madrid, Spain
* Correspondence: garrabou@clinic.cat

Received: 9 September 2020; Accepted: 24 September 2020; Published: 9 October 2020

Abstract: Neuromuscular diseases (NMDs) are a heterogeneous group of acquired or inherited rare disorders caused by injury or dysfunction of the anterior horn cells of the spinal cord (lower motor neurons), peripheral nerves, neuromuscular junctions, or skeletal muscles leading to muscle weakness and waste. Unfortunately, most of them entail serious or even fatal consequences. The prevalence rates among NMDs range between 1 and 10 per 100,000 population, but their rarity and diversity pose difficulties for healthcare and research. Some molecular hallmarks are being explored to elucidate the mechanisms triggering disease, to set the path for further advances. In fact, in the present review we outline the metabolic alterations of NMDs, mainly focusing on the role of mitochondria. The aim of the review is to discuss the mechanisms underlying energy production, oxidative stress generation, cell signaling, autophagy, and inflammation triggered or conditioned by the mitochondria. Briefly, increased levels of inflammation have been linked to reactive oxygen species (ROS) accumulation, which is key in mitochondrial genomic instability and mitochondrial respiratory chain (MRC) dysfunction. ROS burst, impaired autophagy, and increased inflammation are observed in many NMDs. Increasing knowledge of the etiology of NMDs will help to develop better diagnosis and treatments, eventually reducing the health and economic burden of NMDs for patients and healthcare systems.

Keywords: neuromuscular diseases (NMDs); mitophagy; reactive oxygen species (ROS); damage-associated molecular patterns (DAMPs); oxidative stress; mitochondrial respiratory chain (MRC)

1. Introduction

1.1. Neuromuscular Diseases (NMDs)

NMDs are a heterogeneous group of acquired or inherited rare disorders caused by injury or dysfunction of the anterior horn cells of the spinal cord (lower motor neurons), peripheral nerves, neuromuscular junctions (NMJ), or skeletal muscles, resulting in muscle weakness and waste, swallowing and breathing difficulties, and cardiac failure [1]. NMDs share some common features: weakness, twitching, torpidity, and cramps but signs and symptoms of various NMDs might be very different [2]. Unfortunately, most of them entail serious or even fatal consequences.

NMDs exhibit a diversity of symptoms due to large genetic and clinical heterogeneity, as more than 500 genes are implicated in their pathogenesis, setting difficulties for healthcare and research [2,3]. Most NMDs' prevalence ranges between 1 and 10 per 100,000 population [4]. Given the rarity and diversity of NMDs, patients experience long delays in diagnosis (typically 7 years) and 30% are never

achieved [1], probably because many of them lack non-invasive diagnostic and prognostic biomarkers. Likewise, models of disease or therapeutic options are infrequent, but growing interests and knowledge are focused in depicting the etiology of these disorders [5].

Currently, diagnosing NMD starts with clinical observation, which can identify atrophy or loss of muscle bulk or tone. Blood tests can determine abnormal levels of various common metabolites and antigens in certain NMD. In addition, electromyography (EMG) helps to assess the health of muscles and lower motor neuron nerve cells that control those muscles to diagnose a number of NMD [6]. Once muscle affection is assured, multitude of diagnostic algorithms are developed to establish the specific disorder. Usually, muscle biopsy takes part in the diagnostic clues. Depending on the clinical and pathological presentation, the study of mitochondrial DNA (mtDNA) genome and mitochondrial respiratory chain (MRC) function is also required [7]. This fact indicates the mitochondrial etiology of some NMDs and why mitochondrial deregulation may play a role in the rest.

Despite the challenges in NMD diagnosis, genetic diagnosis of these diseases has improved over the last 20 years [8]. Advances in sequencing and understanding the human genome has helped to detect monogenic NMD. Improved diagnosis and increased life expectancy may rise the prevalence of NMD worldwide while massive genome sequencing helps to depict complex disease inheritance and etiology. In addition, research in pathways affected in NMD is essential to improve the treatments and guide toward more personalized therapies in NMDs.

Classification of NMDs

The knowledge about new NMDs is continually increasing and changing. Currently, there are 7 main groups of NMDs, represented in Figure 1, which are [6,9,10]:

- Muscular dystrophies (MD): affect the structure of the muscle cells, causing weakness and degeneration of the skeletal muscles. MD subtypes are described in Table 1.
- Myopathies other than dystrophies: affect tone and contraction of muscles controlling voluntary movements; may include inflammation of muscles or related tissues, resulting in muscular weakness. Numerous myopathies have been described and classified in different groups (Table 2).
- Neuromuscular junction (NMJ) diseases: result from the destruction, dysfunction, or absence of one or more key proteins involved in the transmission of signals between nerves and muscles (Table 3).
- Motor neuron diseases: involve nerve cells in the spinal cord (lower motor neurons). Lower motor neurons progressively lose their function, causing the muscles they control to become weak and eventually non-functional (Table 3).
- Peripheral nerve diseases: involve motor and sensory nerves that connect the brain and spinal cord to the rest of the body causing impaired sensations, movement or other functions (Table 4).
- Mitochondrial diseases: involve errors in metabolism that affect energy production in muscle cells (Table 4).
- Ion channel diseases: diseases associated with defects in proteins forming ion channels, leading to muscular weakness, absent muscle tone, or episodic muscle paralysis (Table 5).

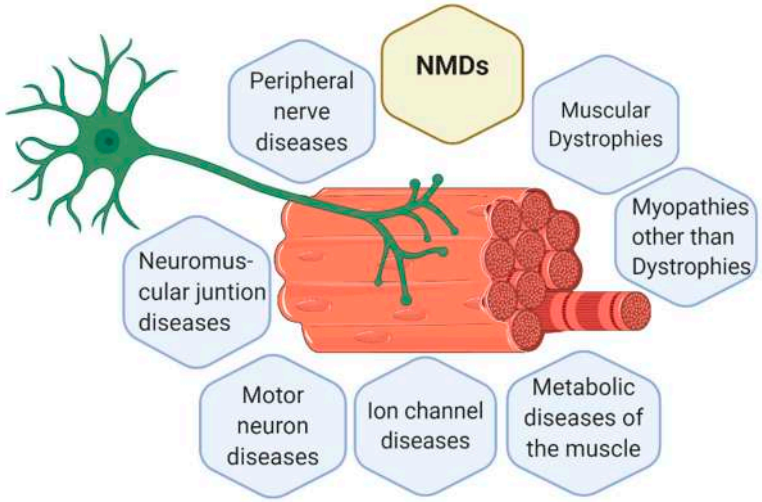

Figure 1. Representation of a motor unit according to the classification of the main neuromuscular diseases (NMDs). Muscle cells and neurons interact in the neuromuscular junction (NMJ) where muscle cells receive the instructions from the lower motor neurons to perform the actions required. Thus, body movement is actioned by muscle fibers but controlled by the nervous system. Consequently, alterations in muscle fibers or nerves can both trigger a NMD. Figure created with BioRender.com.

Table 1. Examples of studies reporting altered mitochondrial functions in muscular dystrophies.

NMD Group	Name of Main Diseases	Description of Principal Disease Features	Description of Main Mitochondrial Alteration	Most Affected Mitochondrial Pathways	Main Evidence Level/Disease Model	Relevant References	Examples of Mutations in Genes
Muscular Dystro-phies (MD)	**Becker MD (BMD)**	Atrophy of the skeletal, cardiac, and pulmonary muscles	Reduced mitochondrial mass, complex I activity and ATP levels, and increased Ca^{2+} levels	Increased MPTP opening, ROS levels, and inflammation	in vitro, cells, animal (*C. elegans*, *mdx* mice), patient (CT)	[11–13]	DMD
	Congenital MD (CMD)	Muscle weakness and possible joint deformities with slow progression and shortened life span	Most common CMD are collagen VI myopathies, with visible mitochondrial dysfunction	Increased MPTP opening and defective autophagy	in vitro, cells, animal (Col6a1 -/- mice), patient (CT)	[2,14,15]	LMNA, DPM3, DAG1, TRAPPC11
	Duchenne MD (DMD)	General muscle weakness and wasting due to lack of dystrophin protein. Shortened lifespan. Rarely affects women (milder symptoms and better prognosis)	Massive aggregates of mitochondria, lower activities of MRC complexes III and IV and increased Ca^{2+}.	Increased MPTP opening, ROS levels and inflammation	in vitro, cells, animal (*C. elegans*, *mdx* mice), patient (CT)	[8,11,12,14,16–21]	DMD
	Emery-Dreifuss MD (EDMD)	Muscular weakness and atrophy of shoulder, upper arm, and shin muscles, with early joint contractures and cardiomyopathy	Reduced expression of MRC complex genes and upregulation of mitochondrial disassembly genes, altered mitochondrial location and morphology	Decreased MRC and altered mitochondrial biogenesis	in vitro and animal models (*C. elegans*, mice)	[2,22–24]	LMNA, EMD, FHL1
	Faciosca-pulohume-ral MD (FSHD)	Muscle weakness that affects mainly facial, shoulder, and arm muscles	Reduced antioxidative response molecules (low levels of zinc, selenium, and vitamin C)	Higher ROS and mitochondrial dysfunction	cells and patient (CT)	[14,17,25,26]	TRPV4, DUX4, SMCHD1
	Limb-girdle MD (LGMD)	Weakness and wasting of the muscles in hips and shoulders	Morphologic mitochondrial abnormalities, including RRF and decreased COX	MPTP dysregulation and mitochondrial dysfunction	in vitro, cells, animal (*521ΔT* mice), patient (CT)	[2,5,14,27]	SGCG, LMNA, DYSF, TCAP, TRIM32, TNPO3 *
	Myotonic dystrophy (MD)	Muscle loss and weakness due to inability to relax them. It affects facial muscles first, but also feet, hands, and neck	Altered mitochondrial proteins (decreased EF-Tu, hsp60, GRP75, dienoyl CoA isomerase) and disruption of ubiquitin-proteasome systems in MD2 (affects proximal muscles)	ER stress and mitochondrial dysfunction	cells and patient (CT)	[14,28,29]	CNBP (ZNF9), DMPK
	Oculopha-ryngeal MD (OPMD)	Weakness of eye, face, and throat muscles leading to drooping eyelids and problems with swallowing	PABPN1 protein aggregates, reduced complex I and V mitochondrial proteins, altered UPR and apoptosis	ER stress, mitochondrial dysfunction and apoptosis	in vitro, cells, animal, patient (CT)	[24,30–32]	PABPN1
	Distal MD (DD) (or Distal myopathy)	Weakness and wasting of muscles of the hands, forearms, and lower legs with slow progression. Many DD diseases	Decreased mitochondrial membrane potential, increased mitochondrial oxygen consumption and Ca^{2+} and deficiencies in MRC complexes I and IV	MPTP opening and ATP depletion	in vitro, cells, patient (CT)	[14,33,34]	FLNC, TTN, DYSF

Family of muscular dystrophies (MD) and their respective disease features, mitochondrial alterations, affected mitochondrial pathways, evidence level of altered mechanisms, mutations in causal genes and relevant references. Examples of genes with mutations causal/related to a MD taken from Muscle gene table (accessed July 2020) [35]. * More LGMD mutations: HNRNPDL, CAPN3, COL6A1, SGCA, SGCB, SGCG, SGCD, POMT1, POMT2, POMGNT1, POMGNT2, FKTN, ANO5, COL6A2, COL6A3, DAG1, PLEC, TRAPPC11, GMPPB, ISPD, POGLUT1, DNAJB6, FKRP, TTN, LAMA2, BVES. Abbreviations: MPTP: mitochondrial permeability transition pore; ROS: reactive oxygen species; CT: clinical trials; RRF: ragged-red fibers; COX: cytochrome c oxidase, MRC complex IV; ER: endoplasmic reticulum; UPR: unfolded protein response.

Table 2. Examples of studies reporting altered mitochondrial functions in myopathies other than dystrophies.

NMD Group	Name of Main Diseases	Description of Principal Disease Features	Description of Main Mitochondrial Alteration	Most Affected Mitochondrial Pathways	Main Evidence Level/Disease Model	Relevant References	Examples of Mutations in Genes
Myopa-thies	**Congenital myopathies**	Inherited diseases that affect the tone and contraction of skeletal muscles causing general muscle weakness	The most frequent congenital myopathies are core myopathies, with reduced MRC activity and near-total depletion of mitochondria	reduced MRC and mitochondrial depletion	in vitro, cells, animal, patient (CT)	[14,29,36,37]	RYR1, DNM2, MTM1, TNPO3, COL6A1/2/3, COL12A1, PYROXD1, MSTO1
	Endocrine myopathies	Weakness and atrophy (shrinking) of the muscles around the shoulders and hips, muscle stiffness, cramps, and slowed reflexes caused by abnormal activity of the thyroid gland. Two types: hypothyroid (reduced hormone levels) and hyperthyroid myopathies (excess in hormones)	Hypothyroid myopathy: decreased TFAM, reduced mitochondrial DNA copy number and mitochondrial alterations (COX- fibers). Hyperthyroid: moderate increase in mitochondrial size and protein aggregates	mitochondrial structure, ER stress (proteotoxicity), autophagy failure	cells	[38–40]	
	Inflammatory myopathies	Chronic muscle inflammation accompanied by prolonged muscle fatigue and weakness. sIBM is the inflammatory myopathy with more mitochondrial alteration	Abnormal mitochondria in sIBM (RRFs and COX- fibers). In sIBM and PM, mtDNA deletions in muscle and altered autophagy	Altered mitochondrial structure, mtDNA deletions and autophagy	in vitro, cells, animal, patient (CT)	[7,14,41,42]	VCP, HNRNPA1, GNE
	Metabolic myopathies	Group of disorders caused each by a different genetic defect that impairs the body's metabolism causing muscle weakness, exercise intolerance, muscle pain or cramps	Altered MRC: substrates are not properly processed or cannot enter mitochondria affecting energy production of the cell. mtDNA or nDNA mutations	reduced MRC and ATP depletion	in vitro, cells, patient (CT)	[7,28,43]	GAA, AGL, GBE1, PYGM, PFKM, PHKA1
	Myofibrillar myopathies (MFM)	Characterized by muscle weakness, cardiomyopathy, myalgia, loss of sensation and weakness in the limbs (peripheral neuropathy), and respiratory failure	Mitochondrial abnormalities with RRF and enlarged mitochondria. Protein aggregates affecting distribution and function of mitochondria. Deficiencies in MRC complex I and IV	MRC dysfunction, autophagy and ER stress, reduced mitochondrial biogenesis	in vitro, cells, patient	[14,44–46]	MYOT, DES, PYROXD1, CRYAB, LDB3, FLNC, BAG3, TTN
	Scapulopero-neal myopathy	Rare genetic disorder characterized by weakness and wasting of specific muscles: shoulder blade area (scapula) and the smaller of the two leg muscle groups below the knee (peroneal)	mtDNA mutations reported in a few cases	mtDNA	cells	[47–49]	VCP, FHL1

Family of myopathies other than dystrophies and their respective disease features, mitochondrial alterations, affected mitochondrial pathways, evidence level of altered mechanisms, mutations in causal genes and relevant references. Examples of genes with mutations causal/related to a myopathy taken from muscle gene table (accessed July 2020) [35]. Abbreviations: MRC: mitochondrial respiratory chain; CT: clinical trials; TFAM: mitochondrial transcription factor A; COX-: cytochrome c oxidase negative fibers; ER: endoplasmic reticulum; sIBM: sporadic Inclusion Body Myositis; RRF: ragged-red fibers; PM: polymyositis; mtDNA: mitochondrial DNA; nDNA: nuclear DNA.

Table 3. Examples of studies reporting altered mitochondrial functions in Neuromuscular Junction Diseases (NMJ) and Motor Neuron Diseases.

NMD Group	Name of Main Diseases	Description of Principal Disease Features	Description of Main Mitochondrial Alteration	Most Affected Mitochondrial Pathways	Main Evidence Level/Disease Model	Relevant References	Examples of Mutations in Genes
Neuro-muscular junction diseases (NMJ)	**Congenital myasthenic syndromes (CMS)**	Weakness and fatigue resulting from problems at NMJ. Different types of CMS, according to the part of the NMJ affected: presynaptic (the nerve cell), postsynaptic (the muscle cell) or synaptic (the space in between)	Gene defect in mitochondrial citrate carrier SLC25A1 underlie deficits in NMJ transmission. SLC25A1 is involved in many biological processes (e.g., glycolysis, autophagy)	NMJ signaling	in vitro, cells, animal (zebrafish, mice), patient (CT)	[50–53]	CHRNA1, PLEC, CHRNB1, CHRND, CHRNE, COLQ, CHAT, SYT2, AGRN, SLC5A7, SYT2
	Lambert-Eaton myasthenic syndrome (LEMS)	Autoimmune disease that attacks the calcium channels in the NMJ and interferes with the ability of nerve cells to send acetylcholine to muscle cells, affecting muscle contraction and causing muscle weakness	Altered calcium channels	NMJ signaling	cells, patient (CT)	[50,54–56]	SYT2
	Myasthenia gravis (MG)	Chronic autoimmune disorder in which antibodies destroy neuromuscular connections. It affects voluntary muscles of the body, especially the eyes, mouth, throat, and limbs	Mitochondrial morphological alterations and RRF	mitochondrial morphology, neuromuscular connections	cells, animal (rat, mice), patient (CT)	[55,57,58]	CHAT
Motor neuron diseases	**Amyotrophic lateral sclerosis (ALS)**	Fatal disease with degeneration of nerve cells in the spinal cord and brain. It affects voluntary control of arms and legs and eventually leads to trouble breathing	Accumulation of mitochondrial in proximal axons, mitochondrial injury by ROS excess, COX I mtDNA mutation and RRF	Increased ROS and altered mitochondrial structure	in vitro, cells, animal (*SOD1G93A* mice), patient (CT)	[7,14,17,18,45,59–65]	SOD1, ALS2, SPG111, HNRNPA1, SQSTM1*
	Spinal-bulbar muscular atrophy (SBMA)	Genetic disorder in which loss of lower motor neurons affect voluntary muscle movement, specifically facial, swallowing muscles and limbs. Only affects men	Reduced MMP. Increased expression of apoptotic proteins that activate mitochondrial caspase pathway. AR unfolding and oligomerization induces toxicity	MPTP opening, increased ROS and apoptosis. Lower mitochondrial mass and ER stress	in vitro, cells, animal, patient (CT)	[66–70]	AR
	Spinal muscular atrophy (SMA)	Genetic disease affecting the central and peripheral nervous system, and voluntary muscle movement, mainly shoulders, hips, thighs, and upper back	Decreased enzyme activities involving MRC complexes I-IV causing mitochondrial dysfunction	mitochondrial dysfunction and altered MRC	in vitro, cells, animal, patient (CT)	[8,14,16–18,67,69–71]	SMN1, IGHMBP2, SIGMAR1, PLEKHG5, DNAJB2, VRK1, TRPV4

Family of neuromuscular junction diseases (NMJ) and motor neuron diseases and their respective disease features, mitochondrial alterations, affected mitochondrial pathways, evidence level of altered mechanisms, mutations in causal genes and relevant references. Example of genes with mutations causal/related to a NMJ diseases taken from muscle gene table (accessed July 2020) [35]. * More ALS mutations: ubiquilin 2, C9orf72, SIGMAR1, CHCHD10, C9orf72, VCP, TDP-43, SETX, FUS, VAPB. Abbreviations: NMJ: neuromuscular junction; CT: clinical trials; RRF: ragged-red fibers; ROS: reactive oxygen species; COX I: cytochrome c oxidase subunit I; mtDNA: mitochondrial DNA; MMP: mitochondrial membrane potential; AR: androgen receptor; MPTP: mitochondrial permeability transition pore; ER: endoplasmic reticulum.

Table 4. Examples of studies reporting altered mitochondrial functions in peripheral nerve diseases and mitochondrial diseases.

NMD Group	Name of Main Diseases	Description of Principal Disease Features	Description of Main Mitochondrial Alteration	Most Affected Mitochondrial Pathways	Main Evidence Level/Disease Model	Relevant References	Examples of Mutations in Genes
Peripheral nerve diseases	**Charcot-Marie-Tooth disease (CMT)**	Inherited disorder that affects nerves outside of your brain and spinal cord, nerves that supply feet, legs, hands, and arms. Two subtypes: CMT1 (demyelinating), CMT2 (axonal)	Altered mitochondrial dynamics and axonal transport of mitochondria, causing axonal degeneration. Mutations in mitochondrial fusion regulatory genes	mitochondrial dynamics and ER stress	in vitro, cells, animal, patient (CT)	[14,17,26,45,67,72–74]	CMT1: PMP22, MPZ. CMT2: MFN2, LMNA, VCP, DNM2, IGHMBP2, DNAJB2, AARS, DYNC1H1, SOD2
	Giant axonal neuropathy (GAN)	Inherited condition characterized by abnormally large and dysfunctional axons. First, limbs have problems with walking, followed by difficulties coordinating movements (ataxia), and require wheelchair assistance	Abnormal and enlarged mitochondria in Schwann cells, deficiencies of complexes I and IV, several mtDNA point mutations and multiple mtDNA deletions.	altered mitochondrial size and mitochondrial dynamics, reduced MRC function	in vitro, cells, animal, patient (CT)	[7,75,76]	GAN
Mitochon-drial diseases	**Mitochon-drial myopathies**	Genetic defects that affect mitochondria can cause muscular and neurological problems (e.g., muscle weakness, exercise intolerance, trouble with balance and coordination). Many mitochondrial myopathies are known	Mutations in mtDNA or nDNA affecting proteins involved in MRC, mitochondrial morphology (RRF) and protein aggregation (UPR)	Altered energy production and redox signaling, mitochondrial morphology and ER stress	in vitro, cells, animal (*ANT*- mice), patient (CT)	[9,77–79]	MRPS25, TIMM22, NDUFAF1, COX6A2, SLC25A42
	Friedreich's ataxia (FA)	Muscle weakness and ataxia, loss of balance and coordination due to reduced synthesis of the mitochondrial protein frataxin. It mostly affects the spinal cord, peripheral nerves and cerebellum	Altered synthesis of frataxin affects mitochondrial iron metabolism and homeostasis and antioxidant protection	oxidative stress, mitochondrial dysfunction	in vitro, cells, patient (CT)	[7,80,81]	FXN

Family of peripheral nerve diseases and mitochondrial diseases and their respective disease features, mitochondrial alterations, affected mitochondrial pathways, evidence level of altered mechanisms, mutations in causal genes and relevant references. Example of genes with mutations causal/related to a peripheral nerve disease or mitochondrial disease taken from muscle gene table (accessed July 2020) [35]. Abbreviations: ER: endoplasmic reticulum; CT: clinical trials; mtDNA: mitochondrial DNA; MRC: mitochondrial respiratory chain; nDNA: nuclear DNA; RRF: ragged-red fibers; UPR: unfolded protein response.

Table 5. Examples of studies reporting altered mitochondrial functions in ion channel diseases.

NMD Group	Name of Main Diseases	Description of Principal Disease Features	Description of Main Mitochondrial Alteration	Most Affected Mitochondrial Pathways	Main Evidence Level/Disease Model	Relevant References	Examples of Mutations in Genes
Ion channel diseases (or Channe-lopathies)	**Andersen-Tawil syndrome**	Altered potassium channel gene affect the heartbeat and the ability of muscles to stay ready to contract. Paralysis may occur	Mitochondrial channelopathies affect the K^+, Ca^{2+}, VDAC and MPTP channels. Reduced channel activity rate results in reduced MMP and delayed repolarization, causing mitochondrial dysfunction. Intracellular Ca^{2+} homeostasis, mitochondrial bioenergetic metabolism, and modulation of cell survival and death are also affected	reduced MMP, mitochondrial dysfunction, apoptosis	in vitro, cells, animal (mice, rat, *C. elegans*, patient (CT)	[82–85]	KCNJ2
	Hyperkalemic periodic paralysis	Genetic alterations in sodium channels results in temporary muscle weakness, and eventually, temporary paralysis					SCN4A, T704M, M1592V
	Hypokalemic periodic paralysis	Genetic defects in calcium or sodium channel cause a loss of muscle excitability when serum potassium is low					SCN4A, CACNA1S, ATP1A2, KCNE3
	Myotonia congenita	Disease caused by mutations in the gene encoding a chloride channel necessary for stopping muscle contraction. Delayed muscle relaxation triggers muscle stiffness					CLCN1 (CLC-1), SCN4A
	Paramyotonia congenita	Mutations in the muscle sodium channel gene prolong the channel's opening, higher muscle excitation triggering episodes of muscle stiffness and weakness, mostly in the face, neck and upper extremities					SCN4A
	Potassium-aggravated myotonia (or Sodium Channel myotonias)	Sustained muscle tensing causes muscle stiffness that worsens after exercise and may be aggravated by eating potassium-rich foods					SCN4A

Family of ion channel diseases and their respective disease features, mitochondrial alterations, affected mitochondrial pathways, evidence level of altered mechanisms, mutations in causal genes and relevant references. Example of genes with mutations causal/related to an ion channel disease taken from muscle gene table (accessed July 2020) [35]. Abbreviations: VDAC: voltage-dependent anion channels; MPTP: mitochondrial permeability transition pore; MMP: mitochondrial membrane potential.

1.2. Muscle and Nerve System

As outlined in the classification of NMDs, either muscle or nerve dysfunction can result in a NMD. Both tissues are formed by highly specialized cells; neurons in the peripheral nervous system and muscle cells (organized into sarcomeres) in skeletal muscles. Although nerve and muscle tissues contain a reservoir of stem cells for tissue remodeling and regeneration (called satellite cells in muscles), the rate of cell and tissue renewal is quite low, and neurons and sarcomeres, once formed, never proliferate. This is one of the features that causes nerve and muscle tissue disease in case of cell injury.

One of the reasons for cell injury is the strong dependence that nerve and muscle tissue have on mitochondrial function. Their high energetic needs are almost entirely sustained by oxidative metabolism (high-energy demands provided by mitochondrial oxidative respiration). Thus, any deficiency at mitochondrial level may endanger cell and tissue function, being the base of NMDs.

At structural level, the interaction of nervous and musculoskeletal system occurs in the NMJ, also called motor end plate [54]. Muscles are organized in bundles, called muscle fibers, made up of myocytes (muscle cells). Muscle fibers together with lower motor neurons form the motor unit. To reach motor units, nerve impulses travel from the central nervous system (CNS) to the spinal cord and to the whole body within peripheral nerves [86]. In Figure 1, a motor unit is represented together with the classification of the main NMDs.

Muscle fibers are innervated with motor neuron axon terminals. The communication of muscle cells with lower motor neurons is mainly based in changes in the membrane potential and ion channel opening and closing. Briefly, when lower motor neurons are stimulated, their membrane potential changes due to exchange of sodium (Na^+) and potassium (K^+) across the cell membrane, prompting the depolarization of the neuron. Inside the neuron, Na^+ entrance through specific channels promotes the release of calcium (Ca^{2+}) ions from the endoplasmic reticulum (ER) into the cytosol, triggering the further release of neurotransmitters out of nerve cells. These neurotransmitters are sensed by muscle cells, promoting the contraction of muscle fibers [87]. Muscle contraction is mainly controlled by Ca^{2+} fluxes.

Ca^{2+} increase in the cytosol of muscle cells allows actin and myosin (contractile proteins), to interact, causing muscle contraction. Right after, Ca^{2+} are pumped back into the ER causing muscle relaxation [87]. Overall, body movement is actioned by muscle fibers controlled by the nervous system.

Energetic supply is essential for ion exchange and NMJ functioning. Based on energetic criteria and mitochondrial metabolism, muscle fibers can be divided into two categories: type I (slow-twitch) fibers and type II (fast-twitch) fibers. Type I fibers contain more mitochondria and myoglobin than type II fibers. Mitochondria generate ATP by cellular respiration, for which oxygen is required and provided by myoglobin, which stores and carries oxygen in muscle cells. Type II fibers synthesize the majority of their energy through anaerobic respiration, without the need of oxygen, a faster process than mitochondrial respiration but that provides lower amount of ATP [88].

Overall, the CNS and muscle require high amount of energy, mostly produced in mitochondria, and that is why mitochondrial defects are causal or remarkable in the development of NMDs [14]. As mitochondria are essential in nerve and muscle tissue function, primary mitochondrial diseases, caused by mutations in a mitochondrial gene, generally manifest as encephalomyopathies [89], mainly affecting brain and muscle tissues. This is the case of mitochondrial encephalomyopathy with lactic acidosis syndrome (MELAS) or myoclonic epilepsy with ragged-red fibers (MERRF). NMD such as Charcot-Marie-Tooth neuropathy type 2A (CMT2A) [74] or amyotrophic lateral sclerosis (ALS) can also be caused by mitochondrial mutations (CMT2A can be caused by mutations in MFN2 and ALS by mutations in SOD1) [59]. Interestingly, mitochondria can also play a secondary role in the development of the rest of NMD when the mutation or deficiency is not directly related or located in the mitochondria, since affected cells will need additional ATP to support homeostatic mechanisms disbalanced (anti-stress or antioxidant responses), while minimizing the production of ROS. If mitochondria are unable to counterbalance cell dysfunction, a secondary mitochondrial disease will appear, like spinal muscular atrophy (SMA) (usually caused by a mutation in SMN1) [71]

or Duchenne muscular dystrophy (DMD) due to mutation in DMD) [90]. Therefore, mitochondrial function is key in the onset or progression of most of NMDs, regardless of their genetic origin.

1.3. Mitochondrial Function

Despite their clinical and pathological diversity, some overlaps can arise among all NMDs. One of them are molecular events revealing metabolic alterations related to the mitochondria. Although originally considered the "powerhouse of the cell" [91], mitochondria are organelles with a central role in multiple cellular processes: ATP production, apoptosis, β-oxidation of fatty acids, iron-sulfur cluster synthesis and in a broader range of signaling pathways. Additionally, in case of troubleshooting, mitochondria are the main center of ROS production and cell death through the control of apoptosis [92]. Thus, mitochondrial health is essential for cell function and any misbalance in bioenergetics can endanger cell, tissue, and patient survival [93].

Mitochondria can multiply their number in case of energy need or survival of cells, through a process called mitochondrial biogenesis [94]. In addition, mitochondria are dynamic organelles that constantly fuse and divide to increase their energy supply (fusion) or target the mitochondria for degradation (fission). This process is called mitochondrial dynamics and triggers changes in mitochondrial number, morphology, and size [92].

Even if the number of mitochondria rises in a cell, impairment of MRC increases the production of ROS [95], which increases the oxidative stress levels in cells, activating mechanisms to counterbalance this excessive ROS. These repair mechanisms start with autophagy and mitophagy. Autophagy is the clearance of damaged organelles and protein aggregates by lysosomal degradation; while mitophagy is a specialized autophagy that degrades dysfunctional mitochondria to maintain mitochondrial integrity [96]. Both processes remove the excess of ROS produced in mitochondria. Excessive ROS can also affect the ER, as it is one of the main sensors of cellular stress. ER and mitochondria are connected through mitochondria-ER membrane contact sites, called mitochondria-associated membranes (MAMs). When ER senses ROS, ER redox status can change, and might induce ER stress [97]. To defend against ER stress and overcome potential protein misfolding, cells can activate an adaptive unfolded protein response (UPR), which increases the size and capacity of ER to reduce ER stress and increase the removal of misfolded proteins by autophagy [98].

In addition, excessive ROS can trigger an intracellular inflammatory response [99] which has an impact in mitochondrial genomic instability and respiratory chain dysfunction [100]. ROS burst, impaired autophagy, and increased inflammation are observed in many NMDs [101], whose prevalence increases with aging. However, these mechanisms have not been thoroughly revised in all groups of NMD and have not been compared before.

Overall, the aim of this review is to point out the role of excessive oxidative stress in mitochondrial function and its impact in autophagy and inflammation in NMDs (Tables 1–5). Increasing knowledge of the etiology of NMDs will help to develop better diagnosis and treatments to modify the natural history of these chronic disabling diseases, eventually reducing both health and economic burdens of NMDs for patients and healthcare systems [9].

2. Mitochondrial Pathways Altered in NMD

2.1. Mitochondrial Genome and mtDNA Mutations

Mitochondria contain their own genome, which encodes 13 proteins, 22 tRNAs, and 2 rRNAs. The remaining proteins involved in mitochondrial structure and function are encoded by the nuclear DNA, translated in the cytosol and translocated into mitochondria [92]. Although mtDNA only encodes ±1% of the mitochondrial proteins, these elements are critical components of the MRC, essential for mitochondrial function [94]. Nuclear and mitochondrial intergenomic communication is essential to build the MRC complexes that enables cell bioenergetics and promotes healthy organ function [102].

If mtDNA mutates, these mutations can be present in all mtDNA copies in the cell (homoplasmy) or only in a fraction (heteroplasmy). Almost all humans carry low levels of heteroplasmic mtDNA point mutations, which could be pathogenic [103]. Both the subcellular distribution of mutated mtDNA and the intrinsic pathogenicity of the mutation itself may also be important in determining whether a mtDNA defect is expressed phenotypically [7]. mtDNA mutations are also related to the aging process or age-associated diseases [94].

The distribution of a mutation in different tissues may change with time depending on the mitotic activity of the tissue [92]. In tissues with ongoing cell division, there is a chance that a defect in mtDNA may be selected in or out. This may explain the predilection for mitochondrial diseases to manifest clinically in postmitotic tissues such as the central nervous system and skeletal muscle. This mechanism may also explain why some mitochondrial phenotypes change with time [7,104].

Pathogenic mtDNA mutations must be present in 60–90% of mitochondria in a cell to trigger MRC dysfunction [105]. Computational models estimate that only mtDNA mutations generated in early life could expand to reach the threshold and cause MRC dysfunction in aging human adults [106]. One of the reasons is because mtDNA is organized into mitochondrial nucleoids [107] and coupled with mitochondrial transcription factor A (TFAM), to make mtDNA less accessible to mutations than naked DNA. In fact, lower amount of TFAM is found in hypothyroid myopathy (endocrine myopathy, Table 2), triggering reduced mtDNA copy number and mitochondrial dysfunction [38].

Other NMDs associated to mtDNA mutations are metabolic myopathies, ALS, CMT2, mitochondrial myopathies, and Friedreich's ataxia (Tables 2–4).

Apart from mtDNA point mutations, single large deletion in mtDNA at high levels cause multisystem diseases in children and NMDs associated with chronic progressive external ophthalmoplegia in adults and proximal myopathy [76,79]. Other NMDs with mtDNA deletions are sporadic inclusion body myositis (sIBM) (reported in 67% of sIBM patients) [108,109] and giant axonal neuropathy (GAN). These deletions are generally spontaneously acquired [105], probably as accidents during mtDNA replication in the oocyte, in the early embryo or later on, along lifetime. Some multiple large mtDNA deletions are inherited, as they are caused by mutations in nuclear genes involved in mtDNA replication, nucleotide synthesis or transport [92]. Spontaneous mtDNA deletions appear to accumulate with time, and may increase the likelihood that tissue function will be impaired with time [7].

Above all, mtDNA variants (mutations and deletions) have a broad range of impact, from the ones that are causal of monogenic disorders to those that are a risky allele for complex diseases, in which clinical penetrance also depend on environmental factors. For example, de novo mtDNA monogenic mutations m.3243A > G and m.8344A > G trigger MELAS and MERRF, respectively, and can arise spontaneously, because of replication errors. Another high impact variant is a large 4,977-bp deletion of mtDNA, the most common cause of Kearns–Sayre syndrome. These mutations usually occur de novo within two or three human generations and, for deletions, tend to affect only one generation [104]. In all cases, the specific mutation, the level of heteroplasmy, the threshold effect that determines the level of phenotypic penetrance and which tissues are affected, directly determine the inheritance of the disease and the onset and progression of these disorders.

2.2. Mitochondrial Respiratory Chain (MRC)

The MRC contains five multimeric enzymatic complexes. Complexes I–IV oxidize and transfer their electrons, in the form of hydrogen ions, to the next complex. Once in complex IV, electrons are transferred to molecular oxygen, producing water [7,95]. Complex V generates ATP from adenosine diphosphate (ADP) using the transmembrane electrical potential generated by proton translocation along the MRC [14]. This production of ATP from the reduction of oxygen, known as mitochondrial coupling, is what generates the energy needed for cellular function [110]. In parallel, MRC generates ROS as a subproduct of oxygen metabolism, especially in case of disease. Mutations in mtDNA can trigger the impairment of MRC, affecting energy production and cellular dysfunction [111], observed

in some NMDs and mitochondrial diseases [112]. mtDNA mutates more than ten times faster than nuclear DNA, and this high mutation rate in mtDNA is based on the proximity of mtDNA to the inner mitochondrial membrane, where ROS are generated as by-products of MRC chain, coupled with a lack of histones and efficient DNA repair mechanisms. In addition, mtDNA has low number of noncoding regions between genes, leading to random mutations that impact coding sequences of genes responsible of MRC.

In particular, most of the muscular dystrophies (MD) have some MRC complexes with impaired or decreased function (Table 1): complex I in Becker MD (BMD), complexes III and IV in DMD, and complexes I and V in oculopharyngeal (OPMD) and in distal MD (DD). Other NMDs with MRC alterations are myofibrillar myopathies (complexes I and IV) (Table 2), ALS (CIV subunit I) (Table 3), SMA (complexes I and IV) (Table 3), GAN (complexes I and IV) (Table 4), and sIBM (complex IV) [108]. Impaired MRC function promotes mitochondrial dysfunction, eventually leading to progressive weakness and muscle wasting.

To understand the extent of the how MRC dysfunction affects the progression of a NMDs or vice versa, here we present the case of hypothyroid myopathy (endocrine myopathy, Table 2) and ALS (motor neuron diseases, Table 3).

In hypothyroid myopathy, there is an abnormal activity of the thyroid gland, leading to reduced hormone levels. Thyroid hormones affect skeletal muscle through T3 receptors, located on the mitochondrial membrane of skeletal muscle fibers [113,114]. This MRC-thyroid hormones connection is mediated by several molecular mechanisms that include both direct and indirect effects on mitochondrial structure, function, and biogenesis. One effect in hypothyroid myopathy is a reduced mitochondrial oxidative metabolism, due to decreased hormonal levels and a reduced amount and activity of complex IV (cytochrome c oxidase negative fibers (or COX-)). In addition, T3 receptors, together with the thyroid hormone receptor, increase the expression of some nuclear-encoded respiratory genes, such as cytochrome c1 and b-F1- ATPase subunit genes [38].

Regarding ALS, ALS-associated P525L mutant interacts with ATP synthase complex subunit TP5B, disrupting the formation of ATP synthase complex, thus inhibiting the production of ATP [115]. Both are examples of the complex and intricated pathways governing NMDs in which mitochondria, and herein explained, MRC, play a role.

2.3. Mitochondrial Quality Control

2.3.1. Mitochondrial Biogenesis

Mitochondrial biogenesis increases the number of mitochondria, what can lead to a higher energy supply and survival of cells; or if mutated mtDNA expands to higher levels, low energy supply, and cell death. Both outcomes depend on random clonal expansion of mitochondria [103]. Although mitochondrial biogenesis is energy-consuming, it helps to increase energy production and often restores mitochondrial function. Mitochondrial biogenesis can react to many external *stimuli*, such as exercise, hormones, and possibly dietary restriction, in addition to mitochondrial dysfunction [92]. In the case of mitochondrial dysfunction, coordination between mitochondrial synthesis (mitochondrial biogenesis) and degradation (mitophagy) regulates mitochondrial content, quality, and function.

To initiate mitochondrial biogenesis, synthesis of more MRC complexes is required. MRC components are both encoded in nuclear and mtDNA, although their transcripts are not synthesized simultaneously. Cytosolic translation unidirectionally controls mitochondrial translation, both orchestrated by the nuclear genome. The nuclear genes coding for the MRC are rapidly induced under nutrient shift, whereas mitochondrial genes coding for the MRC are induced more slowly. Mitochondrial MRC's slow kinetics may underlie the lack of environment-responsive mitochondrial transcription factors. Instead of transcription factors, mitochondria contain mRNA-specific translational activators, involved in initiation, elongation, and feedback control of MRC complexes assembly [102].

If mitochondrial biogenesis is disrupted, it may result in mitochondrial dysfunction and loss of respiratory capacity [103], observed in patients with mitochondrial diseases. However, excessive mitochondrial biogenesis can also be a sign of disease. In fact, in the muscle of patients with mitochondrial disease, mitochondrial biogenesis generates the so-called ragged-red fibers (RRF), an increase in the number of mitochondria surrounding muscle fibers aimed to compensate mitochondrial dysfunction (Figure 2). RRF typically loss COX activity (partially encoded in the mitochondrial genome) and increase complex II function (succinate dehydrogenase, SDH, entirely encoded in the nuclear genome). Thus, RRF mainly accumulate abnormal proliferated mitochondria [94].

Alterations in some pathways may trigger accumulation of mitochondria in RRF (e.g., changes in mitochondrial protein synthesis). In addition, RRF usually contain a higher amount of mutant mtDNA genomes than non-RRF. Overall, RRF are a tag of defective oxidative phosphorylation in the affected muscle fibers [7]. In fact, RRF are found in many NMDs like limb-girdle MD (LGMD), sIBM, myofibrillar myopathies, myasthenia gravis, ALS, and mitochondrial myopathies (Tables 1–4).

2.3.2. Mitochondrial Dynamics

Mitochondria are highly dynamic organelles that continuously fuse, divide, and move, and mitochondrial function is controlled and maintained by these morphologic changes. Mitochondrial fission is mainly mediated by dynamin-related guanosine triphosphatase (GTPase) protein 1 (Drp1); while in mitochondrial fusion, the outer and inner mitochondrial membranes primarily fuse mediated by dynamin-related GTPases mitofusin (Mfn 1 and 2) and optic atrophy 1 (OPA1), respectively [103]. The most direct consequence of mitochondrial division and fusion is the change in size of the mitochondria [105]. Interestingly, these processes promote the exchange of genetic and structural material among participant mitochondria, thus enabling the renewal of damaged components, or its expansion throughout the mitochondrial net (Figure 2). However, mitochondria can also increase in number when there are the specific requirements.

When mitochondria are damaged, they undergo changes in mitochondrial membrane potential (MMP) causing depolarization. Altered MMP can also impact the mitochondrial fission/fusion machinery and thereby mitochondrial morphology. Mitochondrial fission generates fragmented mitochondria with increased ROS production [106], which may help in the separation of dysfunctional mitochondria from healthy mitochondria and is a prerequisite for mitochondrial degradation (in a process called mitophagy) [107]. The detrimental effect of mitochondrial fission is the release of cytochrome c from mitochondria, which could activate apoptosis signaling through activation of Bax/Bak pore [103]. Apoptotic cell death may be an important mediator of nervous system injury in the mitochondrial encephalomyopathies [7]. Other NMD with increased apoptosis are OPMD, spinal-bulbar muscular atrophy (SBMA), and ion channel diseases. Defects in ion channel diseases may directly reduce MMP and delay repolarization, affecting the modulation of cell survival and increasing cell apoptosis.

Mitochondrial dynamics is also implicated in the pathogenesis of NMDs like inherited peripheral neuropathy, GAN [76], infantile-onset encephalopathy [116], autosomal dominant optic atrophy [101], and CMT2A [74]. The last three are characterized by mutations involving mitochondrial fusion regulatory genes, OPA1 and MFN2, respectively [117]. Some mutations in mitochondrial dynamics genes can trigger severe effects or even death. An example is a lethal dominant negative allele of DRP1 that affects mitochondrial and peroxisomes fission in newborns and triggers abnormalities in brain development and optic atrophy [118].

Mitochondrial dynamics have also been thoroughly studied in ALS. As mutations in several genes are responsible of ALS, depending on the gene mutated, fusion or fission of mitochondria are enhanced. For example, TDP-43 mutations enhance Mitochondrial fission 1 protein (Fis 1) expression, which increases DRP1 recruitment, leading to higher mitochondrial fission, and a fragmented morphology of mitochondria. In ALS caused by SOD1, increased DRP1 and reduced

Mfn1/Opa1 lead to higher level of mitochondrial fission and a fragmented mitochondrial network; while in ALS related to C9ORF72 mutation, higher Mfn1 levels triggered increased mitochondrial fusion and an elongated morphology [119]. Thus, the deregulation of mitochondrial dynamics is frequently associated to NMDs and its proper function protects and counteracts the progression of some NMDs.

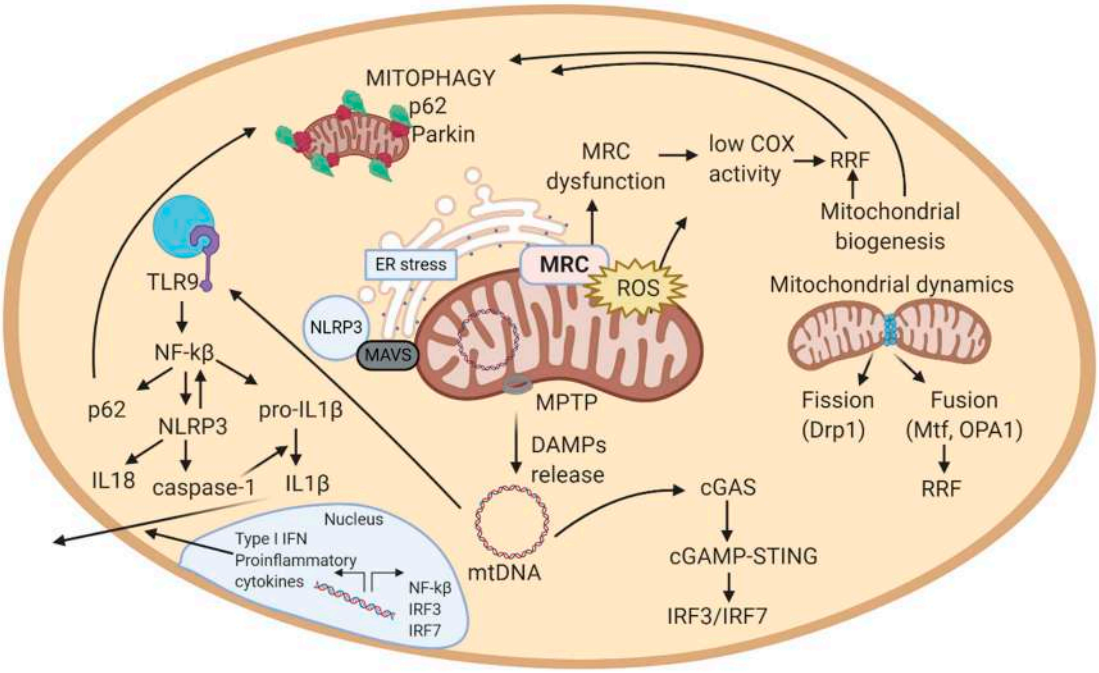

Figure 2. Schematic view of the mechanistic model of mitochondrial-related pathways in a cell. 1. MRC generates ATP in the inner mitochondrial membrane. In this process, also ROS are produced. 2. In case of excessive ROS levels, mitochondrial membrane potential decreases, allowing MPTP to open and release DAMPs (mtDNA, cardiolipin, ceramides) to the cytosol. These DAMPs can trigger an inflammatory response. In this scheme, the inflammatory cascade represented is the one activated by mtDNA. mtDNA activates cGAS in cytosol, that eventually induces the expression of interferon-related genes (IRF3/IRF7). In parallel, mtDNA activates TLR9, which activates NF-kB, and thus, NLRP3 inflammasome, expression of pro-inflammatory cytokines, and among them, IL-1 response. 3. Increased ROS levels can result from MRC dysfunction. To compensate dysfunctional mitochondria, mitochondrial biogenesis increases the number of mitochondria in a cell. Excessive mitochondria around muscle cells form RRF. 4. Excessive ROS, RRF, inflammation, and ER stress damage mitochondria, which alterations are sensed by autophagy and mitophagy. Autophagy and mitophagy remove damaged mitochondria, and consequently stop the inflammatory response, supporting repair mechanisms in the cell. If autophagy and mitophagy are altered, mitochondria cannot be recycled, leading to apoptosis. Abbreviations: MRC: mitochondrial respiratory chain; ROS: reactive oxygen species; MPTP: mitochondrial permeability transition pore; DAMPs: damage-associated molecular patterns; mtDNA: mitochondrial DNA; cGAS: cyclic GMP-AMP synthase; TLR9: toll-like receptor 9; NF-kB: nuclear factor kappa-light-chain-enhancer of activated B cells; NLRP3: NOD-like receptor protein 3; RRF: ragged-red fibers; ER: endoplasmic reticulum; MAVS: mitochondrial antiviral signaling protein. Figure created with BioRender.com.

2.3.3. Autophagy and Mitophagy

Lysosomes were discovered in 1955 [109], and soon was observed that cytoplasmic components could be located in lysosomes [120]. This was the basis for De Duve (1963) to coin the term autophagy [121]. Autophagy is a lysosomal degradation process characterized by the formation of double-membrane autophagosomes from cytoplasmic material and damaged organelles. Autophagosomes fuse with lysosomes to degrade their content by acidic hydrolases. Autophagic

degradation generates amino acids and fatty acids for protein synthesis or oxidation in the MRC to produce ATP for cell survival under starvation conditions. Other functions of autophagy include removal of damaged organelles and protein aggregates, control of cellular biomass and elimination of intracellular pathogens [92]. There are three subtypes of autophagy: macroautophagy, microautophagy, and chaperone-mediated autophagy, divided according to the mechanism used to send intracellular material to be degraded in the lysosomes and the kind of cargo for degradation.

Briefly, mitophagy—the specific autophagy of mitochondria—initiates with the recognition of damaged mitochondria by the E3-ubiquitin ligase Parkin, which decorates the outer mitochondrial membrane proteins with poly-Ub chains [122]. p62 binds polyubiquitinated proteins and damaged organelles and target them to autophagosomal clearance via its ubiquitin association domain (UBA) and LC3 binding motif (LIR), respectively [123]. Absence of specific mitophagy proteins can block autophagosomal or lysosomal clearance leading to an accumulation of damaged proteins and dysfunctional organelles in autophagosomes [124,125].

Mitophagy can occur under several circumstances: metabolic alterations (starvation, particularly), differentiation of some cell types (requiring mitochondrial clearance), and selective targeting and removal of dysfunctional mitochondria [126]. Mitophagy of dysfunctional mitochondria is also called PTEN-induced putative kinase 1 (PINK1)-Parkin-mediated mitochondrial quality-control system [92], since both PTEN and PINK1 are among the main effectors of mitophagy.

The extent of mitophagy varies in different tissues. For instance, heart, skeletal muscle, nervous system, hepatic and renal tissue have higher mitophagy than thymus and spleen [127]. Defects in mitophagy can lead to accumulation of dysfunctional mitochondria and increased levels of mitochondrial ROS and damage-associated molecular pattern (DAMPs), which are self-molecules that resemble pathogenic ones and can trigger an inflammatory response (Figure 2). Both mitochondrial ROS and DAMPs can initiate an inflammatory response [128]. In addition, impaired mitophagy has been linked with aging, metabolic disorders, cancer, senescence, inflammation, and genomic instability [107]. Regarding NMDs, impaired autophagy has been revealed in congenital MD (CMD), endocrine myopathies, inflammatory myopathies, myofibrillar myopathy and congenital myasthenic syndromes, among others.

In CMD linked to collagen VI deficiency, impaired autophagy is responsible for spontaneous apoptosis, dysfunctional mitochondria and myofibers degeneration. Defective autophagy causes accumulation of abnormal organelles and apoptotic degeneration of muscle fibers. Accumulation of defective mitochondria increases oxidative stress and ROS production, which also contribute to increase apoptosis. The cause of defective autophagy in CMD is a reduced protein amount of beclin-1 and Bnip3, what leads to a defective activation of the autophagy process [15].

As mitophagy protects from the accumulation of defective mitochondria and ROS overproduction, this process is frequently impaired in NMDs affecting both nerve and muscle function.

2.4. Mitochondrial ROS and ER Stress

ROS comprises superoxide anion ($O_2^{\bullet -}$), hydrogen peroxide (H_2O_2), hydroxyl radical ($OH^{\bullet}$), peroxyl radical ($ROO^{\bullet}$), and nitric oxide ($NO^{\bullet}$). Although mitochondrial oxidative metabolism is a major source of ROS in many cell types, outside mitochondria there are other enzymes associated with ROS production, like NADPH oxidase, neural nitric oxide synthase, and monoamine oxidase [129]. A balance between oxidative species and antioxidant defense mechanisms is required for cell homeostasis [130]. Briefly, the antioxidant response is mediated by enzymes responsible for metabolizing or neutralizing ROS, such as catalase, glutathione peroxidase, or superoxide dismutase (SODs) [131].

The high proportion of ROS generation in MRC is due to the transfer of electrons in the inner mitochondrial membrane until they encounter oxygen, when electrons are converted in water. Under hypoxia or pathologic conditions this process is not completed, resulting in an increase of superoxide anions [131]. For example, mutation in SOD2, an antioxidant enzyme encoded in the mitochondrial genome, triggers the development of CMT, a NMD [132]. Mutations in SOD1 gene are

found in ALS. SOD1 encodes the Cu-Zn superoxide dismutase, one of three proteins involved in the conversion of free superoxide radicals to molecular oxygen and hydrogen peroxide. Mutations in the SOD1 gene are found in 10–20% of familial ALS cases and 1–5% of sporadic ALS cases globally [133]; so far, more than 170 mutations of the SOD1 gene are known in ALS [119].

Other NMDs in which high ROS levels are not compensated and cells hold excessive oxidative stress are BMD, DMD, FSHD, ALS, SBMA, mitochondrial myopathies, and FA.

When overproduction of ROS cannot be compensated by antioxidant defenses or mitophagy, ER receives ROS signals through MAMs, which may eventually activate cell stress responses to compensate and overcome this adverse situation [134].

ER is the main organelle in charge of protein biosynthesis and folding and one of the main cell sensors to stress insults. Alterations of the ER redox status can negatively affect protein folding and result in ER stress. ER stress occurs when the rate at which new protein entering the ER exceeds its folding capacity, which can lead to the activation of three transmembrane proteins: inositol-requiring enzyme 1α (IRE1α), PKR-like ER kinase (PERK), and the activation transcription factor 6 (ATF6), which altogether trigger a UPR [134]. The UPR is comprised of a series of transcriptional, translational, and post-translational processes that can lower the rate of protein synthesis and increase the protein folding capacity of the ER machinery. This results in an increase of misfolded protein elimination, and escalating the size of the ER compartment thereby reducing the ER stress [98]. Usually, transient ER stress can be overcome by UPR, but if the damaging stimulus persists, inflammatory response genes are activated [131].

ER-mitochondria crosstalk is involved in several pathways including cell proliferation, apoptosis, autophagy, lipid metabolism, Ca^{2+} signaling, UPR, inflammation, and bioenergetics. Alterations in this ER-mitochondria crosstalk are associated with multiple diseases, like motor neuron diseases, myotonic dystrophy, OPMD, endocrine myopathies, myofibrillar myopathies, SBMA, CMT, and mitochondrial myopathies. In ALS, over expression of both wild-type and mutated TDP-43 leads to a decrease in ER-mitochondria physical and functional coupling, affecting Ca^{2+} regulation. Ca^{2+} dysregulation is considered to be a primary cause of motor neuron death in ALS [135]. Ca^{2+} is responsible for the link between metabolic impairment and MAMs interaction. This is seen in cancer cells, which are able to remodel their intracellular Ca^{2+} signaling, enhancing their survival and proliferation. Modulation of ER-mitochondrial Ca^{2+} crosstalk favors resistance to apoptosis [136].

In addition to triggering ER stress, if ROS damage overwhelms these repair mechanisms, MMP may decrease, thus potentially leading to the increase in the permeability of mitochondrial membranes. Higher permeability in mitochondrial membrane can activate the mitochondrial permeability transition pore (MPTP) and thus, the release of DAMPs to the cytosol (mtDNA), ceramides, formaldehyde) [137,138]. MPTP and ROS can also promote the activation of mitochondrial fission and mitophagy to eliminate damaged mitochondria (Figure 2). In mitochondrial fission, MAMs signal the ER tubules to encircle mitochondria and tag the sites for mitochondrial division [139]. Accordingly to mitochondrial implication in NMDs, dysregulation of MPTP opening and defective autophagy have been associated with muscular dystrophies, like collagen VI myopathies (CMD), BMD, DMD, LGMD, and DD [14,15] and, remarkably, most of NMDs show some level of deregulation in most of these pathways.

2.5. Mitochondrially Induced Inflammatory Response

Inflammatory responses recognize pathogen-associated molecular patterns (PAMPs), derived from infection, through a variety of receptors. However, because of the bacterial origin of mitochondria, their proteins are structurally similar to those in bacteria and enable their recognition by the same receptors of the immune system, reinforcing the notion of mitochondria as hubs of immunity [140]. Thus, mitochondrial DAMPs can also trigger an inflammatory response [128]. DAMPs include proteins and peptides, such as N-formyl peptides and TFAM, as well as lipids, and metabolites such as cardiolipin, succinate and ATP, and mtDNA [139].

2.5.1. Implication of mtDNA in Inflammation

In particular, mtDNA is recognized by multiple innate immune receptors: cytosolic cyclic GMP-AMP synthase (cGAS), endosomal Toll-like receptor 9 (TLR9), and NOD, LRR, and Pyrin domain-containing protein 3 (NLRP3) [140]. Here we briefly remark the main effects of these innate immune responses.

Cytosolic mtDNA enhances cytosolic antiviral signaling and expression of interferon-stimulated genes (IRF3/IRF7), which results in the activation of cGAS DNA sensor and STING-IRF3-dependent signaling [141]. These pathways activate transcription factors NF- kB and IRF3 through the kinases IKK and TBK1, respectively. MtDNA stress triggered by TFAM deficiency has been reported to release mtDNA to the cytosol [101].

TLR9 is a nucleic acid sensor that binds to unmethylated CpG DNA, like mtDNA. In basal conditions, TLR9 is located in the ER, but when it is stimulated, TLR9 translocates to the membrane of endosomes or lysosomes, where it binds to ligands and triggers cell inflammation [140].

TLR9 interaction with mtDNA occurs in the endolysosomal compartment and activates the myeloid differentiation primary response protein 88 (MyD88), which induces a number of kinases and transcriptional factors, namely mitogen-activated protein kinases (MAPK) [101]. MAPK leads to nuclear factor-kB (NF-κB) and IRF7 activation to enhance pro-inflammatory and interferon type I (IFN-1) responses, respectively [89]. NF-kB signaling increases the expression of other pro-inflammatory cytokines such as tumor necrosis factor-a (TNF-a), interleukin (IL)-6, IL-1b [128]. Furthermore, TLR9 senses incomplete digestion in lysosomes of damaged mitochondria, because of impaired mitophagy, without the mtDNA release to cytosol.

The activation of the inflammasome NLRP3 involves two sequential signals. The inflammasome priming and assembly signal is induced by NF-κB, which acts downstream of TLRs and other immune receptors [142]. NF-kB activates the expression of inflammasome components and inactive forms of the cytokines, including pro-IL-1b. When active, NLRP3 inflammasome activates caspase-1, which processes pro-IL-1β and pro-IL-18 [100,143]. DAMPs directly activate NLRP3 inflammasome as well. Mitochondria are suggested to regulate the activity of the NLRP3 inflammasome complex, by: activating mitophagy (reduces inflammation by clearing mitochondrial-bound NLRP3 complexes) and releasing mitochondrial ROS (amplifies inflammasome immunogenic signal) [140].

In normal conditions, NLRP3 protein is located on the ER. Under oxidative stress and in response to inflammation, NLRP3 can be translocated to MAMs. MAMs transmit danger signals through physical interaction, promoting coordinated responses to oxidative stress, such as triggering mitophagy to remove damaged mitochondria [131].

Altogether, mitochondria-induced inflammation usually is initiated by mitochondrial ROS, which can cause the activation of MAPKs by inhibiting MAPK phosphatase. Activated MAPK may aid in the production of IL-6 and TNF. Mitochondrial ROS accumulation can also activate NLRP3 inflammasome, which promotes the maturation of IL-1β and IL-18. mtDNA accumulation in the cytosol can interact with TLR-9 (in lysosomes) to induce inflammatory responses (e.g., in autosomal dominant optic atrophy [101]. This pathologic feature has been described in sIBM and in LMNA-related NMDs (CMD, Emery-Dreifuss MD, LGMD, CMT, etc.)) [144]. Further, cytosolic mtDNA can activate cGAS-STING to induce IFN-1 or the NLRP3 inflammasome which can induce the maturation/secretion of pro-inflammatory cytokines [101]. Thus, mtDNA can activate major innate immune responses by acting as a DAMP from the mitochondria. Overall, mtDNA is released from mitochondria to the cytosol, where it is recognized by immune receptors, which trigger a signaling cascade that leads to the production of cytokines or transcription of inflammatory genes in the nucleus (Figure 2) [143]. This close association between mitochondria and inflammation triggered from affected cells, explains why NMDs are usually associated with inflammatory effects.

2.5.2. Implication of Mitochondrial ROS in Inflammation

Regarding mitochondrial ROS, they are sensed by mitochondrial antiviral signaling protein (MAVS), key in viral RNA infections. MAVS can activate pathways that regulate NF-kB and IRF3/IRF7 to induce gene expression [145]. It also can interact with the outer mitochondrial membrane, where mitochondrial ROS can trigger MAVS oligomerization, promoting IFN-1 production. In addition, MAVS can associate with NLRP3 and triggers its oligomerization, leading to caspase-1 activation [146].

NLRP3 is activated by mitochondrial ROS but also by cardiolipin, an inner mitochondrial membrane lipid. Cardiolipin translocates to the outer mitochondrial membrane after mitochondrial membrane depolarization, where it can recruit NLRP3. Cardiolipin-NLRP3 interaction suggests the role of mitochondria as a hub for the activation of innate immunity [143].

Similar to MAVS, NLRP3 also responds to mitochondrial ROS and can cause mitochondrial damage that promotes the generation of additional ROS. NLRP3 drives the production of IL-1β, IL-18, and pyroptosis. mtDNA can also activate NLRP3, and is also sensed by TLR9, which leads to immune and inflammatory gene expression. Mitochondria are therefore critical for signaling by three major innate immune pathways: RIG-I/MAVS, NLRP3, and TLR9 [143]. All these pathways rely on mitochondria-inflammatory response and, consequently, are altered in numerous NMDs.

2.5.3. Feedback Regulation of the Mitochondrial Inflammatory Response

NF-kB has a role as a pro-inflammatory and anti-inflammatory transcription factor in mitochondrial-induced inflammation. NF-kB anti-inflammatory functions prevent premature and excessive NLRP3-inflammasome activation, avoiding chronic inflammatory disease and inflammation caused by cell and tissue stress [147]. Self-limiting inflammation is also important for maintaining homeostasis, tissue repair, and regeneration, which restores integrity of epithelial barriers and thereby attenuates PAMP and DAMP availability [100].

Autophagy is the mechanism underlying NF-kB-mediated inhibition of NLRP3 inflammasome. After inducing the expression of pro-inflammatory cytokines and NLRP3, NF-kB is able to switch the initial pro-inflammatory to an anti-inflammatory state to avoid excessive inflammation. Thus, NF-kB induces the expression of p62, which eliminates NLRP3 by mitophagy [138]. Therefore, the "NF-kB-p62/SQSTM1-mitophagy" pathway provides an essential regulatory loop through which NF-kB orchestrates a reparative inflammatory response and prevents excessive collateral damage [100].

Dysregulation of the NLRP3-inflammasome is frequently associated with diverse inflammatory, metabolic, and malignant diseases, including gouty arthritis, Alzheimer's disease, obesity, type II diabetes, and colorectal cancer [148]. Other NMDs with increased inflammation are ALS (with aberrant activation of NF-kB) [17], muscular dystrophies (like BMD and DMD), and inflammatory myopathies. Therefore, proper control of NLRP3-inflammasome activity and overall inflammatory cascade are critical for preventing disease development.

The aging process itself is linked to elevated low-grade inflammation or para-inflammation, characterized by constitutive production of low amounts of IL-1b, TNF, and IL-6. The NLRP3-inflammasome activation and insufficient mitophagy link accumulation of damaged mitochondria to the para-inflammatory state. Normal, healthy aging may be compromised and greatly enhanced by accumulation of somatically mutated mitochondria, which are more likely to release mitochondrial ROS and fragmented mtDNA that act as direct NLRP3-inflammasome activators [100]. This explains why most of NMDs arise hand by hand to aging processes.

3. Treatment Strategies in NMDs

As stated before, mitochondria play a key role in the early process of nerve and muscle degeneration and affects the progression of NMDs. Although current understanding of mitochondrial dysfunction in NMD is still evolving, there are some potential therapeutic strategies that tackle mitochondrial deregulated pathways.

The number of NMDs for which treatments are available is limited. This scarcity of therapeutic options lays on the rarity and diversity of NMDs, the complexity of their genetic inheritance, the abundance and distribution of muscle tissue, and low treatment efficacy [14]. The rarity of NMDs limits the available patients for recruitment for clinical trials, which highly depends on the quality and reliability of data obtained in cell and animal experiments [149].

Despite there is no cure for most NMDs, some can be effectively managed and treated. Some common interventions include drug therapy, surgery, or patient support groups, to improve physical and psychological wellbeing of NMD patients [6]. Innovative breakthroughs are approaching owing to antisense oligonucleotides (ASO) and gene replacement therapies, currently under development. Here we summarize the main points of different treatment strategies, most of them posing supportive pharmacologic options aimed not to cure but to slow down disease progression.

Drug therapy in NMDs comprises a wide range of treatments. Immunosuppressive drugs are widely used to treat certain muscle, nerve, and NMJ diseases. Anticonvulsants and antidepressants might aid in treating the pain of neuropathy [6]. More specifically, senolytic drugs (e.g., resveratrol) help to remove senescent cells to reduce the overall pro-inflammatory profile, although inflammation differs among tissues and makes it difficult to only target senescent cells [82]. Interestingly, resveratrol has been associated to promote mitochondrial health and renewal through different mechanisms [150].

Other treatment options are being developed to specifically target mitochondria. For example metformin, used as an anticancer drug, increases the activation of AMPK, favoring autophagy of damaged mitochondria (e.g., in mitochondrial diseases and DMD); caloric restriction, which reduces ROS production and thus, DNA damage (in collagen VI myopathies); and mitohormesis, based in inducing mild mitochondrial stress during life to induce an antioxidant response (e.g., by vitamin E). Some dietary supplements boost mitochondrial capacity like niacin (vitamin B3) in mitochondrial myopathy; epicatechin in BMD, or triheptanoin, CoQ10 and tocotrienols in ALS [151].

Moreover, exercise has shown to induce autophagy to overcome sarcopenia (e.g., in metabolic myopathies) [152]. In young and old mice, exercise training has even promoted biogenesis of mitochondria and mitochondrial autophagy to reduce the expression of proinflammatory cytokines by up to 49% [82]. Unfortunately, exercise is not always possible in patients affected by NMDs.

Other mitochondrial pathways that could be tackled therapeutically are dysregulation of MPTP opening, mitochondrial fission, and ER stress. MPTP modifiers (e.g., CsA, cyclophilin D inhibitors) might potentially aid in many NMDs [14]. Targeting mitochondrial fission is based on its direct relation to apoptosis, thus reducing fission might reduce cell death. Treating ER stress could be relevant in many NMD and other proteinopathies [30]. Currently, these therapeutic approaches are under development.

In addition to drug therapy, some NMDs benefit from surgery. Depending on the NMD, patients may receive neurological, thoracic, orthopedic, or other surgeries. Physical, occupational, or rehabilitation therapies may help before or after these interventions [6].

Recently, other approaches more related to personalized medicine are being developed or even in the market, like ASO and gene therapy. ASOs are short, synthetic single-stranded nucleic acids that bind targeted RNAs sequences to promote their degradation or modify splicing by impeding the binding of RNA splicing factors [153]. This approach has been developed in SMA and DMD and approved by FDA. In SMA, an ASO that switches the splicing to include an exon in the pre-mRNA of SMN2 gene has become the first treatment for SMA approved by FDA, commercialized by Biogen (MA, USA) under the name Nusinersen [67].

In DMD, an exon skipping ASO called Eteplirsen is also approved and commercially available. In this case, exon-skipping of damaged dystrophin in DMD generates a shortened but still functional version of dystrophin [154]. Other NMDs like LGMD could benefit from ASO exon skipping, by restoring the disrupted reading frame of the SGCG gene [5,27].

Apart from ASOs, gene replacement therapies are under development. In SMA, there is a gene replacement therapy available for patients younger than 2 years old. In this case, SMN1 gene cDNA is packaged in an adeno-associated virus 9 vector (AAV9), which are non-pathogenic, delivered

intravenously and can cross the blood brain barrier to transduce neurons [155]. Once inside neurons, SMN1 cDNA constitutively expresses, with long-term expression in differentiated cells after a single dose, but not in mitotically active cells. This drug has shown efficacy in infantile SMA patients and is commercialized by Avexis under the name Zolgensma [67,156]. Other gene therapies using CRISPR/Cas-mediated approaches in NMD have shown efficacy in models of DMD, CMD, LGMD, DM1, and FSHD [157], becoming promising therapeutic approaches for further transference into clinical settings.

Altogether, currently there are nearly 200 potential therapies under development for NMD (in preclinical and clinical stages), mainly targeting ALS, SMA, and DMD [158]. Around 43% are small molecules (targeting receptor modulation, epigenetic reprogramming, redox metabolism, etc.), 14% gene therapy and 9% antisense oligonucleotides (ASOs) [159]. This shows that personalized medicine is increasingly offering new treatments for rare diseases, like NMDs. Indeed, the number of molecules in clinical trials for NMD has sharply increased in the last 5 years [158]. This proves NMD therapies are becoming a highly dynamic and potentially achieving field [8].

Notably, treatments not only focus in improving physical health of NMD patients, but also patients and families receive education and counselling to check their wellbeing. This may include getting involved in support groups or genetic counsellors (e.g., physical therapists, nutritionists). Patient's associations are highly interested in creating support groups and analyze the quality of life of NMD patients and carers. One ongoing project, promoted by Share4Rare and released in the beginning of 2020, consists in a study called "Understanding how neuromuscular diseases impact learning and working opportunities for patients and carers." They claim that patients with rare NMDs are a scattered community, often dispersed, and poorly represented. Even with the increased interest in developing research and potential therapeutic options in clinical trials in the last 10 years, little is known about the impact on quality of life of NMDs. With this study, they focus on understanding the psychosocial impact of NMD on patients, families, and caregivers [160].

4. Discussion

Despite we must acknowledge the impossibility of summarizing all previous knowledge in the current review, the present revision aimed to outline the state-of-the-art in the main etiologies of NMDs related to mitochondrial metabolism. The role of oxidative stress, mitochondrial biogenesis, autophagy, and inflammation related to mitochondria have been thoroughly described and linked to the affected NMDs (Figure 2). Overall, mitochondrial defects play a key role in the early process of neuronal and muscle degeneration and further affects the progression of NMDs.

NMDs can appear as a result of damage in nerve, muscle, or both tissues. In fact, the classification of NMDs include seven groups, two of them with primary muscle affection (MD and myopathies other than dystrophies), three of them with primary nerve dysfunction (NMJ diseases, peripheral nerve diseases and motor neuron diseases) and last two with both tissues affected (mitochondrial diseases and ion channel diseases). More attention should be focused on identifying prognostic and diagnostic biomarkers that target a specific pathway to accurately diagnose every NMD and control its progression.

Despite the number of treatments for NMD is still limited, some experimental treatments are currently under development to tackle mitochondrial deregulated pathways in NMDs. Current studies and clinical trials in many disabling NMDs aim to improve the wellbeing of patients and their families, but deep understanding of mitochondrial dysfunction in NMD will be essential to validate and establish further therapeutic targets.

The preclinical and clinical research advances in NMDs in the last years have been astounding. Better cell and animal models have helped in the characterization of many NMDs. Furthermore, the broad diversity and rarity of these diseases have revealed the importance of carefully studying every NMD history and progression. This more accurate approach is translating to more personalized

treatments, as seen with new ASOs and gene therapies recently released to the market, and will eventually lead to a higher success rate in clinical trials for these disabling diseases.

5. Conclusions

- NMDs have a direct or indirect influence of mitochondria in their etiology. Mitochondrial genetic defects directly affect nerves and muscles in NMDs; but when there is an alternative cause of disease, unproper mitochondrial function can limit energetic supply of compensatory mechanisms, thus indirectly conditioning the progression of disease.
- Defects in oxidative metabolism can lead to accumulation of ROS, potentially affecting the ER and triggering inflammation, which eventually may lead to cell death and tissue damage.
- To avoid cell damage and excessive oxidative stress, mitochondrial quality control processes closely monitor changes in mitochondrial metabolism. In case of trouble, different responses arise by the increase in the number of mitochondria (mitochondrial biogenesis), by changing their morphology and size (mitochondrial dynamics) or recycling them (mitophagy). Most of these processes are altered in NMDs, highlighting the relevance of mitochondria in the development and progression of these disorders.
- Understanding nerves, muscles, and mitochondrial defects in NMDs is essential to improve diagnosis and treatments for these major incapacitating diseases.
- Despite growing efforts to clarify the etiology of NMD, the complexity of reality is still far beyond current knowledge and information provided in the present review, challenging new researchers to develop novel approaches.

Author Contributions: Conceptualization: J.C.-S. and G.G.; formal analysis: J.C.-S. and G.G.; investigation: J.C.-S. and G.G.; writing—original draft preparation: J.C.-S.; writing—review and editing: J.C.-S., J.M.G.-J. and G.G.; supervision: J.M.G.-J. and G.G.; project administration: J.M.G.-J. and G.G.; funding acquisition: J.M.G.-J. and G.G. All authors have read and agreed to the published version of the manuscript.

Funding: This research was funded by Instituto de Salud Carlos III (ISCIII) and Fondos Europeos de Desarrollo Regional (FEDER), 'una manera de hacer Europa', FIS PI1800498.

Acknowledgments: We are in dept to all patients and their families, always devoted to collaborate and widen the state-of-the-art in diseases.

Conflicts of Interest: The authors declare no conflict of interest. The funders had no role in the design of the study; in the collection, analyses, or interpretation of data; in the writing of the manuscript, or in the decision to publish the results.

References

1. Diagnosis—European Reference Network—EURO-NMD. Available online: https://ern-euro-nmd.eu/ (accessed on 22 April 2020).
2. Scotton, C.; Passarelli, C.; Neri, M.; Ferlini, A. Biomarkers in rare neuromuscular diseases. *Exp. Cell Res.* **2013**, *325*, 44–49. [CrossRef] [PubMed]
3. Bonne, G.; Rivier, F.; Hamroun, D. The 2018 version of the gene table of monogenic neuromuscular disorders (nuclear genome). *Neuromuscul. Disord.* **2017**, *27*, 1152–1183. [CrossRef] [PubMed]
4. Deenen, C.W.J.; Horlings, G.C.C.; Verschuuren, J.G.M.J.; Verbeek, L.M.A.; van Engelen, G.M.B. The Epidemiology of Neuromuscular Disorders: A Comprehensive Overview of the Literature. *J. Neuromuscul. Dis.* **2015**, *2*, 73–85. [CrossRef] [PubMed]
5. Van Putten, M.; Hmeljak, J.; Aartsma-Rus, A.; Dowling, J.J. Moving neuromuscular disorders research forward: From novel models to clinical studies. *Dis. Model. Mech.* **2020**, *13*, 44370. [CrossRef]
6. Neurology Neuromuscular Disorders Causes & Symptoms Beaumont Health. Available online: https://www.beaumont.org/conditions/neuromuscular-disorders (accessed on 19 May 2020).
7. Nardin, R.A.; Johns, D.R. Mitochondrial dysfunction and neuromuscular disease. *Muscle Nerve* **2001**, *24*, 170–191. [CrossRef]
8. Cowling, B.S.; Thielemans, L. Translational medicine in neuromuscular disorders: From academia to industry. *Dis. Model. Mech.* **2019**, *13*, 41434. [CrossRef]

9. Find A Neuromuscular Disease Muscular Dystrophy Association. Available online: https://www.mda.org/disease/list (accessed on 19 May 2020).
10. GeneTable. Available online: http://www.musclegenetable.fr/index.html (accessed on 7 July 2020).
11. Hewitt, J.E.; Pollard, A.K.; Lesanpezeshki, L.; Deane, C.S.; Gaffney, C.J.; Etheridge, T.; Szewczyk, N.J.; Vanapalli, S.A. Muscle strength deficiency and mitochondrial dysfunction in a muscular dystrophy model of *Caenorhabditis elegans* and its functional response to drugs. *Dis. Model. Mech.* **2018**, *11*. [CrossRef]
12. Heydemann, A. Skeletal muscle metabolism in duchenne and becker muscular dystrophy—Implications for therapies. *Nutrients* **2018**, *10*, 796. [CrossRef]
13. Mendell, J.R.; Sahenk, Z.; Malik, V.; Gomez, A.M.; Flanigan, K.M.; Lowes, L.P.; Alfano, L.N.; Berry, K.; Meadows, E.; Lewis, S.; et al. A phase 1/2a follistatin gene therapy trial for becker muscular dystrophy. *Mol. Ther.* **2015**, *23*, 192–201. [CrossRef]
14. Katsetos, C.D.; Koutzaki, S.; Melvin, J.J. Mitochondrial dysfunction in neuromuscular disorders. *Semin. Pediatric Neurol.* **2013**, *20*, 202–215. [CrossRef]
15. Grumati, P.; Grumati, P.; Coletto, L.; Sabatelli, P.; Cescon, M.; Angelin, A.; Bertaggia, E.; Blaauw, B.; Urciuolo, A.; Tiepolo, T.; et al. Autophagy is defective in collagen VI muscular dystrophies, and its reactivation rescues myofiber degeneration. *Nat. Med.* **2010**, *16*, 1313–1320. [CrossRef] [PubMed]
16. Jongpiputvanich, S.; Sueblinvong, T.; Norapucsunton, T. Mitochondrial respiratory chain dysfunction in various neuromuscular diseases. *J. Clin. Neurosci.* **2005**, *12*, 426–428. [CrossRef] [PubMed]
17. Pleasure, D. Advances in Translational Research in Neuromuscular Diseases. *Arch. Neurol.* **2011**, *68*, 429. [CrossRef]
18. Lamar, K.-M.; Mcnally, E.M. Genetic Modifiers for Neuromuscular Diseases. *J. Neuromuscul. Dis.* **2014**, *1*, 3–13. [CrossRef]
19. Rybalka, E.; Timpani, C.A.; Cooke, M.B.; Williams, A.D.; Hayes, A. Defects in mitochondrial ATP synthesis in dystrophin-deficient Mdx skeletal muscles may be caused by complex I insufficiency. *PLoS ONE* **2014**, *9*, 115763. [CrossRef] [PubMed]
20. Godin, R.; Daussin, F.; Matecki, S.; Li, T.; Petrof, B.J.; Burelle, Y. Peroxisome proliferator-activated receptor γ coactivator 1-α gene transfer restores mitochondrial biomass and improves mitochondrial calcium handling in post-necrotic mdx mouse skeletal muscle. *J. Physiol.* **2012**, *590*, 5487–5502. [CrossRef]
21. Pauly, M.; Daussin, F.; Burelle, Y.; Li, T.; Godin, R.; Fauconnier, J.; Koechlin-Ramonatxo, C.; Hugon, G.; Lacampagne, A.; Coisy-Quivy, M.; et al. AMPK activation stimulates autophagy and ameliorates muscular dystrophy in the mdx mouse diaphragm. *Am. J. Pathol.* **2012**, *181*, 583–592. [CrossRef] [PubMed]
22. Zuela, N.; Dorfman, J.; Gruenbaum, Y. Global transcriptional changes caused by an EDMD mutation correlate to tissue specific disease phenotypes in *C. elegans*. *Nucleus* **2017**, *8*, 60–69. [CrossRef]
23. Puckelwartz, M.; McNally, E.M. Emery-Dreifuss muscular dystrophy. *Handb. Clin. Neurol.* **2011**, *101*, 155–166. [CrossRef]
24. Orphanet. Available online: https://www.orpha.net/consor4.01/www/cgi-bin/?lng=ES (accessed on 22 May 2020).
25. Lemmers, R.J.L.F.; Van Der Vliet, P.J.; Klooster, R.; Sacconi, S.; Camaño, P.; Dauwerse, J.G.; Snider, L.; Straasheijm, K.R.; Van Ommen, G.J.; Padberg, G.W.; et al. A unifying genetic model for facioscapulohumeral muscular dystrophy. *Science* **2010**, *329*, 1650–1653. [CrossRef]
26. Deng, H.-X.; Klein, C.J.; Yan, J.; Shi, Y.; Wu, Y.; Fecto, F.; Yau, H.-J.; Yang, Y.; Zhai, H.; Siddique, N.; et al. Scapuloperoneal spinal muscular atrophy and CMT2C are allelic disorders caused by alterations in TRPV4. *Nat. Genet.* **2010**, *42*, 165–169. [CrossRef] [PubMed]
27. Demonbreun, A.R.; Wyatt, E.J.; Fallon, K.S.; Oosterbaan, C.C.; Page, P.G.; Hadhazy, M.; Quattrocelli, M.; Barefield, D.Y.; McNally, E.M. A gene-edited mouse model of limb-girdle muscular dystrophy 2C for testing exon skipping. *DMM Dis. Model. Mech.* **2020**, *13*. [CrossRef] [PubMed]
28. Lilleker, J.B.; Keh, Y.S.; Roncaroli, F.; Sharma, R.; Roberts, M. Metabolic myopathies: A practical approach. *Pract. Neurol.* **2018**, *18*, 14–26. [CrossRef] [PubMed]
29. CNBP Gene—Genetics Home Reference—NIH. Available online: https://ghr.nlm.nih.gov/gene/CNBP#conditions (accessed on 25 May 2020).
30. Malerba, A.; Klein, P.; Bachtarzi, H.; Jarmin, S.A.; Cordova, G.; Ferry, A.; Strings, V.; Espinoza, M.P.; Mamchaoui, K.; Blumen, S.C.; et al. PABPN1 gene therapy for oculopharyngeal muscular dystrophy. *Nat. Commun.* **2017**, *8*, 1–14. [CrossRef] [PubMed]

31. Malerba, A.; Roth, F.; Harish, P.; Dhiab, J.; Lu-Nguyen, N.; Cappellari, O.; Jarmin, S.; Mahoudeau, A.; Ythier, V.; Lainé, J.; et al. Pharmacological modulation of the ER stress response ameliorates oculopharyngeal muscular dystrophy. *Hum. Mol. Genet.* **2019**, *28*, 1694–1708. [CrossRef]
32. Chartier, A.; Klein, P.; Pierson, S.; Barbezier, N.; Gidaro, T.; Casas, F.; Carberry, S.; Dowling, P.; Maynadier, L.; Bellec, M.; et al. Mitochondrial Dysfunction Reveals the Role of mRNA Poly(A) Tail Regulation in Oculopharyngeal Muscular Dystrophy Pathogenesis. *PLoS Genet.* **2015**, *11*, 1005092. [CrossRef]
33. Rossi, D.; Palmio, J.; Evilä, A.; Galli, L.; Barone, V.; Caldwell, T.A.; Policke, R.A.; Aldkheil, E.; Berndsen, C.E.; Wright, N.T.; et al. A novel FLNC frameshift and an OBSCN variant in a family with distal muscular dystrophy. *PLoS ONE* **2017**, *12*, 186642. [CrossRef]
34. Vincent, A.E.; Rosa, H.S.; Alston, C.L.; Grady, J.P.; Rygiel, K.A.; Rocha, M.C.; Barresi, R.; Taylor, R.W.; Turnbull, D.M. Dysferlin mutations and mitochondrial dysfunction. *Neuromuscul. Disord.* **2016**, *26*, 782–788. [CrossRef]
35. GeneTable. Available online: http://www.musclegenetable.fr/4DACTION/Blob_groupe11/ (accessed on 6 July 2020).
36. Fusto, A.; Moyle, L.A.; Gilbert, P.M.; Pegoraro, E. Cored in the act: The use of models to understand core myopathies. *DMM Dis. Model. Mech.* **2019**, *12*. [CrossRef]
37. Gilbreath, H.R.; Castro, D.; Iannaccone, S.T. Congenital myopathies and muscular dystrophies. *Neurol. Clin.* **2014**, *32*, 689–703. [CrossRef]
38. Siciliano, G.; Monzani, F.; Manca, M.L.; Tessa, A.; Caraccio, N.; Tozzi, G.; Piemonte, F.; Mancuso, M.; Santorelli, F.M.; Ferrannini, E.; et al. Human Mitochondrial Transcription Factor A Reduction and Mitochondrial Dysfunction in Hashimoto's Hypothyroid Myopathy. *Mol. Med.* **2002**, *8*, 326–333. [CrossRef] [PubMed]
39. Lloreta, J.; Roquer, J.; Corominas, J.M.; Serrano, S. Hyperthyroid myopathy with mitochondrial paracrystalline rectangular inclusions. *Ultrastruct. Pathol.* **1996**, *20*, 61–65. [CrossRef] [PubMed]
40. Tan, Y.; Gong, Y.; Dong, M.; Pei, Z.; Ren, J. Role of autophagy in inherited metabolic and endocrine myopathies. *Biochim. Biophys. Acta Mol. Basis Dis.* **2019**, *1865*, 48–55. [CrossRef] [PubMed]
41. Selva-O'callaghan, A.; Pinal-Fernandez, I.; Trallero-Araguás, E.; Milisenda, J.C.; Grau-Junyent, M.; Mammen, A.L. Classification and management of adult inflammatory myopathies. *Lancet Neurol.* **2018**, *17*, 816–828. [CrossRef]
42. Catalan-Garcia, M.; Garrabou, G.; Moren, C.; Guitart-Mampel, M.; Hernando, A.; Diaz-Ramos, A.; Gonzalez-Casacuberta, I.; Juarez, D.-L.; Bano, M.; Enrich-Bengoa, J.; et al. Mitochondrial DNA disturbances and deregulated expression of oxidative phosphorylation and mitochondrial fusion proteins in sporadic inclusion body myositis. *Clin. Sci.* **2016**, *130*, 1741–1751. [CrossRef] [PubMed]
43. Sharp, L.J.; Haller, R.G. Metabolic and mitochondrial myopathies. *Neurol. Clin.* **2014**, *32*, 777–799. [CrossRef]
44. Selcen, D.; Ohno, K.; Engel, A.G. Myofibrillar myopathy: Clinical, morphological and genetic studies in 63 patients. *Brain* **2004**, *127*, 439–451. [CrossRef]
45. Perrone, L.; Squillaro, T.; Napolitano, F.; Terracciano, C.; Sampaolo, S.; Anna, M.; Melone, B. The Autophagy Signaling Pathway: A Potential Multifunctional Therapeutic Target of Curcumin in Neurological and Neuromuscular Diseases. *Nutrients* **2019**, *11*, 1881. [CrossRef]
46. Vincent, A.E.; Grady, J.P.; Rocha, M.C.; Alston, C.L.; Rygiel, K.A.; Barresi, R.; Taylor, R.W.; Turnbull, D.M. Mitochondrial dysfunction in myofibrillar myopathy. *Neuromuscul. Disord.* **2016**, *26*, 691–701. [CrossRef]
47. Pá, E.; Bedekovics Istvá, T.; Ti, G. Familial Scapuloperoneal Myopathy and Mitochondrial DNA Defect. *Eur Neurol.* **1999**, *42*, 211–216.
48. Zukosky, K.; Meilleur, K.; Traynor, B.J.; Dastgir, J.; Medne, L.; Devoto, M.; Collins, J.; Rooney, J.; Zou, Y.; Yang, M.L.; et al. Association of a novel ACTA1 mutation with a dominant progressive scapuloperoneal myopathy in an extended family. *JAMA Neurol.* **2015**, *72*, 689–698. [CrossRef] [PubMed]
49. Chen, D.H.; Raskind, W.H.; Parson, W.W.; Sonnen, J.A.; Vu, T.; Zheng, Y.; Matsushita, M.; Wolff, J.; Lipe, H.; Bird, T.D. A novel mutation in FHL1 in a family with X-linked scapuloperoneal myopathy: Phenotypic spectrum and structural study of FHL1 mutations. *J. Neurol. Sci.* **2010**, *296*, 22–29. [CrossRef] [PubMed]
50. Engel, A.G.; Shen, X.M.; Selcen, D.; Sine, S.M. Congenital myasthenic syndromes: Pathogenesis, diagnosis, and treatment. *Lancet Neurol.* **2015**, *14*, 420–434. [CrossRef]

51. Chaouch, A.; Porcelli, V.; Cox, D.; Edvardson, S.; Scarcia, P.; De Grassi, A.; Pierri, C.L.; Cossins, J.; Laval, S.H.; Griffin, H.; et al. Chaouch et al. Mutations in the Mitochondrial Citrate Carrier SLC25A1. *J. Neuromuscul. Dis.* **2014**, *1*, 75–90. [CrossRef] [PubMed]
52. Finsterer, J. Congenital myasthenic syndromes. *Orphanet J. Rare Dis.* **2019**, *14*, 57. [CrossRef]
53. Bogdanik, L.P.; Burgess, R.W. A valid mouse model of AGRIN-associated congenital myasthenic syndrome. *Hum. Mol. Genet.* **2011**, *20*, 4617–4633. [CrossRef]
54. Kesner, V.G.; Oh, S.J.; Dimachkie, M.M.; Barohn, R.J. Lambert-Eaton Myasthenic Syndrome. *Neurol. Clin.* **2018**, *36*, 379–394. [CrossRef]
55. Hülsbrink, R.; Hashemolhosseini, S. Lambert-Eaton myasthenic syndrome-Diagnosis, pathogenesis and therapy. *Clin. Neurophysiol.* **2014**, *125*, 2328–2336. [CrossRef]
56. Herrmann, D.N.; Horvath, R.; Sowden, J.E.; Gonzales, M.; Sanchez-Mejias, A.; Guan, Z.; Whittaker, R.G.; Almodovar, J.L.; Lane, M.; Bansagi, B.; et al. Synaptotagmin 2 mutations cause an autosomal-dominant form of lambert-eaton myasthenic syndrome and nonprogressive motor neuropathy. *Am. J. Hum. Genet.* **2014**, *95*, 332–339. [CrossRef]
57. Marchiori, P.E.; Levy, J.A.; Carvalho-Alegro, M.S.; Lusvarghi, E.S.; Tsanaclis, A.M.; De Assis, J.L.; Scaff, M. Mitochondrial dysfunction in myasthenia gravis. Report of a case. *Arq. Neuropsiquiatr.* **1989**, *47*, 355–358. [CrossRef]
58. Gilhus, N.E. Myasthenia Gravis. *N. Engl. J. Med.* **2016**, *375*, 2570–2581. [CrossRef] [PubMed]
59. Maruyama, H.; Morino, H.; Ito, H.; Izumi, Y.; Kato, H.; Watanabe, Y.; Kinoshita, Y.; Kamada, M.; Nodera, H.; Suzuki, H.; et al. Mutations of optineurin in amyotrophic lateral sclerosis. *Nat. Lett.* **2010**, *465*. [CrossRef] [PubMed]
60. Mitchell, J.; Paul, P.; Chen, H.-J.; Morris, A.; Payling, M.; Falchi, M.; Habgood, J.; Panoutsou, S.; Winkler, S.; Tisato, V.; et al. Familial amyotrophic lateral sclerosis is associated with a mutation in D-amino acid oxidase. *Proc. Natl. Acad. Sci. USA* **2010**, *107*, 7556–7561. [CrossRef] [PubMed]
61. Hardiman, O.; Van Den Berg, L.H.; Kiernan, M.C. Clinical diagnosis and management of amyotrophic lateral sclerosis. *Nat. Rev. Neurol.* **2011**, *7*, 639–649. [CrossRef]
62. Chiò, A.; Mora, G.; Lauria, G. Pain in amyotrophic lateral sclerosis. *Lancet Neurol.* **2017**, *16*, 144–157. [CrossRef]
63. Comi, G.P.; Bordoni, A.; Salani, S.; Franceschina, L.; Sciacco, M.; Prelle, A.; Fortunato, F.; Zeviani, M.; Napoli, L.; Bresolin, N.; et al. Cytochrome c oxidase subunit I microdeletion in a patient with motor neuron disease. *Ann. Neurol.* **1998**, *43*, 110–116. [CrossRef]
64. Figueroa-Romero, C.; Guo, K.; Murdock, B.J.; Paez-Colasante, X.; Bassis, C.M.; Mikhail, K.A.; Raue, K.D.; Evans, M.C.; Taubman, G.F.; McDermott, A.J.; et al. Temporal evolution of the microbiome, immune system and epigenome with disease progression in ALS mice. *DMM Dis. Model. Mech.* **2020**, *13*. [CrossRef]
65. Lynch, E.; Semrad, T.; Belsito, V.S.; FitzGibbons, C.; Reilly, M.; Hayakawa, K.; Suzuki, M. C9ORF72-related cellular pathology in skeletal myocytes derived from ALS-patient induced pluripotent stem cells. *DMM Dis. Model. Mech.* **2019**, *12*, 1–12. [CrossRef]
66. Ranganathan, S.; Harmison, G.G.; Meyertholen, K.; Pennuto, M.; Burnett, B.G.; Fischbeck, K.H. Mitochondrial abnormalities in spinal and bulbar muscular atrophy. *Hum. Mol. Genet.* **2008**, *18*, 27–42. [CrossRef]
67. Ravi, B.; Antonellis, A.; Sumner, C.J.; Lieberman, A.P. Genetic approaches to the treatment of inherited neuromuscular diseases. *Hum. Mol. Genet.* **2019**, *28*, 1–55. [CrossRef]
68. Giorgetti, E.; Lieberman, A.P. Polyglutamine androgen receptor-mediated neuromuscular disease. *Cell Mol. Life Sci.* **2016**, *73*, 3991–3999. [CrossRef] [PubMed]
69. Grunseich, C.; Miller, R.; Swan, T.; Glass, D.J.; El Mouelhi, M.; Fornaro, M.; Petricoul, O.; Vostiar, I.; Roubenoff, R.; Meriggioli, M.N.; et al. Safety, tolerability, and preliminary efficacy of an IGF-1 mimetic in patients with spinal and bulbar muscular atrophy: A randomised, placebo-controlled trial. *Lancet Neurol.* **2018**, *17*, 1043–1052. [CrossRef]
70. Hashizume, A.; Katsuno, M.; Suzuki, K.; Banno, H.; Takeuchi, Y.; Kawashima, M.; Suga, N.; Mano, T.; Araki, A.; Hijikata, Y.; et al. Efficacy and safety of leuprorelin acetate for subjects with spinal and bulbar muscular atrophy: Pooled analyses of two randomized-controlled trials. *J. Neurol.* **2019**, *266*, 1211–1221. [CrossRef] [PubMed]

71. Passini, M.A.; Bu, J.; Roskelley, E.M.; Richards, A.M.; Sardi, S.P.; O'Riordan, C.R.; Klinger, K.W.; Shihabuddin, L.S.; Cheng, S.H. CNS-targeted gene therapy improves survival and motor function in a mouse model of spinal muscular atrophy. *J. Clin. Investig.* **2010**, *120*, 1253–1264. [CrossRef] [PubMed]
72. Tinelli, E.; Pereira, J.A.; Suter, U. Muscle-specific function of the centronuclear myopathy and Charcot-Marie-Tooth neuropathy-associated dynamin 2 is required for proper lipid metabolism, mitochondria, muscle fibers, neuromuscular junctions and peripheral nerves. *Hum. Mol. Genet.* **2013**, *22*, 4417–4429. [CrossRef]
73. Patel, P.I.; Roa, B.B.; Welcher, A.A.; Schoener-Scott, R.; Trask, B.J.; Pentao, L.; Snipes, G.J.; Garcia, C.A.; Francke, U.; Shooter, E.M.; et al. The gene for the peripheral myelin protein PMP–22 is a candidate for Charcot–Marie–Tooth disease type 1A. *Nat. Genet.* **1992**, *1*, 159–165. [CrossRef]
74. Züchner, S.; Mersiyanova, I.V.; Muglia, M.; Bissar-Tadmouri, N.; Rochelle, J.; Dadali, E.L.; Zappia, M.; Nelis, E.; Patitucci, A.; Senderek, J.; et al. Mutations in the mitochondrial GTPase mitofusin 2 cause Charcot-Marie-Tooth neuropathy type 2A. *Nat. Genet.* **2004**, *36*, 449–451. [CrossRef]
75. Pezeshkpour, G.; Krarup, C.; Buchthal, F.; DiMauro, S.; Bresolin, N.; McBurney, J. Peripheral neuropathy in mitochondrial disease. *J. Neurol. Sci.* **1987**, *77*, 285–304. [CrossRef]
76. Bomont, P.; Cavalier, L.; Blondeau, F.; Hamida, C.B.; Belal, S.; Tazir, M.; Demir, E.; Topaloglu, H.; Korinthenberg, R.; Tüysüz, B.; et al. The gene encoding gigaxonin, a new member of the cytoskeletal BTB/kelch repeat family, is mutated in giant axonal neuropathy. *Nat. Lett.* **2000**, *26*, 370–374. [CrossRef]
77. Milone, M.; Wong, L.-J. Diagnosis of mitochondrial myopathies. *Mol. Genet. Metab.* **2013**, *110*, 35–41. [CrossRef]
78. Khan, N.A.; Auranen, M.; Paetau, I.; Pirinen, E.; Euro, L.; Forsström, S.; Pasila, L.; Velagapudi, V.; Carroll, C.J.; Auwerx, J.; et al. Effective treatment of mitochondrial myopathy by nicotinamide riboside, a vitamin B3. *EMBO Mol. Med.* **2014**, *6*, 721–731. [CrossRef] [PubMed]
79. Vincent, A.E.; Ng, Y.S.; White, K.; Davey, T.; Mannella, C.; Falkous, G.; Feeney, C.; Schaefer, A.M.; Mcfarland, R.; Gorman, G.S.; et al. The Spectrum of Mitochondrial Ultrastructural Defects in Mitochondrial Myopathy. *Sci. Rep.* **2016**, *6*, 30610. [CrossRef]
80. Cook, A.; Giunti, P. Friedreich's ataxia: Clinical features, pathogenesis and management. *Br. Med. Bull.* **2017**, *124*, 19–30. [CrossRef]
81. Alfedi, G.; Luffarelli, R.; Condò, I.; Pedini, G.; Mannucci, L.; Massaro, D.S.; Benini, M.; Toschi, N.; Alaimo, G.; Panarello, L.; et al. Drug repositioning screening identifies etravirine as a potential therapeutic for friedreich's ataxia. *Mov. Disord.* **2019**, *34*, 323–334. [CrossRef] [PubMed]
82. Strickland, M.; Yacoubi-Loueslati, B.; Bouhaouala-Zahar, B.; Pender, S.L.F.; Larbi, A. Relationships between ion channels, mitochondrial functions and inflammation in human aging. *Front. Physiol.* **2019**, *10*, 158. [CrossRef] [PubMed]
83. Jurkat-Rott, K.; Lehmann-Horn, F. State of the art in hereditary muscle channelopathies. *Acta Myol.* **2010**, *29*, 343–350.
84. Pi, Y.; Goldenthal, M.J.; Marín-García, J.; Pi, Y.; Goldenthal, M.J.; Marín-García, J. Mitochondrial channelopathies in aging. *J. Mol. Med.* **2007**, *85*, 937–951. [CrossRef]
85. Vicart, S.; Sternberg, D.; Fontaine, B.; Meola, G. Human skeletal muscle sodium channelopathies. *Neurol. Sci.* **2005**, *26*, 194–202. [CrossRef]
86. Rudolf, R.; Khan, M.M.; Witzemann, V. Motor Endplate—Anatomical, Functional, and Molecular Concepts in the Historical Perspective. *Cells* **2019**, *8*, 387. [CrossRef]
87. Calderón, J.C.; Bolaños, P.; Caputo, C. The excitation-contraction coupling mechanism in skeletal muscle. *Biophys. Rev.* **2014**, *6*, 133–160. [CrossRef]
88. Bach-y-Rita, P.; Ito, F. In vivo studies on fast and slow muscle fibers in cat extraocular muscles. *J. Gen. Physiol.* **1966**, *49*, 1177–1198. [CrossRef] [PubMed]
89. López-Armada, M.J.; Riveiro-Naveira, R.R.; Vaamonde-García, C.; Valcárcel-Ares, M.N. Mitochondrial dysfunction and the inflammatory response. *Mitochondrion* **2013**. [CrossRef] [PubMed]
90. Koenig, M.; Hoffman, E.P.; Bertelson, C.J.; Monaco, A.F.; Feener, C.; Kunkel'tt, L.M. Complete Cloning of the Duchenne Muscular Dystrophy (DMD) cDNA and Preliminary Genomic Organization of the DMD Gene in Normal and Affected Individuals. *Cell* **1987**, *50*, 509–517. [CrossRef]
91. Siekevitz, P. Powerhouse of the Cell. *Nature* **1957**, *197*, 131–144. [CrossRef]

92. Kauppila, T.E.S.; Kauppila, J.H.K.; Ran Larsson, N.-G. Cell Metabolism Review Mammalian Mitochondria and Aging: An Update. *Cell Metab.* **2017**, *25*, 57–71. [CrossRef]
93. Palikaras, K.; Tavernarakis, N. Mitochondrial homeostasis: The interplay between mitophagy and mitochondrial biogenesis. *Exp. Gerontol.* **2014**, *56*, 182–188. [CrossRef]
94. Piantadosi, C.A.; Suliman, H.B. Transcriptional control of mitochondrial biogenesis and its interface with inflammatory processes. *Biochim. Biophys. Acta* **2012**, *1820*, 532–541. [CrossRef]
95. Kepp, O.; Galluzzi, L.; Kroemer, G. Mitochondrial control of the NLRP3 inflammasome. *Nat. Immunol.* **2011**, *12*. [CrossRef]
96. Lazarou, M.; Sliter, D.A.; Kane, L.A.; Sarraf, S.A.; Wang, C.; Burman, J.L.; Sideris, D.P.; Fogel, A.I.; Youle, R.J. The ubiquitin kinase PINK1 recruits autophagy receptors to induce mitophagy. *Nature* **2015**, *524*, 309–314. [CrossRef]
97. Vance, J.E. MAM (mitochondria-associated membranes) in mammalian cells: Lipids and beyond. *Biochim. Biophys. Acta Mol. Cell Biol. Lipids* **2014**, *1841*, 595–609. [CrossRef]
98. Manevski, M.; Muthumalage, T.; Devadoss, D.; Sundar, I.K.; Wang, Q.; Singh, K.P.; Unwalla, H.J.; Chand, H.S.; Rahman, I. Cellular stress responses and dysfunctional Mitochondrial–cellular senescence, and therapeutics in chronic respiratory diseases. *Redox Biol.* **2020**, *33*, 101443. [CrossRef]
99. Saitoh, T.; Fujita, N.; Jang, H.; Uematsu, S.; Yang, B.-G.; Satoh, T.; Omori, H.; Noda, T.; Yamamoto, N.; Komatsu, M.; et al. Loss of the autophagy protein Atg16L1 enhances endotoxin-induced IL-1b production. *Nat. Lett.* **2008**, *456*. [CrossRef]
100. Zhong, Z.; Umemura, A.; Sanchez-Lopez, E.; Liang, S.; Shalapour, S.; Wong, J.; He, F.; Boassa, D.; Perkins, G.; Ali, S.R.; et al. NF-κB Restricts Inflammasome Activation via Elimination of Damaged Mitochondria. *Cell* **2016**, *164*, 896–910. [CrossRef] [PubMed]
101. Rodríguez-Nuevo, A.; Díaz-Ramos, A.; Noguera, E.; Díaz-Sáez, F.; Duran, X.; Muñoz, J.P.; Romero, M.; Plana, N.; Sebastián, D.; Tezze, C.; et al. Mitochondrial DNA and TLR9 drive muscle inflammation upon Opa1 deficiency. *EMBO J.* **2018**, *37*. [CrossRef] [PubMed]
102. Couvillion, M.T.; Soto, I.C.; Shipkovenska, G.; Stirling, L. Synchronized mitochondrial and cytosolic translation programs. *Nature* **2016**, *533*, 499–503. [CrossRef] [PubMed]
103. Tokuyama, T.; Hirai, A.; Shiiba, I.; Ito, N.; Matsuno, K.; Takeda, K.; Saito, K.; Mii, K.; Matsushita, N.; Fukuda, T.; et al. Mitochondrial Dynamics Regulation in Skin Fibroblasts from Mitochondrial Disease Patients. *Biomolecules* **2020**, *10*, 450. [CrossRef] [PubMed]
104. Stewart, J.B.; Chinnery, P.F. The dynamics of mitochondrial DNA heteroplasmy: Implications for human health and disease. *Nat. Rev. Genet.* **2015**, *16*, 530–542. [CrossRef]
105. Picca, A.; Lezza, A.M.S.; Leeuwenburgh, C.; Pesce, V.; Calvani, R.; Landi, F.; Bernabei, R.; Marzetti, E. Fueling inflamm-aging through mitochondrial dysfunction: Mechanisms and molecular targets. *Int. J. Mol. Sci.* **2017**, *18*. [CrossRef]
106. Frank, M.; Duvezin-Caubet, S.; Koob, S.; Occhipinti, A.; Jagasia, R.; Petcherski, A.; Ruonala, M.O.; Priault, M.; Salin, B.; Reichert, A.S. Mitophagy is triggered by mild oxidative stress in a mitochondrial fission dependent manner. *Biochim. Biophys. Acta Mol. Cell Res.* **2012**, *1823*, 2297–2310. [CrossRef]
107. Babbar, M.; Basu, S.; Yang, B.; Croteau, D.L.; Bohr, V.A. Mitophagy and DNA damage signaling in human aging. *Mech. Ageing Dev.* **2020**, *186*. [CrossRef]
108. Bhatt, P.S.; Tzoulis, C.; Balafkan, N.; Miletic, H.; Tran, G.T.T.; Sanaker, P.S.; Bindoff, L.A. Mitochondrial DNA depletion in sporadic inclusion body myositis. *Neuromuscul. Disord.* **2019**, *29*, 242–246. [CrossRef] [PubMed]
109. De Duve, C.; Pressman, B.C.; Gianetto, R.; Wattiaux, R.; Appelmans, F. Tissue fractionation studies. *Biochem. J.* **1955**, *60*, 604–617. [CrossRef] [PubMed]
110. Koopman, W.J.H.; Willems, P.H.G.M.; Smeitink, J.A.M. Monogenic Mitochondrial Diseases. *N. Engl. J. Med.* **2012**, *366*, 1132–1141. [CrossRef] [PubMed]
111. Keogh, M.J.; Chinnery, P.F. Mitochondrial DNA mutations in neurodegeneration. *Biochim. Biophys. Acta Bioenerg.* **2015**, *1847*, 1401–1411. [CrossRef] [PubMed]
112. Lightowlers, R.N.; Taylor, R.W.; Turnbull, D.M. Mutations causing mitochondrial disease: What is new and what challenges remain? *Science* **2015**, *349*, 1494–1499. [CrossRef]
113. Argov, Z.; Renshaw, P.F.; Boden, B.; Winokur, A.; Bank, W.J. Effects of thyroid hormones on skeletal muscle bioenergetics. In vivo phosphorus-31 magnetic resonance spectroscopy study of humans and rats. *J. Clin. Investig.* **1988**, *81*, 1695–1701. [CrossRef] [PubMed]

114. Monzani, F.; Caraccio, N.; Siciliano, G.; Manca, L.; Murri, L.; Ferrannini, E. Clinical and Biochemical Features of Muscle Dysfunction in Subclinical Hypothyroidism. *J. Clin. Endocrinol. Metab.* **1997**, *82*, 3315–3318. [CrossRef]
115. Deng, J.; Wang, P.; Chen, X.; Cheng, H.; Liu, J.; Fushimi, K.; Zhu, L.; Wu, J.Y. FUS interacts with ATP synthase beta subunit and induces mitochondrial unfolded protein response in cellular and animal models. *Proc. Natl. Acad. Sci. USA* **2018**, *115*, E9678–E9686. [CrossRef]
116. Spiegel, R.; Saada, A.; Flannery, P.J.; Burté, F.; Soiferman, D.; Khayat, M.; Eisner, V.; Vladovski, E.; Taylor, R.W.; Bindoff, L.A.; et al. Fatal infantile mitochondrial encephalomyopathy, hypertrophic cardiomyopathy and optic atrophy associated with a homozygous OPA1 mutation. *J. Med. Genet.* **2016**, *53*, 127–131. [CrossRef]
117. Mishra, P.; Carelli, V.; Manfredi, G.; Chan, D.C. Proteolytic cleavage of Opa1 stimulates mitochondrial inner membrane fusion and couples fusion to oxidative phosphorylation. *Cell Metab.* **2014**, *19*, 630–641. [CrossRef]
118. Waterham, H.R.; Koster, J.; van Roermund, C.W.T.; Mooyer, P.A.W.; Wanders, R.J.A.; Leonard, J.V. A Lethal Defect of Mitochondrial and Peroxisomal Fission. *N. Engl. J. Med.* **2007**, *356*, 1736–1741. [CrossRef] [PubMed]
119. Kodavati, M.; Wang, H.; Hegde, M.L. Altered Mitochondrial Dynamics in Motor Neuron Disease: An Emerging Perspective. *Cells* **2020**, *9*, 1065. [CrossRef] [PubMed]
120. Clark, S. Newborn mice studied with the electron mircroscope. *Biophys. Biochem. Cytol.* **1957**, *3*, 349–362. [CrossRef] [PubMed]
121. Ohsumi, Y. Historical landmarks of autophagy research. *Cell Res.* **2014**, *24*, 9–23. [CrossRef] [PubMed]
122. Eiyama, A.; Okamoto, K. PINK1/Parkin-mediated mitophagy in mammalian cells. *Curr. Opin. Cell Biol.* **2015**, *33*, 95–101. [CrossRef] [PubMed]
123. Seabright, A.P.; Fine, N.H.F.; Barlow, J.P.; Lord, S.O.; Musa, I.; Gray, A.; Bryant, J.A.; Banzhaf, M.; Lavery, G.G.; Hardie, D.G.; et al. AMPK activation induces mitophagy and promotes mitochondrial fission while activating TBK1 in a PINK1-Parkin independent manner. *FASEB J.* **2020**, *34*, 6284–6301. [CrossRef] [PubMed]
124. García-Prat, L.; Martínez-Vicente, M.; Perdiguero, E.; Ortet, L.; Rodríguez-Ubreva, J.; Rebollo, E.; Ruiz-Bonilla, V.; Gutarra, S.; Ballestar, E.; Serrano, A.L.; et al. Autophagy maintains stemness by preventing senescence. *Nature* **2016**, *529*, 37–42. [CrossRef]
125. Lemasters, J.J. Selective mitochondrial autophagy, or mitophagy, as a targeted defense against oxidative stress, mitochondrial dysfunction, and aging. *Rejuvenation Res.* **2005**, *8*, 3–5. [CrossRef]
126. Youle, R.J.; Narendra, D.P. Mechanisms of mitophagy. *Nat. Rev. Mol. Cell Biol.* **2011**, *12*, 9–14. [CrossRef]
127. Sun, N.; Yun, J.; Liu, J.; Malide, D.; Liu, C.; Rovira, I.I.; Holmström, K.M.; Fergusson, M.M.; Yoo, Y.H.; Combs, C.A.; et al. Measuring In Vivo Mitophagy. *Mol. Cell* **2015**, *60*, 685–696. [CrossRef]
128. Zhang, Q.; Raoof, M.; Chen, Y.; Sumi, Y.; Sursal, T.; Junger, W.; Brohi, K.; Itagaki, K.; Hauser, C.J. Circulating mitochondrial DAMPs cause inflammatory responses to injury. *Nat. Lett.* **2010**, *464*, 104–107. [CrossRef] [PubMed]
129. Zhang, W.; Hu, X.; Shen, Q.; Xing, D. Mitochondria-specific drug release and reactive oxygen species burst induced by polyprodrug nanoreactors can enhance chemotherapy. *Nat. Commun.* **2019**, *10*, 1–14.
130. Lerner, C.A.; Sundar, I.K.; Rahman, I. Mitochondrial redox system, dynamics, and dysfunction in lung inflammaging and COPD. *Int. J. Biochem. Cell Biol.* **2016**, *81*, 294–306. [CrossRef] [PubMed]
131. Domènech, B.E.; Marfany, G. The Relevance of Oxidative Stress in the Pathogenesis and Therapy of Retinal Dystrophies. *Antioxidants* **2020**, *9*, 347. [CrossRef] [PubMed]
132. Peterman, E.M.; Sullivan, C.; Goody, M.F.; Rodriguez-Nunez, I.; Yoder, J.A.; Kim, C.H. Neutralization of mitochondrial superoxide by superoxide dismutase 2 promotes bacterial clearance and regulates phagocyte numbers in zebrafish. *Infect. Immun.* **2015**, *83*, 430–440. [CrossRef] [PubMed]
133. Andersen, P.M.; Nilsson, P.; Forsgren, L.; Marklund, S.L. CuZn-Superoxide Dismutase, Extracellular Superoxide Dismutase, and Glutathione Peroxidase in Blood from Individuals Homozygous for Asp90Ala CuZn-Superoxide Dismutase Mutation. *J. Neurochem.* **2002**, *70*, 715–720. [CrossRef] [PubMed]
134. Sano, R.; Reed, J.C. ER stress-induced cell death mechanisms. *Biochim. Biophys. Acta Mol. Cell Res.* **2013**, *1833*, 3460–3470. [CrossRef] [PubMed]
135. Smith, E.F.; Shaw, P.J.; De Vos, K.J. The role of mitochondria in amyotrophic lateral sclerosis. *Neurosci. Lett.* **2019**, *710*, 132933. [CrossRef] [PubMed]
136. Naon, D.; Scorrano, L. At the right distance: ER-mitochondria juxtaposition in cell life and death. *Biochim. Biophys. Acta Mol. Cell Res.* **2014**, *1843*, 2184–2194. [CrossRef]

137. Nadalutti, C.A.; Stefanick, D.F.; Zhao, M.-L.; Horton, J.K.; Prasad, R.; Brooks, A.M.; Griffith, J.D.; Wilson, S.H. Mitochondrial dysfunction and DNA damage accompany enhanced levels of formaldehyde in cultured primary human fibroblasts. *Sci. Rep.* **2020**, *10*, 5575. [CrossRef]
138. Nakahira, K.; Haspel, J.A.; Rathinam, V.A.K.; Lee, S.-J.; Dolinay, T.; Lam, H.C.; Englert, J.A.; Rabinovitch, M.; Cernadas, M.; Pyo Kim, H.; et al. Autophagy proteins regulate innate immune responses by inhibiting the release of mitochondrial DNA mediated by the NALP3 inflammasome. *Nat. Immunol.* **2011**, *8*, 222–230. [CrossRef] [PubMed]
139. Pérez-Treviño, P.; Velásquez, M.; García, N. Mechanisms of mitochondrial DNA escape and its relationship with different metabolic diseases. *BBA Mol. Basis Dis.* **2020**, *1866*, 165761. [CrossRef] [PubMed]
140. Rodríguez-Nuevo, A.; Zorzano, A. The sensing of mitochondrial DAMPs by non-immune cells. *Cell Stress* **2019**, *3*, 195–207. [CrossRef] [PubMed]
141. West, A.P. Mitochondrial dysfunction as a trigger of innate immune responses and inflammation. *Toxicology* **2017**, *391*, 54–63. [CrossRef]
142. Baroja-Mazo, A.; Martín-Sánchez, F.; Gomez, A.I.; Martínez, C.M.; Amores-Iniesta, J.; Compan, V.; Barberà-Cremades, M.; Yagüe, J.; Ruiz-Ortiz, E.; Antón, J. The NLRP3 inflammasome is released as a particulate danger signal that amplifies the inflammatory response. *Nat. Immunol.* **2014**, *15*, 738–748. [CrossRef]
143. Mills, E.L.; Kelly, B.; O'Neill, L.A.J. Mitochondria are the powerhouses of immunity. *Nat. Immunol.* **2017**, *18*, 488–498. [CrossRef]
144. Cappelletti, C.; Salerno, F.; Canioni, E.; Mora, M.; Mantegazza, R.; Bernasconi, P.; Maggi, L. Up-regulation of toll-like receptors 7 and 9 and its potential implications in the pathogenic mechanisms of lmna-related myopathies. *Nucleus* **2018**, *9*, 398–409. [CrossRef]
145. Seth, R.B.; Sun, L.; Ea, C.K.; Chen, Z.J. Identification and characterization of MAVS, a mitochondrial antiviral signaling protein that activates NF-κB and IRF3. *Cell* **2005**, *122*, 669–682. [CrossRef]
146. Park, S.; Juliana, C.; Hong, S.; Datta, P.; Hwang, I.; Fernandes-Alnemri, T.; Yu, J.-W.; Alnemri, E.S. The mitochondrial anti-viral protein MAVS associates with NLRP3 and regulates its inflammasome activity 1. *J. Immunol.* **2013**, *191*, 4358–4366. [CrossRef]
147. Deswaerte, V.; Ruwanpura, S.M.; Jenkins, B.J. Transcriptional regulation of inflammasome-associated pattern recognition receptors, and the relevance to disease pathogenesis. *Mol. Immunol.* **2017**, *86*, 3–9. [CrossRef]
148. Lamkanfi, M.; Dixit, V.M. Mechanisms and functions of inflammasomes. *Cell* **2014**, *157*, 1013–1022. [CrossRef] [PubMed]
149. Kornegay, J.N.; Spurney, C.F.; Nghiem, P.P.; Brinkmeyer-Langford, C.L.; Hoffman, E.P.; Nagaraju, K. Pharmacologic Management of Duchenne Muscular Dystrophy: Target Identification and Preclinical Trials. *ILAR J.* **2014**, *55*, 119–149. [CrossRef] [PubMed]
150. Antosh, M.; Whitaker, R.; Kroll, A.; Hosier, S.; Chang, C.; Bauer, J.; Cooper, L.; Neretti, N.; Helfand, S.L. Comparative transcriptional pathway bioinformatic analysis of dietary restriction, Sir2, p53 and resveratrol life span extension in Drosophila. *Cell Cycle* **2011**, *10*, 904–911. [CrossRef] [PubMed]
151. Interventional Studies Neuromuscular Diseases. Available online: https://clinicaltrials.gov/ct2/results?cond=Neuromuscular+Diseases&term=mitochondria&type=Intr&rslt=&age_v=&gndr=&intr=&titles=&outc=&spons=&lead=&id=&cntry=&state=&city=&dist=&locn=&rsub=&strd_s=&strd_e=&prcd_s=&prcd_e=&sfpd_s=&sfpd_e=&rfpd_s=&rfpd_e=&lu (accessed on 29 May 2020).
152. Liang, J.; Zeng, Z.; Zhang, Y.; Chen, N. Regulatory role of exercise-induced autophagy for sarcopenia. *Exp. Gerontol.* **2020**, *130*, 110789. [CrossRef]
153. Schoch, K.M.; Miller, T.M. Antisense Oligonucleotides: Translation from Mouse Models to Human Neurodegenerative Diseases. *Neuron* **2017**, *94*, 1056–1070. [CrossRef]
154. Levin, A.A. Treating disease at the RNA level with oligonucleotides. *N. Engl. J. Med.* **2019**, *380*, 57–70. [CrossRef]
155. Saraiva, J.; Nobre, R.J.; Pereira De Almeida, L. Gene therapy for the CNS using AAVs: The impact of systemic delivery by AAV9. *J. Control. Release* **2016**, *241*, 94–109. [CrossRef]
156. Mendell, J.R. Single-Dose Gene-Replacement Therapy for SMA. *N. Engl. J. Med.* **2017**, *377*, 1713–1722. [CrossRef]
157. Young, C.S.; Pyle, A.D.; Spencer, M.J. CRISPR for Neuromuscular Disorders: Gene Editing and Beyond. *Physiology* **2019**, *34*, 341–353. [CrossRef]

158. Understanding Neuromuscular Disease Care—IQVIA. Available online: https://www.iqvia.com/insights/the-iqvia-institute/reports/understanding-neuromuscular-disease-care (accessed on 28 May 2020).
159. Patridge, E.V.; Gareiss, P.C.; Kinch, M.S.; Hoyer, D.W. An analysis of original research contributions toward FDA-approved drugs. *Drug Discov. Today* **2015**, *20*, 1182–1187. [CrossRef]
160. S4R Registration Share4Rare. Available online: https://www.share4rare.org/registration/understanding-neuromuscular-diseases (accessed on 19 May 2020).

DISCUSSION

IBM is an idiopathic complex disease, with a late onset, unknown pathophysiology, limited disease models and ineffective treatments. Multiple attempts to unravel its origin, genetic variants contributing to the disease, potential disease models and treatments, have still not reached a consensus about how to deal with IBM.

The purpose to perform this project was based on the lack of models in IBM that aid in understanding its pathophysiology, identify potential biomarkers and assay new therapeutical options. In our attempt to be as close as possible to the patient clinical state, we decided to develop cell models based on IBM patients' samples.

This thesis presented four manuscripts about the use of cell models in IBM, including the validation of fibroblasts and myotubes derived from iPSC as disease models for IBM, the use of fibroblasts for analyzing IBM potential comorbidities and their application to multi-omics analysis to identify potential biomarkers and molecular targets.

The first work, using IBM-derived cell fibroblasts, was inspired by the use of fibroblasts in neurodegenerative and mitochondrial diseases. As IBM has degenerative and mitochondrial defects, we tested if these, along with inflammatory alterations, were recapitulated in IBM fibroblasts. Indeed, we confirmed the hypothesis, with IBM fibroblasts revealing inflammatory, degenerative and mitochondrial alterations at transcriptomic and functional level. Specifically, the mRNA seq profile of IBM vs. CTL fibroblasts displayed 778 differentially expressed genes (DEGs) ($|log2FC| \geq 1.5$ and p-value adj < 0.05) associated with inflammation, mitochondria, cell cycle regulation and metabolism gene clusters. In addition, there was a higher cytokine secretion in IBM fibroblasts, and reduced autophagic activity, by a lower expression of

autophagy protein mediators and lower formation of autophagosomes. In mitochondria, the mtDNA genetic content was decreased, together with reduced mitochondrial respiration, COX/CS activity, mitochondrial membrane potential and mitochondrial elongation. By contrast, oxidative stress, antioxidant capacity and organic acids concentration were increased. Moreover, we tried to stratify the IBM cohort in two subgroups, according to their progression or stabilization of the disease. As mentioned before, IBM is a progressive degenerative disease that can evolve through decades and have periods of stability for 4-12 years (11). In our findings, oxidative stress and inflammation were correlated to IBM prognosis, arising as potential markers of disease evolution. These findings could be exported to other muscular diseases, as fibroblasts are a cost-effective model and are being used in multiple biomedical research settings worldwide.

The limitations of this study were the small sample size, as IBM is a rare disease and it is challenging to collect big cohorts of patients for further studies, even for a specialized muscle unit like ours. In addition, the inflammatory response was weaker in fibroblasts, due to these cells not being immune cells.

Alongside fibroblasts, we aimed to develop a cell model closer (in physiology) to the target tissue of IBM, to muscle. This model was based on myotubes derived from iPSC, in an attempt to obtain muscle cells from a non-invasive source (fibroblasts or blood instead of muscle) and characterizing them as a potential disease model. For this, we evaluated the transcriptomic and functional profile, by assessing the inflammatory, degenerative and mitochondrial hallmarks from IBM. The DEGs from the transcriptome were related to myopathic and muscle contraction features in IBM myotubes, recapitulating some of the clinical observation in the muscle. At molecular level, inflammatory cytokine levels between IBM and CTL were similar, revealing an absence of immune response related to IBM, potentially due to a lack of inflammatory crosstalk between differentiated myotubes and immune cells. Autophagy displayed a reduced activity, with a lower concentration of autophagy protein mediators. In mitochondria, an increased anaerobic respiration by significant lactate production and lower COX/CS activity suggested a trends towards mitochondrial dysfunction, but the mitochondrial respiratory profile and antioxidant capacity did not display changes. Briefly, myotubes suggest a trend towards myopathic,

autophagic and mitochondrial changes in IBM. However, inflammation was absent, and the lack of more pronounced alterations could be due to reprogramming, lack of inflammatory crosstalk in myotube vs. immune cells or shortage of time in culture to develop alterations. To address these limitations, we suggest that a co-culture with iPSC-differentiated myotubes and IBM-derived lymphocytes could activate the myotubes and display an inflammatory response. We should examine if the inflammation reduces after the stimulus is removed or if the myotubes keep an inflammatory fingerprint that resembles the IBM muscle inflammatory hallmarks. Nevertheless, we also need to recapitulate the late onset age of IBM, associated with aging. Thus, for this reason, we suggest that myotubes may require contact with ageing factors (chemical, environmental or genetic stressors) to reveal an aged IBM phenotype.

Coming back to the fibroblast model, we decided to look for comorbidities in IBM, in this case with AD and Type 2 Diabetes Mellitus diseases (T2DM). In former studies in IBM, the presence of rimmed vacuoles containing TDP-43, b-amyloid, p62, p-Tau, etc. in the cytoplasm of muscle fibers resembled the b-amyloid plaques in the brain of AD patients. Thus, IBM was formerly called "the Alzheimer in muscle", although this terminology has been already dismissed and no association between IBM patients and a higher prevalence towards AD was found. The association with T2DM could be linked to the patients' lifestyle. Restricted mobility could be associated with the reported misbalanced glucose homeostasis at clinical level, suggesting prediabetes conditions in IBM patients, also observed in other IIMs. This altered glucose metabolism was confirmed at molecular level, as when glucose conditions were changed, fibroblasts were unable to adapt and displayed a reduced mitochondrial respiration and increased anaerobic respiration in IBM, coupled with lower COX/citrate synthase (CS) activity and higher oxidative stress levels. In the three diseases, IBM, AD and T2DM, the mitochondrial dysfunction is present, suggesting mitochondria could be an effective therapeutical target.

The constraints of this study were, again, the limited sample size due to IBM being a rare disease. Moreover, it could be interesting to deep into the glucose metabolism pathways to understand their dysregulation in IBM and check if they share some traits with T2DM. These pathways may be also analyzed in other IIM

like PM to determine if it is a distinctive trait of IBM or shared among the IIM group.

Following with the mitochondrial contribution in IBM, the metabolite findings in the IBM fibroblast model, drive us to search for altered molecules in other fluid samples, such as urine, saliva and plasma samples. Indeed, we found an altered organic acid profile in IBM fibroblasts and urine, highlighting L-pyroglutamic and orotic acids. These associations lead us to pointing the glutathione and orotic acid-related pyrimidine metabolism, specially orotidine, as potential metabolic targets in IBM. These findings firmly support the mitochondrial contribution to IBM. In addition, we found a correlation between the metabolic profile of IBM patients and the metabolic genes with a differential gene expression in the muscle of IBM patients, with L2HGDH, IDH2, OPLAH and ASL genes as potential upstream gene regulators in muscle. In subsequent studies, the analysis of the metabolic state of patients along their disease progression, could aid in understanding disease evolution and metabolic fingerprints might contribute in this, considering IBM is a progressive degenerative disease. The evaluation of IBM progression may aid in the stratification of patients according to their disease progression rate, or in the response to treatment efficacy.

For the previous studies, we performed multiple experimental set-ups, intertwining clinical data from the IBM cohort, with functional and omics analysis. This combination allows to compare the results of a holistic vs. target approach, at omics vs. experimental level. However, the restricted number of patients in our cohort, due to IBM being a rare disease, requires the validation of our findings in bigger cohorts. Moreover, we must point out the technical complexity of setting new cell models, specially iPSCs, as they required cell reprogramming, characterization and differentiation before starting the experiments to obtain results from the model. Additionally, iPSCs need to be approved by several ethical committees, at institutional, regional and national levels before the study, but also, once they are obtained, to be deposited in a national biobank. These processes add complexity in the set-up and performance of the studies.

Aside from the technical and biological complexity of the cell models for IBM herein explained, here we remarked the limitations of disease models alongside

their potential to be useful. From a more theoretical point of view, disease models for preclinical studies are required for understanding disease pathophysiology and to identify potential biomarkers, molecular contributors to the disease and new treatments.

There are several aspects to determine how useful a model could or should be: the first one is face validity, based on characterizing the disease hallmarks in the models and determining if the model displays the pathogenic features of a specific disease (122). This was our focus in the cell models of IBM, to characterize the IBM inflammatory, degenerative and mitochondrial changes in multiple IBM samples. The second one is construct validity, focused on the onset of pathogenic features in the disease model appearing for the same reasons than in the patients (122). The third one, key in translational research, is the predictive validity, meaning that the observations in the model should predict the outcomes in patients (122). This is key in testing potential treatments in preclinical and clinical trials, but also, in understanding the pathophysiological responses, to determine if the same effect is happening in the model and the patients. The predictive validity should cover diverse genetic backgrounds, especially in complex diseases, as several risk loci can display a similar clinical phenotype but same or distinct treatment response (122). We must be receptive to models not entirely recapitulating the human physiology but still being useful for specific disease conditions and aims.

Appropriate preclinical models are required to generate accurate and predictive data. Thus, they should be clinically relevant for all the disease progression, reliable in the model predictions, highly validated and their bias should be previously identified (123). Moreover, there is a need to report negative results in the scientific community and also, to regulate all of the above issues. However, in the case of new treatments from animal to human testing, the failures remain at 90% of the cases for decades (124). In many cases, this is due to unpredicted toxicity, such as cases in which safety issues in animal tests were irrelevant but appeared in human trials, or scarce efficacy (124).

In recent years, several alternatives have appeared to reduce animal testing. The European Union Reference Laboratory for alternatives to animal testing (EURL ECVAM), part of the Joint Research Centre of the European Union, advocates for

the use of non-animal models like cells, organoids, organ-on-a-chip or *in silico* models (125). They published several guidelines that promote the three Rs in animal testing: Replacement, Reduction and Refinement of animal use in basic, applied, translation research and for regulatory purposes (125). Reducing animal use would also decrease study time and costs.

For instance, in the case of AD and PD, both neurodegenerative diseases, they reported the use of non-animal models according to publications between 2013 and 2018 (126). Thus, tissues or fluids derived from patients accounted for 28% of models in AD and 15% in PD (126). Primary or stem cells represented a 11% in AD and 38% in PD, while human-derived cell lines a 9 vs. 11% in AD and PD, respectively. Biochemical (cell-free) assays accounted for 18% in AD and 12% in PD (126). More complex models like co-cultures, organoids, or organ on a chip represented a 4%, 0% and 11% in AD, and 2% in the three cases for PD. *In silico* models constituted a 19% in AD and 18% in PD, respectively (126). All these percentages depicted the progressive introduction of non-animal disease models in research, clinical and regulatory settings.

Coming back to the limited sample size in IBM, IIM and other rare diseases, it impairs the collection of samples for assembling bigger cohorts, needed to obtain robust results. To overcome this, we need the myositis community to collaborate more to share their clinical, molecular and omics data in favor of the scientific community and the patients, for better understanding of the pathophysiology of these diseases, for recruiting patients for clinical trials, and eventually delivering effective treatments to these patients.

Currently, *The International IBM Consortium Genetic Study (IIBMCGS),* led by the University College London (UCL) Institute of Neurology, recruited 750 blood IBM samples for a GWAS to search for genetic variants contributing to IBM and understand the disease pathways in this disease to be able to accelerate treatment options. This study is active till 2027 (127,128). Another consortium, the Myositis Genetic Consortium (MYOGEN), recently published the identification of novel associations in IIMs using genome-wide imputation through a ImmunoChip array (36). They included 2,565 IIM patient samples, from which 252 were IBM samples, and 10,260 ethnically matched control samples (Caucasian ethnicity). They found 3 genetic associations in IIM, in STAT4, SDK2, and LINC00924 genes

(36). In IBM, they identified CCR5, already associated with rheumatic disease (36). These large cohort studies, considering the rarity of IIM and specifically IBM, expand the understanding of the genetic basis in these diseases.

In the search for treatments, the field has revolutionized in recent years with the application of omics profiling of patients. As mentioned before, understanding the genetic or molecular profile of a patient, alongside their clinical history, allows a more precise diagnosis, prognosis and treatment selection for patients, instead of only taking decisions according to their clinical phenotype.

Multiple research consortiums at international levels, have been pioneered in sharing, financing and discussing the latest results in massive data volumes in genomics, cancer, or rare diseases, among others (129). Consortiums such as the Global Alliance for Genomics and Health (GA4GH, www.ga4gh.org) (130), research infrastructures like ELIXIR (131) and Big Data to Knowledge (BD2K) (132), and international initiatives such as the International Cancer Genome Consortium (ICGC), the International Human Epigenome Consortium (IHEC), and the International Rare Disease Consortium (IRDiRC), are an example of these consortiums (129). In the case of GA4GH, they are focused on building technical standards and policy frameworks to secure the use of genomic and other clinical data to apply genomic into clinical practice to predict treatment responses or find patients with the same condition worldwide (130). In rare diseases, IRDiRC is centered in delivering accurate diagnosis, treatments and care to rare disease patients within one year from the disease symptoms onset. IRDiRC committees are focused on tackling gaps and key points in rare diseases by producing guidelines and other resources (133). In order to integrate and reuse scholarly data, multiple stakeholders from academia, industry, funding agencies and publishers established the “The FAIR Guiding Principles for scientific data management and stewardship” (134). FAIR principles stand for findable, accessible, interoperable and reusable data management, to enable open science, reproducibility and faster breakthroughs. The abovementioned consortiums adhered to FAIR principles (134).

It is essential to appreciate the coordinated effort of clinicians, basic and computational researchers, ethical committees, funding and regulatory agencies to maintain international platforms for sharing and interpretating biomedical

data to improve the understanding of multiple diseases and provide a better care for their patients. Moreover, integrating biomedical, clinical and computational level is challenging. An initiative in charge of this is called the Disease Maps Project, which aims to represent disease mechanisms for several diseases (135,136). They integrate signaling pathways, metabolic and gene regulatory networks. Clinicians and basic researchers ensure that all the disease contributors and knowledge are represented appropriately (135,136).

In translational medicine, disease maps are used to interpret omics data (e.g. pathway analysis) and to generate new hypothesis, for predictive analysis (e.g. causal gene variants in a disease) and for clinical support data. There are disease maps available for specific diseases like COVID-19, PD, Asthma, Rheumatoid Arthritis, Cancer, Sarcopenia, hearth failure, atherosclerosis and Sjögren's syndrome, among others (135,136). A disease map for IBM or other IIMs would be valuable.

Indeed, Sjögren syndrome displays an associated comorbidity with IBM (5,30) together with IBM related features like anti-cN-1A antibodies, HLA-DR3 haplotype (predisposes to autoimmune diseases), and an association to T cell large granular lymphocytic leukeamia (30). Hepatitis C virus, displaying immune senescence and T cell exhaustion, also shares traits with IBM(14). Also, some myopathies manifest IBM-like features like pathomorphology (similar histopathological patterns) (in Granulomatous and HIV-associated myositis), immune senescence and T cell exhaustion also in HIV-associated myositis; and mitochondrial damage in NRTI-associated myopathy (14,30). Understanding these interactions among immune pathologies could shed light into the pathogenesis of IBM (30).

However, there is still a knowledge gap to understand the effect of multiple genetic and molecular alterations in the phenotype, complicating the application of molecular studies straightforward to the clinical assistance. Indeed, this is one of the bottlenecks of the bench-to-bed translation in translational research. We expect this gap will narrow in upcoming years with the contribution of the recent scientific developments.

A current project that tackles these gaps is called Treatabolome (137), in charge of determining treatments for untreated rare diseases according to their genetic variants. The aim is to develop a database able to seek for available treatments to be applied to rare diseases, to find gene and variant specific treatments and to reduce the patient's treatment obstacles.

Aligned with this approach, drug repurposing, with the aid of artificial intelligence (AI), is emerging as a new tool to find potential drug candidates for untreated rare diseases. To identify a candidate for drug repurposing, it is required to determine a molecular signature associated with disease severity. With this target, the search for an overlap in previously approved drugs (by FDA or EMA) begins. If drug candidates are found within the approved drugs, some of them are prioritized and tested *in vitro* (e.g. in iPSC-derived myotubes) or *in vivo* (e.g. in animal models). Drug repurposing has advanced hugely with the integration of data allowed by AI models.

Alongside high throughput approaches seeking for new treatments, patients' associations and a significant number of clinicians advocate for implementing quality of life (QoL) assessments in the natural history of IBM patients, in clinical trials, or observational studies, to introduce the patients' view and understand what matters most for them (5). IBM and other IIMs affect the QoL of patients and could lead to long-term disability. However, it is challenging to standardize a protocol to measure QoL. Moreover, as some IIM manifest also outside muscle (e.g. skin rash in DM), indicators of systemic alterations could be beneficial but quite unknown and not yet validated (5).

A therapeutic program directly related to improving the QoL of IIM patients could be the prescription of physical therapy. New findings provide evidence that exercise is both safe and beneficial for adults with IIM, as it has been shown to enhance muscle function and QoL in individuals with IIM (5). Exercise programs designed to enhance strength and function activate specific molecular pathways that regulate aerobic capacity, promote capillary growth, and facilitate muscle remodeling, while alleviating the inflammatory response within the muscles (5). Consequently, it is advisable to include exercise, under the guidance of physical therapists, as an early intervention for IIM patients, with gradual progression tailored to each individual's response. The majority of patients tolerate exercise

well, experiencing no adverse effects (5). Considering the favorable outcomes, physical exercise should be regarded as a standard treatment for IIMs.

In summary, with this thesis we provided an insight into IBM molecular mechanisms with the aid of cellular models derived from IBM patients. The development of fibroblasts and iPSC-differentiated myotubes models for IBM have allowed the characterization of muscle histopathology findings, which are inflammation, degeneration and mitochondrial changes, outside the muscle tissue but keeping the patients' genetic background. Alternative models, such as mice models, cannot replicate the patients' genetic background to that extent. Moreover, we assessed if our cohort of IBM fibroblasts displayed comorbidities with other prevalent diseases like AD or T2DM diseases, all sharing mitochondrial dysfunction within their pathophysiology. In an attempt to have a broader view of IBM pathophysiology, we perform a gene expression analysis by mRNA seq of the target tissue, muscle, compared to fibroblasts and iPSC-differentiated myotubes. DEGs of each of the samples provided an overview of what pathological pathways were altered and which ones were shared between the cell models and the target tissue. Moreover, the additional screening of fluid samples, like urine or plasma, was aimed to check and support the presence of systemic alterations related to the IBM hallmarks, as well as facilitating their detection in a non-invasive manner. However, we must acknowledge the limited sample size of our cohorts as well as the supportive information the cell models herein displayed can provide to the muscle biopsy required in the diagnosis of IBM. In addition, we should take advantage of the knowledge provided by other pathologies with shared mechanisms, like AD and PD related to mitochondrial and degeneration alterations; or Sjögren syndrome disease map, as anti-cN-1A antibodies, HLA-DR3 haplotype and an association to T cell large granular lymphocytic leukemia are shared with IBM. Moreover, we must keep in mind that IBM is a rare disease, and IBM-related consortiums are key to validate results from proof of concept studies in bigger cohorts of patients. In this step, we have to acknowledge the importance of including, sharing and protecting clinical data registries for IBM and all rare diseases, to move faster from research to clinical applications. Overall, the coordination of multiple stakeholders including basic researchers, clinicians, regulatory and funding agencies and pharmaceutical companies is key in providing a better understanding, care and treatments in

multiple diseases, including IBM. We hope our study sheds light on alternative models for IBM and provides ideas to progress in the IBM care context.

CONCLUSIONS

The conclusions derived from this thesis are the following ones:

1. Fibroblasts from inclusion body myositis patients revealed the presence of inflammatory, degenerative and mitochondrial disturbances, resembling those present in the muscle tissue, becoming a potential disease model for inclusion body myositis and eventually other neuromuscular diseases.
2. Skeletal muscle cells derived from induced pluripotent stem cells obtained from inclusion body myositis patients fibroblasts' displayed myopathic, autophagic and mitochondrial changes resembling the target tissue of the disease.
3. The comorbidity of inclusion body myositis with other age-related diseases revealed that pre-diabetes conditions were found in inclusion body myositis fibroblasts in relation to Diabetes mellitus type 2, but no correlation with Alzheimer's disease was found.
4. Metabolic disarrangements in inclusion body myositis fibroblasts and fluid samples revealed that L-pyroglutamic and orotic acids could be potential biomarkers for inclusion body myositis.
5. Cell models derived from inclusion body myositis patients are a tool to investigate the etiology of the disease, aid in the identification of biomarkers and in the evaluation of potential comorbidities with other diseases.
6. The role of the metabolic and mitochondrial component in inclusion body myositis is relevant and could be also affected in other muscular diseases.
7. Despite inclusion body myositis is a muscular disease without clinical symptoms outside of the muscle, there are molecular changes in other tissues, suggesting that there might be a systemic alteration.
8. The identification of altered genes at transcriptomic level in inclusion body myositis could aid in identifying upstream regulators and affected signaling pathways that shed light into inclusion body myositis pathophysiology.

REFERENCES

1. Cantó-Santos J, Grau-Junyent JM, Garrabou G. The Impact of Mitochondrial Deficiencies in Neuromuscular Diseases. Antioxidants [Internet]. 2020 Oct 9;9(10):964. Available from: https://www.mdpi.com/2076-3921/9/10/964

2. Bonne G, Rivier F, Hamroun D. The 2018 version of the gene table of monogenic neuromuscular disorders (nuclear genome). Neuromuscular Disorders. 2017 Dec 1;27(12):1152–83.

3. Deenen C W J, Horlings G C C, Verschuuren J G M J, Verbeek L M A, van Engelen G M B. The Epidemiology of Neuromuscular Disorders: A Comprehensive Overview of the Literature - PubMed. J Neuromuscul Dis. 2015;2(1):73–85.

4. van Putten M, Hmeljak J, Aartsma-Rus A, Dowling JJ. Moving neuromuscular disorders research forward: from novel models to clinical studies. Dis Model Mech. 2020 Feb 1;13(2):dmm044370.

5. Lundberg IE, Fujimoto M, Vencovsky J, Aggarwal R, Holmqvist M, Christopher-Stine L, et al. Idiopathic inflammatory myopathies. Nat Rev Dis Primers. 2021;7(1):1–22.

6. Selva-O'callaghan A, Pinal-Fernandez I, Trallero-Araguás E, Milisenda JC, Grau-Junyent M, Mammen AL. Classification and management of adult inflammatory myopathies. Lancet Neurol [Internet]. 2018 [cited 2020 May 26];17:816–28. Available from: www.thelancet.com/neurology

7. Nagy S, Khan A, Machado PM, Houlden H. Inclusion body myositis: from genetics to clinical trials. J Neurol [Internet]. 2023 Mar 18;270(3):1787–97. Available from: https://link.springer.com/10.1007/s00415-022-11459-3

8. Naddaf E, Shelly S, Mandrekar J, Chamberlain AM, Hoffman EM, Ernste FC, et al. Survival and associated comorbidities in inclusion body myositis. Rheumatology (United Kingdom). 2022 May 1;61(5):2016–24.

9. Weihl CC. Sporadic Inclusion Body Myositis and Other Rimmed Vacuolar Myopathies. CONTINUUM: Lifelong Learning in Neurology [Internet]. 2019 Dec;25(6):1586–98. Available from: http://journals.lww.com/10.1212/CON.0000000000000790

10. Greenberg SA. Pathogenesis of inclusion body myositis. Curr Opin Rheumatol [Internet]. 2020 Nov 1;32(6):542–7. Available from: https://journals.lww.com/10.1097/BOR.0000000000000752

11. Greenberg SA. Inclusion body myositis: clinical features and pathogenesis. Nat Rev Rheumatol [Internet]. 2019 May 5 [cited 2021 Dec 13];15(5):257–72. Available from: https://www.nature.com/articles/s41584-019-0186-x

12. Jackson CE, Barohn RJ, Gronseth G, Pandya S, Herbelin L, Muscle Study Group. Inclusion body myositis functional rating scale: A reliable and valid measure of disease severity. Muscle Nerve. 2008 Apr;37(4):473–6.

13. Lin AY, Siener CS, Faino A V., Seiffert M, Weihl CC, Wang LH. Optimizing hand-function patient outcome measures for inclusion body myositis. Neuromuscular Disorders. 2020 Oct 1;30(10):807–14.

14. Perez-Rosendahl M, Mozaffar T. Inclusion body myositis: evolving concepts. Curr Opin Neurol. 2022 Oct 1;35(5):604–10.

15. Lundberg IE, Tjärnlund A, Bottai M, Werth VP, Pilkington C, Visser M de, et al. 2017 European League Against Rheumatism/American College of Rheumatology classification criteria for adult and juvenile idiopathic inflammatory myopathies and their major subgroups. Ann Rheum Dis. 2017 Dec;76(12):1955–64.

16. MR R. 188th ENMC International Workshop: Inclusion Body Myositis, 2-4 December 2011, Naarden, The Netherlands. Neuromuscul Disord [Internet]. 2013 Dec [cited 2021 Oct 26];23(12):1044–55. Available from: https://pubmed.ncbi.nlm.nih.gov/24268584/

17. Catalán M, Selva-O'Callaghan A, Grau JM. Diagnosis and classification of sporadic inclusion body myositis (sIBM). Autoimmun Rev [Internet]. 2014 Apr [cited 2019 Apr 16];13(4–5):363–6. Available from: http://www.ncbi.nlm.nih.gov/pubmed/24424185

18. Benarroch L, Bonne G, Rivier F, Hamroun D. The 2023 version of the gene table of neuromuscular disorders (nuclear genome). Neuromuscular Disorders [Internet]. 2023 [cited 2023 Apr 26];33:76–117. Available from: www.sciencedirect.comwww.elsevier.com/locate/nmd

19. Perez-Rosendahl M, Mozaffar T. Inclusion body myositis: evolving concepts. Curr Opin Neurol [Internet]. 2022 Oct 1;35(5):604–10. Available from: https://journals.lww.com/10.1097/WCO.0000000000001095

20. Askanas V, Engel WK, Nogalska A. Sporadic inclusion-body myositis: A degenerative muscle disease associated with aging, impaired muscle protein homeostasis and abnormal mitophagy. Biochim Biophys Acta Mol Basis Dis [Internet]. 2015 Apr 1 [cited 2020 Oct 23];1852(4):633–43. Available from: http://dx.doi.org/10.1016/j.bbadis.2014.09.005

21. Brady S, Squier W, Sewry C, Hanna M, Hilton-Jones D, Holton JL, et al. A retrospective cohort study identifying the principal pathological features useful in the diagnosis of inclusion body myositis Setting: Specialist muscle services at the John. BMJ Open. 2014;4:4552.

22. Greenberg SA, Pinkus JL, Kong SW, Baecher-Allan C, Amato AA, Dorfman DM. Highly differentiated cytotoxic T cells in inclusion body myositis. Brain [Internet]. 2019 [cited 2020 Apr 21];142:2590–2604. Available from: https://academic.oup.com/brain/article-abstract/142/9/2590/5536587

23. Goyal NA, Coulis G, Duarte J, Farahat PK, Mannaa AH, Cauchii J, et al. Immunophenotyping of Inclusion Body Myositis Blood T and NK Cells. Neurology [Internet]. 2022 Mar 29 [cited 2023 Mar 14];98(13):e1374–83. Available from: https://n-neurology-org.sire.ub.edu/content/98/13/e1374

24. Pluk H, Van Hoeve BJA, Van Dooren SHJ, Stammen-Vogelzangs J, Van Der Heijden A, Schelhaas HJ, et al. Autoantibodies to cytosolic 5′-nucleotidase 1A in inclusion body myositis. Ann Neurol. 2013;73(3):397–407.

25. Tawara N, Yamashita S, Zhang X, Korogi M, Zhang Z, Doki T, et al. Pathomechanisms of anti–cytosolic 5′-nucleotidase 1A autoantibodies in sporadic inclusion body myositis. Ann Neurol. 2017 Apr 1;81(4):512–25.

26. Pinal-Fernandez I, Casal-Dominguez M, Derfoul A, Pak K, Plotz P, Miller FW, et al. Identification of distinctive interferon gene signatures in different types of myositis. Neurology [Internet]. 2019 Sep 17;93(12):e1193–204. Available from: https://www.neurology.org/lookup/doi/10.1212/WNL.0000000000008128

27. Milisenda JC, Pinal-Fernandez I, Lloyd TE, Grau JM, Miller FW, Selva-O'Callaghan A, et al. Accumulation of autophagosome cargo protein p62 is common in idiopathic inflammatory myopathies. Clin Exp Rheumatol [Internet]. 2021 Mar 1 [cited 2022 Feb 17];39(2):351–6. Available from: https://www.clinexprheumatol.org/abstract.asp?a=15178

28. Nogalska A, D'Agostino C, Terracciano C, Engel WK, Askanas V. Impaired autophagy in sporadic inclusion-body myositis and in endoplasmic reticulum

stress-provoked cultured human muscle fibers. American Journal of Pathology. 2010 Sep 1;177(3):1377–87.

29. Yu L, Chen Y, Tooze SA. Autophagy pathway: Cellular and molecular mechanisms. Autophagy. 2018;14(2):207–15.

30. Nelke C, Kleefeld F, Preusse C, Ruck T, Stenzel W. Inclusion body myositis and associated diseases: an argument for shared immune pathologies. Vol. 10, Acta Neuropathologica Communications. BioMed Central Ltd; 2022.

31. Balakrishnan A, Aggarwal R, Agarwal V, Gupta L. Inclusion body myositis in the rheumatology clinic. Int J Rheum Dis. 2020;23(9):1126–35.

32. Bhatt PS, Tzoulis C, Balafkan N, Miletic H, Tuong G, Tran T, et al. Mitochondrial DNA depletion in sporadic inclusion body myositis. Neuromuscular Disorders. 2019;29:242–6.

33. Rygiel KA, Miller J, Grady JP, Rocha MC, Taylor RW, Turnbull DM. Mitochondrial and inflammatory changes in sporadic inclusion body myositis. Neuropathol Appl Neurobiol. 2015;41(3):288–303.

34. Rothwell S, Cooper RG, Lundberg IE, Gregersen PK, Hanna MG, Machado PM, et al. Immune-Array Analysis in Sporadic Inclusion Body Myositis Reveals HLA–DRB1 Amino Acid Heterogeneity Across the Myositis Spectrum. Arthritis and Rheumatology. 2017 May 1;69(5):1090–9.

35. Rothwell S, Cooper RG, Lundberg IE, Gregersen PK, Hanna MG, Machado PM, et al. Immune-Array Analysis in Sporadic Inclusion Body Myositis Reveals HLA–DRB1 Amino Acid Heterogeneity Across the Myositis Spectrum. Arthritis and Rheumatology. 2017 May 1;69(5):1090–9.

36. Rothwell S, Amos CI, Miller FW, Rider LG, Lundberg IE, Gregersen PK, et al. Identification of Novel Associations and Localization of Signals in Idiopathic Inflammatory Myopathies Using <scp>Genome-Wide</scp> Imputation. Arthritis & Rheumatology [Internet]. 2023 Jun 20;75(6):1021–7. Available from: https://onlinelibrary.wiley.com/doi/10.1002/art.42434

37. Inflammatory & Immune Myopathies [Internet]. [cited 2023 Apr 11]. Available from: https://neuromuscular.wustl.edu/antibody/infmyop.htm#ibm

38. Scotton C, Passarelli C, Neri M, Ferlini A. Biomarkers in rare neuromuscular diseases. Exp Cell Res. 2013;325:44–9.

39. Search of: Recruiting, Active, not recruiting Studies | Interventional Studies | Inclusion Body Myositis - List Results - ClinicalTrials.gov [Internet]. [cited 2023 Apr 11]. Available from: https://clinicaltrials.gov/ct2/results?cond=Inclusion+Body+Myositis&recrs=a&recrs=d&age_v=&gndr=&type=Intr&rslt=&Search=Apply

40. Connolly CM, Plomp L, Paik JJ, Allenbach Y. Best Practice & Research Clinical Rheumatology Possible future avenues for myositis therapeutics : DM , IMNM and IBM. Best Pract Res Clin Rheumatol. 2022;36(2):101762.

41. Advanced therapy medicinal products: Overview | European Medicines Agency [Internet]. [cited 2023 Apr 11]. Available from: https://www.ema.europa.eu/en/human-regulatory/overview/advanced-therapy-medicinal-products-overview

42. Mendell JR, Sahenk Z, Al-Zaidy S, Rodino-Klapac LR, Lowes LP, Alfano LN, et al. Follistatin Gene Therapy for Sporadic Inclusion Body Myositis Improves Functional Outcomes. Molecular Therapy. 2017;25(4):870–9.

43. S4R Registration | Share4Rare [Internet]. [cited 2020 May 19]. Available from: https://www.share4rare.org/registration/understanding-neuromuscular-diseases

44. Inclusion Body Myositis - Clinical Trials | Cure IBM [Internet]. [cited 2021 Nov 11]. Available from: https://cureibm.org/treatment/clinical-trials/

45. The Myositis Association | Your Myositis Community [Internet]. [cited 2021 Nov 11]. Available from: https://www.myositis.org/

46. Diagnosis – European Reference Network – EURO-NMD [Internet]. [cited 2020 Apr 22]. Available from: https://ern-euro-nmd.eu/

47. Disease model [Internet]. 2023 [cited 2023 Jun 4]. Available from: https://www.nature.com/subjects/disease-model

48. Avior Y, Sagi I, Benvenisty N. Pluripotent stem cells in disease modelling and drug discovery. Nat Rev Mol Cell Biol. 2016;17(3):170–82.

49. Speciale AA, Ellerington R, Goedert T, Rinaldi C. Modelling neuromuscular diseases in the age of precision medicine. Vol. 10, Journal of Personalized Medicine. MDPI AG; 2020. p. 1–17.

50. Hasin Y, Seldin M, Lusis A. Multi-omics approaches to disease. Genome Biol [Internet]. 2017 Dec 5;18(1):83. Available from: https://genomebiology.biomedcentral.com/articles/10.1186/s13059-017-1215-1

51. Avior Y, Sagi I, Benvenisty N. Pluripotent stem cells in disease modelling and drug discovery. Vol. 17, Nature Reviews Molecular Cell Biology. Nature Publishing Group; 2016. p. 170–82.

52. Britson KA, Ling JP, Braunstein KE, Montagne JM, Kastenschmidt JM, Wilson A, et al. Loss of TDP-43 function and rimmed vacuoles persist after T cell depletion in a xenograft model of sporadic inclusion body myositis. Sci Transl Med [Internet]. 2022 Jan 19;14(628):9196. Available from: https://www.science.org/doi/10.1126/scitranslmed.abi9196

53. Greenberg SA. Pathogenesis of inclusion body myositis. Curr Opin Rheumatol [Internet]. 2020 Nov;32(6):542–7. Available from: https://journals.lww.com/10.1097/BOR.0000000000000752

54. Sugarman MC, Yamasaki TR, Oddo S, Echegoyen JC, Murphy MP, Golde TE, et al. Inclusion body myositis-like phenotype induced by transgenic overexpression of βAPP in skeletal muscle. Proc Natl Acad Sci U S A. 2002;99(9):6334–9.

55. Ahmed M, Machado PM, Miller A, Spicer C, Herbelin L, He J, et al. Targeting protein homeostasis in sporadic inclusion body myositis. Sci Transl Med [Internet]. 2016 Mar 23 [cited 2019 Apr 16];8(331):331ra41-331ra41. Available from: https://www.science.org/doi/10.1126/scitranslmed.aad4583

56. Fosse V, Oldoni E, Gerardi C, Banzi R, Fratelli M, Bietrix F, et al. Evaluating Translational Methods for Personalized Medicine—A Scoping Review. J Pers Med [Internet]. 2022 Jul 19;12(7):1177. Available from: https://www.mdpi.com/2075-4426/12/7/1177

57. Lin YY. Muscle diseases in the zebrafish. Neuromuscul Disord. 2012;22(8).

58. Howe K, Clark MD, Torroja CF, Torrance J, Berthelot C, Muffato M, et al. The zebrafish reference genome sequence and its relationship to the human genome. Nature 2013 496:7446. 2013 Apr 17;496(7446):498–503.

59. Dowling JJ, Arbogast S, Hur J, Nelson DD, McEvoy A, Waugh T, et al. Oxidative stress and successful antioxidant treatment in models of RYR1-related myopathy. Brain. 2012 Apr 1;135(4):1115–27.

60. Hewitt JE, Pollard AK, Lesanpezeshki L, Deane CS, Gaffney CJ, Etheridge T, et al. Muscle strength deficiency and mitochondrial dysfunction in a muscular dystrophy model of Caenorhabditis elegans and its functional response to drugs. Dis Model Mech. 2018;11.

61. Fibroblast [Internet]. [cited 2023 Apr 13]. Available from: https://www.genome.gov/genetics-glossary/Fibroblast

62. Wei K, Nguyen HN, Brenner MB. Fibroblast pathology in inflammatory diseases. Journal of Clinical Investigation. 2021;131(20):1–11.

63. Kendall RT, Feghali-Bostwick CA. Fibroblasts in fibrosis: novel roles and mediators. Front Pharmacol [Internet]. 2014 May 27;5. Available from: http://journal.frontiersin.org/article/10.3389/fphar.2014.00123/abstract

64. Ortuño-Costela M, García-López M, Cerrada V, Gallardo ME. <scp>iPSC</scp> s: A powerful tool for skeletal muscle tissue engineering. J Cell Mol Med [Internet]. 2019 Jun [cited 2020 Oct 28];23(6):3784–94. Available from: https://onlinelibrary.wiley.com/doi/10.1111/jcmm.14292

65. Tokuyama T, Hirai A, Shiiba I, Ito N, Matsuno K, Takeda K, et al. Mitochondrial Dynamics Regulation in Skin Fibroblasts from Mitochondrial Disease Patients. Biomolecules. 2020 Mar 13;10(3):450.

66. Auburger G, Klinkenberg M, Drost J, Marcus K, Morales-Gordo B, Kunz WS, et al. Primary skin fibroblasts as a model of Parkinson's disease. Mol Neurobiol. 2012;46(1):20–7.

67. González-Casacuberta I, Morén C, Juárez-Flores DL, Esteve-Codina A, Sierra C, Catalán-García M, et al. Transcriptional alterations in skin fibroblasts from Parkinson's disease patients with parkin mutations. Neurobiol Aging. 2018;65:206–16.

68. González-Casacuberta I, Juárez-Flores DL, Morén C, Garrabou G. Bioenergetics and Autophagic Imbalance in Patients-Derived Cell Models of Parkinson Disease Supports Systemic Dysfunction in Neurodegeneration. Front Neurosci. 2019 Sep 10;13(September):1–20.

69. González-Casacuberta I, Juárez-Flores DL, Ezquerra M, Fucho R, Catalán-García M, Guitart-Mampel M, et al. Mitochondrial and autophagic alterations in skin fibroblasts from Parkinson disease patients with Parkin mutations. Aging

[Internet]. 2019 Jun 1 [cited 2020 Jun 26];11(11):3750–67. Available from: https://pubmed.ncbi.nlm.nih.gov/31180333/

70. Alvarez-Mora MI, Garrabou G, Barcos T, Garcia-Garcia F, Grillo-Risco R, Peruga E, et al. Bioenergetic and Autophagic Characterization of Skin Fibroblasts from C9orf72 Patients. Antioxidants 2022, Vol 11, Page 1129. 2022 Jun 8;11(6):1129.

71. Onesto E, Colombrita C, Gumina V, Borghi MO, Dusi S, Doretti A, et al. Gene-specific mitochondria dysfunctions in human TARDBP and C9ORF72 fibroblasts. Acta Neuropathol Commun. 2016;4(1):47.

72. Mesdom P, Colle R, Lebigot E, Trabado S, Deflesselle E, Fève B, et al. Human Dermal Fibroblast: A Promising Cellular Model to Study Biological Mechanisms of Major Depression and Antidepressant Drug Response. Curr Neuropharmacol. 2019;18(4):301–18.

73. Collier JJ, Guissart C, Oláhová M, Sasorith S, Piron-Prunier F, Suomi F, et al. Developmental Consequences of Defective ATG7-Mediated Autophagy in Humans. New England Journal of Medicine [Internet]. 2021 Jun 24;384(25):2406–17. Available from: http://www.nejm.org/doi/10.1056/NEJMoa1915722

74. Park SY, Byun EJ, Lee JD, Kim S, Kim HS. Air Pollution, Autophagy, and Skin Aging: Impact of Particulate Matter (PM 10) on Human Dermal Fibroblasts. International Journal of Molecular Sciences Article.

75. Nadalutti CA, Stefanick DF, Zhao ML, Horton JK, Prasad R, Brooks AM, et al. Mitochondrial dysfunction and DNA damage accompany enhanced levels of formaldehyde in cultured primary human fibroblasts. Sci Rep. 2020 Dec 27;10(1):5575.

76. Weider M, Schröder A, Docheva D, Rodrian G, Enderle I, Seidel CL, et al. A human periodontal ligament fibroblast cell line as a new model to study periodontal stress. Int J Mol Sci. 2020;21(21):1–10.

77. Madelaire CB, Klink AC, Israelsen WJ, Hindle AG. Fibroblasts as an experimental model system for the study of comparative physiology. Comp Biochem Physiol B Biochem Mol Biol. 2022;260(December 2021):110735.

78. Takahashi K, Yamanaka S. Induction of pluripotent stem cells from mouse embryonic and adult fibroblast cultures by defined factors. Cell. 2006 Aug 25;126(4):663–76.

79. Chang CY, Ting HC, Liu CA, Su HL, Chiou TW, Harn HJ, et al. Induced Pluripotent Stem Cells: A Powerful Neurodegenerative Disease Modeling Tool for Mechanism Study and Drug Discovery. Cell Transplant. 2018;27(11):1588–602.

80. Takahashi K, Tanabe K, Ohnuki M, Narita M, Ichisaka T, Tomoda K, et al. Induction of pluripotent stem cells from adult human fibroblasts by defined factors. Cell. 2007 Nov 30;131(5):861–72.

81. Takahashi K, Yamanaka S. A decade of transcription factor-mediated reprogramming to pluripotency. Nat Rev Mol Cell Biol. 2016;17(3):183–93.

82. Maffioletti SM, Gerli MFM, Ragazzi M, Dastidar S, Benedetti S, Loperfido M, et al. Efficient derivation and inducible differentiation of expandable skeletal myogenic cells from human ES and patient-specific iPS cells. Nat Protoc. 2015;10(7):941–58.

83. Chal J, Oginuma M, Al Tanoury Z, Gobert B, Sumara O, Hick A, et al. Differentiation of pluripotent stem cells to muscle fiber to model Duchenne muscular dystrophy. Nat Biotechnol. 2015 Sep 10;33(9):962–9.

84. Incitti T, Magli A, Magli A, Jenkins A, Lin K, Yamamoto A, et al. Pluripotent stem cell-derived skeletal muscle fibers preferentially express myosin heavy-chain isoforms associated with slow and oxidative muscles. Skelet Muscle. 2020;10(1):1–11.

85. Caron L, Kher D, Lee KL, McKernan R, Dumevska B, Hidalgo A, et al. A Human Pluripotent Stem Cell Model of Facioscapulohumeral Muscular Dystrophy-Affected Skeletal Muscles. Stem Cells Transl Med. 2016 Sep;5(9):1145–61.

86. Moretti A, Fonteyne L, Giesert F, Hoppmann P, Meier AB, Bozoglu T, et al. Somatic gene editing ameliorates skeletal and cardiac muscle failure in pig and human models of Duchenne muscular dystrophy. Nature Medicine 2020 26:2 [Internet]. 2020 Jan 27 [cited 2022 Jun 22];26(2):207–14. Available from: https://www-nature-com.sire.ub.edu/articles/s41591-019-0738-2

87. Maniscalco E, Abbadessa G, Giordano M, Grasso L, Borrione P, Racca S. Metformin regulates myoblast differentiation through an AMPK-dependent mechanism. PLoS One. 2023;18(2 February):1–22.

88. Mournetas V, Massouridès E, Dupont JB, Kornobis E, Polvèche H, Jarrige M, et al. Myogenesis modelled by human pluripotent stem cells: a multi-omic study of Duchenne myopathy early onset. J Cachexia Sarcopenia Muscle [Internet]. 2021

Feb 1 [cited 2022 May 2];12(1):209–32. Available from: https://onlinelibrary.wiley.com/doi/full/10.1002/jcsm.12665

89. Nogalska A, D'Agostino C, Engel WK, Askanas V. Sodium phenylbutyrate reverses lysosomal dysfunction and decreases amyloid-β42 in an in vitro-model of inclusion-body myositis. Neurobiol Dis. 2014 May 1;65:93–101.

90. Safety and Tolerability of Phenylbutyrate in Inclusion Body Myositis - Full Text View - ClinicalTrials.gov [Internet]. [cited 2021 Nov 10]. Available from: https://clinicaltrials.gov/ct2/show/NCT04421677?recrs=abd&type=Intr&cond=Inclusion+Body+Myositis&draw=4&rank=3

91. Ahmed M, Machado PM, Miller A, Spicer C, Herbelin L, He J, et al. Targeting protein homeostasis in sporadic inclusion body myositis. Sci Transl Med [Internet]. 2016 Mar 23;8(331):331-ra41. Available from: https://www.science.org/doi/10.1126/scitranslmed.aad4583

92. Zhao Z, Chen X, Dowbaj AM, Sljukic A, Bratlie K, Lin L, et al. Organoids. Nature Reviews Methods Primers. 2022;2(1).

93. Clevers H. Modeling Development and Disease with Organoids. Cell. 2016;165(7):1586–97.

94. Fernández-Garibay X, Ortega MA, Cerro-Herreros E, Comelles J, Martínez E, Artero R, et al. Bioengineered in vitro 3D model of myotonic dystrophy type 1 human skeletal muscle. Biofabrication [Internet]. 2021 Jul 1 [cited 2021 Apr 30];13(3):035035. Available from: https://iopscience.iop.org/article/10.1088/1758-5090/abf6ae

95. Xia Y, Izpisua Belmonte JC. Design Approaches for Generating Organ Constructs. Cell Stem Cell. 2019 Jun 6;24(6):877–94.

96. Shendure J. Next-generation human genetics. Genome Biol. 2011 Sep 14;12(9):1–3.

97. Cummings BB, Marshall JL, Tukiainen T, Lek M, Donkervoort S, Foley AR, et al. Improving genetic diagnosis in Mendelian disease with transcriptome sequencing. Sci Transl Med [Internet]. 2017 Apr 19;9(386). Available from: https://www.science.org/doi/10.1126/scitranslmed.aal5209

98. Momeni Z, Hassanzadeh E, Saniee Abadeh M, Bellazzi R. A survey on single and multi omics data mining methods in cancer data classification. Vol. 107, Journal of Biomedical Informatics. Academic Press Inc.; 2020.

99. Taudt A, Colomé-Tatché M, Johannes F. Genetic sources of population epigenomic variation. Nature Reviews Genetics 2016 17:6. 2016 May 9;17(6):319–32.

100. Roadmap Epigenomics Consortium, Kundaje A, Meuleman W, Ernst J, Bilenky M, Yen A, et al. Integrative analysis of 111 reference human epigenomes. Nature 2015 518:7539. 2015 Feb 18;518(7539):317–30.

101. Schmitz SU, Grote P, Herrmann BG. Mechanisms of long noncoding RNA function in development and disease. Cell Mol Life Sci. 2016 Jul 1;73(13):2491–509.

102. Morán I, Akerman I, Van De Bunt M, Xie R, Benazra M, Nammo T, et al. Human β cell transcriptome analysis uncovers lncRNAs that are tissue-specific, dynamically regulated, and abnormally expressed in type 2 diabetes. Cell Metab. 2012 Oct 3;16(4):435–48.

103. Barrett SP, Salzman J. Circular RNAs: analysis, expression and potential functions. Development [Internet]. 2016 Jun 1 [cited 2023 Apr 16];143(11):1838–47. Available from: https://journals.biologists.com/dev/article/143/11/1838/47513/Circular-RNAs-analysis-expression-and-potential

104. Mann M, Jensen ON. Proteomic analysis of post-translational modifications. Nature Biotechnology 2003 21:3. 2003 Mar 1;21(3):255–61.

105. Shin SY, Fauman EB, Petersen AK, Krumsiek J, Santos R, Huang J, et al. The Multiple Tissue Human Expression Resource (MuTHER) Consortium 13 , Melanie Waldenberger 14. Nature Publishing Group. 2014;46(6):16.

106. Palsson B, Zengler K. The challenges of integrating multi-omic data sets. Nature Chemical Biology 2010 6:11. 2010 Oct 18;6(11):787–9.

107. Emilsson V, Thorleifsson G, Zhang B, Leonardson AS, Zink F, Zhu J, et al. Genetics of gene expression and its effect on disease. Nature [Internet]. 2008 Mar 16 [cited 2023 Apr 16];452(7186):423–8. Available from: https://www.nature.com/articles/nature06758

108. Johnson JO, Chia R, Miller DE, Li R, Kumaran R, Abramzon Y, et al. Association of Variants in the SPTLC1 Gene with Juvenile Amyotrophic Lateral Sclerosis. JAMA Neurol. 2021;78(10):1236–48.

109. Zhang W, Gong J, Ding L, Zhang Z, Pan X, Chen X, et al. Functional validation of a human GLUD2 variant in a murine model of Parkinson's disease. Cell Death Dis. 2020 Oct 1;11(10).

110. Su Z, Łabaj PP, Li S, Thierry-Mieg J, Thierry-Mieg D, Shi W, et al. A comprehensive assessment of RNA-seq accuracy, reproducibility and information content by the Sequencing Quality Control Consortium. Nature Biotechnology 2014 32:9. 2014 Aug 24;32(9):903–14.

111. Peixoto L, Risso D, Poplawski SG, Wimmer ME, Speed TP, Wood MA, et al. How data analysis affects power, reproducibility and biological insight of RNA-seq studies in complex datasets. Nucleic Acids Res. 2015 Jul 3;43(16):7664–74.

112. Conesa A, Beck S. Making multi-omics data accessible to researchers. Sci Data [Internet]. 2019 Oct 31;6(1):251. Available from: https://www.nature.com/articles/s41597-019-0258-4

113. Gonorazky HD, Naumenko S, Ramani AK, Nelakuditi V, Mashouri P, Wang P, et al. Expanding the Boundaries of RNA Sequencing as a Diagnostic Tool for Rare Mendelian Disease. Am J Hum Genet. 2019 Mar 7;104(3):466–83.

114. Foote AG, Wang Z, Kendziorski C, Thibeault SL. Tissue specific human fibroblast differential expression based on RNAsequencing analysis. BMC Genomics [Internet]. 2019 Dec 23 [cited 2021 Sep 13];20(1):308. Available from: https://bmcgenomics.biomedcentral.com/articles/10.1186/s12864-019-5682-5

115. GTEX [Internet]. [cited 2023 Mar 10]. Available from: https://gtexportal.org/home/

116. Amici DR, Pinal-Fernandez I, Christopher-Stine L, Mammen AL, Mendillo ML. A network of core and subtype-specific gene expression programs in myositis. Acta Neuropathol. 2021 Nov 1;142(5):887–98.

117. Guo K, Savelieff MG, Rumora AE, Alakwaa FM, Callaghan BC, Hur J, et al. Plasma Metabolomics and Lipidomics Differentiate Obese Individuals by Peripheral Neuropathy Status. Journal of Clinical Endocrinology and Metabolism. 2022;107(4):1091–109.

118. Britson KA, Ling JP, Braunstein KE, Montagne JM, Kastenschmidt JM, Wilson A, et al. Loss of TDP-43 function and rimmed vacuoles persist after T cell depletion in a xenograft model of sporadic inclusion body myositis. Sci Transl Med

[Internet]. 2022 Jan 19;14(628):9196. Available from: https://www.science.org/doi/10.1126/scitranslmed.abi9196

119. Cheng Y, Straube R, Alnaif AE, Huang L, Leil TA, Schmidt BJ. Systems Medicine. Vol. 2486, Methods in Molecular Biology. 2022. 129–179 p.

120. Safran M, Dalah I, Alexander J, Rosen N, Iny Stein T, Shmoish M, et al. GeneCards Version 3: the human gene integrator. Database (Oxford). 2010;2010:1–16.

121. Zhang W, Gong J, Ding L, Zhang Z, Pan X, Chen X, et al. Functional validation of a human GLUD2 variant in a murine model of Parkinson's disease. Cell Death Dis. 2020 Oct 1;11(10).

122. Tadenev ALD, Burgess RW. Model validity for preclinical studies in precision medicine: precisely how precise do we need to be? Mammalian Genome [Internet]. 2019;30(5–6):111–22. Available from: https://doi.org/10.1007/s00335-019-09798-0

123. Fosse V, Oldoni E, Bietrix F, Budillon A, Daskalopoulos EP, Fratelli M, et al. Recommendations for robust and reproducible preclinical research in personalised medicine. BMC Med [Internet]. 2023 Jan 8;21(1):14. Available from: http://www.ncbi.nlm.nih.gov/pubmed/36617553

124. Marshall LJ, Bailey J, Cassotta M, Herrmann K, Pistollato F. Poor Translatability of Biomedical Research Using Animals — A Narrative Review. Alternatives to Laboratory Animals. 2023 Mar 7;026119292311577.

125. EU Science Hub. Non-animal methods in science and regulation [Internet]. 2023. Available from: https://joint-research-centre.ec.europa.eu

126. EU Science Hub. Advanced Non-animal Models in Biomedical Research Neurodegenerative Diseases [Internet]. 2021. Available from: https://ec.europa.eu/jrc

127. International Inclusion Body Myositis (IBM) Genetics Consortium [Internet]. 2020 [cited 2023 Jun 1]. Available from: https://www.ucl.ac.uk/centre-for-neuromuscular-diseases/news/2020/jul/international-inclusion-body-myositis-ibm-genetics-consortium-reaches-750-samples

128. The International IBM Consortium Genetic Study: Using Next Generation Sequencing to Unravel the Pathogenesis of Sporadic Inclusion Body Myositis (IBM) [Internet]. [cited 2023 Jun 1]. Available from: https://www.ucl.ac.uk/centre-for-neuromuscular-

diseases/research/experimental-clinical-trials/muscle/muscle-open-trials/international-ibm-consortium-genetic

129. Cirillo D, Valencia A. Big data analytics for personalized medicine. Curr Opin Biotechnol. 2019 Aug 1;58:161–7.

130. About us – GA4GH [Internet]. [cited 2023 May 31]. Available from: https://www.ga4gh.org/about-us/

131. Durinx C, McEntyre J, Appel R, Apweiler R, Barlow M, Blomberg N, et al. Identifying ELIXIR Core Data Resources. F1000Res. 2017;5.

132. Margolis R, Derr L, Dunn M, Huerta M, Larkin J, Sheehan J, et al. The National Institutes of Health's Big Data to Knowledge (BD2K) initiative: capitalizing on biomedical big data. [cited 2023 May 31]; Available from: http://bd2k.nih.

133. Who we are – IRDiRC [Internet]. [cited 2023 May 31]. Available from: https://irdirc.org/who-we-are-2/

134. Wilkinson MD, Dumontier M, Aalbersberg IjJ, Appleton G, Axton M, Baak A, et al. Comment: The FAIR Guiding Principles for scientific data management and stewardship. Sci Data. 2016 Mar 15;3.

135. Mazein A, Ostaszewski M, Kuperstein I, Watterson S, Le Novère N, Lefaudeux D, et al. Systems medicine disease maps: community-driven comprehensive representation of disease mechanisms. NPJ Syst Biol Appl. 2018 Dec 1;4(1).

136. Ostaszewski M, Gebel S, Kuperstein I, Mazein A, Zinovyev A, Dogrusoz U, et al. Community-driven roadmap for integrated disease maps. Brief Bioinform. 2019 Mar 22;20(2):659–70.

137. Treatabolome [Internet]. [cited 2023 Jun 1]. Available from: https://treatabolome.cnag.crg.eu/#/